Cyclopentadiene-Maleimide Platform for Thermally Reversible Polymers

Jeremy Brent Stegall

Dissertation Submitted to the Faculty of Virginia Polytechnic Institute and State University in partial fulfillment of the requirements for the degree of

Doctor of Philosophy

In

Chemistry

Paul A. Deck, Chair

Paul R. Carlier

Harry W. Gibson

Louis A. Madsen

October 17th, 2014

Blacksburg, Virginia

Keywords: Diels-Alder reaction, cyclopentadiene, maleimide, reversible, fluoroaromatic, step-growth polymer

Cyclopentadiene-Maleimide Platform for Thermally Reversible Polymers

Jeremy Brent Stegall

Abstract

This dissertation describes a new platform for the synthesis of thermally reversible polymers, based on Diels-Alder reactions of bis-cyclopentadienes (bis-CPDs) and bis-maleimides (bis-MIs), that meets two main objectives. First, the bis-CPD must resist characteristic self-coupling. Second, the CPD-MI adducts should undergo the *retro*-Diels-Alder (rDA) reaction (i.e., thermal depolymerization) in a temperature regime that is comparable or slightly higher than that of the freely reversible bis-furan/bis-MI polymers (rDA between 80 °C and 130 °C) but much lower than that of bis-CPD homopolymers (rDA above 160 °C).

Structure-reactivity relationships gleaned from the literature and from related but as yet unpublished work in our own laboratories led to our main hypothesis that a CPD moiety bearing one sterically encumbering substituent such as isopropyl (*i*Pr) or tert-butyl (*t*Bu) and one electron-withdrawing substituent such as perfluoroaryl would have the desired reactivity and adduct stability in combination with an *N*-substituted maleimide. Synthetic considerations led to a bis-CPD monomer design in which two alkylcyclopentadiene groups (alkyl = *i*Pr or *t*Bu) are connected by an octafluorobiphenylene linker.

As an initial fundamental step (Chapter 3), 1-(nonafluorobiphenyl-4'-yl)-4-*tert*-butylcyclopentadiene (**1**) was synthesized to provide a monofunctional model for the proposed difunctional CPD monomer. Reactions of **1** and *N*-(4-fluorophenyl)maleimide (**FMI**) afforded up to five regio- and stereo-isomeric adducts (of fourteen possible). Variable-temperature reactivity studies combined with NMR spectroscopic analysis, X-ray crystallography, and computational modeling enabled product distributions to be understood according to a conventional kinetic-vs-

thermodynamic framework. These studies also predicted the microstructure of polymers derived from the proposed bis-CPD monomer, which is structurally analogous to **1**, and bis-MIs. Moreover, **1** does not undergo DA self-coupling under ordinary conditions (T < 180 °C). Thermolysis studies of the major adducts revealed that the rDA becomes observable on a laboratory timescale (hours) at about 140 °C, which is at the upper end of the temperature range reported for furan+MI adducts but well below that of CPD+CPD adducts. In contrast, adducts formed from either of the analogous monosubstituted cyclopentadienes (tBuC$_5$H$_5$ and C$_6$F$_5$C$_5$H$_5$) do not undergo rDA below 180 °C. These results strongly support the proposed bis-CPD monomer design.

In a second fundamental step (Chapter 4), the hypothesis that an electron-withdrawing CPD substituent would destabilize a CPD-MI adduct was further tested by reacting *N*-(4-fluorophenyl)maleimide with a series of triarylated cyclopentadienes (1,2,3-Ar$_3$C$_5$H$_3$ and 1,2,4-Ar$_3$C$_5$H$_3$, Ar = C$_6$F$_5$, C$_6$F$_4$CF$_3$, and Ar = C$_5$F$_4$N). The perfluorophenyl- and perfluorotolyl-substituted compounds were previously reported, but the perfluoropyridyl-substituted cyclopentadienes were prepared for this study using S$_N$Ar reactions of pentafluoropyridine and sodium cyclopentadienide. The least electron deficient cyclopentadiene in each series (Ar = C$_6$F$_5$) reacted the most quickly and with the highest ultimate equilibrium binding constant, confirming the electron-effects hypothesis as well as the underlying presumption that DA reactions of even relatively electron-poor CPDs with MI would behave according to normal-electron-demand principles.

In the main section of this dissertation (Chapter 5) the proposed bis(cyclopentadiene)s reacted with a series of previously reported bis(maleimides) to form linear polymers having molecular weights (M_n) up to 40 kDa. Relationships among the length and flexibility of the bis-MI linker

(C_6H_{12}, $C_{12}H_{24}$, $C_6H_4OC_6H_4$, and $(C_2H_4O)_2$), the identity of the CPD alkyl substitutent ($CHMe_2$, CMe_3 and CMe_2Ph) and the glass transition temperature (T_g) as measured by differential scanning calorimetry (DSC) were understood in terms of a general model of local segmental mobility and free volume. Solution thermolysis of a model polymer system (bis-MI linker = C_6H_{12} (**7)**, CPD alkyl substituent = *t*Bu) showed a rapid decrease in molecular weight at 160 °C as determined by size exclusion chromatography (SEC). Solution thermolysis in the presence of excess **FMI** (as a trap for free CPD moieties) revealed that the onset temperature for rDA on a laboratory time scale (hours) was as low as 120 °C. In the bulk, thermolysis above 250 °C under vacuum led to recovery of a small portion of the bis-CPD monomer, but bulk thermolysis at 200 °C did not reveal a change in molecular weight as determined by SEC. The current interpretation of these observations is that limited mobility in these glassy polymers prohibits retro-DA decoupling. These findings largely validate the main hypothesis of this dissertation.

Acknowledgements

I would like to thank my advisor, Prof. Paul A. Deck, for introducing me to this project and providing guidance when reactions did not proceed as expected, his enthusiastic approach to all things, not just chemistry. I also thank my committee members for their support through every stage of my graduate career and the valuable discussions that led to answers to questions as well as the development of new and interesting questions. I appreciate Prof. Richard Turner's contributions as a substitute committee member. I would like to thank members of the Chemistry Department's analytical services and support staff: Geno Iannaccone, Bill Bebout, Sr., Ken Knott, Geno, Ken, and Tom Wertalik, Sharelle Dillon, Emillie Shephard, Laurie Good, Angie Miller, Joli Huynh, and the many others that keep the department functioning. I would also like to thank Claire Santos for her support and my former advisors from Roanoke College, Dr. Benjamin Huddle and Dr. W. Gary Hollis, Jr., who inspired me to pursue chemistry and explore research.

I thank Alison Schultz, Evan Margaretta, Keren Zhang, and other members of Prof. Tim Long's research group for the use of their SEC, as well as Scott Radzinski in Prof. John Matson's research group for the use of their SEC. I also thank Bruce Orler from the Moore research group who provided valuable discussions related to TGA and DSC. I thank members of the Deck research group, both past and present, for their research groundwork, support and friendship: Dr. Jessica Evans, Dr. Sanghamitra Sen, Chuck Carfagna, Jr., Brian Hickory, and Kevin Kaurich.

I also wish to thank my parents, Ronald and Mary Stegall, and my sister Keri for their continued support through my journey in graduate school and the rest of my life, their belief that I can achieve my goals has been fundamental to my desire to continue learning. I also thank Shelby Jenkins, who has provided love and companionship since before I embarked on this journey and throughout.

Table of Contents

List of Figures

List of Tables

List of Schemes

Common Abbreviations

DA	Diels-Alder
rDA	*Retro*-Diels-Alder
CPD	Cyclopentadiene
MI	Maleimide
*t*Bu	*Tert*-butyl
*i*Pr	Isopropyl
HOMO	Highest Occupied Molecular Orbital
LUMO	Lowest Unoccupied Molecular Orbital
DFB	Decafluorobiphenyl
o-DCB	1,2-dichlorobenzene
THF	Tetrahydrofuran
S_NAr	Nucleophilic Aromatic Substitution
DP	Degree of Polymerization
DMSO	Dimethylsulfoxide
T_g	Glass Transition Temperature
DSC	Differential Scanning Calorimetry
SEC	Size Exclusion Chromatography
ESI	Electrospray Ionization
TGA	Thermogravimetric Analysis

Chapter 1 Introduction to the Diels-Alder Reaction and Applications in Macromolecular Structures

The Diels-Alder (DA) reaction (Scheme 1) is a concerted [4+2] cycloaddition of a diene and another unsaturated species (the dienophile), usually a substituted alkene or alkyne. Over the past century, the DA reaction has become a primary method of forming six-membered rings in synthetic organic chemistry for several key reasons. First, two new C-C bonds are formed simultaneously and with *syn* diastereoselectivity. This feature is highly prized in a field where a new method for the stereoselective formation of just one C-C bond is considered a breakthrough. Second, the reaction is thermally driven, and therefore neither catalysts, external reagents, nor photochemical stimulation are required, and no byproducts are formed. Because functional group tolerance is limited only by thermal stability, the scope of the DA reaction (variation in diene and dienophile structure) is broad. On the other hand, enantioselectivity can be achieved using optional catalysts.[1] For this dissertation, however, the third and most important feature of the DA reaction is its reversibility. In principle, the six-membered ring of the adduct (Scheme 1) can cleave to re-form the diene and dienophile.

Scheme 1-1

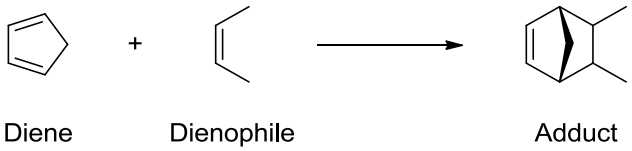

Basic Diels-Alder reaction

This chapter describes macromolecular syntheses that use DA chemistry to produce cleanly reversible polymeric materials. Monomers terminated with dienes and dienophiles can undergo step-growth polymerization at a particular temperature, but then subsequently, at some higher temperature, the retro-Diels-Alder (rDA) reaction becomes thermodynamically favorable, and the polymer spontaneously disassembles. Even if depolymerization is only partial, which is the most

common situation, changes in physical properties can be dramatic. Finally, the polymer may again re-polymerize at the lower temperature, ideally enabling repeated cycling. These changes can all be followed by rigorous experimental techniques including size-exclusion chromatography (SEC), rheometry, and NMR spectroscopy, and in the case of reversible cross-links, effects such as dissolution of a gel can be detected visually. Herein we describe the main DA functional groups and reactions used in reversible polymer synthesis, illustrate the range of polymeric systems that have been prepared using this approach, and highlight their applications.

By far, the most common dienes[1] (Scheme 1-2) used in DA polymerizations are furans, cyclopentadienes, and the occasional anthracene.[2] Furans are aromatic compounds, which restricts the range of side-reactions while favoring the rDA process through the restoration of aromaticity. The most typical means of incorporating either cyclopentadienes or furans is through nucleophilic substitution. Both cyclopentadiene and furfuryl alcohol are inexpensive substances. The most common dienophile moiety is the maleimide, which is reactive (because it is electron-deficient) and easy to incorporate synthetically into structurally diverse monomers through bonding at the N atom (Scheme 1-2). Although not completely general, the mild conditions ($T < 100$ °C, Ac_2O, NaOAc) make these maleimides quite accessible.

In the simplest and most popular implementation (Scheme 1-3), combining a bis-furan and a bis-maleimide under mild conditions (25 °C $< T < 60$ °C) affords a step-growth polymer that undergoes rDA above about 80 °C – although the temperature at which rDA "happens" depends highly on how "happens" is defined and how it is measured. The "onset" of rDA has been reported from 80 °C to 120 °C.

Scheme 1-2

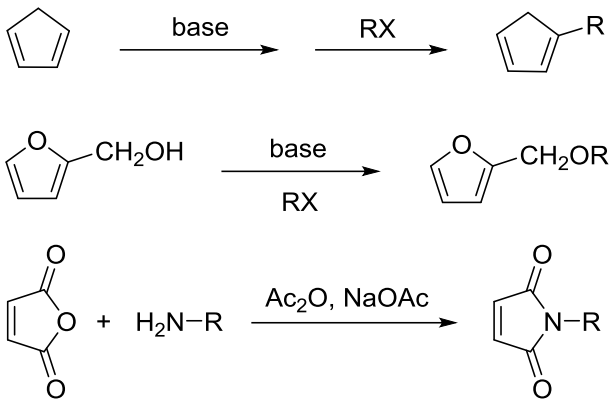

General diene and maleimide substitution

Scheme 1-3

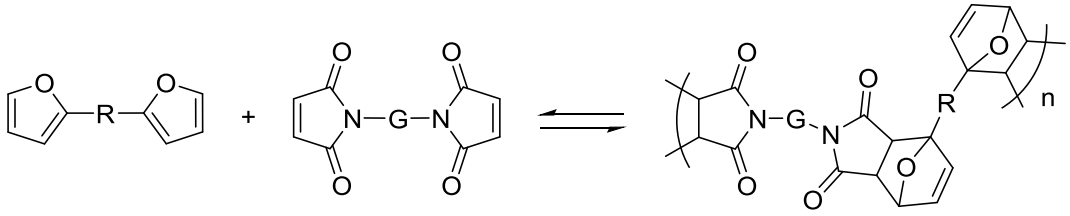

General polymerization of a bis-furan and bis-maleimide

Gandini recently (2013) reviewed the utility of the furan/maleimide system in macromolecular chemistry in great depth.[3,4] Rather than simply reiterate his most recent review, I prefer to illuminate some of the notable examples and provide my own assessment of the methods and findings. Although the furan-MI systems have captured the attention of the polymer community, the claim of facile reversibility seems to be founded on a handful of papers that suffer from incompleteness, vague conclusions, and missing experimental details that would lead to a more complete picture.

A careful theoretical and spectroscopic study of the reaction of some 2- and 3-substituted furans with maleimides has highlighted the general trends as the furan substituent changes from electron donating to electron withdrawing.[5] In this example, Northrop and co-workers perform calculations on seven furan compounds: furan, 2-methylfuran, 3-methylfuran, 2-methoxyfuran, 3-

methoxyfuran, 2-furfural, and 3-furfural; with four maleimide derivatives: maleimide, *N*-methylmaleimide, *N*-alylmaleimide, and *N*-phenylmaleimide. As the "normal electron demand" regime states that the DA reaction is favored with electron rich dienes and electron poor dienophiles, adducts should be stabilized by electron donating groups on the diene and destabilized by electron withdrawing groups (EWGs). The authors confirmed this general trend although the placement of the substituent (whether at the 2- or 3-position of the furan) exerted a significant secondary effect.[5,6] Substituents and their positions of attachment on the diene are often not explored in much depth in many published accounts of DA polymerization, yet it is important in our own chemistry and therefore the subject of exploration in this dissertation.

The DA reaction can result in two stereochemically distinct products, *endo* and *exo*, each of which might also form pairs of enantiomers if the dienophile is asymmetrically substituted (Scheme 1-4). *Endo* isomers are preferred kinetic products according to the Alder Rule, whereas *exo* isomers are typically the more thermodynamically stable. Studies on solvent and other reaction conditions (e.g., pressure, microwave irradiation, etc.)[7] have been conducted, in addition to catalytic methods for achieving enantioselection,[1] but these details are beyond the scope of this dissertation.

Scheme 1-4

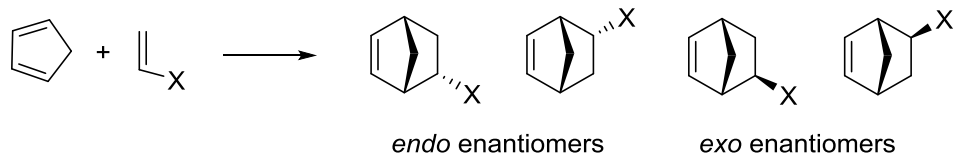

Selectivity in the Diels-Alder reaction

The literature offers essentially two main methods of studying dynamic reversibility in the DA reaction, especially as applied to macromolecular systems. In the first, direct approach, free and bound diene and dienophile moieties are determined spectrometrically. Just as common, however,

is a second, indirect approach that infers rDA events from changes in physical properties such as molecular weight or gelation. In a simple example of the direct approach (Scheme 1-5), a bis-furan derived from adipic acid combines with a bis-maleimide derived from methylenedianiline, adhering to the general monomer design approach shown in Scheme 1-2. The article also highlights some of the inconsistencies and omissions common in the literature of reversible DA polymerization. Polymerization at 60 °C (20 h) purportedly affords a polymer having a DP_n of 30-40. Subsequent thermal cycling was monitored by UV-vis spectrophotometry as the free maleimide (MI) has a characteristic absorption band at λ_{max} = 315 nm. The authors claimed to have observed repeated cycles of depolymerization (90 °C, 2 h, 60% free MI) and repolymerization (60 °C, 20 h, 30% free MI). These variations are reasonable over that temperature range. However, 30% free MI corresponds to a DP of 2-3, so the initial preparation of the polymer at DP = 30 is called into question. The thermal cycling experiments may possibly have been done at much lower concentrations, but the hundredfold decrease in concentration needed to reach a DP of 3 is probably still not a sufficient dilution (10 mM) for direct UV-vis spectrophotometric analysis using standard 1-cm cuvettes. The authors do not report either the concentrations at which these experiments are performed or the details of their analytical work.[8]

Scheme 1-5

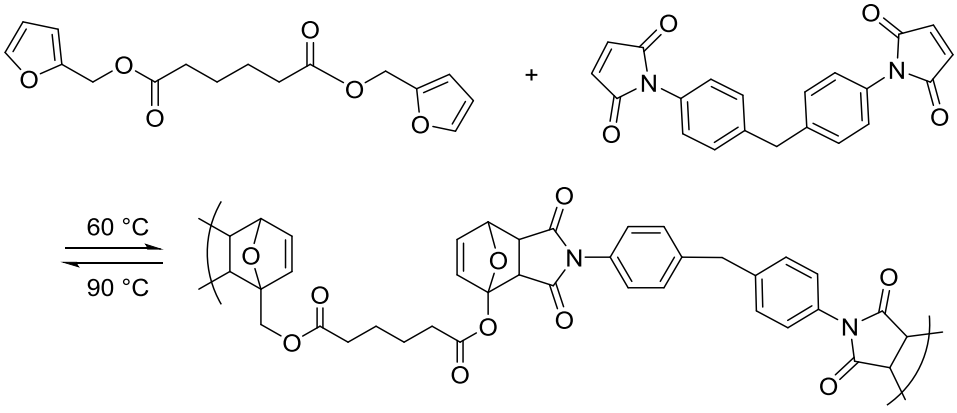

Polymerization of a bis-furan and bis-maleimide: direct approach

An example of more indirect inference of rDA events is shown in Scheme 1-6. Acetalization of furfural with pentaerythritol formed bis-furans that were polymerized with bis-maleimides at relatively low DP (5 – 10), which the authors attributed to premature precipitation. TGA analysis of these polymers showed degradation around 250 °C, which is partially attributed to rDA, among other decomposition pathways, but there were no efforts to study depolymerization in solution (the authors claimed the polymers were not sufficiently soluble). Spectroscopic studies were limited to infrared analysis.[9]

Scheme 1-6

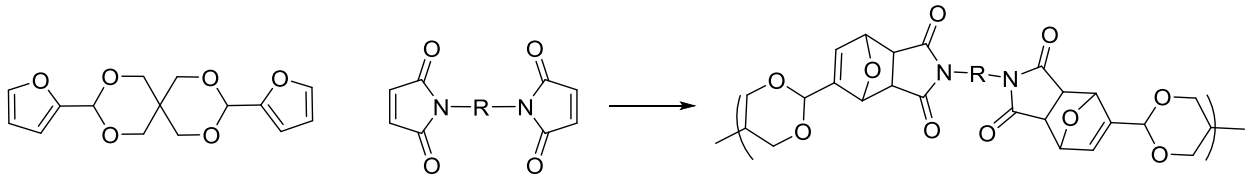

Polymerization of a bis-furan and bis-maleimide: indirect approach

Because furan-MI polymers are intrinsically unstable, researchers have developed techniques for increasing their overall DPs. Polymerizations at higher concentration give higher DP, as the DP increases as the square root of the starting monomer concentration.[10,11] Another trick is to build most of the molecular weight into a furan- or MI-terminated telechelic polymer. As shown in Scheme 1-7, polymerization of a telechelic poly(ethylene adipate) (PEA) with bis-and tris-maleimides occurred at 60 °C. The DP of the linear system only increased twofold (SEC), although the formation of a three-dimensional network structure was claimed for $f = 3$ maleimides. The observation of scant improvement in DP is attributed to the low concentration of furan end groups, which seems like a potentially addressable issue. The crowning achievement of the study was the thermal cycling of the polymer, depolymerizing at 145 °C for 20 min and repolymerizing

at 60 °C for 15 h, and over four cycles the MW alternated neatly between 18 kDa (DP ~ 2) and 8.8 kDa, the molecular weight of the telechelic PEA.[12]

Scheme 1-7

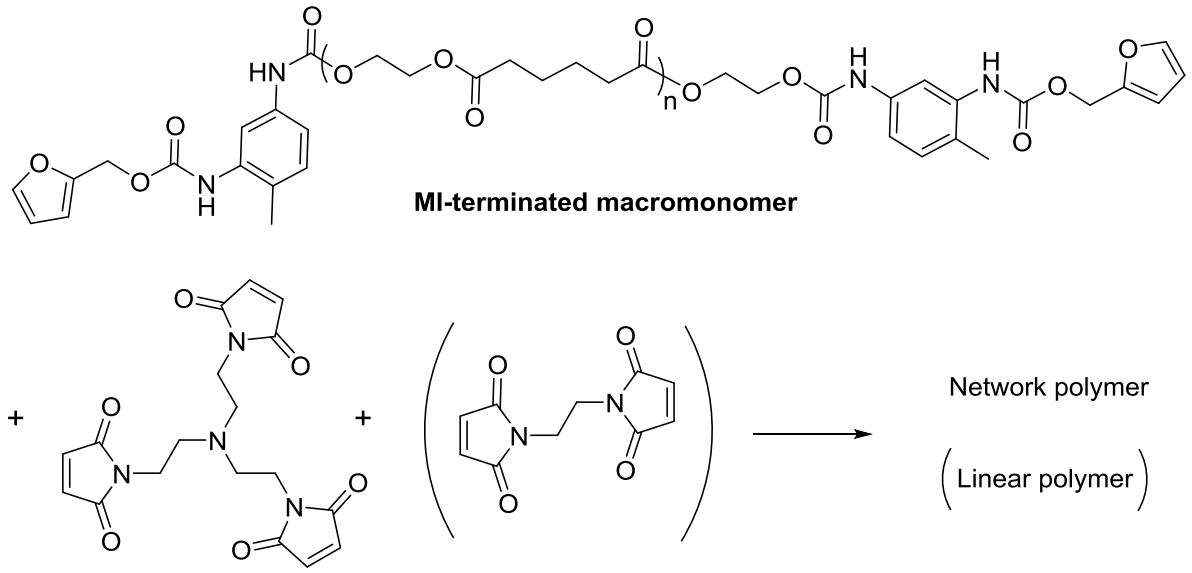

Telechelic bis-furan and tris-maleimide forming a network polymer

In perhaps one of the more in-depth studies, a furan-terminated trehalose compound was polymerized with bis-maleimides to produce linear polymers (Scheme 1-8) with M_n ~ 15 kDa, (DP ~ 20). A broad endotherm in the DSC (100 – 200 °C) was assigned to rDA in the bulk. A second endothermic transition in the thermogram was written off as solvent loss rather than a glass transition, although a second heating cycle could have confirmed this assignment. Solution studies of monomer and polymer samples showed a decrease in molecular weight with SEC (Figure 1-1) as temperature was raised went from 100 to 140 °C.[13]

Scheme 1-8

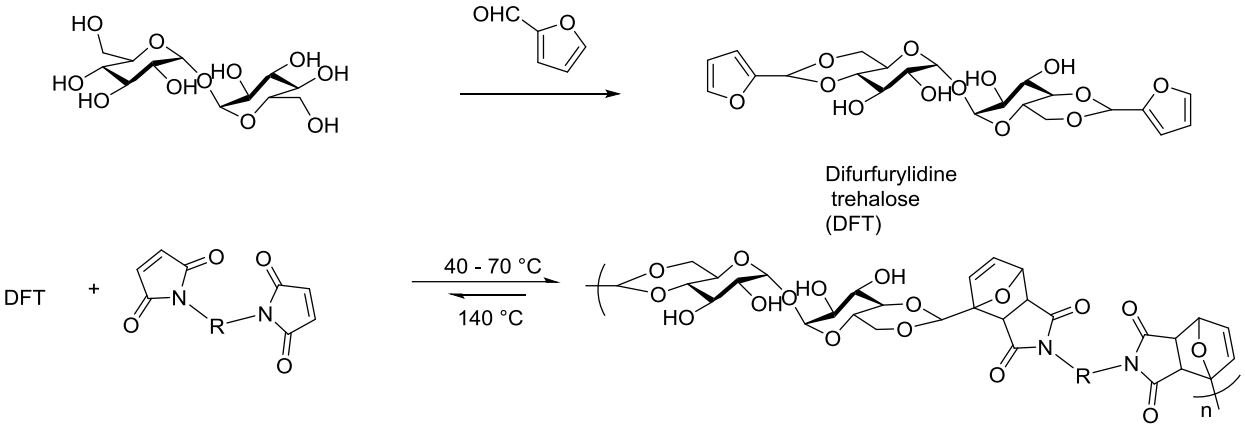

Synthesis of DFT and polymerization with a bis-maleimide

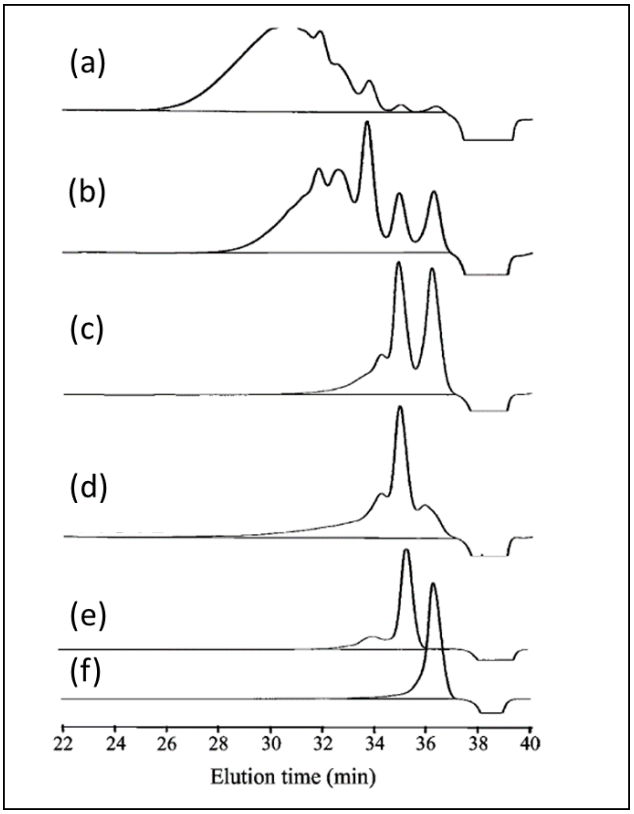

Figure 1-1. Size exclusion chromatograms of polymer derived from furan-terminated trehalose and bis(maleimide) as shown in Scheme 1-7. (a) untreated polymer with M_n ~ 15 kDa and PDI ~ 1.5; (b) polymer heated to 100 °C showing partial reversion to monomers, (c) polymer heated to 140 °C showing complete reversion to monomer, (d) polymer 140 °C for 3 h, (e) starting trehalose, and (f) starting bis-maleimide. The figure was reproduced from Teramoto et al.[13] and relabeled for clarity.

The lack of a truly detailed and thorough study of furan-maleimide coupling and uncoupling[4] in linear polymers points to an intrinsic feature (i.e., limitation) of their chemistry: Adducts are too unstable to form useable polymers without some form of stabilization (aromatization, cross-linking). A general method for dehydrative aromatization of the oxanorborene moiety using acetic anhydride (Scheme 1-9) was reported to be effective at temperatures as low as 80 °C. While these temperatures are already in the regime where rDA becomes competitive, the coupling equilibrium is driven toward the adduct by the subsequent irreversible aromatization.[14] Polymers formed by this method, however, are typically described as intractable brown solids and must be characterized by methods such as infrared spectroscopy.

Scheme 1-9

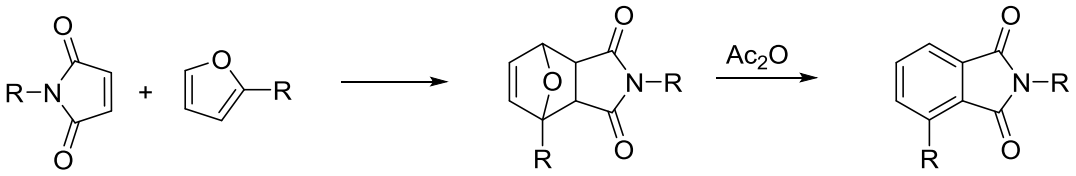

Simple reaction of a maleimide and a furan and subsequent aromaticization

More prevalent in the literature are examples of cross-linked structures obtained by attaching furan or maleimide moieties to a polymer chain (pendant) or as $f = 3$ monomers. In either case, the complementary monomer is used to create reversibly branched polymers, networks, and gels that soften or solubilize under rDA conditions. The lability of the furan-MI coupling is advantageous in these systems. In perhaps one of most convincing examples of DA crosslinking, Chujo and co-workers described the formation of reversible hydrogels with furan and MI functionalized (ca. 4%) poly(*N*-acetylethylenimine) (PAEI) (Scheme 1-10). Each functionalized polymer did not exhibit gelation on its own, yet when simultaneously cast into a homogenous film and left to stand for days, the resulting material could be swollen by water, in which it is insoluble.

The gel would begin to reverse at relatively low temperatures (ca. 80 °C), evidenced by subsequent solubility in solutions of methanol and water.[15]

Scheme 1-10

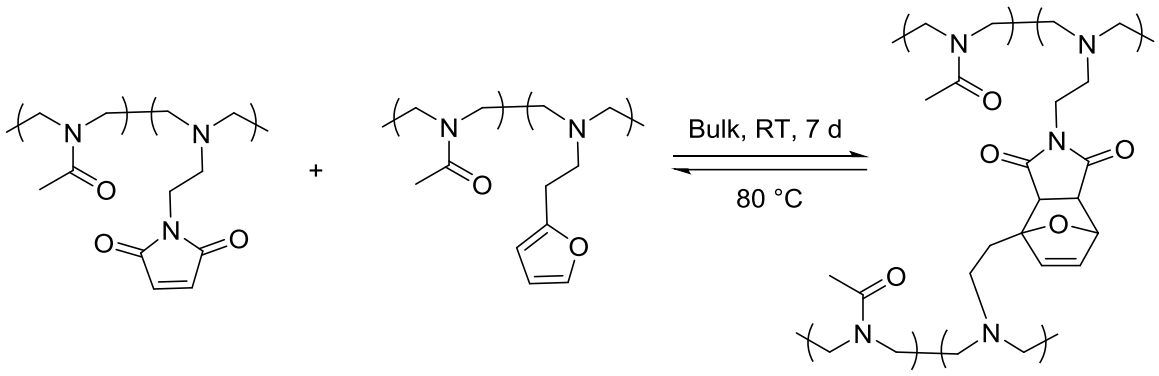

Cross-linking of furan and maleimide-functionalized PAEI

Stevens and Jenkins showed that maleimide functionalized polystyrene could be cross-linked by difurfuryl adipate quickly at 80 °C, but did not report any reversibility studies.[16] Later, Canary and Stevens showed this same system (Scheme 1-11) would cross-link in about a day at room temperature and in less than two hours at 64 °C. Their investigation of rDA showed the gel underwent rapid solubilization at 150 °C, but they did not report the state of the material between 80 and 150 °C.[17] This is a good example of furan-maleimide coupling to form a reversible material, but the lack of data on the state of the material between the two temperatures makes the reversibility study incomplete.

Scheme 1-11

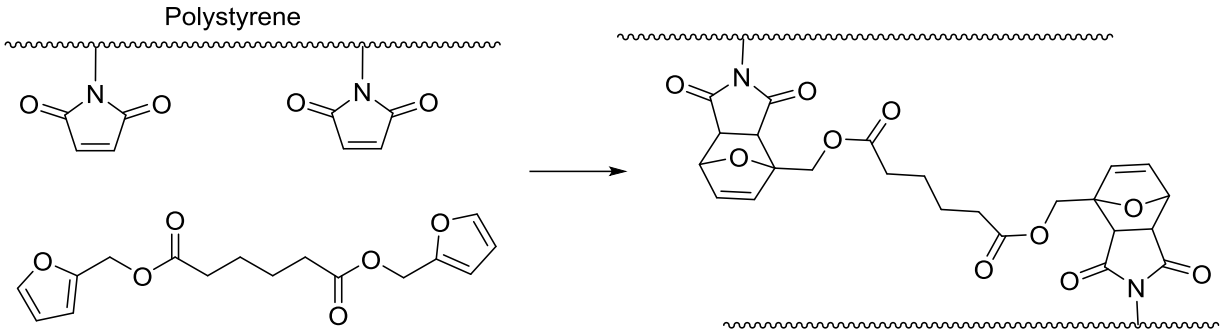

Cross-linking of maleimide-functionalized PS with a bis-furan

Multifunctional furan and maleimide moieties can assemble into networks. In a celebrated example (Scheme 1-12, T_p = 75 °C), ca. 12 % of the linkages are broken at 130 °C (30 min) and twice as many at 150 °C (30 min). The authors also reported tensile, flexural, and compression strengths to be similar to that of epoxy resins and unsaturated polyesters.[18] These examples show that in cross-linked or network materials, robust materials with impressive thermal responsiveness are possible even though decoupling is only partial.

Scheme 1-12

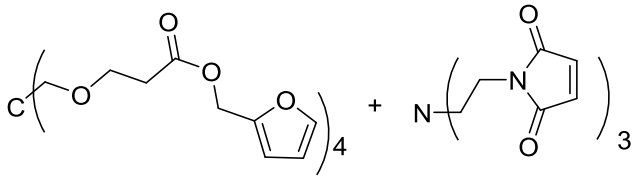

c

In addition to traditional linear polymers and cross-linked materials, the DA reaction has found utility in self-healing composites,[19] dendritic structures,[20-22] thermally labile foams and surfactants,[23,24] and aggregation[25] through covalent bonding. While these materials are interesting, they are beyond the scope of this introduction and even further beyond the scope of this dissertation, they are mentioned here to provide examples of other useful materials that can be prepared using DA chemistry.

In summary, while there are many examples of furan-MI materials, some of the fundamentals of their DA/rDA behavior are still unclear. Also, furans are generally derivatives of furfuryl alcohol and are singly substituted on the furan ring. Coupling to *N*-substituted maleimides occurs at room temperature slowly and reaches maximum conversion as T approaches ca. 80 °C, whereas un-coupling commences at ca. 80 °C and becomes predominant at ca. 150 °C, depending on reaction concentration. A key aspect of furan/MI chemistry that has received sparse treatment is the question of the relative stabilities of the *endo* and *exo* isomers,[5,8,12] even though this intrinsic feature of the chemistry likely explains, at least in part, the broad range of temperatures reported for thermal responsiveness via rDA events.

Cyclopentadiene (CPD) differs from furan in several respects, the most obvious of which is its ability to serve as both diene and dienophile. This feature, which will be described in much more detail below, enables a bis-CPD to be used in so-called "one component" polymers, behaving like an AB monomer. The utility of this method is diminished by the difficulty in controlling that coupling and thus arresting the polymerization of a polymer when it is not desired. Furthermore, the retro-DA reaction requires high temperatures where other, undesired reactions can occur. CPD derivatives are synthetically accessible and substituted CPDs are often still reactive, unlike many substituted furans. Substitution, however, allows for tautomerization (Scheme 1-13), resulting in a complex mixture of product regio- and stereochemistries. Furans neither dimerize nor tautomerize, simplifying adduct mixtures, but present a different set of challenges such as decreased reactivity as substituents become complex and a general decrease in adduct stability.

Scheme 1-13

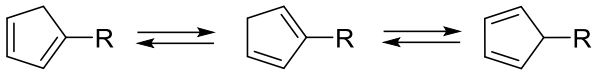

Tautomerization of a substituted cyclopentadiene

The pioneering work by Stille and Plummer (Scheme 1-14) described the DA reaction of CPD terminated alkanes to afford linear polymers.[26] Although their work included both single and two-component (bis-CPD/bis-maleimide) polymers, they did not investigate the reversibility of these polymers nor did they present any molecular weight or thermal data. They reported conversions up to 97% in refluxing benzene. However, the monomers were hard to purify because they were not able to prevent self-coupling during purification.

Scheme 1-14

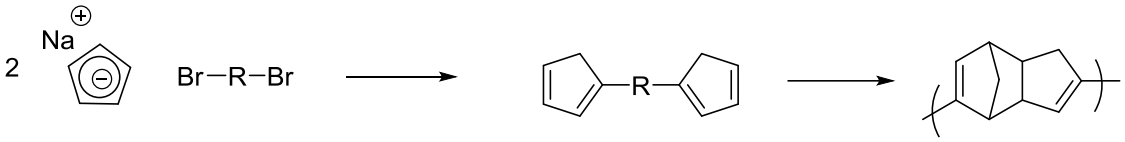

Synthesis of a bis-cyclopentadiene and subsequent dimerization to form a polymer

CPD-terminated telechelic polyisobutylenes (PIBs) oligomerize rapidly at 80 °C (Scheme 1-15).[27-29] Once again, detailed reversibility studies were not conducted, likely due to the high temperature required for rDA to become the predominant decomposition pathway; it was only speculated that "cracking" of CPD dimers would occur at elevated temperatures.

Scheme 1-15

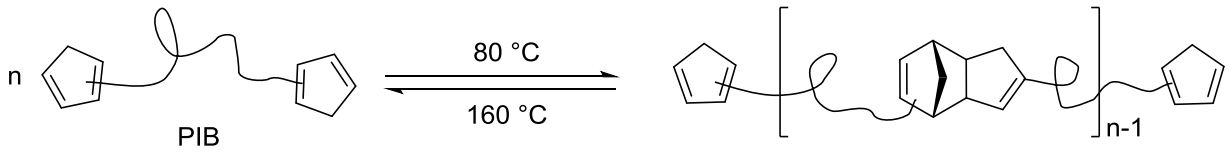

Polymerization of a telechelic bis-cyclopentadiene

The same authors also showed that TMS-substituted CPDs would not undergo self-dimerization, but would react with bis-maleimides to oligomerize in two-component fashion (Scheme 1-16).[30] As PIB size increased, so did overall molecular weight, but at the cost of the degree of DA polymerization (DP). An 11-kDa macromonomer polymerized to $DP_n = 11.4$, while a 25-kDa macromonomer polymerized only to $DP_n = 4.5$, indicating a dilution of reactive ends. The reversibility of these polymers was also not studied.

Scheme 1-16

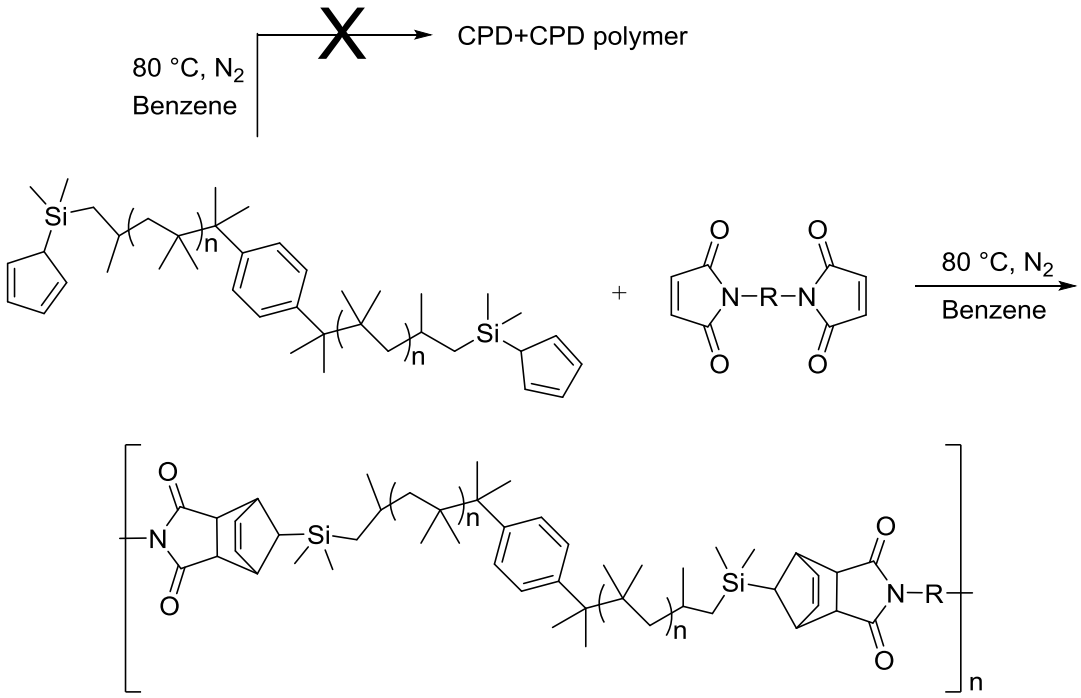

Arresting the dimerization of CPD by the addition of a TMS substituent

A further method for studying depolymerization of a DA polymer is to heat the polymer in the presence of a monofunctional trapping agent that is generally present in excess, driving the rDA process in accord with the le Chatelier principle. An example of this trapping approach is shown in Scheme 1-17. Cyclopentadienylated ethylene-propylene rubber was cross-linked and gelled at room temperature in 72 h, at which point is was heated to 215 °C in the presence of maleic

anhydride in hexachlorobutadiene. The gel solubilized at this temperature. The authors do not indicate why a temperature of 215 °C was needed, when CPD dimers generally are understood to decouple around 180 °C.

Scheme 1-17

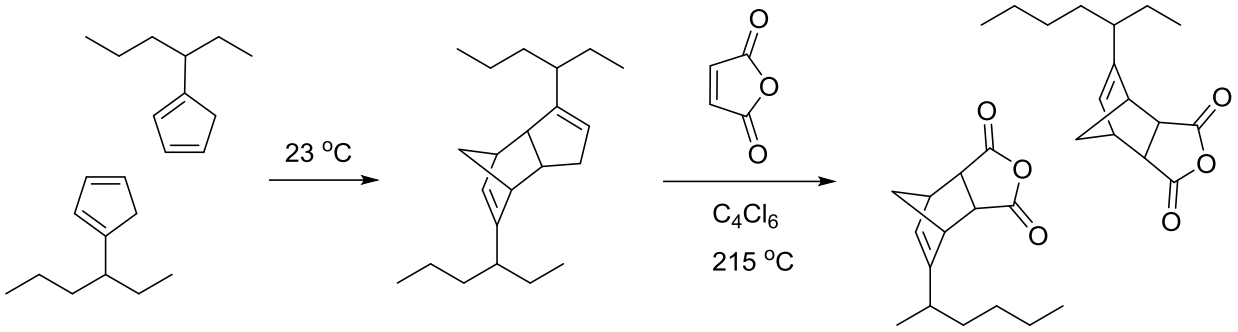

Cross-linking of a CPD-functionalized polymer and subsequent trapping with maleic anhydride

One of the most important goals of reversible polymers is finding systems that can be re-polymerized after undergoing de-polymerization. Ideally, desirable and measureable properties will be maintained through multiple cycles of de-polymerization/re-polymerization.[12] Murphy and Wudl developed a "single-component" DA monomer, based on cyclopentadiene.[31] Murphy's monomer, a ring closed bis-cyclopentadiene (Scheme 1-18), could be purified while controlling self-dimerization. The monomer is also exclusively *endo*-coupled which means that it will undergo rDA under conditions that are somewhat milder than ordinary CPD dimers.

Scheme 1-18

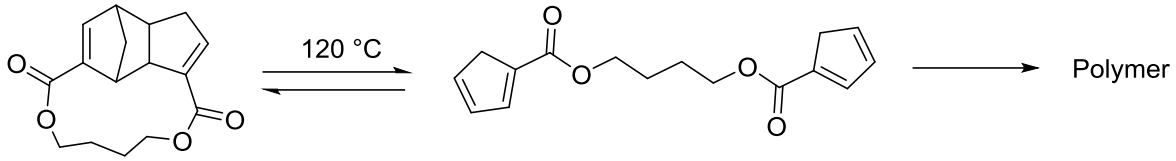

Murphy and Wudl's single-component bis-CPD based monomer

Murphy and Wudl showed that polymers prepared from this monomer, once thermally opened and chain extended, could undergo multiple depolymerization and healing steps. Figure 1-2 shows what might be happening in a bulk polymer sample when cracked and then healed. The proposed mechanism for this healing is that new DA linkages can be formed across the crack interface once held together and heated. This requires sufficient mobility of reactive ends and high enough reactive end concentration. Cross-linking is also evident in the system as remaining unsaturation exists in the CPD adduct. "Trimers" could form as the double bond in the adduct moiety acts as a dienophile for further reaction with cyclopentadienes. Murphy showed that single component CPD polymers could be restored to roughly 50% of their initial mechanical properties, such as three point bending stress, after several cycles of fracture testing and re-mending.[32]

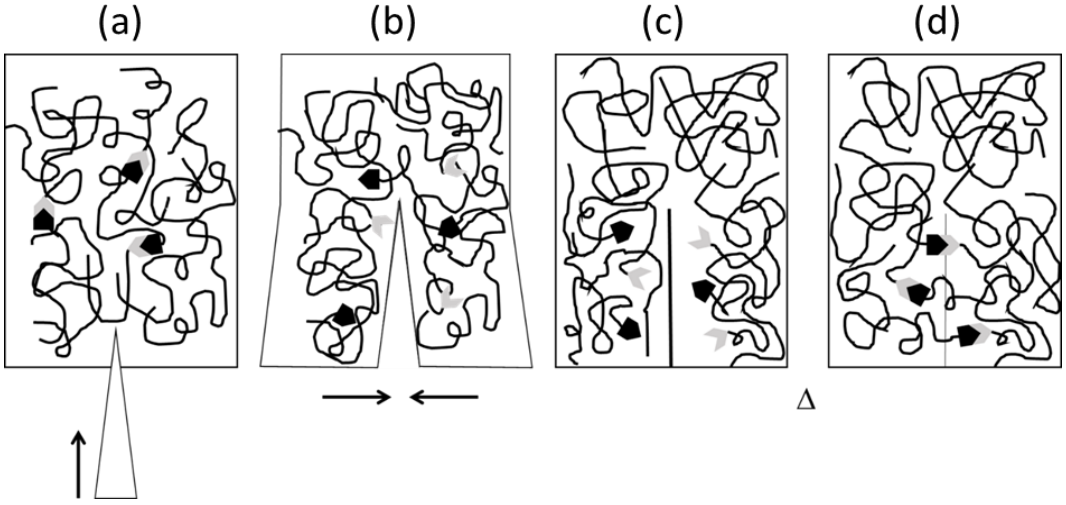

Figure 1-2. Healable polymer after cracking and thermal mending. (a) as prepared material being cracked with a wedge, (b) cracked material, with broken linkages, being pressed together, (c) thermal treatment of material to afford while clamped; end groups migrate toward reactive site; (d) "repaired" material with reformation of broken linkages.

In summary, much of the published work in the area of reversible DA polymers suffers from significant deficiencies that prevent us from understanding the fundamental underlying chemistry such as rates and enthalpies of the DA and rDA processes, particularly as a function of temperature, and taking into account primary issues such as endo/exo isomerism and substituent effects. Many of the "pioneering" papers highlighted in reviews and textbooks do not describe basic experimental methods such as reaction conditions and analytical techniques, and studies of the uncoupling (rDA) process too often rely on indirect evidence such as DSC thermograms, solution viscosity, and polymer solubility. Even the detailed model study of furan/mleimide reactivity published by Northrop[5] in 2011 does not address all of the issues experimentally. So, even though the Diels-Alder reaction is 100 years old, we still lack a clear experimental basis for establishing structure/reactivity relationships that are sufficiently clear to predict how DA polymers will behave, even in solution. And in the bulk phase, the relationship of the DA/rDA process to other thermal transitions (notably the glass transition) has not been explored in any depth, although it has long been thought to play an important role in thermal cycling behavior.[33]

Despite these shortcomings, the literature offers numerous examples of the utility of the Diels-Alder reaction in macromolecular synthesis. Furan/MI is the predominant combination of functional groups, followed by CPD-CPD. Furan/MI is convenient from the standpoint of monomer synthesis, as the MI nitrogen and the furfuryl moiety (especially the alpha oxygen of furfuryl alcohol) are general connection points to other organic species. This combination offers an attractive thermal profile, because both polymerization (40 – 60 °C) and reversion (above about 80 °C) occur under mild conditions. On the other hand, because rDA occurs at temperatures so close to the optimum polymerization temperature, the adducts may actually be too unstable for some applications. Not surprisingly, then, applications in linear polymers are scarce, while

systems that benefit the most from facile rDA – cross-linked, hyperbranched, and network materials – are the most prominent. Finally, the furan-MI system is already structurally optimized for adduct stability in the sense that changing substitution on either the furan or the maleimide will either destabilize adducts further or put the cost of the starting materials completely out of reach.[5]

Cyclopentadiene self-coupling polymers (CPD-CPD systems) are interesting because they only require a single component, and CPD can be attached to monomers reasonably efficiently using the C_5H_5 anion as a nucleophile. However, as a single-component system with a low barrier to polymerization, the onset cannot be controlled, and in some cases the monomers cannot even be purified. Finally, the CPD-CPD adduct is so stable that temperatures exceeding 160 °C are needed to drive rDA. These challenges make CPD-CPD systems hard to use in dynamic material applications. On the other hand, there is considerable room for structural optimization. For example, it is known that multi-substituted CPDs, especially those with bulky substituents, are more stable toward dimerization.[34-39] Also, in Murphy and Wudl's system, if indeed rDA of the CPD-CPD linkage is occurring at 120 °C as they suggest, then one has to consider the electron withdrawing influence of the ester functionality, the exclusively *endo* geometry, and perhaps some strain in the cyclic monomer as possible structural influences on adduct stability.

At the same time, thorough studies of CPD-MI couplings are sparse. Stille showed that bis-CPDs would polymerize with bis-MIs, but he made no effort to exclude competitive CPD homopolymerization.[26] CPD-CPD coupling was later shown to be arrested by substitution of the CPD with a silyl (R_3Si) group, enabling the synthesis of AA+BB step growth polymers from bis-CPDs and bis-MIs.[30] However, the latter account does not address reversibility of the polymerization, likely because the process would not occur below 160 °C, where other decomposition reactions would likely take over.

Nevertheless, the marriage of CPDs with maleimides could still be promising. We know from the published preliminary studies that CPD dimerization can be arrested through relatively simple structural modifications. We also know that CPDs and MIs react slowly at room temperature but proceed quickly above 80 °C, and we know that CPD-MI adducts are comparable in stability to CPD-CPD adducts from the few studies that are available,[40] but detailed studies of these important kinetic and thermodynamic parameters as a function of cyclopentadiene substitution are not available at all.

This dissertation focuses on the development of thermally reversible two-component Diels-Alder polymers based on cyclopentadienes and maleimides. CPD design needs to both prevent competitive self-dimerization (the easier task) and also destabilize the MI adduct (probably more challenging) without completely frustrating the forward DA coupling reaction. Our strategy will focus on a combination of steric and electronic contributions from CPD substituents and their placement on the CPD ring.

Chapter 2 Substituent Effects in the Retro-Diels-Alder Reaction: Thermal Stabilities of the Adducts of *tert*-Butylcyclopentadiene and (Pentafluorophenyl)cyclopentadiene and *N*-(4-Fluorophenyl)maleimide

Foreward. This chapter represents a study that will become part of a larger manuscript on DA reactions of fluoroarylated cyclopentadienes that will include reactions of **FMI** with bis(pentafluorophenyl)cyclopentadienes. The entire study will bring together the work of several undergraduate and graduate students including but not necessarily limited to Charles S. Carfagna, Jr., Tabitha A. Clem, and Brett W. Van der Goetz.

2.1 Introduction

The main objective of this dissertation is the development of a bis-CPD / bis-MI Diels-Alder polymerization that excludes self-dimerization of the CPD, while destabilizing the CPD-MI adduct through the combined effects of one sterically encumbering substituent (*i*Pr or *t*Bu) and one electron-withdrawing substituent, introduced as an octafluorobiphenylene linker connection the two CPDs. Although both the model studies presented in Chapter 3 and the polymerization/depolymerization studies presented in Chapter 5 strongly support this objective, we wanted to investigate the extent to which either a single bulky group (*t*Bu) or a single perfluoroaryl substituent on CPD would be adequate to meet either of the key reactivity criteria. Therefore we prepared both *tert*-butylcyclopentadiene[41,42] and pentafluorophenylcyclo-pentadiene[43] and subjected each to reactions with *N*-(4-fluorophenyl)maleimide. Already we know that pentafluorophenylcyclopentadiene readily undergoes characteristic CPD+CPD self-dimerization and that the dimer is relatively stable.[36] Methylcyclopentadiene dimerizes slowly at room temperature and completely at 60 °C in 2 h,[44] while cracking of the dimer occurs only above about 160 °C.[45]

Tert-butylcyclopentadiene, on the other hand, dimerizes much more slowly at room temperature. The latter reaction is controversial. A report by Christoffers and co-workers[34] claimed that the dimer was recovered from a reaction of *tert*-butylcyclopentadiene in which the temperature was maintained at RT or below, but in our hands a solution of the dimer in C_6D_6 solution in an NMR tube did not dimerize over a 1-week period. We surmise that Christoffers may have used a commercial sample of *tert*-butylcyclopentadiene that was already contaminated with the dimer. Our laboratory has also, in the past, received partially dimerized samples of this compound from commercial sources and found it difficult to distill, and in fact the compound is no longer available from catalog retailers, probably because of its longer-term instability issues. We know from the detailed work of Kennedy and co-workers that $RSiMeC_5H_5$ (R = alkyl) does not dimerize up to 80 °C, [30] although another report suggests that $Cl_3SiC_5H_5$ dimerizes.[46]

The DA product of cyclopentadiene with maleic anhydride is reportedly stable (unobserved free cyclopentadiene) toward rDA up to 210 °C.[40] The *endo* adduct of cyclopentadiene and maleimide is slightly less stable, undergoing rDA above its melting point, 187 °C.[47] It is important to understand, however, that the melting point may represent an upper bound on the temperature required for rapid rDA because the lack of mobility in the solid frustrates reactivity. Unfortunately we are not aware of more detailed studies of CPD-MI adduct rDA reactions in solution, and this gap in the knowledge base largely motivated the present work.

The reactivity of cyclopentadienes can be influenced by highly fluorinated aromatics, such as the pentafluorophenyl group, since they are strongly electron withdrawing.[48] We hypothesize that CPD/MI adducts can be destabilized by electron-withdrawing substituents. While there is a well-known tendency of the Diels-Alder reaction to be slower with electron-poor dienes because of the increase in the energy gap between the diene HOMO and the dieneophile LUMO, we recognize

that there is a "leap of faith" when extending that *kinetic* trend to adduct stability, which is a *thermodynamic* quantity.

2.2 Experimental

2.2.1 General Methods.

Solvents were used as received from commercial suppliers unless noted otherwise. 4-Fluoro-aniline was used as received from Matrix Scientific. Sodium *tert*-butylcyclopentadienide,[41] and *N*-(4-fluorophenyl)maleimide (**FMI**),[49,50] were prepared as previously reported. Samples of *tert*-butylcyclopentadiene were obtained by hydrolysis of sodium *tert*-butylcyclopentadienide with water, extraction of the diene into pentane, drying over magnesium sulfate, filtration, and rotary evaporation of the solvent at RT. NMR spectra were acquired on either a Varian Inova 400 NMR spectrometer, an Agilent 400-MR DD2 NMR spectrometer or a Bruker Avance II 500 NMR spectrometer. Proton chemical shifts were referenced to $CHCl_3$ (7.26 ppm) in $CDCl_3$. ^{19}F chemical shifts were referenced to external C_6F_6 (−183.0 ppm) in $CDCl_3$. Mass spectra were obtained using an Agilent 6220 instrument (LC-ESI-TOF featuring 5-ppm mass accuracy) operating in positive ion mode. Melting points (uncorrected) were acquired using open capillaries on a Buchi B-545 apparatus.

2.2.2 Reaction of *t*-Butylcyclopentadiene with *N*-(4-Fluorophenyl)maleimide

A solution of *tert*-butylcyclopentadiene (0.50 g, 4.1 mmol) and *N*-(4-fluorophenyl)maleimide (0.25 g, 1.3 mmol) in ca. 4 mL of diethyl ether was allowed to stand at room temperature. The solution turned from pale yellow (the characteristic color of the starting maleimide) to colorless over 2 h. A 200-mg aliquot was removed after 2 h and the solvent was evaporated to afford ca. 30 mg of a pale residue. ^1H NMR analysis showed that all of the starting maleimide had been consumed, and the crude mixture contained mostly unreacted diene, with smaller amounts of

adducts and < 5% of *t*BuCPD dimer. After standing another ca. 15 h, the solvent was evaporated to afford 0.630 g of an oily residue, which was subjected to liquid chromatography on silica gel (5 cm x 6 cm column, 66 g), eluting with 40% ethyl acetate in hexanes. Ten 50-mL fractions were collected followed by one 150-mL fraction. Based on TLC analysis, fractions 3 and 4 were combined and evaporated to afford 219 mg of a pale yellow oil that crystallized upon standing to afford adduct **1a**, which was found to be pure by ^{1}H NMR spectroscopic analysis. [Structures of adducts **1 - 4** are defined in Scheme 2-1 on p. 42 below]. Fraction 5 was evaporated to afford 40 mg of a residue containing a mixture of adducts **1a** and **3a** according to ^{1}H NMR spectroscopic analysis. Fractions 6 and 7 were combined and evaporated to afford 75 mg of adduct **3a**, which was found by ^{1}H NMR spectroscopic analysis to be about 90% pure. Fractions 8 through 11 were combined and evaporated to afford 50 mg of residue that contained traces of **1a** and **3a** along with a third, unidentified compound. Fractions 1 and 2 were discarded. The overall combined yield of adducts **1a** and **3a** was 334 mg (81%). Analytically pure samples of **1a** and **3a** were obtained by recrystallization from hexanes. A similar reaction in toluene at 100 °C showed an increase in *t*-BuCPD dimer along with compounds **1a**, **2a**, and **3a**.

Data for 1a: mp 91.5–92.3 °C. ^{1}H NMR (400 MHz, $CDCl_3$) δ 7.1 (s, 2H), 7.1 (d, 2H, $^{3}J_{HF}$ = 2 Hz), 6.3 (d, 1H, *J* = 6 Hz), 6.2 (dd, 1H, *J* = 6 Hz, 3 Hz), 3.5 (dd, 1H, *J* = 8 Hz, 4 Hz), 3.4 (m 2H), 1.72 (dd, 2H, *J* = 9 Hz, 1.9 Hz), 1.6 (d, 2H, *J* = 9 Hz), 1.1 (s, 9H). ^{13}C NMR (100 MHz, $CDCl_3$) δ 176.6 (s), 176.4 (s), 163.2 (d, $^{1}J_{CF}$ = 257 Hz), 136.4 (s), 133.6 (s), 128.6 (d, $^{3}J_{CF}$ = 8.8 Hz), 128.0 (d, $^{4}J_{CF}$ = 3 Hz), 116.1 (d, $^{2}J_{CF}$ = 23 Hz), 68.4 (s), 52.6 (s), 49.0 (s), 45.8 (s), 44.4 (s), 31.8 (s), 28.3 (s). $C_{19}H_{20}FNO_2$ HRMS (ESI-TOF): *m/z* calcd. for $C_{19}H_{21}FNO_2$ $(M+H)^+$ 314.1556, found $(M+H)^+$ 314.1557. Anal. Calcd for $C_{19}H_{20}FNO_2$: C, 72.82; H, 6.73; N, 4.47. Found: C, 72.86; H, 6.45; N, 4.56. **Data for 3a**: mp 144–145 °C, ^{1}H NMR (400 MHz, $CDCl_3$) δ 7.2 – 7.1 (m, 4H), 5.9 (dd,

1H, *J* = 1.5 Hz, 3 Hz), 3.5 – 3.4 (m, 4H), 1.8 (dt, 1H, *J* = 2 Hz, 8 Hz), 1.7 (dt, 1H, *J* = 1 Hz, 8 Hz), 1.0 (s, 9H). ^{13}C NMR (100 MHz, $CDCl_3$) δ 177.1 (s), 176.7 (s), 162.2 (d, $^1J_{CF}$ = 248 Hz), 160.7 (s), 128.5 (d, $^3J_{CF}$ = 9 Hz), 127.9 (d, $^4J_{CF}$ = 3 Hz), 124.1 (s), 116.2 (d, $^2J_{CF}$ = 23 Hz), 55.3 (s), 47.3 (s), 47.1 (s), 46.6 (s), 44.8 (s), 32.9 (s), 29.6 (s). $C_{19}H_{20}FNO_2$ HRMS (ESI-TOF): *m/z* calcd. for $C_{19}H_{21}FNO_2$ $(M+H)^+$ 314.1556, found $(M+H)^+$ 314.1551. Anal. Calcd for $C_{19}H_{20}FNO_2$: C, 72.82; H, 6.73; N, 4.47. Found: C, 72.85; H, 6.37; N, 4.57.

Preparation of Thermodynamic Adduct 4a. A sample of **1a** was heated in bulk at 160 °C for 72 h. NMR analysis revealed a mixture of **1a** (3%), **3a** (ca. 53%), and **4a** (ca. 44%). Preparative thin layer chromatography on silica gel eluting with 40% ethyl acetate in hexanes yielded an analytically pure sample of **4a**, mp 136 – 138 °C. ^{1}H NMR ($CDCl_3$) δ 7.3 – 7.1 (m, 4H), 5.8 (d, 1H, *J* = 3 Hz), 3.4 (m, 1H), 3.3 (m, 1H), 2.9 (m, 2H), 1.6 (d, 1H, *J* = 10 Hz), 1.4 (d, 1H, *J* = 10 Hz), 1.1 (s, 9H). ^{13}C NMR (100 MHz, $CDCl_3$) δ 177.4 (s), 177.3 (s), 162.3 (d, $^1J_{CF}$ = 248 Hz), 162.1 (s), 128.3 (d, $^3J_{CF}$ = 9 Hz), 127.9 (d, $^4J_{CF}$ = 3 Hz), 126.7 (s), 116.3 (d, $^2J_{CF}$ = 23 Hz), 49.2 (s), 48.5 (s), 46.5 (s), 46.2 (s), 43.5 (s), 33.6 (s), 28.6 (s). $C_{19}H_{20}FNO_2$ HRMS (ESI-TOF): *m/z* calcd. for $C_{19}H_{21}FNO_2$ $(M+H)^+$ 314.1556, found $(M+H)^+$ 314.1557.

2.2.3 Reaction of Pentafluorophenylcyclopentadiene with N-(4-Fluorophenyl)maleimide

A solution of pentafluorophenylcyclopentadiene (3.72 g, 16.0 mmol) in THF (20 mL) was slowly dripped through a reflux condenser into a solution of *N*-(4-fluorophenyl)maleimide (2.85 g, 14.9 mmol) in THF (40 mL) under reflux over 1 h. The resulting mixture was stirred for an additional 1.5 h at reflux and then cooled to room temperature. The solvent was removed using a rotary evaporator (bath temperature 55 °C) to give a pasty yellow residue. The crude material contained primarily **3b**, **1b**, **FMI**, *t*BuCPD and dimer, and small quantities of **2b** and **4b**. [Structures of adducts **1 - 4** are defined in Scheme 2-1 on p. 42 below]. The yellow residue was

triturated with hexanes (2 x 10 mL). A colorless liquid was decanted and then evaporated to afford a colorless, viscous oil and some crystals. This mixture largely contained all adducts, unreacted FMI, *t*BuCPD and dimer. The yellow residue remaining after trituration (4.74 g) was triturated again with a larger volume of hexanes (100 mL) and a tan solid (0.941 g) was filtered and dried and found to be nearly pure **3b** by NMR analysis. The supernatant hexane was evaporated to yield a yellow paste (3.8 g). This solid was subjected to silica gel chromatography (250 g silica gel, 6 cm x 19 cm), eluting with 30% ethyl acetate in hexanes. Ten fractions were collected (100 mL each) followed by one fraction of 1 L and finally 1 L of pure ethyl acetate. The fractions were spotted and developed on a TLC plate using 30% ethyl acetate in hexanes and like fractions were combined and evaporated. Fractions 1 – 3 contained primarily pentafluorophenylcyclopentadiene dimer, fractions 4 – 6 contained traces of dimer and adduct isomers **2b** and **4b**, fraction 7 contained a mixture of adduct isomers **1b**, **2b**, and **4b**, fractions 8 – 11 contained **1b** and un-reacted *N*-(4-fluorophenyl)maleimide, and the final column flush contained **3b**. The yields were **1b**: 1.34 g; **2b**: 0.126 g (calculated from an NMR mixture with **1b**); **3b**: 1.72 g; and **4b**: 0.090 g (calculated from an NMR mixture with **2b**). Analytically pure samples of **1b** and **3b** were prepared by crystallization from hexanes/ethyl acetate. Compounds **2b** and **4b** were not isolated.

Data for **1b**: mp = 106 – 107 °C, ^{1}H NMR (400 MHz, $CDCl_3$) δ 7.2 – 7.1 (m, 4H), 6.7 (dt, 1H), 6.4 (dd, 1H, $^{3}J_{HH}$ = 6 Hz, $^{4}J_{HH}$ = 3 Hz), 3.9 (d, 1H, *J* = 8 Hz), 3.7 (dd, 1H, ^{3}J = 8 Hz, ^{4}J = 5 Hz), 3.6 (m, 1H), 2.4 (d, 1H, $^{3}J_{HH}$ = 9 Hz), 2.1 (dd, 1H, $^{3}J_{HH}$ = 9 Hz, $^{4}J_{HH}$ = 1 Hz). ^{19}F NMR (376 MHz, $CDCl_3$) δ –112.1 (dt, 1F, $^{4}J_{FH}$ = 8, $^{3}J_{FH}$ = 5 Hz), –139.2 (d 2F, $^{3}J_{FF}$ = 17 Hz), –154.8 (tt, 1F, $^{4}J_{FF}$ = 21, $^{3}J_{FF}$ = 2 Hz), –161.5 (m, 2F). ^{13}C NMR (100 MHz, $CDCl_3$) δ 175.7, 174.9, 162.5 (d, $^{1}J_{CF}$ = 249 Hz), 145.3 (d, $^{1}J_{CF}$ = 250 Hz), 140.6 (d, $^{1}J_{CF}$ = 250 Hz), 138.2 (d, $^{1}J_{CF}$ = 250 Hz), 135.5 (t, *J* = 7 Hz), 134.3, 128.4 (d, *J* = 9 Hz), 127.6 (d, *J* = 3 Hz), 116.3 (d, *J* = 23 Hz), 57.4 (t, *J* = 4 Hz),

56.3, 49.6 (t, J = 3 Hz), 47.0, 44.7. HRMS (APCI) *m/z* calcd for $C_{21}H_{12}F_6NO_2$ $(M+H)^+$ 424.0772, found 424.0770.

Data for **2b**, assigned as part of a mixture with **1b**: ^{1}H NMR (400 MHz, $CDCl_3$) δ 7.1 – 7.2 (m, 4H), 6.5 (dd, 1H, $^3J_{HH}$ = 6 Hz, $^4J_{HH}$ = 2 Hz), 6.5 (m, 1H), 3.5 (m, 1H), 3.4 (d, 1H, $^3J_{HH}$ = 7 Hz), 3.1 (d, 1H, $^3J_{HH}$ = 7 Hz), 2.2 (d, 1H, $^3J_{HH}$ = 10 Hz), 2.1 (m, 1H). ^{19}F NMR (376 MHz, $CDCl_3$) δ –112.2 (m, 1F), –138.5 (overlapping with signals from **1b**) (broad s, 1F), –143.4 (broad s, 1F), –155.3 (t, 1F, $^3J_{HF}$ = 21 Hz), –161.7 (overlapping with signals from **1b**) (broad s, 1F), –162.6 (overlapping with signals from **1b**) (broad s, 1F).

Data for **3b**: m.p. 156 – 158 °C, ^{1}H NMR (400 MHz, $CDCl_3$) δ 7.1 (s, 2H), 7.1 (s, 2H), 6.7 (d, 1H, $^3J_{HH}$ = 2 Hz), 4.1 (m, 1H), 3.7 (m, 1H), 3.6 (dd, 2H, $^3J_{HH}$ = 3 Hz, $^4J_{HH}$ = 2 Hz), 2.1 (dt, 1H, $^3J_{HH}$ = 9 Hz, $^4J_{HH}$ = 2 Hz), 1.8 (d, 1H, 8.9 Hz). ^{19}F NMR (376 MHz, $CDCl_3$) δ –112.4 (dt, 1F, $^3J_{HF}$ = 7, $^4J_{HF}$ = 7 Hz), –139.4 (dd, 2F, $^3J_{FF}$ = 22, $^4J_{FF}$ = 7 Hz), –154.1 (tt, 1F, $^3J_{FF}$ = 21, $^4J_{FF}$ = 2 Hz), –161.8 (m, 2F). ^{13}C NMR (100 MHz, $CDCl_3$) δ 175.9, 175.5, 162.2 (d, J = 248 Hz), 144.6 (d, J = 250 Hz), 140.6 (d, J = 250 Hz), 137.9 (d, J = 250 Hz), 137.6 (dt, J = 6 Hz, J = 1 Hz), 134.5 (d, J = 2 Hz), 127.9 (d, J = 9 Hz), 127.5 (d, J = 3 Hz), 116.0 (d, J = 22 Hz), 52.6, 48.1 (t, J = 5 Hz), 46.7, 46.4, 46.3. HRMS (ESI) *m/z* calcd for $C_{21}H_{12}F_6NO_2$ $(M+H)^+$ 424.0772, found 424.0778.

Data for **4b**: ^{1}H NMR (400 MHz, $CDCl_3$) δ 7.1 – 7.2 (m, 4H), 6.8 (d, 1H, J = 2.6 Hz), 3.8 (s, 1H), 3.6 (s, 1H), 3.1 (d, 1H, $^3J_{HH}$ = 7 Hz), 3.0 (d, 1H, $^3J_{HH}$ = 7 Hz), 1.9 (d, 1H, $^3J_{HH}$ = 10 Hz), 1.6 (d, 1H, $^3J_{HH}$ = 10 Hz). ^{19}F NMR (376 MHz, $CDCl_3$) δ –112.3 (m, 1F), –140.4 (dd, 2F, J = 7.5, ^3J = 22 Hz), –155.1 (t, 1F, J = 22 Hz), –162.2 (m, 2F).

2.2.4 Thermolyses of Butylated Diels-Alder Adducts

Thermolyses of **1a** and **3a** were carried out in the melt by heating small samples (ca. 10 mg) of each adduct in an open NMR tube maintained in a thermostat-controlled oil bath for a fixed

interval (typically several hours), quenching the sample to RT, and then dissolving the residue in $CDCl_3$ and analyzing the mixture using NMR spectrometry. Observed product distributions are collected in Table 2-1.

Table 2-1. Products of thermolysis of adducts **1a** and **3a** (see Scheme 2−1, below) of *tert*-butylcyclopentadiene and *N*-(4-fluorophenyl)maleimide in the melt.

			Product distribution				
Substrate	**T (°C)**	**t (h)**	**1a**	**2a**	**3a**	**4a**	**FMI**[a]
1a	100	4	100%	--	--	--	--
1a	120	4	98%	--	2%	Trace	Trace
1a	140	4	84%	--	12%	4%	--
1a	160	4	44%	--	39%	16%	1%
3a	160	4	2%	--	97%	1%	Trace

2.2.5 Thermolyses of Perfluorophenyl-Substituted Diels-Alder Adducts

Thermolyses of **3b** and of **1b** were carried out by heating ca. 5 mg of each sample, separately, dissolved in 1,2-dichlorobenzene (0.5 mL) in an NMR tube in a thermostat controlled oil bath. Samples were heated for several hours (t = 4 – 12 h) at 120 – 160 °C. After heating, the samples were removed and quenched in cool water. A coaxial insert containing DMSO-d_6 was used for lock and shim. Because the reaction solvent was not deuterated, ^{19}F NMR spectra were used to follow reaction progress. The chemical shift of the *p*-fluorine of *N*-(4-fluorophenyl)maleimide changes noticeably with the structure of the adduct and shifts significantly upfield when liberated as the free maleimide. Therefore this signal was used to determine the extent of isomerization of the starting adduct, which is presumed to occur via rate-limiting rDA. Table 2-2 shows the product distributions.

Table 2-2. Product distributions from thermolysis of adducts **1b** and **3b** (Scheme 2-1, below) of pentafluorophenylcyclopentadiene and *N*-(4-fluorophenyl)maleimide in 1,2-dichlorobenzene solution, cumulative reaction times. [a]Performed in bulk melt.

			Product distribution				
Substrate	**T (°C)**	**t (h)**	**1b**	**2b**	**3b**	**4b**	**FMI**[a]
1b	100[a]	6	93%	1%	3%	--	2%
1b	120	6	72%	4%	24%	--	Trace
1b	120	18	17%	8%	63%	10%	2%
1b	130	6	6%	10%	71%	12%	2%
1b	140	18	Trace	7%	79%	13%	1%
1b	150	6	Trace	4%	80%	14%	2%
1b	160	18	Trace	Trace	81%	18%	1%
3b	120	--	--	--	100%	--	--
3b	165[a]	10	2%	1%	94%	2%	1%

2.2.6 Computational Studies

Relative overall enthalpies of Diels-Alder adducts of either *tert*-butylcyclopentadiene or pentafluorophenylcyclopentadiene were calculated using a semi-empirical method (PM3) via the WebMO interface (Table 2-3).

Table 2-3. Relative adduct enthalpies calculated using PM3. The most stable adduct isomers **4a** and **4b** are set to zero on this scale.

Compound	**ΔΔH, kcal/mol**	**Compound**	**ΔΔH, kcal/mol**
1a	6.8	**1b**	6.4
2a	8.6	**2b**	8.7
3a	0.8	**3b**	2.5
4a	0	**4b**	0

2.2.7 Crystallographic Studies

Experimental paragraphs on crystallographic data collection, solution, and refinement were written by Dr. Carla Slebodnick. A colorless plate of **1a** (0.34 x 0.18 x 0.04 mm^3) was centered on the goniometer of an Agilent Nova diffractometer operating with CuKα radiation. The data collection routine, unit cell refinement, and data processing were carried out with the program CrysAlisPro.[51] The Laue symmetry and systematic absences were consistent with the monoclinic

space group $P2_1/n$. The structure was solved using SHELXS-2013[52] and refined using SHELXL-2013[52] via OLEX2.[53] The final refinement model involved anisotropic displacement parameters for non-hydrogen atoms and a riding model for all hydrogen atoms.

A colorless plank of **3a** (0.05 x 0.14 x 0.46 mm^3) was centered on the goniometer of an Agilent Nova diffractometer operating with CuKα radiation. The data collection routine, unit cell refinement, and data processing were carried out with the program CrysAlisPro. The Laue symmetry and systematic absences were consistent with the monoclinic space group $P2_1/n$. The structure was solved using SHELXS-2013 and refined using SHELXL-2013 via OLEX2. The final refinement model involved anisotropic displacement parameters for non-hydrogen atoms and a riding model for all hydrogen atoms.

A colorless plate of **1b** (0.01 x 0.30 x 0.59 mm^3) was centered on the goniometer of an Agilent Nova diffractometer operating with CuKα radiation. The data collection routine, unit cell refinement, and data processing were carried out with the program CrysAlisPro. The Laue symmetry and systematic absences were consistent with the monoclinic space group $P2_1/c$. The structure was solved using olex2.solve and refined using SHELXL-2013 via OLEX2. The final refinement model involved anisotropic displacement parameters for non-hydrogen atoms and a riding model for all hydrogen atoms. Olex2 was used for molecular graphics generation.

A colorless rod of **3b** was cut (0.21 x 0.36 x 0.39 mm^3) and centered on the goniometer of an Agilent Gemini E Ultra diffractometer operating with MoKα radiation. The data collection routine, unit cell refinement, and data processing were carried out with the program CrysAlisPro. The Laue symmetry and systematic absences were consistent with the monoclinic space group $P2_1/c$. The structure was solved using olex2.solve and refined using SHELXL-2014 via OLEX2.

The final refinement model involved anisotropic displacement parameters for non-hydrogen atoms and a riding model for all hydrogen atoms. Olex2 was used for molecular graphics generation.

2.3 Results and Discussion

2.3.1 Synthesis of Diels-Alder Adducts

As shown in Scheme 2-1, adducts were prepared directly from the corresponding dienes and **FMI**. Both dienes exist in solution as slowly interconverting mixtures of two tautomers. Tautomers in which the substituent group is in the 5-position of the cyclopentadiene are not observed in solution NMR spectra. The possibility that the 5-substituted isomers might nevertheless exist at low, steady-state concentration, and thereby combine with maleimide to drive the tautomerization equilibrium was not ignored, but the corresponding adducts (with R at the 7-position of the norbornene system) were not observed in the product mixture. Each tautomer can also, in principle, form both *endo* or *exo* adducts.

Scheme 2-1

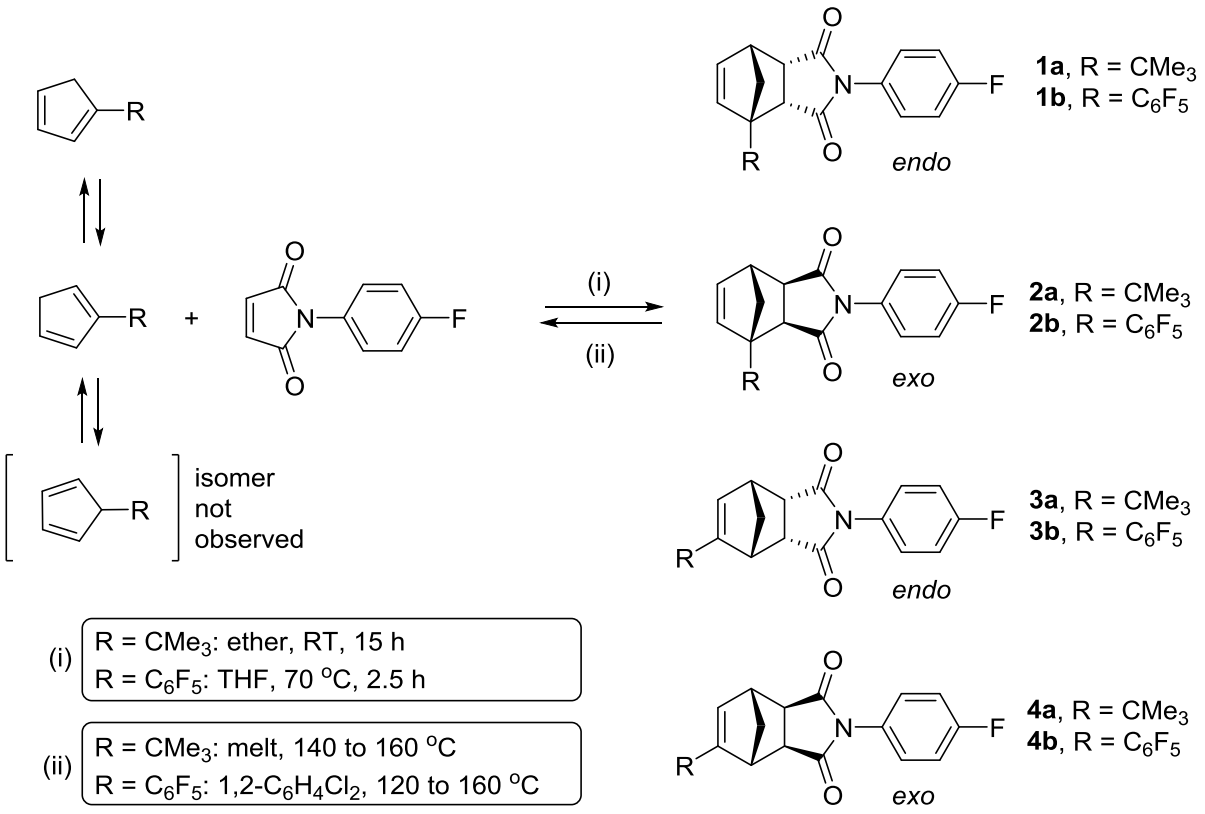

Reaction of substituted cyclopentadienes tautomers with **FMI**

In the case of *tert*-butylcyclopentadiene (R = CMe_3), combination of the reactants at room temperature in diethyl ether formed three of the four anticipated isomers (**1a**, **3a**, and **4a**). Starting maleimide was absent after only 4 h at RT, and NMR spectroscopic analysis showed that the crude product mixture contained **1a**, **3a**, and **4a** in a 12:7:1 ratio. Silica gel chromatography effected a nearly complete separation and final purification of the two isomeric products was achieved by recrystallization. Compound **2a** is unobserved experimentally.

In the case of pentafluorophenylcyclopentadiene (**b**, R = C_6F_5), a preliminary reaction of a 1:1 mixture of diene and maleimide in ether at room temperature slowly afforded a complex mixture that contained a significant quantity of the dimerized diene and unreacted maleimide. Therefore, we carried out the main preparative-scale reaction in THF under reflux with slow addition of the

diene to the maleimide to minimize CPD dimerization. Isolation of the products was much more difficult than it was for the butylated adducts. Because of the relatively large scale of the reaction, the product mixture was first fractionated using a simple trituration procedure, but ultimately the products were mostly separated using liquid chromatography and then purified by recrystallization. It was evident from crude NMR spectra and obtained masses of each adduct that the two *endo* isomers (**1a** and **1b**) were the major products (> 90%). The other two minor isomers, **2a** and **2b**, were present at less than 10% of the total adduct mixtures. Their assignment was not trivial, and was the result of carefully integrated ^{1}H and ^{19}F spectra and comparison to spectra of isolated **1a** and **1b**, respectively. Integration of the ^{19}F spectrum enabled the identification of signals arising from **2b** and by extension of ratios of **1b** to **2b**, the ^{1}H spectrum was also assigned. In a similar spectral analysis, **4b** was deconvoluted from overlapping signals with **3b**.

Isomeric products of the Diels-Alder reactions shown in Scheme 2-1 were easily characterized using ^{1}H NMR spectrometry. The location of the substituent group on the norbornene skeleton was easily inferred from the number of vinyl vs methine CH signals in the ^{1}H NMR spectrum, while *endo* stereochemistry was assigned to those compounds using NOE spectrum measurements in which irradiation of protons alpha to the carbonyl groups resulted in an enhancement of the proximal proton at the 7-position of the norbornene. ^{19}F NMR spectra were largely unremarkable except for the spectrum of the *exo* adduct **2b**, which showed exchange-broadened resonances for the *ortho* and *meta* fluorines of the C_6F_5 group positioned at the norbornene bridgehead. Examination of models suggested a steric interaction of the *ortho* fluorine and the nearby carbonyl oxygen.

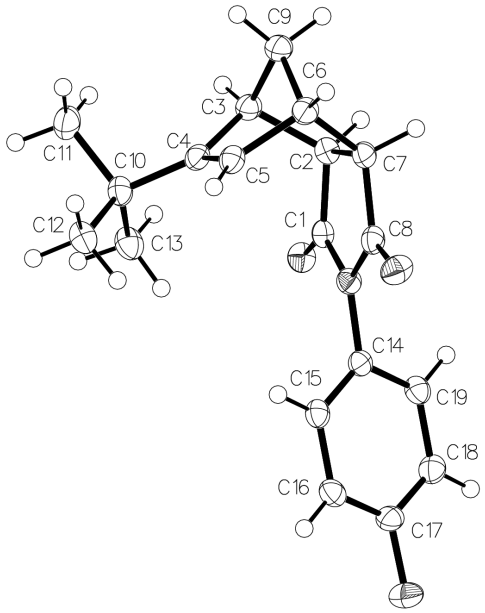

Figure 2-1. Ellipsoid plot (50% probability) of the molecular structure of crystalline adduct **3a** showing *endo* stereochemistry and attachment of *t*Bu group at the 2-carbon (C=C double bond) of the norbornene. The atom attached to C17 is F17. Hydrogen atoms are numbered according to the carbon atoms to which they are attached.

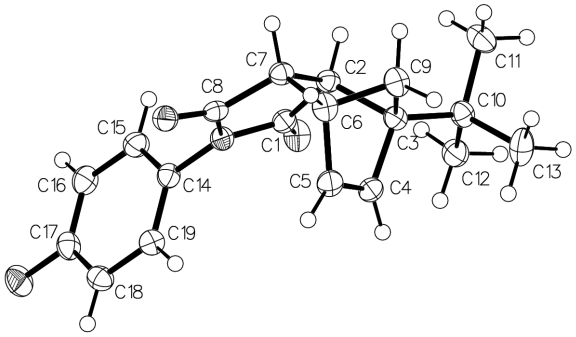

Figure 2-2. Ellipsoid plot (50% probability) of the molecular structure of crystalline adduct **1a** showing *endo* stereochemistry and attachment of *t*Bu group at the 1-carbon (bridgehead) of the norbornene. The atom attached to C17 is F17. Hydrogen atoms are numbered according to the carbon atoms to which they are attached.

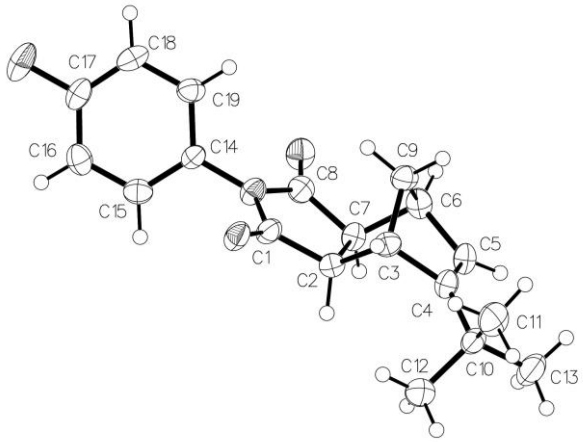

Figure 2-3. Ellipsoid plot (50% probablitiy) of the molecular structure of crystalline **4a** showing *exo* stereochemistry and attachment of the *t*Bu group at the 2-carbon (C=C double bond) of the norbornene. The atom attached to C17 is F17. Hydrogen atoms are numbered according to the carbon atoms to which they are attached.

2.3.2 rDA Reactions of CPD-MI Adducts

Table 2-1 and Figure 2-4 show the results of thermolyses of **1a** and **3a** carried out between 100 and 160 °C. The reaction is quite slow, even at 160 °C. Isomerization is assumed to occur by rate-limiting rDA and recombination of the diene and the maleimide. The *exo* isomer **2a**, having a bridgehead *tert*-butyl group and the least stable according to PM3 calculations (Table 2-3), is not formed. The emergence at 160 °C of the *exo* isomer **4a**, having a vinyl *tert*-butyl group, is consistent with its stability (most stable according to PM3), but its slow formation is also consistent with the inaccessibility of *exo* transition states according to the Alder rule.

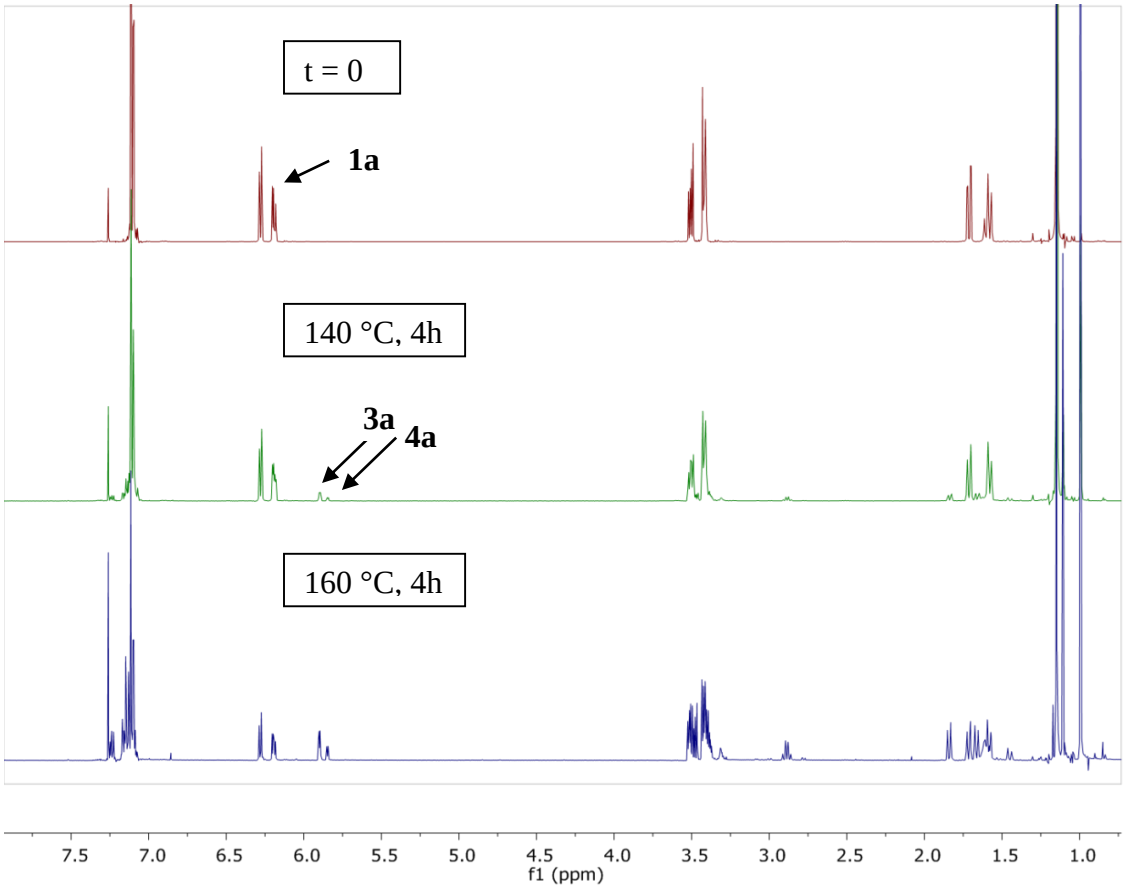

Figure 2-4. ^{1}H NMR spectra (400 MHz, $CDCl_3$) of compound **1a** before (top) and after heating to 140 °C (middle) and 160 °C (bottom), for 4 h each. Adduct **1a** has undergone rDA to produce compound **3a** at δ 5.90 ppm, compound **4a** at δ 5.85 ppm and also **FMI** at δ 6.85 ppm. Longer reaction times showed >97% conversion of **1a** to **3a** and **4a**.

The data in Table 2-1 and in Figure 2-5 show that **3a** undergoes rDA reluctantly even at 160 °C. These data, taken together, show that *tert*-butylcyclopentadiene forms robust adducts with **FMI**; however the adducts with the *tert*-butyl group in the 1-position of the norbornene moiety are decidedly less stable toward rDA.

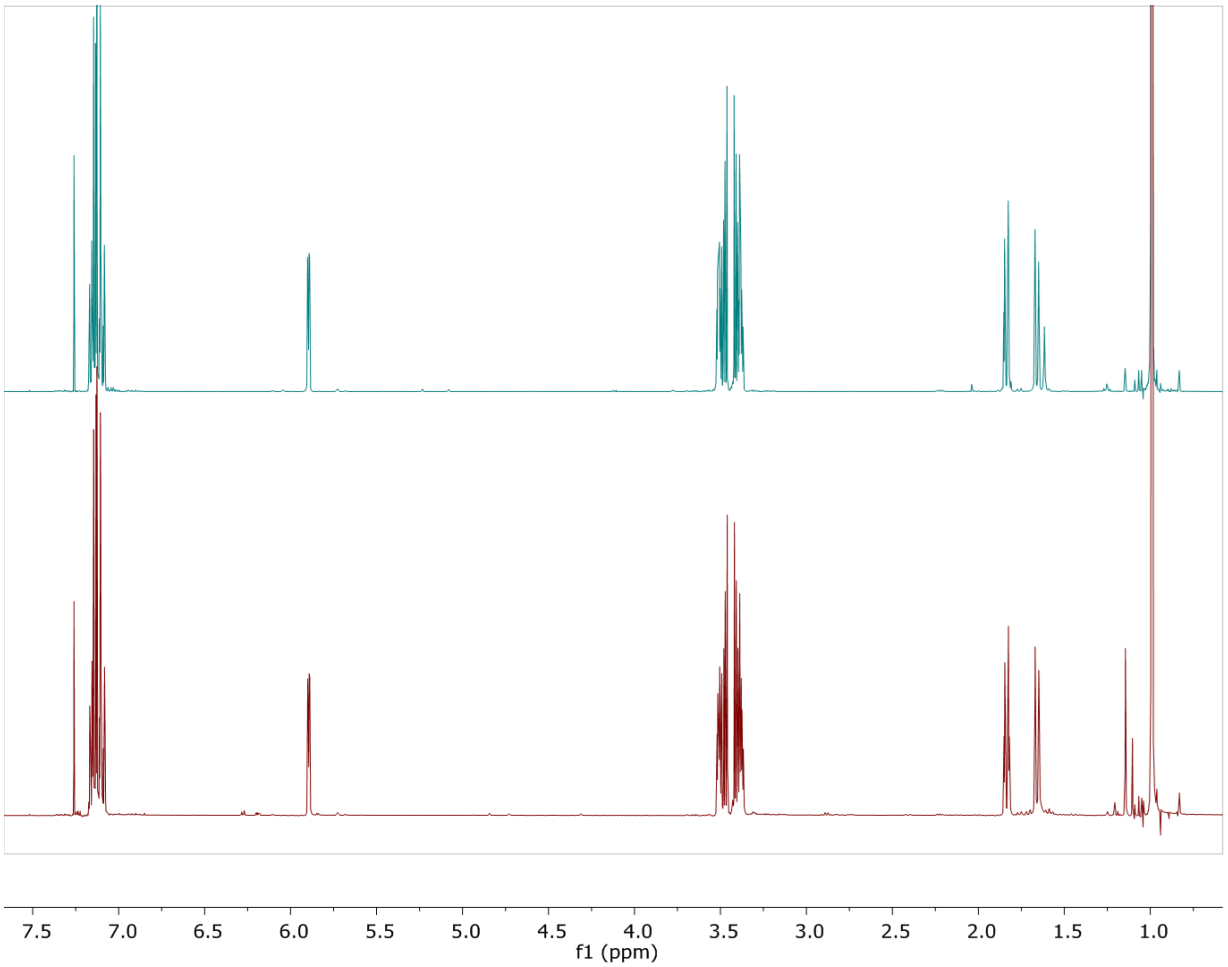

Figure 2-5. ^{1}H NMR (400 MHz, $CDCl_3$) of compound **3a** before (top) and after heating to 160 °C (bottom). It is evident that a major rDA process has not occurred due to the lack of *maleimide* protons which normally appear at δ 6.85 ppm.

In stark contrast to the *tert*-butylated adduct **1a**, thermolysis of the C_6F_5-substituted congener **1b** underwent isomerization at 120 °C after only 4 h (Table 2-2). This is an important finding because it means that the C_6F_5 group is highly destabilizing of the adduct toward rDA, especially when the C_6F_5 group is in the 1-position of the norbornene moiety. In the thermolysis of **1b**, formation of the unstable 1-substituted *exo* adduct **2b** (highest adduct energy by PM3, Table 2-3) was observed but only in single-digit percentages and in proportions that gradually decline at higher temperatures. The isomer presumed (and calculated by PM3) to be the lowest-energy adduct is a minor product in all cases; further experiments at still higher temperatures are expected to show that **4a** and **4b** are the ultimate thermodynamic adducts in the butylated and

perfluorophenylated systems, respectively. Another interesting observation is the rather small changes in the proportion of **1b** and **3b** in the thermolysis of **3b** when the temperature is raised from 120 °C to 160 °C. These results suggest that the activation barrier to rDA of **3b** is already overcome at 120 °C and that the ratio of **1b**:**3b** could be under thermodynamic control at the higher temperatures. The relatively large difference in their PM3 energies argues against this conclusion, but an experiment in which the mixture is maintained at 150 °C for a much longer time would help answer this question.

2.4 Conclusions

The model studies presented in this chapter show that a perfluoroaryl substituent, and to a lesser extent a bulky alkyl substituent, are both capable of destabilizing DA adducts toward rDA. These findings suggest that placing both substituents on a single cyclopentadiene may arrest self-dimerization while weakening DA adducts with N-substituted maleimides. The question of whether the destabilization effects will be sufficient to allow CPD-MI chemistry to serve as the basis for thermally reversible DA polymerization is addressed in Chapter 3 and Chapter 5 of this dissertation.

Chapter 3 Models for Diels-Alder Adduct Formation in Cyclopentadiene-Maleimide Polymers

Jeremy B. Stegall, Carla Slebodnick, and Paul A. Deck*

Department of Chemistry, Virginia Tech, Blacksburg, VA 24061

Keywords: Diels-Alder reaction, cycloaddition, substituent effects, cyclopentadiene, maleimide, NMR spectroscopy, molecular modeling, DFT

Foreward. With the exception of supporting information relegated to the end of the dissertation, this chapter represents a stand-alone manuscript in preparation for submission to the *Journal of Organic Chemistry*. I performed all of work reported in this chapter except as follows: Dr. Carla Slebodnick performed the crystallographic data collection, structure solution, and refinement; Bill Bebout performed the mass spectroscopic analyses; Atlantic Microlab, Inc. (Norcross, GA) performed the microanalyses, and Prof. Paul A. Deck supervised my work.

3.1 Abstract

Thermal reactions of 1-(nonafluorobiphenyl-4'-yl)-4-tert-butylcyclopentadiene and *N*-(4-fluorophenyl)maleimide afford mixtures of Diels-Alder (DA) adducts in high overall yields. Product mixtures are complex because the starting diene tautomerizes and because each tautomer can – and with one exception does – form both *endo* and *exo* DA adducts. Generally, however, the products are separable by silica gel chromatography and are characterized by a combination of NMR spectrometry and X-ray crystallography. The product distribution is influenced strongly by reaction temperature; B3LYP/6-31G(d) studies support the conclusion that the adducts favored at higher reaction temperatures are "thermodynamic" products. Thermal cleavage, via a rate-limiting retro-Diels-Alder (rDA) process, of each of the two major adducts formed at 150 °C was demonstrated in solution either by observing its isomerization or by exchanging the adduct-bound *N*-(fluorophenyl)maleimide with *N*-phenylmaleimide present in large excess. It was found that 1,3-endo adduct **3d** exchanged most rapidly, followed by 2,4-endo **3b** and finally 1,3-exo **3c**; these data are largely consistent with B3LYP/6-31G(d) studies highlighting relative adduct stability.

3.2 Introduction

The Diels-Alder (DA) reaction has found widespread use as a means of introducing thermal reversibility into macromolecules. Reversible attachment of functional groups provides a means to tune polymer properties such as surface activity.[23,24] Grafting, dendronization, and other structural modifications can also be made reversible using the DA approach.[2,21,22] The DA reaction has also been used to propagate linear polymers that can subsequently be thermally depolymerized, at least partially, under relatively mild conditions.[9,54] This strategy is an entry point for thermally re-mendable ("self-healing") materials[32,55-57] and for facilitating melt-processing of polymers[58,59] DA chemistry can also introduce thermally reversible cross-links,[28,60] which also can facilitate processing[61] and thermal healing,[31,32,57] as well as control physical behavior such as gelation[15,16,62,63] and viscoelastic response.[64]

The DA reaction requires two reactive components: a diene and a dienophile. The most common dienophile moiety in macromolecular synthesis is the *N*-substituted maleimide (MI),[47] which is typically prepared from a primary amine (or diamine) and maleic anhydride. Diamines are likewise converted to bis(maleimides), which can serve as step-growth monomers with bis-dienes or as cross-linking agents with diene-functionalized polymers. The diene moiety varies more widely but is still generally limited to cyclic diene specie, notably furans[3,5,9,12,17,22,24,63,65,66] and cyclopentadienes,[26,27,31,67] and to a lesser extent anthracenes[2,68] and a few others.[32] Of these, furans are used most commonly because they are relatively easy and inexpensive to introduce synthetically (from furfural and related derivatives),[13,69] and because their maleimide adducts decouple at temperatures (80-100 °C) well below the onset of general thermal decomposition of common organic functionalities.[18,70]

Cyclopentadiene (CPD) is unique in the sense that it serves both as diene and dienophile. Cyclopentadiene moieties can be attached to monomer end-groups and to other structures using polymethylene tethers but are usually otherwise unfunctionalized. This feature enables linear polymerization of bis(cyclopentadienes)[26,31] as well as cross-linking of cyclopentadiene-substituted polymers without requiring the addition of a curing agent.[28,29] Unfortunately, monoalkylated cyclopentadienes also require harsh conditions for retro-Diels-alder (rDA) reactions: Thermal cracking of methylcyclopentadiene dimer occurs ca. 160–180 °C.[44] Meanwhile the dimerization (DA) reaction occurs so readily that the process cannot easily be arrested even long enough to purify a bis(cyclopentadiene) monomer.[34] The latter property precludes their use in two-component systems (e.g., CPD + MI) because the self-reaction (CPD + CPD) always competes with the cross-DA process.

Despite these issues, cyclopentadiene derivatives offer promise for use in Diels-Alder reactions in the context of thermally reversible macromolecular chemistry for two main reasons. First, functionalization of cyclopentadiene is a highly developed area of synthetic chemistry, such that one can often control not only the number and placement of substituents but also their electron-donating or electron-withdrawing character. Second, [as we showed in Chapter 2,] certain CPDs bearing one bulky substituent, such as *tert*-butylcyclopentadiene[41,42] and especially trimethylsilylcyclopentadiene,[30] are fairly resistant to dimerization, and whereas methylcyclopentadiene[35] and pentafluorophenylcyclopentadiene[36] both dimerize readily at or near room temperature, the analogous disubstituted compounds dimethylcyclopentadiene,[35] di-*tert*-butylcyclopentadiene,[38] bis(pentafluorophenyl)cyclopentadiene,[36] and 4-*tert*-butyl-1-pentafluorophenylcyclopentadiene[37] do not. These observations suggest that disubstituted cyclopentadienes could be useful in two-component, thermally reversible coupling systems (e.g.,

CPD + MI), possibly with thermochemical profiles ("onset temperatures") for DA and rDA that are complementary to or possibly even competitive with analogous furan-based systems.

This article describes the DA chemistry of a model disubstituted cyclopentadiene (**1**) and a model maleimide (**FMI**)[1] shown generically in Scheme 3-1. As diene **1** tautomerizes freely, and as the DA reaction generally affords both *exo* and *endo* adducts, the reaction of **1** and **FMI** gives a mixture of isomeric products in high overall conversion. We show that the product distribution depends on the reaction temperature in a manner that suggests temperature regimes of kinetic and thermodynamic control. We also show that the DA adducts **3** undergo clean thermal reversion starting at 120 °C.

Scheme 3-1

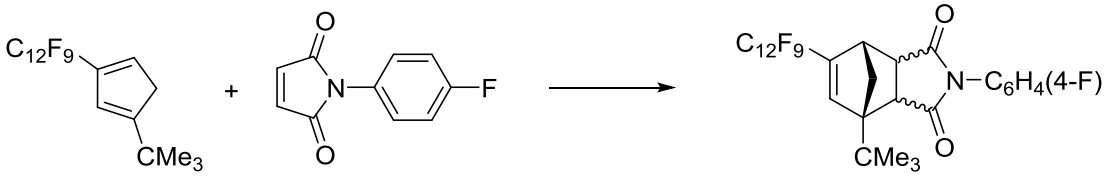

1a **FMI** **3**

Reaction of **1a** with **FMI** to form adduct **3**

3.3 Experimental

3.3.1 General Methods

Solvents were used as received from commercial suppliers unless noted otherwise. Hexafluorobenzene was used as received from Oakwood Products (Columbia, SC) or Apollo Scienfitic (UK). Decafluorobiphenyl, 4-fluoroaniline, and 2,6-difluoroaniline were used as received from Matrix Scientific. Sodium *tert*-butylcyclopentadienide,[41] *N*-(4-fluorophenyl)maleimide (**FMI**),[49,50] *N*-(2,6-difluorophenyl)maleimide (**2b**),[50] and *N*-

[1] In the manuscript the maleimide **FMI** is designated **2a**. We use the designator **FMI** here for consistency throughout the dissertation.

phenylmaleimide (**2c**) were prepared as previously reported and have physical and spectroscopic data consistent with those reports. Maleic anhydride and aniline were used as received from Aldrich. NMR spectra were acquired on a Varian Inova 400 NMR spectrometer, an Agilent 400-MR DD2 NMR spectrometer or a Bruker Avance II 500 NMR spectrometer. Proton chemical shifts were referenced to $CHCl_3$ (7.26 ppm) in $CDCl_3$. ^{19}F chemical shifts were referenced to external C_6F_6 (−183.0 ppm) in $CDCl_3$. Mass spectra were obtained using an Agilent 6220 instrument (LC-ESI-TOF featuring 5-ppm mass accuracy) operating in positive ion mode. Melting points (uncorrected) were acquired using open capillaries on a Buchi B-545 apparatus.

3.3.2 Synthesis of 2-(nonafluorobiphenyl-4'-yl)-4-tert-butylcyclopentadiene (1a) and tautomers (1b and 1c)

To a stirred mixture of decafluorobiphenyl (4.6 g, 14 mmol) and sodium hydride (1.0 g, 42 mmol) in THF (25 mL) maintained at −78 °C under a nitrogen atmosphere was added a solution of sodium *tert*-butylcyclopentadienide (2.0 g, 14 mmol) in THF (25 mL) over 0.5 h, using a cannula. The resulting mixture was stirred and allowed to warm to room temperature over several hours and then stirred at room temperature for two additional days under nitrogen. The reaction was followed by acidic, aqueous workup of small aliquots (0.1 mL), extracting with $CDCl_3$, and analysis by ^{19}F NMR to monitor the disappearance of the well-resolved signal at −150.19 ppm assigned to the *para* fluorine of decafluorobiphenyl. The rest of the procedure was conducted under air. The reaction mixture was diluted with dichloromethane (100 mL), quenched with 10% aqueous sulfuric acid (100 mL), washed with water (2 x 100 mL) and then brine (100 mL), dried with anhydrous magnesium sulfate, and evaporated to afford 5.9 g (98%) of a dark, viscous oil. Elution through a pad of silica gel with 50% dichloromethane in hexanes and rotary evaporation of the solvent yielded a yellow oil that was found by NMR spectroscopic analysis to contain about 10% of an additional compound tentatively assigned (later confirmed, see below) to the diarylated

cyclopentadiene **4**. Flash chromatography (silica gel, 7.5 cm x 20 cm) eluting with hexanes (2 L) and rotary evaporation of the solvent afforded a yellow crystalline solid. Sublimation (100 mTorr, 100 °C) afforded 3.0 g (6.9 mmol, 49%) of a white microcrystalline solid, mp 112–115 °C. NMR spectroscopic analysis revealed that the product comprised a mixture of tautomers. Compound **1a** was observed as a trace component of the mixture and was assigned on the basis of the upfield methylene protons (3.13 ppm) compared to the downfield chemical shift (3.48 ppm) for the methylene protons in **1b** and **1c** which are vicinal to the electron-withdrawing C_6F_5 group. Furthermore the assignment of **1b** vs. **1c** is ambiguous. **Data for 1a** (trace component of the product mixture): ^{1}H NMR (400 MHz, $CDCl_3$) δ 6.7 (s, 1H), 6.4 (s, 1H), 3.1 (s, 2H), 1.2 (s, 9H). ^{19}F NMR data was not resolved for **1b** and **1c**. **Data for 1b** (56 % of mixture): ^{1}H NMR (400 MHz, $CDCl_3$) δ 7.3 (s, 1H), 6.2 (s, 1H), 3.5 (m, 2H), 1.2 (s, 9H); ^{19}F NMR (376 MHz, $CDCl_3$) δ −137.3 (m, 2F), −140.1 (m, 1F), −140.2 (m, 1F), −150.9 (dt, 1F, $^3J_{FF}$ = 21 Hz, $^4J_{FF}$ = 3 Hz), −160.9 (m, 2F). **Data for 1c** (44% of mixture): ^{1}H NMR (400 MHz, $CDCl_3$) δ 7.2 (s, 1H), 6.3 (s, 1H), 3.5 (m, 4H), 1.2 (s, 9H); ^{19}F NMR (376 MHz, $CDCl_3$) δ −137.3 (m, 2F), −140.4 (m, 1F), −140.5 (m, 1F), −151.1 (dt, 1F, $^3J_{FF}$ = 21 Hz, $^4J_{FF}$ = 3 Hz), −161.0 (m, 2F). HRMS (ESI) *m/z* calcd for $C_{21}F_9H_{13}$ $(M+H)^+$ 437.0952, found 437.0950. Anal. Calcd for $C_{21}F_9H_{13}$: C, 57.81; H, 3.00. Found: C, 58.07; H, 2.95.

3.3.3 Synthesis of Diels-Alder Adducts (3)

A stirred solution of diene **1** (mixture of isomers, 0.23 g, 0.53 mmol), *N*-(4-fluorophenyl)maleimide (**FMI**, 0.1 g, 0.524 mmol) in *o*-dichlorobenzene (10 mL) in a 25-mL Schlenk flask was heated at the selected reaction temperature for at least 24 h (reaction temperatures and product distributions are collected in Table 3-1 in the Results and Discussion section below). The reaction was followed by periodic removal of an aliquot (0.1 mL), from which

the solvent was evaporated using a vacuum pump and the residue subjected to NMR spectroscopic analysis in $CDCl_3$ solution. Reaction progress was monitored by disappearance of the well-resolved, single ^{19}F NMR signal of maleimide **FMI**. When no further reaction progress was observed, the solvent was evaporated using a vacuum pump. First the crude mixture was analyzed by ^{1}H NMR spectrometry to obtain a product distribution for that reaction temperature, and then the residue was subjected to flash chromatography on silica gel, eluting with 20% ethyl acetate in hexanes. Unreacted diene (**1**) and residual dichlorobenzene eluted first, followed by DA adducts (**3**), followed by unreacted maleimide (**FMI**). Adduct **3e** was not observed in any of the reactions. Adduct **3f** was only observed in reactions carried out at 80 °C or below.

Data for 2,4-Exo-Adduct 3a: mp 205–207 °C. ^{1}H NMR (400 MHz, $CDCl_3$) δ 7.3 – 7.1 (m, 4H), 6.8 (s, 1H), 3.9 (s, 1H), 3.3 (d, ^{3}J = 7 Hz, 1H,), 2.9 (d, 1H, ^{3}J = 7 Hz), 1.9 (d, ^{2}J = 10 Hz, 1H), 1.7 (d, ^{2}J = 10 Hz, 1H), 1.2 (s, 9H); ^{19}F NMR (376 MHz, $CDCl_3$) δ −112.4 (m, 1F), −137.6 (m, 2F), −139.0 (m, 2F), −140.0 (m, 2F), −150.4 (tt, $^{3}J_{FF}$ = 21 Hz, ^{4}J = 3 Hz), −160.8 (m, 2F). HRMS (ESI) *m/z* calcd for $C_{31}F_{10}H_{20}NO_2$ $(M+H)^+$ 628.1334, found 628.1339. Anal. Calcd for $C_{31}F_{10}H_{19}NO_2$: C, 59.34; H, 3.04; N, 2.23. Found: C, 59.61; H, 3.23; N, 2.24. Notebook reference JBS-1-154-5

Data for 2,4-Endo-Adduct 3b: mp 152–166 °C. ^{1}H NMR (400 MHz, $CDCl_3$) δ 7.1 (m, 4H), 6.9 (s, 1H), 4.1 (d, 1H, ^{3}J = 3 Hz), 3.7 (dd, 1H, ^{3}J = 8 Hz, ^{3}J = 4 Hz), 3.6 (d, 1H, ^{3}J = 8 Hz), 2.0 (d, 1H, ^{2}J = 9 Hz), 1.8 (d, 1H, ^{2}J = 8.9 Hz), 1.2 (s, 9H). ^{19}F NMR (376 MHz, $CDCl_3$) δ −112.9 (m, 1F), −137.3 (m, 2F), −138.7 (m, 2F), −139.1 (m, 2F), −150.5 (t, 1F, ^{3}J = 21 Hz), −160.8 (m, 2F). HRMS (ESI) *m/z* calcd for $C_{31}F_{10}H_{23}N_2O_2$ $(M+NH_4)^+$ 645.1600, found 645.1613. Anal. Calcd. For $C_{31}F_{10}H_{19}NO_2$: C, 59.34; H, 3.04; N, 2.23. Found: C, 59.55; H, 3.10; N, 2.72. Notebook reference JBS-1-153-5, jbs-1-165-4

Data for 1,3-Exo-Adduct 3c : mp 149–151 °C. ^{1}H NMR (400 MHz, $CDCl_3$) δ 7.2 (m, 4H), 6.0 (s, 1H), 3.5 (s, 1H), 3.5 (d, 1H, ^{3}J = 7 Hz), 3.1 (d, 1H, ^{3}J = 7 Hz), 2.3 (d, 1H, ^{2}J = 10 Hz), 2.2 (d, 1H, ^{2}J = 10 Hz), 1.2 (s, 9H). ^{19}F NMR (376 MHz, $CDCl_3$) δ −112.3 (m, 1F), −136.7 (bs, 1F), −137.4 (bs, 1F), −138.0 (bs, 1F), −138.4 (bs, 1F), −139.9 (bs, 1F), −142.9 (bs, 1F), −150.8 (t, 1F, ^{3}H = 21 Hz), −161.0 (bs, 1F), −161.2 (bs, 1F). HRMS (ESI) *m/z* calcd for $C_{31}F_{10}H_{20}NO_2$ $(M+H)^+$ 628.1334, found 628.1339. Anal. Calcd for $C_{31}F_{10}H_{19}NO_2$: C, 59.34; H, 3.04; N, 2.23. Found: C, 58.92; H, 3.07; N, 2.17. Notebook reference JBS-1-154-2

Data for 1,3-Endo Adduct 3d: mp 199–201 °C. ^{1}H NMR (400 MHz, $CDCl_3$) δ 7.2–7.1 (m, 4H), 6.4 (m, 1H), 4.1 (d, 1H, ^{3}J = 8 Hz), 3.7 (dd, 1H, ^{3}J = 8 Hz, ^{3}J = 4 Hz), 3.6 (d, 1H, ^{3}J = 4 Hz), 2.47 (d, 1H, ^{2}J = 9 Hz), 2.3 (d, 1H, ^{2}J = 9 Hz), 1.1 (s, 9H). ^{19}F NMR (376 MHz, $CDCl_3$) δ −112.6 (m, 1F), −137.5 (m, 3F), −138.7 (m, 3F), −150.6 (tt, 1F, ^{3}J = 21 Hz, ^{4}J = 3 Hz), −160.9 (m, 2F). HRMS (ESI) *m/z* $(M+H)^+$ calcd for $C_{31}F_{10}H_{20}NO_2$ 628.1334, found $(M+H)^+$ 628.1339. Anal. Calcd for $C_{31}F_{10}H_{19}NO_2$: C, 59.34; H, 3.04; N, 2.23. Found: C, 59.48; H, 3.10; N, 2.21. Notebook reference JBS-1-176-4

Data for 1,4-Endo Adduct 3f: This compound was not isolated in pure form. NMR data for **3f** were obtained from a spectrum of a sample containing 4% of **3a**, 33% of **3f**, and 63% of **3c**. ^{1}H NMR (400 MHz, $CDCl_3$): 7.2–7.1 (m, 4H), 6.7 (m, 1H), 6.4 (d, 1H, J = 6 Hz), 4.1 (d, 1H, ^{3}J = 7.8 Hz); 3.7 (d, 1H, ^{3}J = 8 Hz), 2.4 (d, 1H, ^{2}J = 9 Hz), 2.1 (d, 1H, ^{2}J = 9 Hz). ^{19}F NMR (376 MHz, $CDCl_3$): −112.6 (m, 1F), −137.4 (m, 2F), −137.7 (m, 2F), −138.6 (m, 2F), −150.5 (tt, 1F, ^{3}J = 21 Hz, ^{4}J = 3 Hz), −160.9 (m, 2F). Notebook reference JBS-1-153-2.

3.3.4 Synthesis of 1,2-bis(nonafluorobiphenyl-4'-yl)-4-tert-butylcyclopentadiene (4)

A stirred slurry of decafluorobiphenyl (4.7 g, 14 mmol) and sodium hydride (0.35 g, 15 mmol) in THF (50 mL) maintained under a nitrogen atmosphere was cooled to −78 °C in a dry ice/acetone

bath. Sodium *t*-butylcyclopentadienide (1.0 g, 6.9 mmol) in THF (20 mL) was added using a cannula over 0.5 h. The mixture warmed slowly to room temperature and was then stirred at room temperature for 15 h and then under reflux for an additional 4 h. The reaction was followed by removal of small aliquots (0.1 mL) followed by acidic aqueous workup, extracting into $CDCl_3$, and analysis of the product mixture by ^{19}F NMR to monitor the disappearance of decafluorobiphenyl. The rest of the procedure was conducted in air. The reaction mixture was diluted with dichloromethane (100 mL), quenched with 10% aqueous sulfuric acid (100 mL), washed with water (2 x 100 mL) and brine (100 mL), dried with anhydrous magnesium sulfate, and evaporated to afford 5.0 g of a viscous red oil, of which 3.0 g was purified by silica gel chromatography (7.5 cm x 10 cm), eluting with hexanes, evaporation of the solvent, and crystallization of the resulting yellow oil from hexanes to obtain large colorless crystals (2.0 g, 2.7 mmol, 39%), mp 132–133 °C. ^1H NMR (400 MHz, $CDCl_3$) δ 6.4 (s, 1H), 3.7 (s, 2H), 1.3 (s, 9H); ^{19}F NMR (376 MHz, $CDCl_3$) δ −137.4 (m, 4F), −138.5 (m, 2F), −138.8 (m, 2F), −139.6 (m, 2F), −140.3 (m, 2F), −150.6 (t, 1F, ^3J = 21 Hz), −150.7 (t, 1F, ^3J = 21 Hz), −161.0 (m, 4F). HRMS (ESI) *m/z* calcd for $C_{33}F_{18}H_{12}$ $(M-H)^-$ 749.0573, found $(M-H)^-$ 749.0618. Anal. Calcd for $C_{33}F_{18}H_{12}$: C, 52.82; H, 1.61. Found: C, 52.86; H, 1.85. Notebook reference jbs-1-136 – jbs-1-138.

3.3.5 Equilibrium studies

A solution of diene **1** (mixture of isomers, 0.191 g, 0.100 mmol) and *N*-(4-fluorophenyl)maleimide (**FMI**, 0.436 g, 0.100 mmol) in *o*-dichlorobenzene (1.88 g, 1.45 mL) in a small reaction tube was maintained at 80 °C under nitrogen for ca. 645 hours. An aliquot (0.1 g of the solution) was removed at periodic intervals (t = 25, 100, 200, 430, and 645 hours), diluted with $CDCl_3$, and subjected to ^1H and ^{19}F spectroscopic NMR analysis. The integral of the spectral

region downfield of the **FMI** signal (−111.0 to −113.0 ppm in the ^{19}F NMR spectrum, assigned to DA adducts) was normalized to the integral of the **FMI** signal at −113.52 ppm to determine the relative quantities of adduct and **FMI** in the mixture. Relative quantities of diene were calculated by subtracting the adduct quantity from initial diene quantity based on the assumption that diene is consumed only by the DA reaction. The total volume of the reaction mixture was assumed to be the volume of 1,2-dichlorobenzene based on its density at 20 °C. This method further assumes that the solution volume was not changed by dissolution of the reactants (that is, the solution was ideal). Absolute concentrations of the three species were determined from their relative concentrations, their absolute initial quantities, and the total solution volume. Concentrations were also assumed to be unaffected by the removal of aliquots.

3.3.6 Maleimide exchange reaction

A solution of adduct **3c** (0.010 g, 0.02 mmol) and *N*-phenylmaleimide (**2c**, 0.028 g, 0.16 mmol) in 1,2-dichlorobenzene (0.6 mL) was prepared in an NMR tube. A sealed DMSO-d_6 capillary was inserted for lock and shim. The tube was sealed with a polypropylene cap and an initial NMR spectrum was acquired. The tube was then placed in an oil bath maintained at 130 °C for a few hours. The tube was removed from the oil bath and quenched by placing in a bath of cool water. An ^{19}F NMR spectrum was acquired. The tube was then returned to the oil bath and heated for a total of 200 hours. ^{19}F NMR spectra were acquired at t (h) = 24, 48, 72, and 200. Unbound **FMI** (ca. 1%) was observed after only 4 h. This increased with time: t = 24, **FMI** = 12%; t = 48, **FMI** = 27%; up to about 68% at 200 h. Notebook reference JBS-2-171-(3-7)

3.3.7 Computational Studies

All calculations were conducted using the WebMO[71] interface to Gaussian.[72] Geometry optimizations of diene **1** (5 isomers) and DA adducts **3** (14 isomers) used the B3LYP[73-76] level of

theory with a 6-31G* basis set.[77,78] Vibrational frequency calculations gave relative free energies of formation at 298 K. Studies of the perfluoroaryl torsional barriers in DA adduct isomers **3c** and **3d** used the Coordinate Scan feature of the WebMO interface to calculate electronic energies every 10° over a 180° range at the PM3 level of theory.[79,80]

3.3.8 Crystallographic Studies

Crystalline samples of **3a**, **3b**, **3c**, and **4** were obtained by cooling or evaporation of hexane solutions containing up to 10% of ethyl acetate. Crystallographic data are provided in the Supporting Information. The following experimental procedures describing data collection, structure solution, and final refinement were written by Dr. Carla Slebodnick.

A colorless rod of **3a** was cut into a prism (0.13 x 0.16 x 0.19 mm^3) and centered on the goniometer of an Oxford Diffraction SuperNova A diffractometer operating with CuKα radiation. The data collection routine, unit cell refinement, and data processing were carried out with the program CrysAlisPro.[51] The Laue symmetry and systematic absences were consistent with the monoclinic space groups *C*2/*c* and *Cc*. The centric space group *C*2/*c* was chosen. The structure was solved using SHELXS-97[52] and refined using SHELXL-97[52] via OLEX2.[53] The final refinement model involved anisotropic displacement parameters for non-hydrogen atoms and a riding model for all hydrogen atoms.

A colorless wedge of **3b** (0.09 x 0.12 x 0.48 mm^3) was centered on the goniometer of an Oxford Diffraction SuperNova A diffractometer operating with CuKα radiation. The data collection routine, unit cell refinement, and data processing were carried out with the program CrysAlisPro. The Laue symmetry and systematic absences were consistent with the monoclinic space group $P2_1/c$. The structure was solved using SHELXS-97 and refined using SHELXL-97 via OLEX2. After refining the main residue, large residual electron density peaks remained in a solvent channel.

These are presumed to be from disordered hexanes, but could not be modeled effectively. The SQUEEZE subroutine of the PLATON[81] program package was used to subtract from the solvent channels a total of 58 e^- / unit cell (0.29 e^- / asymmetric unit). The 58 electrons correspond to 1.16 hexanes/unit cell (0.29 hexanes / asymmetric unit). The final refinement model involved anisotropic displacement parameters for non-hydrogen atoms and a riding model for all hydrogen atoms.

A colorless prism of **3c** was cut into a plate (0.05 x 0.16 x 0.21 mm^3) and centered on the goniometer of an Oxford Diffraction SuperNova A diffractometer operating with CuKα radiation. The data collection routine, unit cell refinement, and data processing were carried out with the program CrysAlisPro. The Laue symmetry and systematic absences were consistent with the monoclinic space groups *C*2/*c* and *Cc*. The centric space group *C*2/*c* was chosen. The structure was solved using SHELXS-97 and refined using SHELXL-97 via OLEX2. The final refinement model involved anisotropic displacement parameters for non-hydrogen atoms and a riding model for all hydrogen atoms.

A colorless needle of **4** was cut (0.21 x 0.35 x 0.51 mm^3) and centered on the goniometer of an Oxford Diffraction SuperNova A diffractometer operating with CuKα radiation. The data collection routine, unit cell refinement, and data processing were carried out with the program CrysAlisPro. The Laue symmetry and systematic absences were consistent with the orthorhombic space groups *Pbcm* (the standard setting of *Pcam*) and $Pca2_1$. Only $Pca2_1$ yielded a satisfactory structure solution, giving 2 molecules in the asymmetric unit. Inspection of the packing diagram of the $Pca2_1$ structure indicates there is no *m* || (001). Thus, $Pca2_1$ with *Z*'=2 was chosen as the space group. The structure was solved using SHELXS-97 and refined using SHELXL-97 via OLEX2. The final refinement model involved anisotropic displacement parameters for non-

hydrogen atoms and a riding model for all hydrogen atoms. The *t*-butyl groups of both crystallographically unique molecules were each modeled with 2-position disorder. Relative occupancies of the two conformations of C30-C33 refined to 0.456(6) and 0.544(6). The two conformations of C64-C66 had relative occupancies 0.492(8) and 0.508(8). The bond lengths in the cyclopentadiene ring also suggest disorder in the location of the sp^3 hybridized carbon in both molecules. A 2-position disorder model was used and relative occupancies were constrained to 0.50.

3.4 Results and Discussion

3.4.1 Synthesis of substituted cyclopentadienes

We briefly considered *tert*-butyl-pentafluorophenylcyclopentadiene (**A**) for our study of cyclopentadiene-maleimide (CPD + MI) reactions because **A** was already available[37] and because the C_6F_5 group is a good spectroscopic probe (^{19}F NMR).[82] Furthermore, we hypothesized that the electron-withdrawing character of the C_6F_5 group might destabilize the maleimide adduct, enabling rDA to occur at lower temperatures than those observed for corresponding adducts of the parent CPD. However the low-melting point and high solubility of **A** made its purification cumbersome and inefficient. We reasoned that the larger aryl group in **1** (abbreviated $C_{12}F_9$ hereafter) would increase the intrinsic crystallinity of the compound and facilitate both purification and handling.

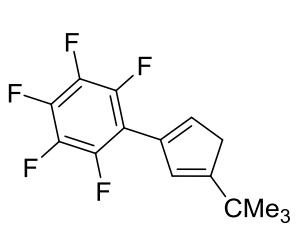

A

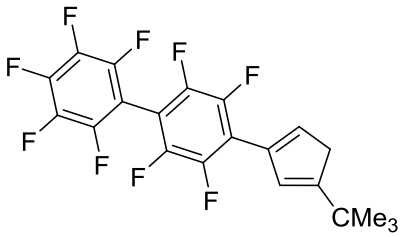

1a

As shown in Scheme 3-2, sodium *tert*-butylcyclopentadienide reacts with 1 equiv of decafluorobiphenyl to afford diene **1** as a mixture of three tautomers as determined by NMR spectroscopic analysis. Tautomer **1a** is present in smallest quantity, likely due to its less stable, cross-conjugated structure (see computational studies below). Tautomers **1b** and **1c** are present in roughly equal quantities, suggesting a lack of preference for the *tert*-butyl group to be attached to the 3-carbon or the 4-carbon of the diene moiety. Tautomers **1a**-**1c** co-elute in TLC analysis and co-crystallize, and are therefore inseparable by these methods. The crude product mixture also contains about 10% of the homologous, diarylated cyclopentadiene **4** (see below). Twofold substitution of decafluorobiphenyl to afford bis-diene **C** is not observed; based on our earlier work the formation of **C** should require a higher temperature (ca. 65 °C).[41] Evidently the anionic intermediate **B** cannot undergo S_NAr nearly as readily as decafluorobiphenyl. Isomers of **1** in which the aryl and *tert*-butyl groups are vicinal are not observed. The steric bulk of the *tert*-butyl group defends the vicinal positions of the cyclopentadiene from attack by the electrophilic perfluoroarene except under forcing conditions.[41]

Scheme 3-2

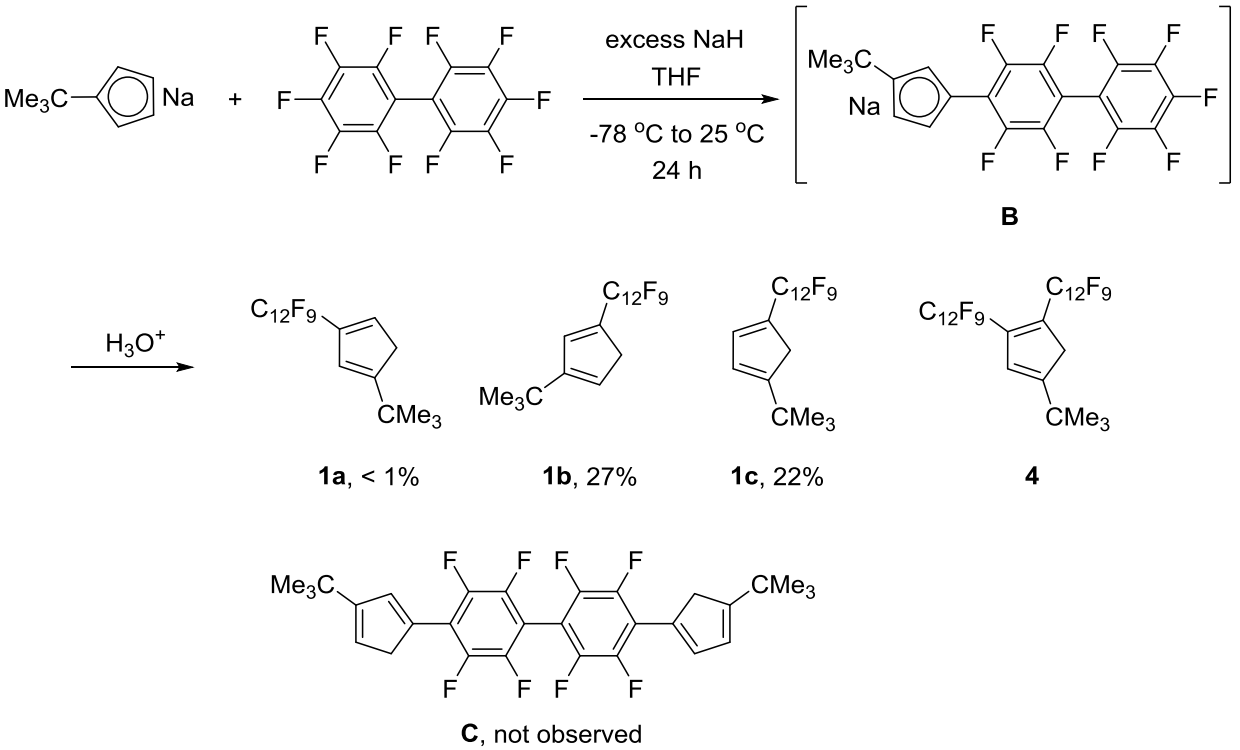

Synthesis of tautomeric diene mixture **1**

To confirm the assignment of **4** (Scheme 3-2), we conducted an analogous arylation (Scheme 3-3) using 2 equiv. of decafluorobiphenyl and increasing the reaction temperature gradually to reflux (in THF). The reaction proceeds to high conversion according to NMR spectroscopic analysis of small aliquots, but recovery of the analytically pure was somewhat inefficient and can likely benefit from further optimization of workup and purification methods.

Scheme 3-3

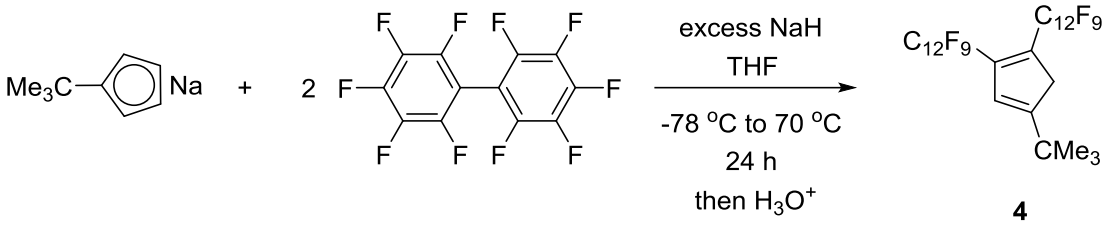

Synthesis of diene **4**

Diene **4** was characterized crystallographically. An ellipsoid plot of the molecular structure of crystalline **4** is provided in the supporting information toward the end of this dissertation. The molecular structure confirms the connectivity shown in the diagram of **4** but otherwise does not exhibit anything especially noteworthy. The aryl-cyclopentadiene torsion angles are ca. 47°. The deviation from a more coplanar conformation likely arises from vicinal steric repulsions of the two aryl substituents.[83] The structure of the diene portion of the molecule is consistent with that of the bis(pentafluorophenyl) analogue.[37] My colleague, Charles S. Carfagna, Jr., has studied the DA chemistry of diene **4** in great detail and will report those results in his own dissertation.

3.4.2 Synthesis of Diels-Alder adducts

Diene **1** reacted with **FMI** to yield mixtures of DA adducts (Scheme 3-4). Reaction progress was readily monitored by ^{19}F NMR spectrometry,[82,84] as the chemical shifts of both the 4-fluorine of the phenyl substituent on the MI and the 4'-fluorine of the $C_{12}F_9$ on the diene are sensitive to adduct formation, although not all five of the adduct signals are resolved from one another. All three of the observed tautomers of diene **1** participate in the formation of adducts, and both *endo* and *exo* forms are observed except for the *exo* isomer of the adduct bearing both substituents at bridgehead positions (**3e**).

Scheme 3-4

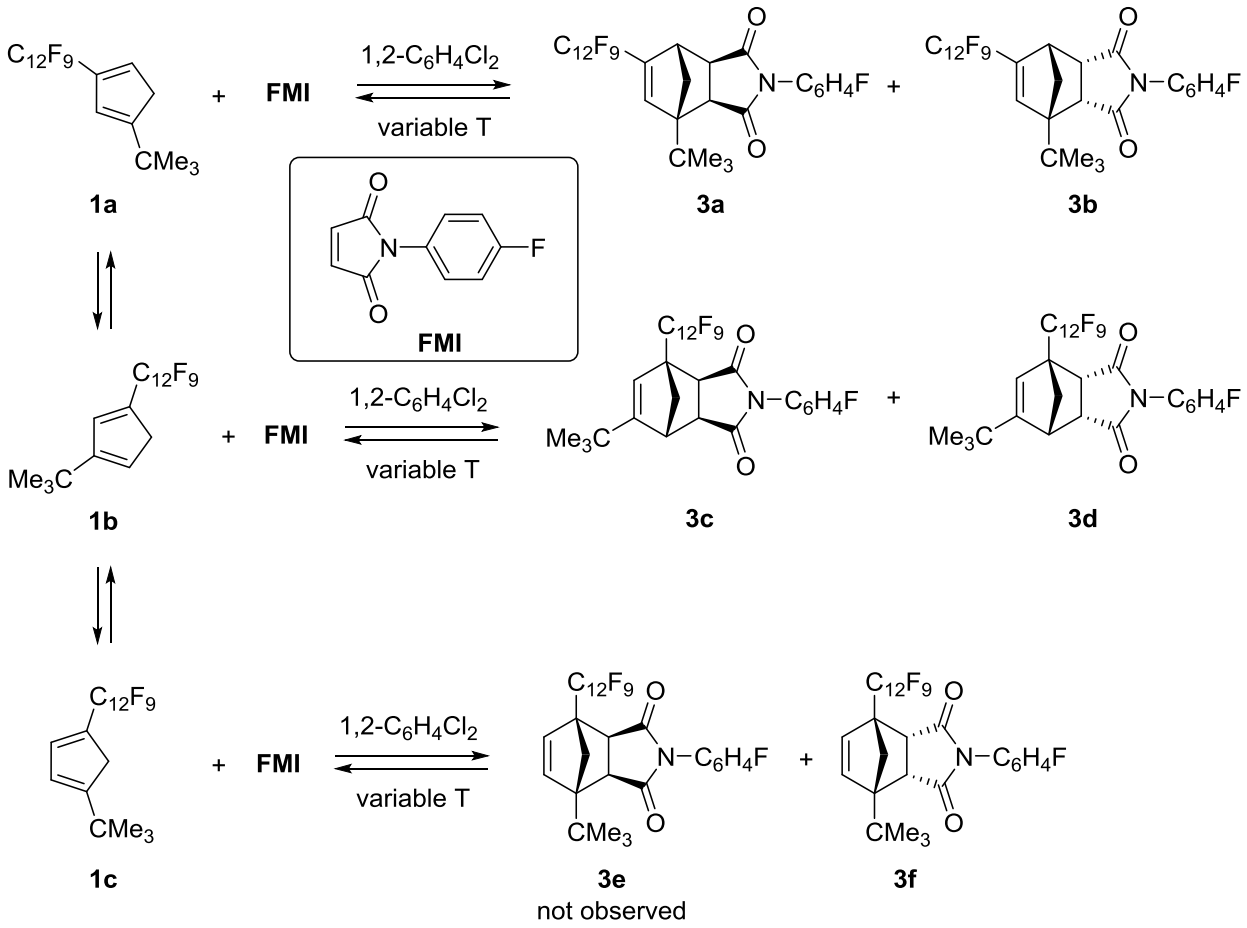

Reaction of tautomeric diene mixture **1b** with **FMI** to for adduct mixture **3**

Adducts **3a-d** were separated by liquid chromatography, and after identifying those four isomers, we were able to assign the fifth isomer **3f** to the minor (ca 35%) component of an additional chromatographic fraction containing **3c** and **3a**. X-ray diffraction studies unequivocally assigned three of the isomers (**3a**, **3b**, and **3c**). Ellipsoid plots are provided in the Supporting Information. Aside from confirming the connectivity and stereochemistry (*exo* vs. *endo*) of the adducts, the structures do not exhibit any especially noteworthy features. Attempts to obtain X-ray-quality crystals of isomer **3d** were unsuccessful. 2D NOE spectrumSY spectra (^{1}H) of the crystallographically characterized isomers were obtained, and only the *endo* isomer **3b** exhibits a through-space interaction of the methine protons α to the carbonyl carbons and one proton of the

methylene bridge. Observation of the corresponding NOE spectrum enhancements in isomers **3d** and **3f** (using 1D-NOE spectrum experiments) thereby confirmed their *endo* stereochemical assignments. Figure 3-2 shows an example of the use of NOE spectrum measurements to characterize adduct stereochemistry. Irradiation of the proximal 7-methylene proton results in NOE spectrum enhancement of the two methine protons adjacent to the carbonyls as well as the geminal methylene proton and a small enhancement of the tert-butyl protons. (Irradiation of the geminal methylene proton at 2.0 ppm does not result in enhancement of the methine signals. Likewise irradiation of the methine protons results in enhancement of just the proximal proton on the 7-methylene.)

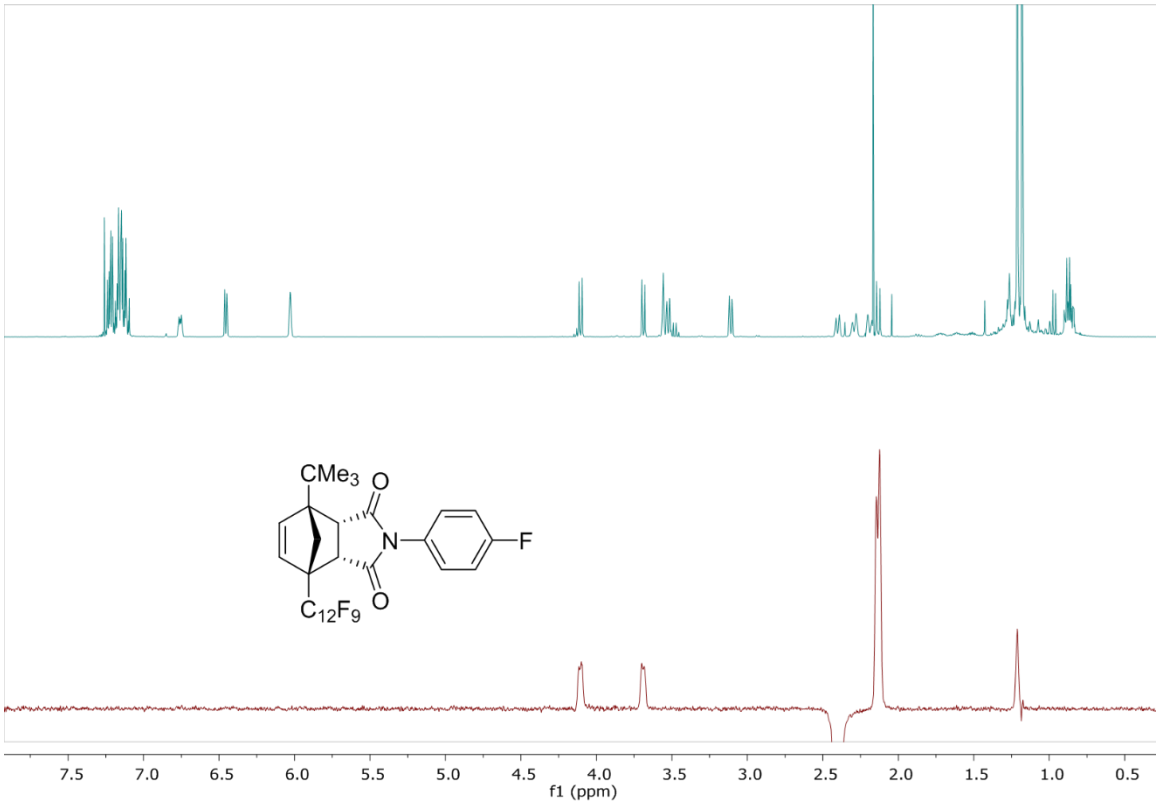

Figure 3-2. Top: ^{1}H (400 MHz, $CDCl_3$) NMR spectrum of **3f** and **3c** mixture; Bottom: 1D ^{1}H NOE spectrum of **3f**: irradiation of methylene proton at δ 2.40 ppm and observed enhancement of methine protons α to the carbonyls δ 4.11 and 3.69 ppm. Enhancement at δ 2.0 and 1.0 are due to the other methylene proton and the *t*-Bu group, respectively.

Isomer **3d** exhibits one vinyl CH signal, whereas isomer **3f** exhibits two vinyl CH signals so their connectivity was assigned on that basis. Isomer **3c** exhibits splitting and exchange-broadening of the ^{19}F NMR signals arising from the $C_{12}F_9$ substituent. Only isomer **3c** has both *exo* stereochemistry and a bridgehead $C_{12}F_9$ substituent. PM3 calculations reveal that the barrier to rotation about the bridgehead-$C_{12}F_9$ bond is much higher in the *exo* isomer **3c** (12 kcal/mol) than in the *endo* isomer **3d** (6 kcal/mol). This feature seems a bit of a curiosity here, but in some of our other, related studies the observation of signal broadening in an ^{19}F NMR spectrum was leading evidence for the formation of *exo* DA adducts with bridgehead perfluoroaryl substituents. Finally, the ^{1}H NMR chemical shifts of the protons adjacent to the carbonyl groups trend upfield with a smaller mutual coupling constant for the two *exo* isomers (2.93 and 3.31 ppm, ^{3}J = 7 Hz for **3a**; 3.11 and 3.52 ppm, ^{3}J = 7 Hz for **3c**), downfield with slightly larger mutual coupling for *endo* isomers (3.63 and 3.72 ppm, J = 8 Hz for **3b**; 3.64 and 3.69 ppm, ^{3}J = 8 Hz for **3d**); the chemical shifts of the corresponding protons in **3f** are consistent with the *endo* assignment (3.69 and 4.11 ppm, ^{3}J = 8 Hz).

3.4.3 Effects of Temperature on Adduct Distribution

The cycloaddition reaction shown in Scheme 3-3 was performed at six temperatures over a 195 °C range (Table 3-1). At lower temperatures, isomer **3f** is formed in significant amounts for two possible reasons. First, the transition state leading to the formation of **3f** from **1c** may be lower in energy than corresponding transition states leading to other products, i.e., kinetic product. As both adducts **3e** and **3f** arise from the same diene isomer **1c**, the observation of only **3f** does seem to present an example of the Alder rule, favoring the formation of *endo* products under kinetic control, whereas the only *exo* isomer formed at low temperature is **3c**. Second, the isomers of **1** may interconvert sufficiently slowly at lower temperatures that the low proportion of diene **1a** in

the reactant mixture could limit the formation of adducts **3a** and **3b**. Similarly *endo* isomer **3d** also seems to be a kinetic product.

The higher reaction temperatures favor formation of isomers **3b** and **3c**, which are apparently the thermodynamic products *within the temperature and reaction time ranges that we studied*. Interestingly, at the highest two temperatures the *exo* isomer **3a** is emerging, whereas the proportion of *endo* isomer **3b** has apparently reached a maximum; *exo* isomers generally are the more stable products in Diels-Alder reactions of cyclopentadienes and furans. We presume that isomers **3e** and **3f** are formed in vanishing quantities at the higher reaction temperatures because of the steric repulsions resulting from two bridgehead substituents. These trends are explored below in the discussion of our computational studies.

Table 3-1. Distributions of products from reactions shown in Scheme 3-4 at varying reaction temperature (T). Each set of products is normalized to a total of 100%.

T (°C)	5	25	50	80	150	200
time, h	3700	160	360	24	20	4
3a	0	0	0	2	8	22
3b	5	15	36	53	49	34
3c	33	38	21	24	40	40
3d	19	20	15	12	3	4
3e	0	0	0	0	0	0
3f	43	27	13	9	0	0

3.4.4 Equilibrium determination

The overall equilibrium constant for the reaction of **1** and **FMI** was determined by heating a solution of the two compounds at 80 °C and periodically subjecting small aliquots to NMR spectroscopic analysis. The relative integrations of **FMI** and adduct concentrations (and presumably also diene concentrations) reached a steady state after 200 hours, in which the ratio of adduct to unreacted FMI was 50(4):1. This ratio represents an equilibrium constant of approximately 4.0(4) x 10^3 M^{-1}. In a further experiment, the temperature was increased to 100 °C

for an additional 670 hours resulting in an increase in the relative total concentration of adducts to FMI (ca. 180:1). We did not determine that these concentrations represented a steady state, but if they did, then the equilibrium constant for binding would be 5.0×10^4 M^{-1}. This value therefore represents a minimum for K_{eq} at 100 °C. We would expect K to decrease as T increases, because of the negative value for the change in entropy for adduct formation. We surmise that the large increase in apparent K_{eq} is caused by the formation of a different distribution of products (specifically, more stable adducts) at higher temperature, in accord with the data presented in Table 3-1.

3.4.5 Computational Studies

The reaction shown in Scheme 3 was subjected to ground-state computational modeling (B3LYP/6-31G*). The formation of DA adduct **3b** as a major product arising from a minor reactant isomer (diene **1a**) suggested the inclusion, in our computational studies, of the two additional diene tautomers **1d** and **1e**, which give rise to another 8 possible DA adducts (Scheme 3-5), even though none of the additional compounds shown in Scheme 3-5 were observed in any of our reactions.

Scheme 3-5

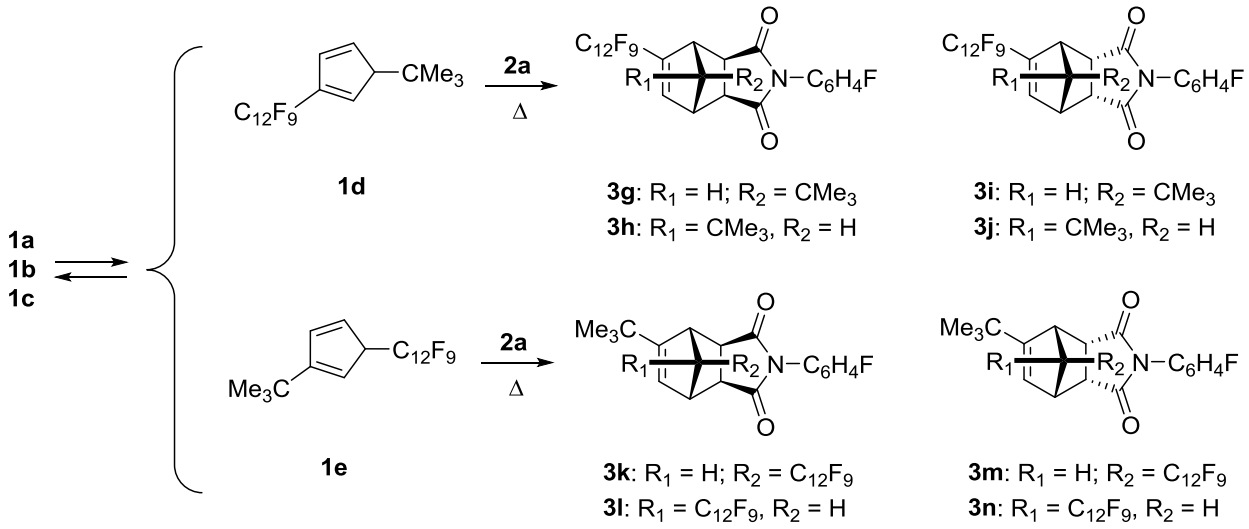

Possible reaction of diene tautomers **1d** and **1e** to form adducts **3g-n**

Geometry optimization and electronic energy calculations (B3LYP/6-31G*) and vibrational frequency calculations afforded the room-temperature free energies collected in Table 3-2. The energies of the 5 possible diene tautomers (**1**) are roughly consistent with the observation of **1b** and **1c** as the major observed isomers of **1** (Scheme 3-1). The cross-conjugated isomer **1a** is calculated to be 2-3 kcal/mol higher than **1b** or **1c** and is observed as a minor component (< 1%). Diene isomers **1d** and **1e** (Scheme 3-5) have electronic energies that are 6-9 kcal/mol higher than **1b** or **1c** and are not observed at all. Isomer **1e** has lost the conjugation of the perfluoroaryl group to the diene moiety and is calculated to have the highest electronic energy of the 5 tautomers.

Table 3-2. Relative enthalpies of formation (kcal/mol) and relative HOMO energies (kcal/mol) of dienes **1** and Diels-Alder adducts **3** that are possible products in the reactions shown in Schemes 3-2 and 3-4. Calculated using B3LYP/6-31G*. Only **1a**, **1b**, **1c**, **3a**, **3b**, **3c**, **3d**, and **3f** were observed.

			ΔΔH of DA adducts with 2a			
Diene	**ΔΔH**	**E_{HOMO}**	***Exo* isomers**		***Endo* isomers**	
1a	3.10	2.3	**3a**, 1.42		**3b**, 1.00	
1b	0.00	3.3	**3c**, 0.00		**3d**, 3.75	
1c	0.05	6.1	**3e**, 8.44		**3f**, 8.93	
1d	7.36	0.4	**3g**, 13.67	**3h**, 2.56	**3i**, 7.51	**3j**, 4.30
1e	8.91	0	**3k**, 5.86	**3l**, 3.87	**3m**, 4.52	**3n**, 6.20

The calculated adduct free energies agree qualitatively with the product distributions observed at higher temperatures (Table 1). Adducts **3a**, **3b**, **3c**, and **3d** are among the most stable, and the two isomers formed at the highest reaction temperature (200 °C), **3b** and **3c**, have the lowest relative free energies. It is curious, however, that **3a** appears at the very highest reaction temperatures, arguably closest to a true thermodynamic regime, yet **3c** was calculated to have the lowest energy. The calculated energy differences among **1a**, **1b**, and **1c** are relatively small. Intuitively, the *exo* isomer having the aryl group conjugated to the double bond (**1a**) should be the most stable. Finally, even though the "wrong" isomers (**3g–3n**) were not observed, the relatively low calculated free energy of **3h** has alerted us to the possibility that DA adducts arising from transient diene isomers may arise in other, closely related systems.

Calculations of transition state energies for the processes shown in Schemes 2 and 4 are well beyond the scope of this work. One could envision a much higher barrier toward formation of adducts **3e** and **3f** because of the presence of two bulky groups (*tert*-butyl, perfluoroaryl) at the reactive carbon atoms of diene **1c**, but **3f** is nevertheless formed at low reaction temperatures. To rationalize this observation we calculated the HOMO energies for diene isomers **1a**–**1e** (Table 2). Presuming that our Diels-Alder reactions operate under "normal" electronic constraints (diene HOMO + dienophile LUMO), a higher diene HOMO energy should facilitate a reaction. Diene

1c is found to have the highest HOMO energy of the five diene isomers (ca. 6 kcal/mol higher than **1e**) and exhibits reactivity at the lowest reaction temperature (5 °C) that is comparable to the less sterically encumbered isomer **1b**, which has the next-highest HOMO energy of the 5 diene isomers (ca. 3 kcal/mol higher than the HOMO of **1e**).

3.4.6 rDA Reactions

Retro-Diels-Alder (rDA) reactions of isolated model adducts **3b**, **3c** and **3d** were examined by three methods. In all cases the *p*-fluorine signal of the maleimide is a clear spectroscopic handle for following reaction progress. In the first method (Scheme 3-6), heating the pure adduct sample in 1,2-dichlorobenzene above 120 °C results in isomerization to a mixture of compounds consistent with the product distributions shown in Table 3-1 for T = 150 °C, the closest reaction temperature to the 120 °C threshold temperature. Isomerization is observed in just 2 h, although it generally requires longer reaction times (ca. 24 h) to observe the ratios reported in Table 3-1. Isomerization is presumed to occur via a rate-limiting rDA reaction.

Scheme 3-6

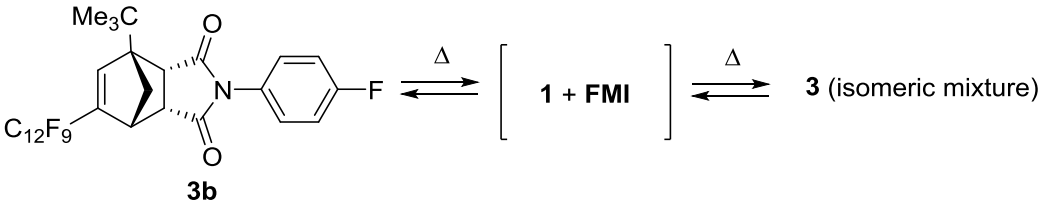

3b

Thermolysis of adduct **3b** to form isomeric mixture **3**

The next method (Scheme 3-7) uses a second monofunctional maleimide in excess, serving as a sink for free diene as it disconnects from the initial maleimide, again following the reaction by the emergence of the characteristic *p*-fluorine signal of free **FMI** (Figure 3-3). Adducts **3b**, **3c**, and **3d** were subjected to this test, gradually increasing the temperature until unbound **FMI** was observed. Adduct **3d** exhibited exchange (ca 15%) with the second maleimide after only 1 hour of heating at 130 °C. Adduct **3c** required approximately 20 hours at 130 °C to show the same level

of maleimide exchange, suggesting it is more resistant to rDA than **3d**. Adduct **3b**, however, exhibited unbound **FMI** (ca 20%) after heating at 130 °C for 8 hours, suggesting it is less resistant to rDA than **3c** and more resistant to rDA than **3d**. This experiment is in agreement with the calculated adduct stabilities from Table 3-2. Figure 3-3 also illustrates the characteristic exchange-broadened spectra that we invariably observe for *exo* adducts having a 1-perfluoroaryl group. If the $C_{12}F_9$ group rotated freely about the C1-aryl bond, one would expect to observe only five signals in addition to the fluorine arising from the maleimide *N*-4-fluorophenyl group downfield.

Scheme 3-7

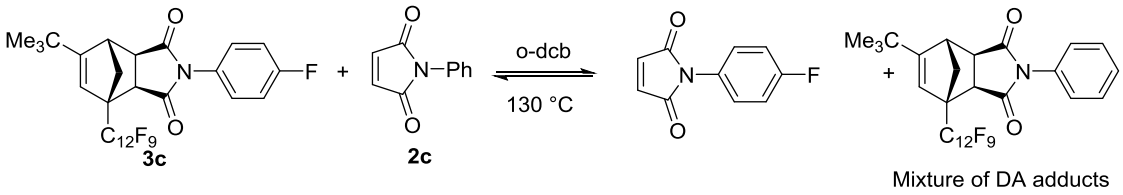

Maleimide exchange reaction of adduct **3c** and maleimide **2c**

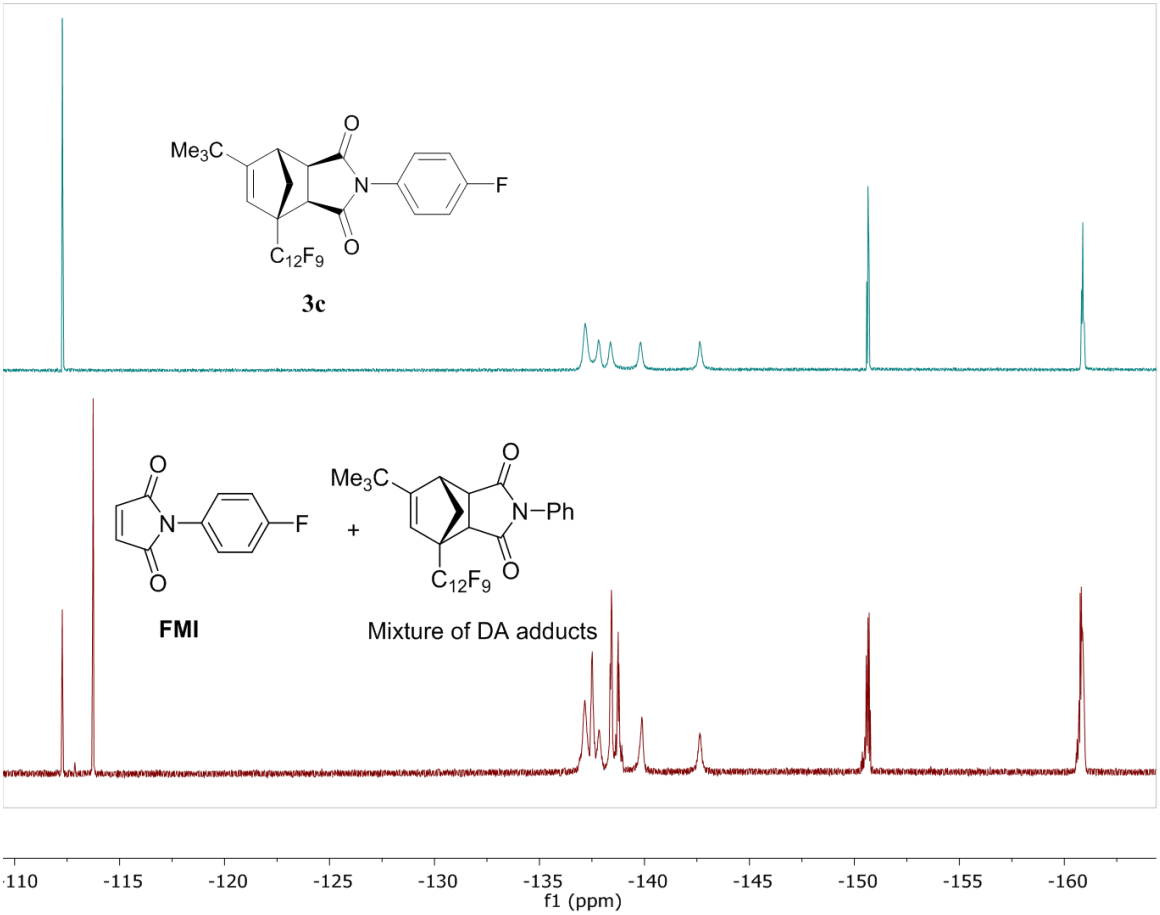

Figure 3-3. ^{19}F (376 MHz, $CDCl_3$) NMR spectrum of **3c** (top); and the appearance of **FMI** (δ -113.52 ppm) and the isomerization of **3c** upon thermolysis (bottom) in the presence of *N*-phenylmaleimide.

The final test was intended as a crude proxy for what might occur in a polymer sample in bulk. Heating the solid model adduct (**3b**) sample to 145 °C for several hours did not show any appreciable isomerization or other evidence of rDA (Figure 3-4). Heating the same sample, however, just above its melting point (152 °C) momentarily, shows complete re-equilibration of the adduct mixture: the adduct reverted, the diene reached tautomeric equilibrium (for the time and temperature allowed), and then reacted with the free maleimide, just as shown in Scheme 3-6 but without any added solvent. Figure 3-5 illustrates these observations. We infer that some solid-phase mobility of the adduct is required for rDA to occur and we surmise that melting of the

crystalline adduct might be analogous to the glass transition process for a polymer linked by DA couplings.

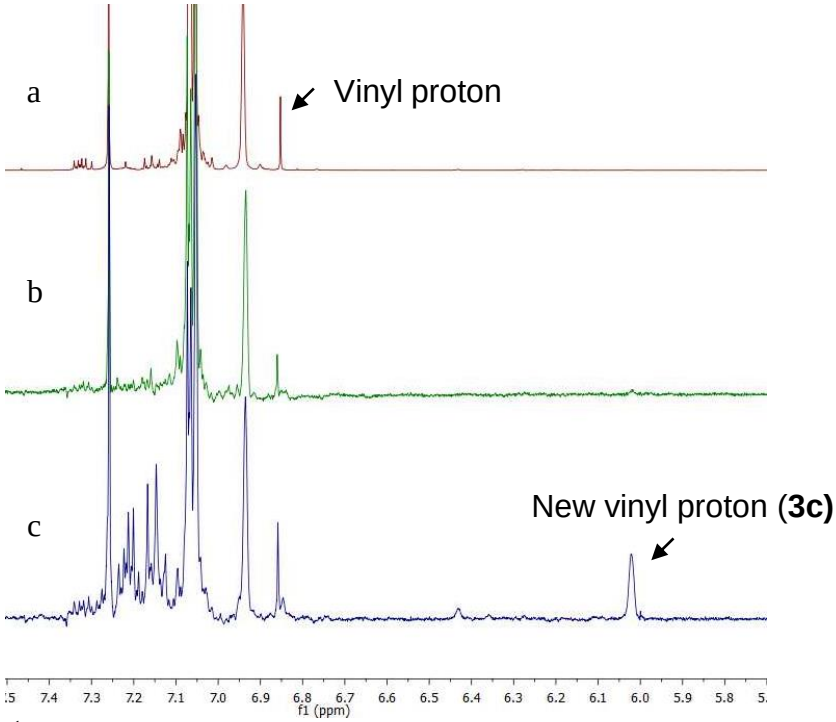

Figure 3-4. ^{1}H (400 MHz, $CDCl_3$) NMR spectra of the vinyl region of model adduct **3b** in $CDCl_3$: **(**a) Initial sample of pure **3b**; (b) Sample after standing overnight at 145 °C; (c) Sample after melting at 152 °C and then immediately quenching to RT.

3.5 Conclusions

A cyclopentadiene bearing one *tert*-butyl substituent and one perfluoroaryl substituent (**1**) undergoes smooth, complete reaction with **FMI**, a typical DA dienophile. Unlike typical monosubstituted cyclopentadienes, however, **1** does not undergo self-dimerization even up to 180 °C, as evidenced by the lack of dimer in reaction mixtures with **FMI**. However, the arrangement of substituents does destabilize the maleimide adduct: the rDA process begins at temperatures as low as 120 °C. These findings confirm our hypothesis that the correct choice and placement of substituents on the cyclopentadiene can both arrest self-dimerization and facilitate rDA.

Chapter 4 Electronic Effects of Isosteric Substituents on Diels-Alder Reactions of Substituted Cyclopentadienes and N-(4-Fluorophenyl)maleimide

Jeremy B. Stegall, Carla Slebodnick, Kimberly F. Tetterton,[2] and Paul A. Deck*

Department of Chemistry, Virginia Tech, Blacksburg, VA 24061

Keywords: Diels-Alder reaction, cycloaddition, electronic substituent effects, reaction kinetics, binding constants, NMR spectroscopy, molecular modeling

Foreward. With the exception of supporting information relegated to the end of the dissertation, this chapter represents a stand-alone manuscript in preparation for submission to the *Journal of Organic Chemistry*. Preliminary work on the synthesis of 1,2,3-tris(perfluoro-4-pyridyl)cyclopentadiene, and 1,2,4-tris(perfluoro-4'-pyridyl)cyclopentadiene, and 1,2,3,4-tetrakis(perfluoro-4'-pyridyl)cyclopentadiene was carried out by Kimberly F. Tetterton, an undergraduate research participant from Hampton University. I performed all of the other experimental work except as follows: Dr. Carla Slebodnick performed the crystallographic data collection, structure solution, and refinement; Bill Bebout performed the mass spectroscopic analyses; Atlantic Microlab, Inc. (Norcross, GA) performed the microanalyses, and Prof. Paul A. Deck supervised my work.

4.1 Abstract

Sodium cyclopentadienide reacts with excess pentafluoropyridine and excess sodium hydride in refluxing THF solution to afford a ca. 1:10:1 mixture of 1,2,3-tris(tetrafluoro-4'-pyridyl)cyclopentadiene (**1c**), 1,2,4-tris(tetrafluoro-4'-pyridyl)cyclopentadienes (**2c**), and 1,2,3,4-tetrakis(tetrafluoro-4'-pyridyl)cyclopentadienes (**7**) in 70% total yield, from which the 1,2,4-triarylated compound (major product) is readily isolated as a pure substance. Both triarylated dienes (**1c** and **2c**), as well as their respective, previously reported pentafluorophenyl- and

[2] Undergraduate research participant.

perfluoro-4-tolyl-substituted congeners, reacted with *N*-(4-fluorophenyl)maleimide to afford Diels-Alder adducts with complete *exo* stereoselectivity. Using NMR spectroscopy, initial rates of adduct formation for the less sterically-encumbered 1,2,3-triarylcyclopentadienes are shown to be 1.35×10^{-2}, 7.38×10^{-3}, and 1.17×10^{-3} $M^{-1}min^{-1}$ for aryl = C_6F_5, 4-$C_6F_4CF_3$, and 4-C_4F_5N, respectively. Rates for the corresponding 1,2,4-triarylcyclopentadienes are 1.22×10^{-3}, 3.82×10^{-4}, and 3.65×10^{-4} $M^{-1}min^{-1}$, respectively. Because electron-withdrawing power of the substituents increases in the order $C_6F_5 < C_6F_5CF_3 < C_4F_5N$, these observations suggest that these Diels-Alder reactions proceed according to a "normal electron demand" scenario in which the HOMO of the diene engages the LUMO of the dienophile. Increasingly electron-withdrawing substituents stabilize the HOMO, increasing the energy gap between HOMO and LUMO and thereby increasing the activation barrier toward cycloaddition and lowering the observed reaction rate. In addition, none of the aforementioned cycloadditions proceed to completion at the temperatures (100 – 150 °C) and concentrations (ca. 0.08 – 0.09 M) at which the reactions were studied. Rather, they approach temperature-dependent, steady-state concentrations of diene, dienophile, and adduct suggesting that adduct formation is reversible and that binding constants (15 – 500 M^{-1}) are considerably lower than those observed for unsubstituted cyclopentadiene. B3LYP/6-31G(d) calculations of orbital energy levels and overall reaction enthalpies generally supported these conclusions.

4.2 Introduction

In synthetic chemistry, the Diels-Alder (DA) reaction is prized for the production of two new C—C bonds, with useful regio- and stereoselectivity, and for its generally strong overall thermodynamic driving force. Because no additional stoichiometric reagents are needed and no by-products are formed, the Diels-Alder reaction also represents the ideal of atom economy.[85] In principle, however, the Diels-Alder reaction should always be reversible unless the adduct

undergoes further reaction (e.g., oxidation[86-88] or electrocyclic extrusion[89]) or is deliberately modified in a manner that disrupts its cyclohexene core structure. Moreover, the retro-Diels-Alder (rDA) reaction can be useful, either in protective-group strategies or in the development of materials, such as re-mendable polymers,[18,19,31,90] in which a purely thermal, reversible bond formation/rupture process is needed to adjust physical properties[16,17,91-93] or chemical functionality.[24,94]

All aspects of the Diels-Alder reaction (relative rates, overall driving forces, and selectivity factors) are strongly influenced by reactant substituents. The "normal" preference for electron-rich dienes and electron-deficient dienophiles is described in many standard textbooks of organic chemistry:[95] this combination minimizes the HOMO-LUMO energy gap corresponding to the electronic reaction barrier. Steric effects are more difficult to investigate in a systematic, quantitative way and can often complicate the analysis of electronic effects. For example, reactivity studies of 2-substituted butadienes [96,97] required deconvolution of the equilibrium *s*-cis conformer populations from the observed reaction rates. This problem is avoided by using conformationally rigid (i.e., cyclic) dienes such as furan, anthracene, and triazole,[5,63,65,98-100] which also conform to "normal electron demand" substituent-effects theory.

As part of our ongoing exploration of fluoroaryl-substituted cyclopentadienes,[48] we are interested generally in their reactivity as dienes in the Diels-Alder reaction and more specifically in their use as reactive groups in thermally reversible polymerization. We are motivated to work somewhat against the normal substituent effect preferences to find systems with *decreased* overall driving force such that adduct formation might be more freely reversible. In this report we demonstrate the effects of fluoroaryl substituents on the course of Diels-Alder reactions of tris(fluoroaryl)cyclopentadienes.

There are relatively few systematic studies of substituent effects on Diels-Alder reactions of cyclopentadienes, probably because cyclopentadiene tautomerization presents an additional, annoying complication (Figure 4-1). Depending on the substituents (R), interconversion among tautomers might occur at rates that are competitive with cycloaddition, resulting in a quite complicated overall kinetic picture. It is perhaps for this reason that all published accounts have explored either substitution of the dienophile in reactions of the unsubstituted parent cyclopentadiene,[96] or reactions of cyclopentadiene derivatives that do not tend to tautomerize such as 6,6-diarylfulvenes[99,101] or tetracyclones,[102] both of which show slower reactions with more electron-withdrawing substituents. Additionally, phenyl-substituted cyclopentadienes are generally hard to synthesize,[83,103-105] which makes conventional Hammett-type studies unappealing.

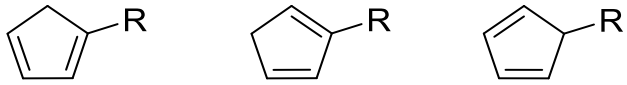

Figure 4-1. Tautomers of a monosubstituted cyclopentadiene. The 5-substituted tautomer is preferred only in special cases such as R = $SiMe_3$ or R = $SnMe_3$.

We have four reasons for selecting 1,2,3- and 1,2,4-tris(fluoroaryl)cyclopentadienes for the present study (please see Figure 4-2): (1) We expected that the fluoroaryl groups would frustrate Diels-Alder adduct formation, but we didn't know by how much; (2) the preference for fluoroaryl groups to conjugate with the double bonds of the cyclopentadiene ring limits tautomerization; (3) we have developed a general synthesis of the compounds based on nucleophilic aromatic substitution chemistry; and (4) *the isosteric nature of the three readily available perfluoroaryl substituents allows us to study electronic substituent effects in isolation*. The perfluoro-4-pyridyl-substituted dienes **1c** and **2c** are new substances and their syntheses and characterization are described below. We chose a "normal," electron-deficient dienophile, *N*-(4-fluorophenyl)maleimide, which also provides a "label" that enables reactions to be followed using

^{19}F-NMR spectrometry. [The maleimide is assigned the number **FMI** to be consistent throughout the dissertation, but in the manuscript it will have the designator **3**.]

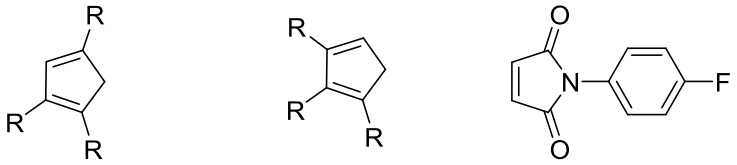

1a: R = C_6F_5
1b: R = 4-$C_6F_4CF_3$
1c: R = 4-C_5F_4N

2a: R = C_6F_5
2b: R = 4-$C_6F_4CF_3$
2c: R = 4-C_5F_4N

FMI

Figure 4-2. Substrate cyclopentadienes and maleimide dienophile selected for a study of electronic substituent effects in the Diels-Alder reaction.

4.3 Experimental Section

4.3.1 General Considerations.

Air-sensitive solids were handled inside an Innovative Technology nitrogen glove box maintained at an oxygen partial pressure of ca. 1 ppm. NMR spectra were acquired on either a Varian Inova 400 NMR spectrometer, an Agilent 400-MR DD2 NMR spectrometer or a Bruker Avance II 500 NMR spectrometer. ^{1}H NMR spectra were referenced to $CHCl_3$ (7.26 ppm) in $CDCl_3$. ^{19}F NMR spectra were referenced to external C_6F_6 in $CDCl_3$ (−183.0 ppm). Mass spectra were recorded using an Agilent 6220 Accurate-Mass TOF LC/MS using direct infusion into 2:1 methanol/water (0.1% formic acid) at a flow rate of 0.4 mL/min. Melting points were acquired using open capillaries on a Buchi B-545 melting point apparatus and are uncorrected. Solvents were used as received from Fisher or Aldrich except THF, which was further purified by passage through molecular sieves, and $CDCl_3$, which was obtained from Cambridge Isotope Laboratories. Maleimide **FMI**,[50] sodium cyclopentadienide,[106] dienes **1a** and **2a**,[83] and dienes **1b** and **1c**,[107] were prepared as previously reported. Elemental microanalyses were performed by Columbia Analytical Services (Tucson, AZ) or Atlantic Microlab (Norcross, GA).

4.3.2 Aliquot analysis method

An aliquot (0.5-mL) was removed from the reaction using a disposable syringe and injected into a test tube or vial containing 1 mL of 10% aqueous sulfuric acid and 1 mL of $CDCl_3$. The lower organic layer was washed with water (1 mL) and brine (1 mL), dried over $MgSO_4$, and then filtered through ca 1 cm of diatomaceous earth into a small flask. The solvent was removed by rotary evaporation and the residue taken up in a new 0.6-mL portion of $CDCl_3$ for NMR analysis.

4.3.3 Synthesis of Tris(perfluoro-4-pyridyl)cyclopentadienes (1c and 2c)

Under an atmosphere of dry nitrogen, a mixture of sodium cyclopentadienide (2.00 g, 22.7 mmol), sodium hydride (2.20 g, 91.7 mmol), and anhydrous THF (50 mL) in a septum-sealed 200-mL Schlenk flask was cooled to 0 °C with magnetic stirring. Pentafluoropyridine (14.9 g, 87.9 mmol) was added in small portions over several minutes using a syringe. The mixture was stirred and gradually warmed to room temperature over 0.5 h, during which interval it turned yellow, then green, and finally brown. A condenser was fitted, and the mixture was stirred at reflux for 48 h. After cooling, the THF was evaporated under vacuum to a liquid nitrogen trap. Dichloromethane (100 mL) was added to the brown residue, and the resulting slurry was quenched with 10% H_2SO_4 (100 mL), and the resulting biphasic mixture was separated. The organic layer was washed with water (2 x 100 mL) and brine (100 mL), dried over $MgSO_4$, filtered through diatomaceous earth, and evaporated to afford 10.7 g (92% crude) of a brown solid. The crude product was subjected to liquid chromatography through a 10-cm (width) x 7-cm (height) bed of silica gel, eluting with dichloromethane. Three bands were collected. The first band afforded 3.0 g of a pale solid that was found by NMR spectroscopic analysis to contain dienes **1c** and **2c** as a 10:1 mixture. A second, darker fraction (0.5 L of solvent) was evaporated to afford 3.2 g of a brown pasty solid that was found to contain **1c**, **2c**, and **7** in a 65:15:20 ratio according to NMR analysis. A third fraction (3 L) was evaporated to afford 0.7 g of a tan solid that was mostly **7** with small amounts of **1c** and

2c. A 1.0-g portion of the solid recovered from the first chromatographic band was dissolved in 100 mL of hot toluene containing 1.0 g of trifluoroacetic acid, filtered through a thin pad of silica gel to decolorize, and cooled in a freezer (−10 °C) to afford a microcrystalline solid, which was collected on a filter and dried under vacuum to afford 570 mg of **1c** (NMR purity > 98%). Attempts to find liquid chromatographic conditions to separate these species further, in order to isolate the minor 1,2,3-substituted isomer **2c**, were not successful. NMR data for **1c** was obtained from a pure sample; data for **2c** was obtained from a sample containing **1c** (major) and **2c** (minor).

Data for diene **1c**: mp 168-174 °C. ^{1}H NMR (400 MHz, $CDCl_3$): δ 7.7 (s, 1H), 4.4 (s, 2H). ^{19}F NMR (376 MHz, $CDCl_3$): δ −88.3 (m, 2F), −88.4 (m, 2F), −90.4 (m, 2F), −141.1 to −141.4 (m, 6F). Anal. calcd. for $C_{20}F_{12}H_3N_3$: C, 46.80; H, 0.59; N, 8.19. Found: C, 46.73; H, 0.53; N, 8.23.

Data for diene **2c**: ^{1}H NMR (400 MHz, $CDCl_3$): δ 7.3 (s, 1H), 4.0 (s, 2H). ^{19}F NMR (376 MHz, $CDCl_3$): δ −87.7 (m, 2F), −88.4 (m, 2F), −88.7 (m, 2F), −141.6 (m, 4F) −142.2 (m, 2F). HRMS analysis of the isomeric mixture (ESI-TOF): *m*/*z* calcd. for $C_{20}F_{12}H_2N_3$ $(M-H)^-$ 512.0063, found $(M-H)^-$ 512.0105. Anal calcd for $C_{20}F_{12}H_3N_3$ C, 46.80; H, 0.59; N, 8.19. Found C, 46.73; H, 0.53; N, 8.23.

4.3.4 Synthesis of Diels-Alder Adducts 5 and 6

All of the DA adducts reported herein were prepared in the manner illustrated as follows for adduct **6a**. A solution of 1,2,3-tris(pentafluorophenyl)cyclopentadiene (0.285 g, 0.505 mmol) and maleimide **3** (0.104 g, 0.547 mmol) in 1.0 g of toluene or 1,2-dichlorobenzene was heated under nitrogen at 100 °C for 145 h. The initially pale-yellow solution turned a deep red color over the reaction interval. Cooling and evaporation of the solvent afforded a dark purple residue that was found by ^{1}H NMR spectroscopic analysis to contain a single Diels-Alder adduct (**6a**). The residue was dissolved in a solution of ethyl acetate (30%) in hexanes with the intention to perform liquid

chromatography, but a microcrystalline solid formed instead, which was collected on a filter and dried to afford 75 mg (0.10 mmol, 20%) of a pink solid, which was found to be the pure adduct **6a** by NMR analysis. The mother liquor was then subjected to silica gel chromatography, eluting with 30% ethyl acetate in hexane. The first UV-active band (400 mL) was concentrated, and upon standing a microcrystalline solid formed, which was collected on a filter, and dried under vacuum to afford an additional 0.150 g (0.20 mol, 39%) of **6a**: mp 225–227 °C, with yellowing. ^{1}H NMR (400 MHz, $CDCl_3$): δ 7.2 (m, 4H), 3.9 (d, *J* = 8 Hz, 1H), 3.8 (s, 1H), 3.8 (d, *J* = 8 Hz, 1H), 3.1 (d, *J* = 10 Hz, 1H), 2.3 (d, *J* = 11 Hz, 1H). ^{19}F NMR (376 MHz, $CDCl_3$): δ −111.3 (s, 1F), −134.5 (broad s, 1F), −137.4 (d, *J* = 19 Hz, 2F), −138.5 (d, *J* = 23 Hz, 1F), −140.6 (broad s, 1F), −140.9 (d, *J* = 23 Hz, 1F), −149.4 (t, *J* = 20 Hz, 1F), −150.9 (t, *J* = 20 Hz, 1F), −151.8 (t, *J* = 20 Hz, 1F), −159.1 (m, 1F), −159.7 (m, 2F), −160.0 (broad s, 1F), −161.6 (broad s, 1F). HRMS (ESI-TOF): m/z calcd. for $C_{33}F_{16}H_9NO_2$ $(M-H)^-$ 754.0305, found $(M-H)^-$ 754.0367. The structure of **6a** was confirmed crystallographically as described below.

Data for Adduct 5a. Prepared according to the general procedure illustrated above for **6a**, except that the reaction time was 20 d, and the product was obtained by crystallization directly from the reaction mixture at −10 °C, collected on a filter, and washed with hexanes to afford 170 mg (43%) of a white solid, mp 185–190 °C. ^{1}H NMR (400 MHz, $CDCl_3$): δ 6.8 (s, 1H), 4.0 (d, 1H, *J* = 7 Hz), 3.7 (d, 1H, *J* = 7 Hz), 3.4 (d, 1H, *J* = 11 Hz), 2.8 (d, 1H, *J* = 11 Hz). ^{19}F NMR (376 MHz, $CDCl_3$): δ −111.1 (m, 1F), −134.9 (br s, 1F), −138.4 (br s, 1F), −140.0 (br s, 3F), −142.6 (br s, 1F), −150.6 (t, *J* = 21 Hz, 1F), −151.9 (t, *J* = 21 Hz, 1F), −153.0 (t, *J* = 21 Hz, 1F), −160.2 to −161.2 (two br s, 6F). HRMS (ESI-TOF): m/z calcd. for $C_{33}F_{16}H_8NO_2$ $(M-H)^-$ 754.0305, found $(M-H)^-$ 754.0380. Anal. Calcd. for $C_{33}F_{16}H_9NO_2$: C, 52.5; H, 1.20; N, 1.85. Found: C, 52.42; H, 1.15; N, 2.01. The structure of **5a** was confirmed crystallographically as described below.

Synthesis of Adduct 6b. Prepared according to the general procedure illustrated above for **6a**, except that the reaction time was 20 d, and the product was obtained by crystallization directly from the reaction mixture at −10 °C, collected on a filter, and washed with hexanes to afford 361 mg (90%) of a solid that was found by NMR analysis to contain about 10% of **FMI**. An analytical sample was obtained by crystallization by layering a 1,2-dichlorobenzene solution of the crude compound with hexanes. mp 210–215 °C. ^{1}H (400 MHz, $CDCl_3$): δ 7.4 – 7.1 (m, 4H), 4.0 (d, *J* = 7.4 Hz, 1H), 3.9 (s, 1H), 3.8 (d, *J* = 7.5 Hz, 1H), 3.2 (d, *J* = 11.1 Hz, 1H), 2.3 (d, *J* = 10.8 Hz, 1H). ^{19}F (376 MHz, $CDCl_3$): δ −57.4 (m, 9F), −111.9 (m, 1F), −133.9 (br s, 1F), −136.5 (m, 2F), −137.4 (m, 1F), −137.8 (br s, 1F), −138.7 (m, 2F), −139.1 (m, 1F), −139.5 (br s, 1F), −140.0 (m, 1F), −141.6 (br s, 1F). $C_{36}F_{22}H_9NO_2$ HRMS (ESI-TOF): *m/z* calcd. for $C_{36}F_{22}H_8NO_2$ $(M-H)^-$ 904.0209, found $(M-H)^-$ 904.0213. Anal. Calcd. for $C_{36}F_{22}H_9NO_2$: C, 47.76; H, 1.00; N, 1.55. Found: C, 48.04; H, 0.98; N, 1.79. The structure of **6b** was confirmed crystallographically as described below.

Synthesis of Adduct 5b. NMR analysis showed that 44% of the starting diene had been captured as a DA adduct, which was isolated in ca. 20% overall yield as a pale solid. mp 197-198 °C. ^{1}H (400MHz, $CDCl_3$) δ ppm: 7.1 (m, 4H), 6.9 (s, 1H), 4.1 (d, 1H, *J* = 7 Hz), 3.8 (d, 1H, *J* = 8 Hz), 3.5 (d, 1H, 11 Hz), 2.9 (d, 1H, *J* = 11 Hz). ^{19}F (376MHz, $CDCl_3$) δ ppm: −56.3 to −56.5 (m 9F), −111.6 (m, 1F), −136.6 (broad, 2F), −138.1 (4F), −138.3 (broad, 2F), −140.0 (broad, 2F), −140.7 (broad, 2F). The compound appears to undergo rDA within the electrospray ionization apparatus of the mass spectrometer; efforts to find instrumental parameters to enable the observation of a molecular ion were not successful. An insufficient quantity of this compound was available for microanalysis. Evidence of substantial bulk purity can be obtained by examination of the NMR spectra provided in the supporting information toward the end of this dissertation.

Synthesis of Adduct 6c. Because diene **2c** was only observed as an inseparable minor component of mixtures with the isomeric diene **1c**, we had to react them as a mixture in order to obtain data for the adduct **6c**. As a result, several of the signals in the NMR spectra are occluded by signals from **5c** and the starting dienes. In the ^{1}H NMR spectrum (400 MHz, $CDCl_3$), the region from 2-3 ppm typically only contains signals for the protons attached to the 7-carbon of the norbornene moiety, and we were able to observe two signals assigned to **6c** at 2.9 (d, 1H, J = 8 Hz) and 2.0 (d, 1H. 11 Hz). In the ^{19}F NMR spectrum ($CDCl_3$, 376 MHz), the signal arising from the 4-fluorophenyl group is well resolved at −111.7 (m, 1F). Because **6c** is a minor component of a complex mixture, mass spectral data and microanalyses are not available. The assignment of **6c** should be considered tentative.

Synthesis of Adduct 5c. The procedure for **6b** was followed, except that the reaction time was 20 days and the conversion was still very low at that time. An analytical sample was obtained by preparative TLC on silica gel, eluting with 20% ethyl acetate in hexanes to afford a few milligrams of a white solid. mp 167–168 °C. ^{1}H (400MHz, $CDCl_3$) δ ppm: 7.0 (s, 1H), 4.1 (d, 1H, J = 7), 3.9 (d, 1H, J = 7 Hz), 3.5 (d, 1H, J = 10 Hz), 2.9 (d, 1H, J = 10 Hz). ^{19}F (376MHz, $CDCl_3$) δ ppm: −110.7 (m, 1F), −87.7 (m, 2F), other fluorine signals are co-incident with starting diene **1c**. Insufficient compound was available for microanalysis, and the adduct is not stable under the conditions of electrospray mass spectrometry.

Synthesis of 7. Under an atmosphere of dry nitrogen, a mixture of sodium cyclopentadienide (1.00 g, 10.9 mmol), sodium hydride (1.30 g, 54.2 mmol), and DMPU (20 mL) in a septum-sealed 200-mL Schlenk flask was cooled to 0 °C with magnetic stirring. Pentafluoropyridine (9.1 g, 54 mmol) was added in one portion using a syringe. Stirring was maintained and the mixture was heated at 150 °C for 24 h. The reaction was monitored by the aliquot method described above.

Once complete, the reaction was quenched using 10% H_2SO_4 (25 ml) and DI H_2O (25 mL) followed by further dilution with CH_2Cl_2 (50 mL). The dark purple solution was washed with water (6 x 50 mL) to remove DMPU and then rotary evaporated to afford a thick viscous purple oil. The oil was then taken up in methanol and triturated with 10% H_2SO_4 then filtered. The filter cake was washed with 10% H_2SO_4 (3 x 50 mL) and DI H_2O (50 mL), dried on the frit for several hours, then by vacuum with liquid nitrogen trap overnight. A light purple solid was recovered (5.3 g, 74%). Attempts to determine a melting point result only in gradual decomposition to a black substance. ^{1}H (400MHz, $CDCl_3$) δ ppm: 4.4 (s, 2H). ^{19}F (376MHz, $CDCl_3$) δ ppm: −86.5 (m, 4F), −87.3 (m, 4F), −140.9 (m, 4F), −141.0 (m, 4F). HRMS (ESI-TOF): *m/z* calcd. for $C_{25}F_{16}HN_4$ $(M-H)^-$ 660.9951 found $(M-H)^-$ 660.9977.

4.3.5 Reaction Rate and Equilibrium Constant Measurements

Initial rate constants for Diels-Alder reaction of dienes **1** and **2** with **FMI** were determined using ^{19}F NMR spectroscopy. Solutions having diene and maleimide concentrations of ca. 0.0800 M and 0.0900 M, respectively, were prepared in 1,2-dichlorobenzene in an NMR tube. A sealed capillary containing DMSO-d_6 was inserted as an external reference for deuterium frequency lock, magnetic field homogeneity adjustments (shims), and approximate calibration of the chemical shift. The NMR tube was placed into an oil bath maintained at 100 °C using a thermostat. Samples were removed, quickly cooled to room temperature for ^{19}F NMR spectroscopic analysis, and then returned to the oil bath. Reactions of 1,2,3-triarylcyclopentadienes (**2**) were monitored every ten minutes, whereas reactions of 1,2,4-triarylcyclopentadienes (**1**) were slower and were monitored hourly, until 10% conversion was reached. The 4-fluorophenyl signal of **FMI** shifted downfield by ca. 2 – 3 ppm upon incorporation into the adduct. Integration of the free and bound maleimide signals provided a reproducible means of determining reaction progress.

4.3.6 Computational Modeling.

WebMO was used to perform PM3 geometry optimization and then calculate the HOMO for dienes **1** and **2** using B3LYP/6-31G(d). The same methods were used to calculate the LUMO for maleimide FMI. This enabled the HOMO-LUMO gap between the dienes and the maleimide to be determined. Data from these calculations are presented in Table 4-2 below.

4.3.7 Crystallography (Dr. Carla Slebodnick wrote these experimental procedures)

A colorless prism (0.10 x 0.35 x 0.66 mm^3) of diene **1c** was centered on the goniometer of an Agilent Gemini E Ultra diffractometer operating with MoKα radiation. The data collection routine, unit cell refinement, and data processing were carried out with the program CrysAlisPro.[51] The Laue symmetry and systematic absences were consistent with the monoclinic space group $P2_1/n$. The structure was solved using SHELXS-97[52] and refined using SHELXL-97[52] via OLEX2.[53] The final refinement model involved anisotropic displacement parameters for non-hydrogen atoms and a riding model for all hydrogen atoms. The site of the sp^3-hybridized carbon of the cyclopentadiene group was modeled as being disordered between C3 and C5, with relative occupancies that refined to 0.560(16) and 0.440(16), respectively. This type of disorder is a common feature of crystalline substituted cyclopentadienes.

Multiple crystals of **5a** were screened and none were single. A colorless needle (0.03 x 0.04 x 0.20 mm^3) was chosen and centered on the goniometer of an Agilent Nova diffractometer. Ninety-nine percent of reflections from the crystal could be fit to a 2-component system. The data was processed as a non-merohedral twin, generating an "HKLF 5" file to be used in the refinements. The Laue symmetry was consistent with the triclinic space groups P1 and P-1. The centric space group P-1 was chosen. The data collection routine, unit cell refinement, and data processing were carried out with the program CrysAlisPro. The structure was solved using SHELXS-2013 and

refined using SHELXL-2013 via OLEX2. The final refinement model involved anisotropic displacement parameters for non-hydrogen atoms and a riding model for all hydrogen atoms. The relative ratios of the two components refined to 0.5332(13).

A colorless plate (0.07 x 0.21 x 0.32 mm^3) of **6b** was centered on the goniometer of an Agilent Nova diffractometer. The data collection routine, unit cell refinement, and data processing were carried out with the program CrysAlisPro. The Laue symmetry and systematic absences were consistent with the orthorhombic space group Pbca. The structure was solved using SHELXS-2013 and refined using SHELXL-2013 via OLEX2. The final refinement model involved anisotropic displacement parameters for non-hydrogen atoms and a riding model for all hydrogen atoms. The residual electron density map suggested minor disorder of the $-CF_3$ groups, accounting for the relatively large residual electron density peak. The secondary conformations were minor, and attempts to model the disorder required excessive restraints with minimal impact on the refinement statistics. The disorder models were abandoned.

A colorless rod (0.05 x 0.08 x 0.245 mm^3) of **6a** was centered on the goniometer of an Agilent Nova diffractometer. The data collection routine, unit cell refinement, and data processing were carried out with the program CrysAlisPro. The structure was solved using SHELXS-2013 and refined using SHELXL-2013 via OLEX2. The Laue symmetry and systematic absences were consistent with the monoclinic space groups $P2_1$ and $P2_1/m$. In addition, the reflections for the *n*-glide were systematically weak. The structure could be solved in both $P2_1$ and $P2_1/n$., but not $P2_1/m$. Refinement in $P2_1/n$ converged to R1= 13.14% and the structure model displayed elongated anisotropic displacement ellipsoids in the $C_{33}H_9F_{16}NO_2$ moiety. Because of symmetry constraints, the structure model in $P2_1/n$ required that a disordered $CHCl_3$ be modeled with 50% occupancy at each site. In space group $P2_1$, relative occupancies of the $CHCl_3$ refined to 0.861(3)

and 0.139(3) and the refinement converged to R1 = 4.07%. The final refinement model in $P2_1$ involved anisotropic displacement parameters for non-hydrogen atoms, except the minor $CHCl_3$ component. A riding model was used for all hydrogen atoms. The structure was refined as an inversion twin and the Flack parameter refined to 0.492(18).[108] All anisotropic displacement ellipsoids were of reasonable shape and magnitude. Overlay of the "pseudo-equivalent" molecules in $P2_1$ showed RMSD ($C_{33}H_9F_{16}NO_2$ moiety) = 0.224 Å and RMSD ($CHCl_3$) = 0.095 Å.

4.4 Results and Discussion

4.4.1 Substituted Cyclopentadiene Synthesis and Characterization

Dienes **1a**, **1b**, **2a**, and **2b** were already in hand from our previous work.[48,83,107] The new dienes **1c** and **2c** were prepared as shown in Scheme 4-1.

Scheme 4-1

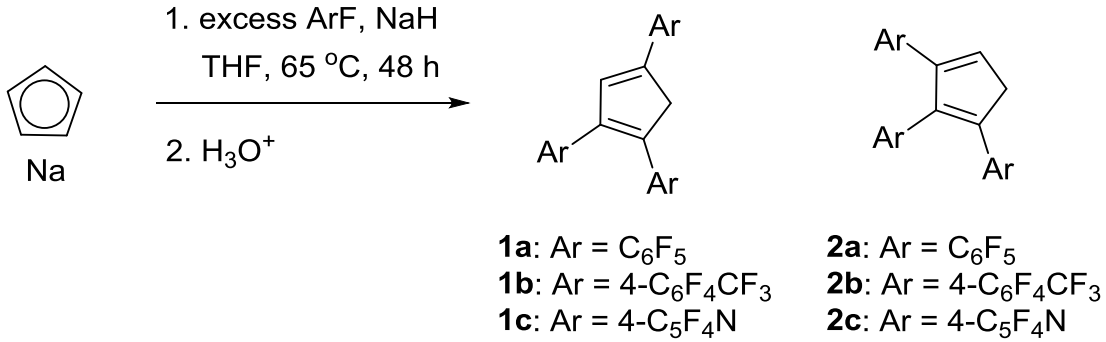

Synthesis of tri-substituted dienes **1** and **2**

Compounds tentatively identified as the mono- and diarylated analogues of **1c** and **2c** were observed as intermediates at lower reaction temperatures and shorter reaction times by working up small aliquots and analyzing the mixtures obtained by NMR spectroscopy; their isolation and use as ligands for transition metals will be reported elsewhere.[109] A small signal at 4.45 ppm in the ^1H NMR spectrum was assigned to the tetraarylated cyclopentadiene **7** (see below). The proportion of **2c** in the crude product mixture was typically 10% - 15%. In preliminary work performed by Kimberly F. Tetterton, the ratios of **1a**:**2a** and **1b**:**2b** were less lopsided than **1c:2c**. While we

were unable to separate **1c** and **2c** on a column (or even by TLC), the small proportion of **2c** enabled us to obtain **1c** cleanly by crystallization from toluene acidified with TFA.

In order to confirm the assignment of diene **7** we deliberately prepared this compound using an analogous nucleophilic arylation reaction at a higher temperature (Scheme 4-2). While NMR spectra of the crude products clearly indicate its formation (one CH_2 signal in the proton spectrum and two chemically distinct C_5F_4N groups in the fluorine spectrum), its purity was perhaps about 80%. The best purification method so far seems to be reprecipitation of a methanol solution in 10% aqueous sulfuric acid. The observation of selectivity for the formation of the tetraarylcyclopentadiene under forcing conditions has precedent in our earlier accounts[83,107] of the C_6F_5- and $C_6F_4CF_3$-substituted analogues. Compound **7** was outside the scope of our present study so we did not pursue it further.

Scheme 4-2

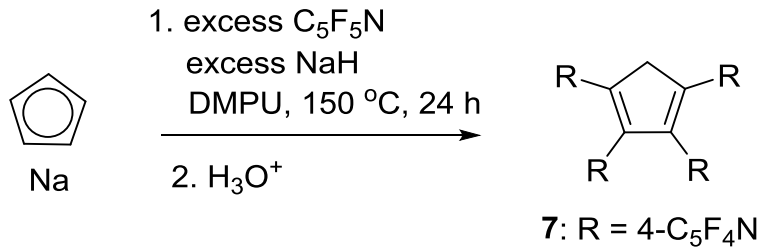

Synthesis of tetra-substituted diene **7**

The new compounds **1c**, **2c**, and **7** were characterized primarily by NMR spectroscopy. Both triarylated compounds show a single vinyl CH signal and a single CH_2 signal: however, Deck and co-workers have previously shown that the CH_2 signal of the 1,2,4-triarylated isomer is downfield of the corresponding signal in the 1,2,3-triarylated isomer because of the proximity of two electron-withdrawing fluoroaromatic groups to the methylene.

The structure of diene **1c** was confirmed using single-crystal X-ray diffraction. Crystallographic data prepared by Dr. Carla Slebodnick are provided in the Supporting

Information section at the end of this dissertation. A thermal ellipsoid plot of the molecular structure of diene **1c** is shown in Fig. 4-1. Bond distances and angles are consistent with the published structure of **1b**. Upon first glance, it may seem strange that the two bonds C3−C4 (1.439 Å) and C4−C5 (1.417 Å) are comparable in length; however a positional disorder (see inset in Figure 4-3) exchanges the CH_2 and CH carbons throughout the crystal lattice, causing those bond distances to adopt values that are intermediate between a strict double bond such as C1=C2 (1.355 Å) and strict carbon(sp^2)-carbon(sp^3) single bonds C2−C3 (1.485 Å) and C5−C1 (1.477 Å). The two vicinal aryl groups show somewhat larger torsional angles with respect to the C_5 ring (52° for the aryl group joined to C1 and 50° for the aryl group joined to C2) compared to the more coplanar arrangement of the aryl group joined to C4 (38 °), likely because of steric crowding between *ortho* fluorine atoms. This feature of the structure is also consistent with the published structure of **1b**. *These findings support the assertion that the three perfluoroaryl substituents do not exhibit different steric effects on the reactive portion of the cyclopentadiene.*

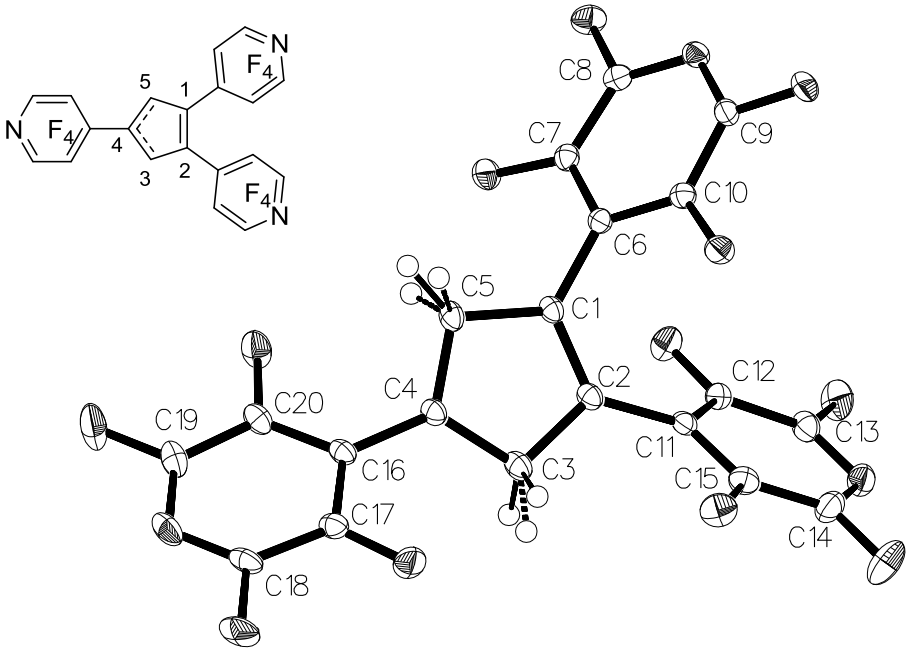

Figure 4-3. Ellipsoid plot (50% probability) of the molecular structure of crystalline diene **1c**. Fluorine atoms are numbered according to the carbon atoms to which they are attached. Selected bond distances (Å): C1−C2, 1.355; C2−C3, 1.485; C3−C4, 1.439; C4−C5, 1.417; C5−C1, 1.477. Selected torsional angles (deg): C1−C2−C11−C12, 52; C2−C1−C6−C10, 50; C3−C4−C6−C17, 38. **Inset**: Diagram showing positional disorder of CH_2 and CH carbons (C3 and C5).

4.4.2 Adduct Synthesis and Characterization

Dienes **1** and **2** reacted with maleimide **FMI** in toluene solution to afford Diels-Alder adducts **5** and **6**, respectively (Scheme 4-3). Reactions were performed at high reactant concentrations and a relatively mild temperature to maximize conversion to the adducts, which was still incomplete in all cases. The tendency for these reactions to reach steady-state concentrations of adducts vs. reactants is described in detail below. All of the adducts reflect selective *exo* stereochemistry for the cycloaddition under the described conditions. The Alder rule predicts *endo* adducts as kinetic products. However, the reactions shown in Scheme 4-3 should more accurately be described as dynamic equilibria that favor the thermodynamic *exo* isomers. Relative energies of formation for equilibrium geometries determined computationally (B3LYP/6-31G(d), data provided in the Supporting Information), indicated that *exo* isomers are favored by 6-9 kcal mol^{-1}. NOE spectrum

measurements do not show interactions between the protons alpha to the carbonyl groups and the protons on the 7-carbon of the norbornene moiety, further supporting the assignment of *exo* stereochemistry. Finally, our confidence in this assignment increased dramatically upon obtaining X-ray crystal structures of **5a**, **6a**, and **6b**, all of which are *exo* adducts.

Scheme 4-3

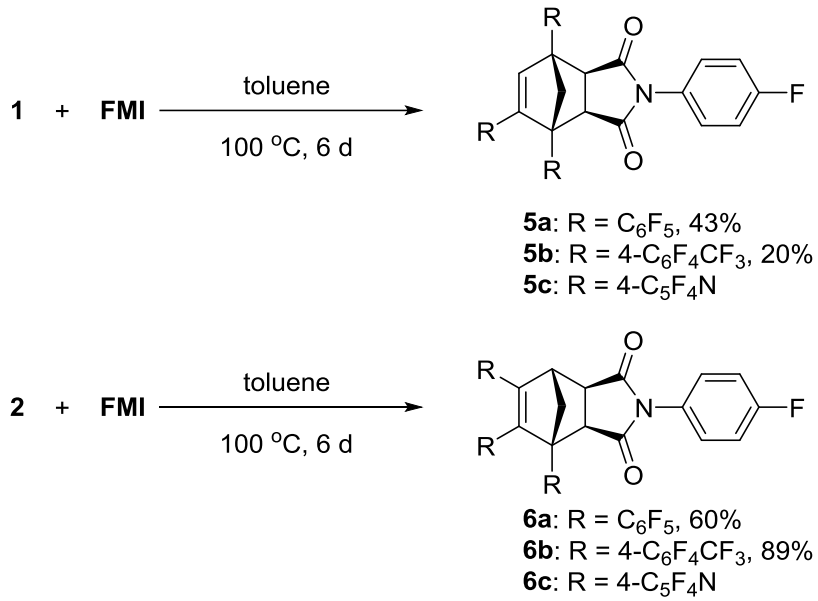

Reaction of dienes **1** or **2b** with **FMI** to form adducts **5** and **6**

It should be pointed out that four of the DA adducts reported here (**5a**, **6a**, **5b**, and **6b**) are well characterized compounds with clean NMR spectra and, in three cases, crystallographic conformation of the molecular structure. The adducts **5c** and **6c** were much more difficult to isolate for two main reasons. First, the diene **2c** is only observed as a minor component in samples of **1c** and efforts to isolate **2c** chromatographically (including TLC) failed. Therefore, the adduct **6c** is also only observed as the minor component of a complex mixture. Second, while the diene **1c** can be obtained in pure form by recrystallization of a **1c**/**2c** mixture, **1c** also is the most electron deficient diene in the study and reacts very slowly and only to low conversion with FMI. Therefore, also this compound was difficult to isolate in an analytically pure form. We are relying

on the commonalities among the NMR spectra of the three spectra in each isomeric set (123 vs. 124) as confirmation, however tentative, of the structures of adducts **5c** and **6c**.

4.4.3 Reaction Kinetics

We are interested in developing fluoroarylated cyclopentadienes as reactive monomer and telomer end groups in thermally reversible polymer synthesis based on Diels-Alder chemistry. Toward that end we aim to understand, in detail, how fluoroaromatic groups influence both the rate and the equilibrium constant for adduct formation. The six diene substrates chosen for the present study will help us learn the effects of overall structure (cyclopentadiene isomer) and the more subtle variations that attend changes in the electron-withdrawing power of the fluoroaromatic group, which we know increases in the order $C_6F_5 < C_6F_4CF_3 < C_5F_4N$ based on previous work by Deck and co-workers.[48] Moreover they are isosteric for the present purpose. We chose a "normal" electron-deficient dienophile, *N*-(4-fluorophenyl)maleimide (**3**), for these studies. Bis(maleimides) have been used as the dienophile component in Diels-Alder polymerization and are easy to synthesize from diamines. The 4-fluorophenyl group serves as a quantitative spectroscopic probe (^{19}F-NMR) that can be used in common for all of our dienes.

Reactions for rate measurements were performed in sealed NMR tubes using 1,2-dichlorobenzene as the solvent, with diene and maleimide concentrations of ca. 0.0800 M and 0.0900 M, respectively and at a constant temperature of 100 °C. Excess maleimide was used so that there would be a consistent spectroscopic label for a reactant even at high conversion. We quickly found that the 1,2,3-trisubstituted dienes reacted much faster than the 1,2,4-trisubstituted congeners, so measurements were required every ten minutes compared to every hour for the 1,2,4 species. We monitored conversion to 10% to establish a linear plot where initial rate should be constant and follow pseudo-first-order behavior. Once this level of conversion was complete, the

samples were allowed to remain in the oil bath until adduct concentrations remained relatively constant, which in some cases was very slow: The perfluoropyridyl-substituted dienes were still showing slow reaction progress after three months.

NMR analysis of the adduct *p*-fluorophenyl signal relative to the maleimide *p*-fluorophenyl allowed for facile determination of relative concentrations of each since the adduct signal shifted downfield by 2 – 3 ppm. The region of the spectrum assigned to the fluoroaromatic substituents of the diene did not show useful resolution of free diene from the adduct, so these signals could not be used to determine reactant and product concentrations. Figures 4-2 and 4-3 present two example of concentration-time data. The other four are provided in the supporting information at the end of this dissertation. Rate constants (k_1 for adduct formation) were obtained directly from the slopes of the regression lines for the six plots and are reported in Table 1. Regression analysis displays less than 5% error in all experiments.

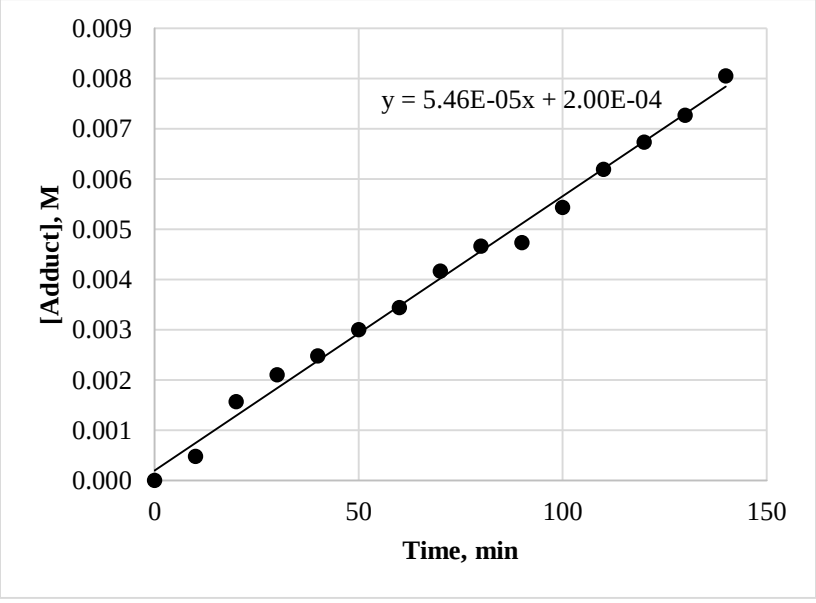

Figure 4-4. Concentration of adduct **6b** vs time for the reaction of diene **2b** (initially 0.0799 M) and **FMI** (initially 0.0925 M) in 1,2-dichlorobenzene at 100 °C.

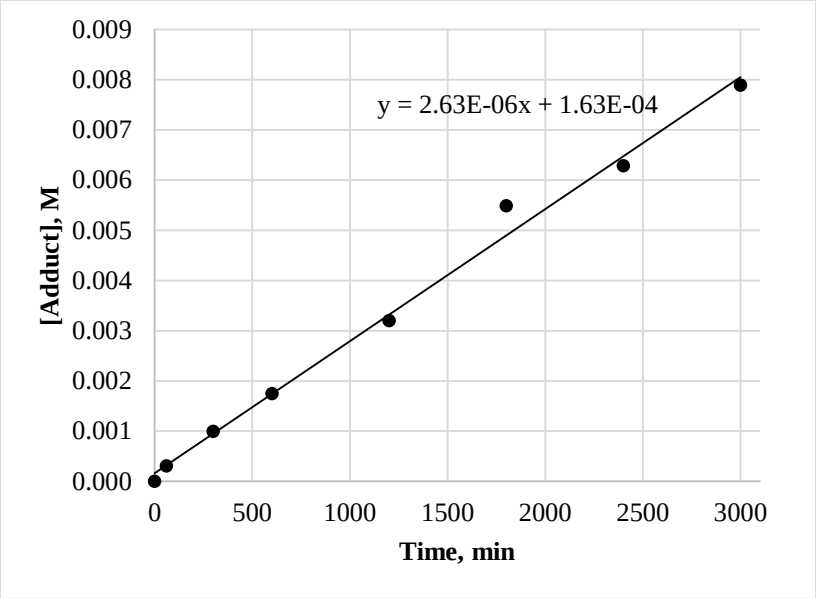

Figure 4-5. Concentration of adduct **5b** vs time for the reaction of diene **1b** (initially 0.0777 M) and **FMI** (initially 0.0885 M) in 1,2-dichlorobenzene at 100 °C.

Table 4-1. Initial, pseudo-first-order rate constants for reactions of triarylated cyclopentadienes **1a-c** and **2a-c** with FMI at conversions lower than 10%.

Diene	10^{-4} x k_1, (M^{-1} min^{-1})	**Diene**	10^{-4} x k_1, (M^{-1} min^{-1})
1a	11.7(2)	**2a**	135(4)
1b	3.82(13)	**2b**	73.8(15)
1c	3.65(14)	**2c**	12.2(5)

Clearly the 1,2,4-triarylated dienes **5** react more slowly than the corresponding 1,2,3-triayrlated isomers **6**. The simplest explanation is the additional steric encumbrance at the carbon atoms where new bonds are forming, and which become the bridgehead carbons in the norbornene moieties of the adducts. Both series reflect the "normal electron demand" tendency for more electron-deficient dienes to undergo slower reactions, as the perfluoroaryl substituents exhibit increasing electron-withdrawing power in the order C_6F_5 < $C_6F_4CF_3$ < C_5F_4N. The observation that dienes **5b** and **5c** react at the same rate seems somewhat anomalous but is reproducible. The data in Table 1 also show that the effects of these different perfluoroaryl substituents is relatively modest, as rates across each series vary by no more than a factor of three, even though all three substituent groups are changed. The effect of changing one substituent (e.g., in fine-tuning the

design of a monomer for Diels-Alder polymerization) might be more modest still or perhaps even negligible.

Ideally, in order to determine the effects of CPD substitution on the stability of DA adducts, we wanted to obtain not only rate constants for binding (from low-conversion data as described above) but also the ultimate binding constants for adducts **5** and **6**. Unfortunately, the reactions at the temperature chosen for the study are so slow that only in one case (for the **2a**) were steady-state concentrations ([**2a**], [**FMI**], and [**6a**]) reached. We therefore resorted to numerical modeling of the adduct concentration-time curves as follows.

For the equilibrium reaction shown in eq 1, the initial concentration of adduct was zero, as reactions were started with pure diene (**1** or **2**) and **FMI**.

Diene (**1** or **2**) + **FMI** = Adduct (**5** or **6**) (1)

As the forward rate is a bimolecular process with rate k_1, and the reverse reaction is a unimolecular decomposition with rate k_{-1}, then the equilibrium constant is found as in eq 2.

$$K_{eq} = \frac{[adduct]}{[diene][\boldsymbol{FMI}]} = \frac{k_1}{k_{-1}} \quad (2)$$

Concentration-time curves for the three reactants were calculated using changes in concentration according to the differential rate equations for the system (eq 3-6).

$$\Delta = k_1[diene][FMI] - k_{-1}[adduct] \quad (3)$$

$$[diene]_{t+1} = [diene]_t - \Delta \quad (4)$$

$$[FMI]_{t+1} = [FMI]_t - \Delta \quad (5)$$

$$[adduct]_{t+1} = [adduct]_t + \Delta \quad (6)$$

Starting from the initial concentrations actually used in the experiment, the three concentrations were increased or decreased according to eq 3-6 in 1-minute increments. The calculated curve for [adduct] vs. time was compared visually to the actual data determined using NMR integrals, and the equilibrium constant and forward rate constant k_1 were adjusted as parameters. The "optimized" value for k_1 was typically found to be about 10% higher than the same rate constant obtained using low-conversion data assuming pseudo-first-order behavior. The binding constants obtained in this manner for **1a**, **2a**, **1b**, and **2b** are 75, 500, 15, and 70 M^{-1}, respectively. A rough estimate of the error in the determination of the equilibrium constants for adducts **5a**, **6a**, **5b**, and **6b** is about 20%. Dienes **1c** and **2c** proceeded only to 30% and 10% conversion, respectively, over the interval of the experiment and their data could not be modeled to extract an equilibrium binding constant. Clearly the less encumbered 1,2,3-trisubstituted dienes bind **FMI** more tightly, and the binding constant decreases with increasing electron-withdrawing power of the substituent.

4.4.4 Computational Studies

The energy of the LUMO for the maleimide and the energies of the HOMO of each diene were calculated using B3LYP on the Department of Chemistry's CEREBRO cluster using the WebMO interface to Gaussian™. Results are collected in Table 4-2. The energetic differences observed follow the same order as the experimentally determined initial rate, or k_1, for the same set of compounds.

Table 4-2. Energy gaps between the HOMO of dienes **1a-c** and **2a-c**, and the LUMO of maleimide **3** calculated using B3LYP/6-31g(d).

Diene	Gap Energy (kcal/mol)	Diene	Gap Energy (kcal/mol)
1a	88.4	**2a**	73.1
1b	90.3	**2b**	88.1
1c	99.4	**2c**	92.7

The difference between 1,2,3-substituted CPDs and 1,2,4-CPDs appears to be primarily due to steric repulsion. The less sterically encumbered dienes **2** have the smallest energy gap and therefore have a larger k_1. Within each diene series the energy gap increases as electron withdrawing ability increases. Comparing the gap energy from **1a** to **1b**, and **2a** to **2b** elucidates this difference. There is a substantial difference from **2a** to **2b**, approximately 15 kcal/mol, yet this difference is much smaller from **1a** to **1b**, roughly 2 kcal/mol. Steric repulsion adds ~15 kcal/mol to the energy gap from **2a** to **1a**, supporting the observed decrease in rate (an order of magnitude) as presented in Table 4-1. The difference in steric effect is less in magnitude from **2b** to **1b** (~2 kcal/mol) and also from **2c** to **1c** (~7 kcal/mol). The electronic effect imparts a larger impact on dienes **2** as the range from **2a** to **2c** is almost 20 kcal/mol while the range for **1a** to **1c** is only 10 kcal/mol, again supporting the substantial differences in observed rates within the two sets.

4.5 Conclusions

Pentafluoropyridine reacts with sodium tert-butylcyclopentadienide at elevated temperature to yield mixtures of 1,2,3- and 1,2,4-tris(perfluoro-4-pyridyl)cyclopentadienes or relatively pure 1,2,3,4-tetrakis(perfluoro-4-pyridyl)cyclopentadiene depending on the reaction conditions. Tris(perfluoroaryl)cyclopentadienes react with the typical DA dieneophile *N*-4-fluorophenylmaleimide to form exclusively *exo* adducts. The initial rates of substituted cyclopentadienes with a maleimide are overall substantially faster with the 1,2,3-triarylated cyclopentadienes because they are less sterically encumbered than the corresponding 1,2,4-triarylated isomers. The effect of variation in the aryl substituent itself is more modest, but reaction rates decrease along the trend from C_6F_5 > $C_6F_4CF_3$ > C_5F_4N, in accordance with the "normal electron demand" theory of electronic effects in the DA reaction, and in agreement with LUMO-

HOMO energy gaps calculated using DFT/6-31g(d). Theoretical calculations of the most stable adduct form (*endo*/*exo*) agree with the experimentally observed exo adducts. The sluggishness of adduct formation of these triarylated dienes and the low binding constants of the adducts suggest that the tris(perfluoroaryl)cyclopentadiene moiety is not a good choice for use in the monomers for step-growth Diels-Alder polymers.

Chapter 5 Linear Polymers Based on Diels-Alder Reactions of Bis(cyclopentadienes) and Bis(maleimides)

Jeremy B. Stegall, Sanghamitra Sen, Carla Slebodnick, and Paul A. Deck*

Department of Chemistry, Virginia Tech, Blacksburg VA 24061-0212

Keywords: Diels-Alder reaction, step-growth polymer, cyclopentadiene, maleimide, size exclusion chromatography, thermo-gravimetric analysis, differential scanning calorimetry

Foreward. With the exception of supporting information relegated to the end of the dissertation, this chapter represents a manuscript in preparation for *Macromolecules*. I performed all of work reported in this chapter except as follows: Dr. Sanghamitra Sen performed preliminary synthetic experiments and developed the method for trapping transient cyclopentadiene end groups using *N*-(4-fluorophenyl)maleimide; Dr. Carla Slebodnick performed the crystallographic data collection, structure solution, and refinement; Bill Bebout performed the MS analyses; Atlantic Microlab (Norcross, GA) performed the microanalyses, and Prof. Paul A. Deck supervised my work.

5.1 Abstract

Octafluoro-4,4'-biphenylene-linked bis(alkylcyclopentadienes) (alkyl = $CHMe_2$, CMe_2Ph, and CMe_3) and bis(maleimide)s linked by $(CH_2)_{12}$, $(CH_2CH_2(OCH_2CH_2)_2$, $(CH_2)_6$, or $(C_6H_4OC_6H_4)$ moieties undergo step-growth Diels-Alder polymerization at 80–100 °C to afford thermally cleavable linear polymers having M_n ~ 25 kDa. The polymers exhibit relatively sharp glass transitions (DSC) with T_g ranging from ca. 140 to 255 °C depending strongly on the flexibility of the bis(maleimide) linker and to a lesser extent on the cyclopentadiene alkyl substituent, which is believed to exert a secondary effect on the glass transition through changes in local free volume. T_g increases in the order of bis-maleimide linker structure listed above and in the order of cyclopentadiene alkyl substituent listed above. Although TGA shows relatively high decomposition temperatures (T_d is typically 280–300 °C), thermal depolymerization is shown by trapping of transient end-groups to commence at temperatures as low as 120 °C in solution.

5.2 Introduction

The Diels-Alder (DA) reaction offers a method of propagating, cross-linking, and functionalizing polymers without catalysts, initiators, or transfer agents, and without the need to remove by-products as in polycondensation, but with attractive prospects for thermal responsiveness of the resulting polymers through controlled thermal (retro DA) decoupling.[15,19,20,22-25] DA polymers have found promising applications in self-healing ("re-mendable") macromolecular systems[31,32,57,91] that are free of small-molecule additives (binders or linkers) that may leach or otherwise degrade material performance.[32]

DA polymers are prepared by two general approaches. The single-component approach is limited to cyclopentadiene (CPD) as the reactive species because CPD can serve as both diene and dienophile. Self-couplings of monoalkylated cyclopentadienes are highly facile even at room temperature (such that monomers can be difficult to purify and store)[26] but difficult to reverse (retro-DA begins above 160 °C).[29] Side reactions can also occur at the double-bond of the substituted norbornene moiety formed by CPD self-coupling, leading sometimes to cross-linking.[31] Whether these features are advantageous depends, of course, on the application.

The alternative, two-component approach has mostly used furan-maleimide chemistry because these functional groups are easily manipulated synthetically.[3,5] Furans and maleimides (MIs) undergo DA coupling as low as 0 °C and rDA decoupling starting around 80 °C, although the perceived temperature at which rDA commences depends greatly on the method of its estimation. The relatively mild coupling/decoupling conditions of the furan-maleimide system are prized for their practical utility, yet they introduce other challenges associated with their decreased adduct stability. Moreover, the furan-maleimide system seems already to be optimized in terms of substituent effects, as species other than derivatives of furfuryl alcohol are either unreactive (in the

case of bulky or electron-withdrawing substituents at the 2-position of furan) or prohibitively expensive (in the case of 3-substituted furans generally).[5]

Our aim is to develop a two-component DA polymerization system in which the resulting polymers would be thermally stable well above 60 °C but would also demonstrate thermal responsiveness (rDA decoupling) at temperature below 150 °C. Our approach is based on couplings of bis(cyclopentadienes) and bis(maleimides). As we have described in Chapter 3, the key problems of arresting CPD self-coupling and of enabling the rDA process to occur under less than forcing conditions are both overcome by careful choice of CPD substituents. This report describes the synthesis of polymers derived from three closely-related bis(CPD) monomers and four bis(maleimides), elementary physical and thermal characterization of these polymers, and experiments demonstrating their ability to undergo thermal decoupling starting at 120 °C.

5.3 Experimental

5.3.1 General Methods.

Solvents were used as received from commercial suppliers unless noted otherwise. Hexafluorobenzene was used as received from Oakwood Products. Decafluorobiphenyl and 4-fluoroaniline were used as received from Matrix Scientific. THF was purified by the method of Pangborn et al.[110] Sodium *tert*-butylcyclopentadienide[37] and *N*-(4-fluorophenyl)maleimide (**FMI**)[50,111,112] were prepared as previously reported. Isopropylcyclopentadiene was prepared by lithium aluminum hydride reduction of dimethylfulvene according to a literature account.[42] Sodium isopropylcyclopentadienide was prepared from isopropylcyclopentadiene wand sodium hydride.[37] Diamines were used as received from Matrix Scientific, Sigma-Aldrich, Alfa Aesar, Acros Organics, and Chemsavers. Maleic anhydride 99% was used as received from Aldrich Chemical Co. Sodium hydride was purchased as a 60% dispersion in mineral oil from Aldrich, washed thoroughly with hexanes, dried under vacuum and stored in an Innovative Technology

nitrogen glove box. NMR spectra were acquired on either a Varian Inova 400 NMR spectrometer, an Agilent 400-MR DD2 NMR spectrometer or a Bruker Avance II 500 NMR spectrometer. NMR data was processed using Mestrelab Research MestReNova software. Proton chemical shifts were referenced to $CHCl_3$ (7.26 ppm) in $CDCl_3$. ^{19}F chemical shifts were referenced to external C_6F_6 (−163.0 ppm) in $CDCl_3$. Mass spectra were obtained using an Agilent 6220 instrument (LC-ESI-TOF featuring 5-ppm mass accuracy). Melting points (uncorrected) were acquired using open capillaries on a Buchi B-545 apparatus. Differential scanning calorimetry (DSC, TA Instruments Q2000) determined thermal transitions using a standard heat/cool/heat method with 10 °C/min heating rate and 100 °C/min cooling rate under constant N2 purge. All glass transition temperature (Tg) values are reported from the second heats. Thermogravimetric analysis (TGA, TA Instruments Q50) recorded the 5%-weight loss temperature (Td,5%) of the polymers when subjected to a 10 °C/min temperature ramp under constant N2 purge. TA Instruments Universal Analysis 2000 software (version 4.5A) was used for data processing.

5.3.2 Monomer Synthesis

4,4'-Bis(4''-*tert*-butylcyclopentadien-1''-yl)octafluorobiphenyl (**1**) and **4,4'-Bis(4''-cumylcyclopentadien-1''-yl)octafluorobiphenyl** (**3**) were prepared as reported by Evans.[41] Compound (**1**) was purified by silica gel chromatography, eluting with hexanes (mp 127 – 128 °C). Compound (**3**) was purified by silica gel chromatography (gradient: 2% CH_2Cl_2 in hexanes → 50% CH_2Cl_2 in hexanes) followed by recrystallization from hot toluene (mp 159 – 160 °C). NMR spectra of previously reported compounds were consistent with data provided in those reports.

4,4'-Bis(4''-isopropylcyclopentadien-1-yl)octafluorobiphenyl (2). Under nitrogen, a mixture of sodium isopropylcyclopentadienide (0.540 g, 4.15 mmol), sodium hydride (0.100 g, 4.16 mmol),

and THF (20 mL) was cooled using an ice-brine bath (0 °C) with magnetic stirring. With continued cooling and stirring, a solution of decafluorobiphenyl (0.630 g, 1.89 mmol) in 20 mL of THF was added over a period of 1 h. When the addition was complete, the reaction was allowed to warm slowly to room temperature and then stirred at room temperature for a total reaction time of 2 d. Progress was followed by working up small aliquots of the reaction mixture and observing the disappearance of the ^{19}F NMR signal assigned to the *para*-fluorines of decafluorobiphenyl (δ −152 ppm). The solvent was then evaporated, and the residue was quenched with 10% aqueous sulfuric acid (100 mL). The product was extracted into dichloromethane (50 mL), which was washed with water (2 x 50 mL) and brine (50 mL), dried over anhydrous $MgSO_4$, filtered, and evaporated to afford 0.79 g (1.5 mmol, 82%) of a dark, viscous oil. Filtration of a hexanes solution through a short column of silica gel followed by concentration of the yellow eluent and then crystallization at −5 °C (overnight in the freezer) afforded a pale yellow crystalline solid (0.400 g, 41%). The solid was washed with a small amount of cold methanol and dried under vacuum: mp 96 – 98 °C. ^{1}H NMR: **major isomers** (**2a/b**) δ 7.3 (s, 1H), 6.3 (s, 1H), 3.6 (q, 2H, J = 2 Hz), 2.7 (sept, 2H, ^3J = 13, J = 6Hz), 1.2 (d, 6H, J = 7 Hz); (**2a/b**) 7.3 (s, 1H), 6.3 (s, 1H), 3.5 (t, 2H, J = 2 Hz), 2.81 (sept, 2H, ^3J = 13, J = 6 Hz), 1.2 (d, 6H, J = 7 Hz); **minor isomer** (**2c**) 6.8 (s,1H), 6.5 (s, 1H), isopropyl CH proton obscured at 2.7 ppm, isopropyl CH_3 group obscured at 1.2 ppm, 3.2 (s, 2H). ^{19}F NMR: δ −140.1 (2F), −140.3 (2F), −140.6 (2F), −141.1 (2F).**Synthesis of Bis(maleimide)s**. Bis-maleimides **4-7** were prepared from the respective diamines following published literature procedures.[93,111,113,114] Melting points and NMR chemical shifts agreed with the published values. Routine data are provided here for the benefit of other members of our research group embarking on related research programs. This data will not be reproduced in the manuscript sent to *Macromolecules*.

Diphenylether bis-4,4'-(*N*-maleimide) (**4**) was dissolved in dichloromethane and reprecipitated in methanol, m.p. 170 – 176 °C, lit.[115] mp 175 – 176.5 °C; ^{1}H NMR (400 MHz, $CDCl_3$): δ ppm 7.3 (m, 4H), 7.1 (m, 4H), 6.9 (s, 4H).

1,6-bis(maleimido)hexane (**5**) was sublimed (160 °C, 10^{-3} mmHg). m.p. 140 – 141 °C, lit[113] 138 – 139 °C; ^{1}H NMR (400 MHz, $CDCl_3$): δ 6.7 (s, 4H), 3.5 (t, 4H, N-CH_2), 1.5 (m, 4H, CH_2), 1.3 (m, 4H, CH_2); ^{13}C NMR (376 MHz, $CDCl_3$): δ 170.8 (C=O), 134.0 (C=C), 37.6 (N-CH_2), 28.3 (CH_2), 26.1 (CH_2).

1,12-Bis(maleimido)dodecane (6) was sublimed (120 °C, 0.1 mmHg). mp 116 – 117 °C, lit[93] mp 109 – 111 °C. ^{1}H NMR (400 MHz, $CDCl_3$): δ 6.6 (s, 4H), 3.5 (t, 4H, N-CH_2), 1.5 (m, 4H, CH_2), 1.2 (m, 16H, CH_2).

1,2-bis(2-maleimidoethoxy)ethane (7) was sublimed (140 °C, $1x10^{-5}$ Torr). m.p. 97.5 – 98.5 °C, lit[116] 98.05 °C. ^{1}H NMR (400 MHz, $CDCl_3$): δ 6.7 (s, 4H), 3.6 (t, 4H, N-CH_2), 3.5 (t, 4H, CH_2), 3.5 (s, 4H, CH_2) ^{13}C NMR (100 MHz, $CDCl_3$): δ 170.6, 134.1, 70.0, 67.8, 37.1.

Adduct of Bis(diene) 1 and 2 Equiv of FMI (Mixture of Isomers) (9). A solution of diene **1** (0.5 g, 0.9 mmol) and *N*-(4-fluorophenyl)maleimide (**FMI**, 0.4 g, 2 mmol) were in toluene (5 mL) was stirred at 80 °C under nitrogen for 24 h. The reaction was followed by ^{19}F NMR monitoring for adduct signals between -112 and -113 ppm as described in Chapter 3. The solvent was evaporated and the residue subjected to silica gel chromatography (90 g, 180 mm x 40 mm) eluting with 50% ethyl acetate in hexanes to afford afforded twenty 10-mL fractions. Fractions were spotted and developed on a TLC plate using 50% ethyl acetate in hexanes, and like fractions were combined. Fractions 1 – 3 had no UV visible spots, fraction 4 – 8 contained two spots (136 mg after solvent removal), fraction 9 – 14 contained 3 spots (380 mg after solvent removal), and fractions 15 – 22 contained two major spots and two minor spots (408 mg after solvent removal).

The minor spots were carryover from all previous fractions. A single diadduct product was cleanly isolated after column chromatography from fractions 15 – 22, precipitating after the addition of hexanes yielding 68 mg (8%) of a white powder. Isomers were not further isolated as the purpose was simply for comparison to polymer trapping experiments described later. The NMR spectra of the mixture (**9**) are described in detail below.

5.3.3 Crystallography (Dr. Carla Slebodnick wrote these experimental procedures)

A colorless plate of **2** (0.08 x 0.20 x 0.39 mm^3) was centered on the goniometer of an Oxford Diffraction SuperNova A diffractometer operating with MoKα radiation. The data collection routine, unit cell refinement, and data processing were carried out with the program CrysAlisPro.[51] The Laue symmetry and systematic absences were consistent with the monoclinic space groups *Cc* and *C*2/*c*. The centric space group *C*2/*c* was chosen. The structure was solved using SHELXS-97[52] and refined using SHELXL-97[52] via OLEX2.[53] The final refinement model involved anisotropic displacement parameters for non-hydrogen atoms and a riding model for all hydrogen atoms. The sp^3 hybridized site of the cyclopentadiene was modeled as being disordered between C2 and C5, with relative occupancies that refined to 0.53(2) and 0.47(2), respectively. Structure and data table can be found in **Appendix D**.

5.3.4 DA Polymer Synthesis

Generally, DA polymers were prepared by combining a bis(CPD) monomer and a bis(MI) monomer in rigorously equimolar quantities based on ca. 0.5000 g of the bis(CPD) to establish a consistent scale. Solvent was added such that the weight ratio of solvent to monomer was 2:1. Polymerizations were conducted under dry nitrogen atmosphere at 80 °C or 100 °C (toluene), or at 150 °C (1,2-dichlorobenzene) for at least 24 h. Polymers were isolated by precipitation of the cooled/quenched reaction mixture in methanol saturated with sodium chloride, stirring for 1 h,

filtering, washing with methanol, and drying under vacuum. Specific reaction conditions, yields, and thermal data can be found in Table 5-1. An example polymerization procedure is as follows: Monomer **1** (0.5001 g, 0.9287 mmol) and monomer **6** (0.3347 g, 0.9286 mmol) were combined with dry toluene (1.6 g) in a small reaction tube and purged with dry nitrogen. The mixture was magnetically stirred and heated at 80 °C for 96 hours. The solution was cooled to RT and diluted with a small amount of toluene and then poured into rapidly stirred methanol (100 mL). The resulting precipitate was collected on a filter and dissolved in chloroform (2 – 3 mL) and then re-precipitated in rapidly stirred methanol (100 mL). The resulting precipitate was collected on a filter and dried to yield ca. 0.800g (96%) of a pale white solid.

Table 5-1. Reaction conditions, product yields, and molecular weight data (SEC-MALLS, see below) for selected Diels-Alder polymers formed from dienes **1**-**3** (R-C_5H_4-$C_6F_4C_6F_4$-C_5H_4-R) and maleimides **4**-**7** (MI-G-MI). **[M]** represents concentration of diene monomer.

Polymer	CPD	MI	R	G	T, °C	t, hr	[M]	Yield, %	M_n, kDa	PDI	DP_n
P1	**1**	**4**	*t*Bu	-$C_6H_4OC_6H_4$-	80	140	0.22	91	17	1.8	19
P2	**1**	**5**	*t*Bu	-$(CH_2)_6$-	80	24	0.53	90	34	1.6	42
P2	**1**	**5**	*t*Bu	-$(CH_2)_6$-	80	2	0.54	98	9	1.6	11
P2	**1**	**5**	*t*Bu	-$(CH_2)_6$-	80	24	0.11	77	10	1.3	12
P2	**1**	**5**	*t*Bu	-$(CH_2)_6$-	80	160	0.53	99	22	1.9	27
P2	**1**	**5**	*t*Bu	-$(CH_2)_6$-	80	24	1.06	92	25	1.5	31
P3	**1**	**6**	*t*Bu	-$(CH_2)_2(O(CH_2)_2)_2$-	80	68	0.29	93	17	1.6	18
P4	**1**	**7**	*t*Bu	-$(CH_2)_{12}$-	80	24	0.48	93	32	1.9	36
P4	**1**	**7**	*t*Bu	-$(CH_2)_{12}$-	80	96	0.49	96	32	2.1	36
P4	**1**	**5**	*t*Bu	-$(CH_2)_{12}$-	140	60	0.17	87	25	1.4	28
P4	**1**	**5**	*t*Bu	-$(CH_2)_{12}$-	100	90	0.48	95	27	1.9	30
P5	**2**	**4**	*i*Pr	-$C_6H_4OC_6H_4$-	100	45	0.49	82	27	2.0	31
P5	**2**	**4**	*i*Pr	-$C_6H_4OC_6H_4$-	60	48	0.02	70	4	2.2	5
P6	**2**	**5**	*i*Pr	-$(CH_2)_6$-	80	24	0.57	87	21	1.9	27
P7	**2**	**6**	*i*Pr	-$(CH_2)_2(O(CH_2)_2)_2$-	100	45	0.52	80	12	2.3	15
P8	**2**	**7**	*i*Pr	-$(CH_2)_{12}$-	80	24	0.49	95	29	1.7	33
P8	**2**	**7**	*i*Pr	-$(CH_2)_{12}$-	80	24	0.50	86	17	1.3	20
P9	**3**	**4**	cumyl	-$C_6H_4OC_6H_4$-	100	45	0.42	87	19	1.7	19
P10	**3**	**5**	cumyl	-$(CH_2)_6$-	100	32	0.45	90	8	1.7	8
P11	**3**	**6**	cumyl	-$(CH_2)_2(O(CH_2)_2)_2$-	100	45	0.44	79	14	1.65	14
P12	**3**	**7**	cumyl	-$(CH_2)_{12}$-	80	24	0.43	84	25	1.9	24
P13	**1**	**7**	*t*Bu	-$(CH_2)_{12}$-	150	48	0.60	84	46	1.74	51
P14	**1**	**4**	*t*Bu	-$C_6H_4OC_6H_4$-	150	24	0.77	91	20	2.61	22
P15	**1**	**5**	*t*Bu	-$(CH_2)_6$-	150	24	0.80	--	24	1.98	29

5.3.5 Size Exclusion Chromatography

Differential refractive index values for all polymers were obtained using a Wyatt Optilab T-rEX maintained at 35 °C with solutions (filtered through 0.45μm PTFE membrane) of polymer in THF (1 mg/mL → 5 mg/mL) sequentially injected using a syringe pump at 15 mL/h until refractive index for each dilution stabilized. A linear fit through each step yielded the slope, or differential refractive index (dη/dc). Tetrahydrofuran (THF) SEC at 30 ºC using a flow rate of 1.0 mL/min through three Polymer Laboratories PLgel 5 μm MIXED-C columns determined the molecular weights of the obtained polymers. SEC instrumentation included a Waters 717 plus autosampler equipped with Waters 515 HPLC pump, Waters 2414 refractive index detector, and Wyatt miniDawn MALLS detector operating at 690 nm. Alternately, molecular weights were calculated using a Waters Isocratic HPLC pump with 2 Agilent 10 um Mixed-B LS columns in series (300 x 7.5 mm each) at 30 °C in THF at 1 mL/min. A Wyatt Helios-II LS detector and an Optilab rEX RI detector at 30 °C. Molecular weights were calculated based on 100% mass recovery. All relevant size exclusion chromatograms are provided in the supporting information.

5.3.6 Depolymerization Studies

Depolymerization of polymers was carried out by four methods. In **solution method 1** the polymer was simply heated in 1,2-dichlorobenzene solution at 160 °C for several hours. The work-up procedure differed in that the solution was immediately quenched in either cold hexanes or methanol. Isolation and drying was carried out in the same way as the initial polymer synthesis. In **solution method 2**, the polymer sample was dissolved in *o*-dichlorobenzene and heated at 150 °C with the addition of a 20 equiv of a monofunctional maleimide (**FMI**) which served to trap transient diene end-groups formed during rDA events. Work-up was carried out in the same manner as initial polymer synthesis. The resulting product mixture was separated by silica gel chromatography and analyzed by ^{1}H and ^{19}F NMR. In **bulk method 1**, a polymer film sample was

heated at 200 °C in an oven for several hours. It was considered quenched when removed to ambient temperatures quickly. In **bulk method 2** a sample (film or powder) of polymer was heated in a tube furnace (250 °C, 1 h) under vacuum, using a tube having a condenser separated from the hot zone by a constriction fitted with a plug of glass wool to prevent any erupted solid transferring to the condenser (Fig 5-1. Residue was recovered from the condenser by dissolving it in acetone and evaporation of the solvent to afford a solid that was subjected to ^{1}H NMR spectroscopic analysis.

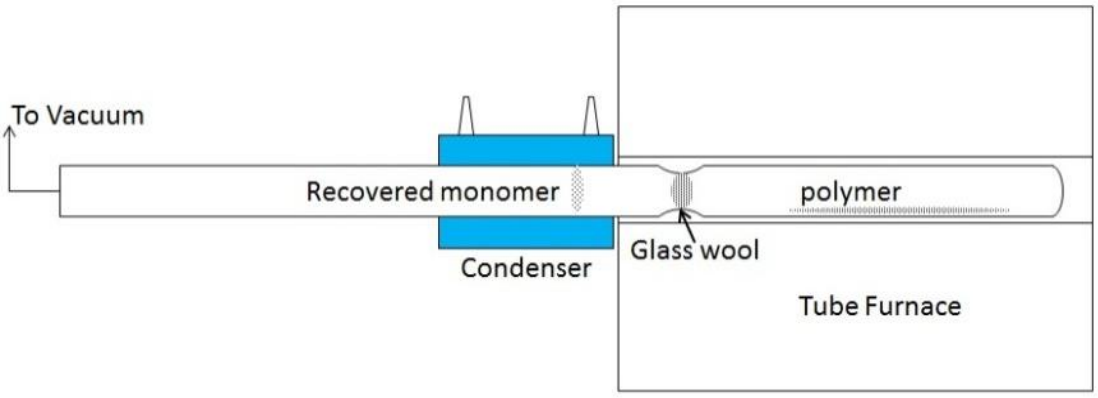

Figure 5-1. Tube furnace setup for bulk thermolysis of DA polymers.

5.4 Results and Discussion

5.4.1 Monomer Design and Rationale

Monomers for two-component (bis-CPD + bis-MI) DA polymerization were designed with three criteria in mind. First, self-coupling of the CPDs must be arrested. Second, the bis(CPD) must react smoothly with the bis(MI) under mild conditions. Finally, the adducts must become labile at a temperature between ca. 100-140 °C so the polymers may be considered both reasonably stable but also thermally reversible. As we showed in Chapter 3, these criteria can all be met if the cyclopentadiene bears one *tert*-butyl group and one perfluoroaryl group. Our monomer "design" therefore required only the replacement of the perfluoroaryl group with a ditopic perfluoroarylene linker. We knew from the work of Evans[41] and of Deck and co-workers[117] that

octafluorobiphenylene-linked bis-cyclopentadienes are easily established by nucleophilic substitution of decafluorobiphenyl. In fact, monomer **1** was reported by Evans as an intermediate in the synthesis of bis(cyclopentadienone) monomers for use in DA polymerizations leading to Stille-Muellen-type polyphenylenes.[41]

5.4.2 Monomer Synthesis

Bis(diene) monomers were prepared according to Scheme 5-1. Monomer **1** was prepared previously by Dr. Jessica P. Evans in our laboratory, and monomer **3** was prepared by Kelly M. Daly in our laboratory under Dr. Evans's supervision.[41] Their samples needed only purification by silica gel chromatography or recrystallization.

Scheme 5-1

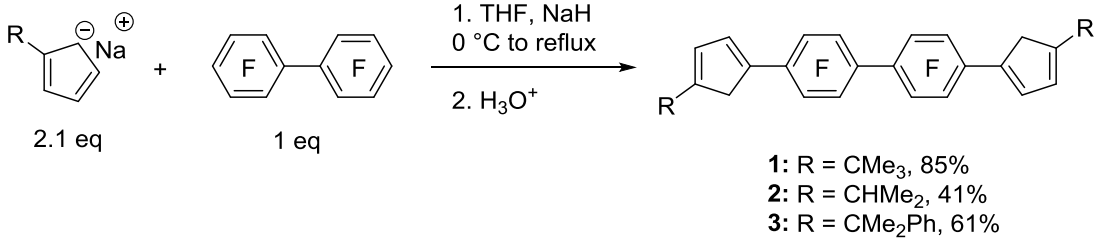

Synthesis of bis-diene monomers **1**, **2**, and **3**

In her doctoral dissertation, Dr. Evans detailed the isomerism that these bis(diene) compounds exhibit, so the issue needs only cursory treatment here.[41] Essentially, each diene moiety can adopt one of three slowly interconverting tautomeric forms as shown in Scheme 5-2.

Scheme 5-2

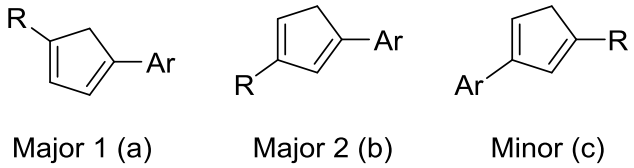

Tautomeric forms of a di-substituted cyclopentadiene

Bis(maleimides) **4 – 7** were prepared (Scheme 5-3) by the reaction of the diamine with excess maleic anhydride at 0 °C overnight, followed by isolation of the amic acid intermediate. Starting

with the amic acid intermediate, modifications to published literature procedures were used to close the ring affording the desired bis(maleimide). Each BMI was recrystallized or sublimed to ensure 99%+ purity as determined by NMR spectroscopic analysis.

Scheme 5-3

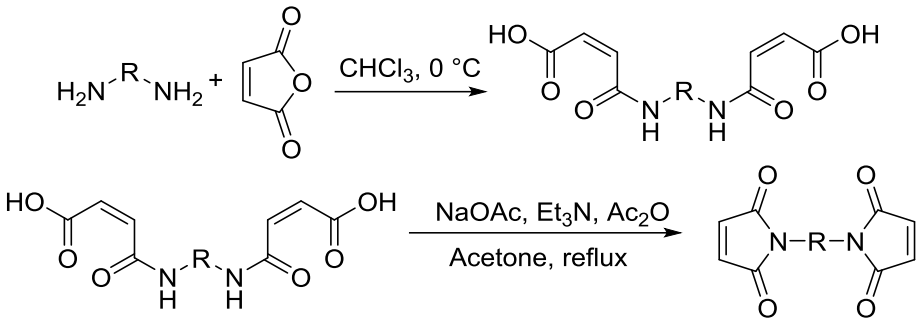

Synthesis of a bis-maleimide

5.4.3 Model Chemistry

Chapter 3 of this dissertation describes the synthesis and DA chemistry of a cyclopentadiene (**A**) bearing one *tert*-butyl and one nonafluorobiphenyl substituent. In that chapter we showed that the diene, which exists as three primary tautomers (as in Scheme 5-2), may react to form up to six isomeric adducts, as each of the diene isomers can form *endo* and *exo* adducts. We now extend this model to the reaction of bis(diene) **1** with maleimide **FMI** to afford the bis-adduct **9** (Scheme 5-4).

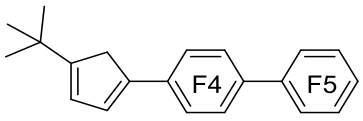

A

Scheme 5-4

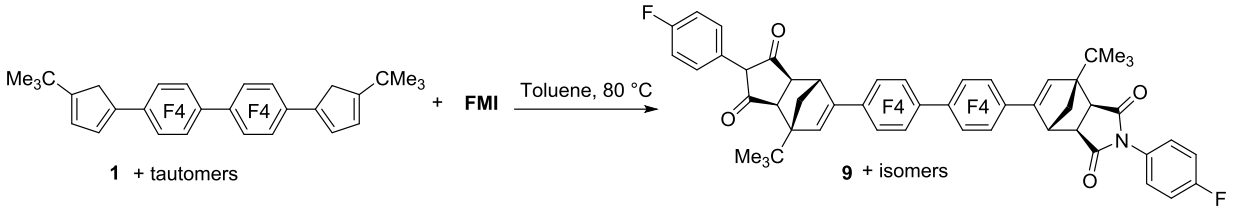

Reaction of monomer **1** with **FMI** to form adduct mixture **9**

The isomers present in the mixture **9** were mostly identified by comparing their ^{1}H NMR spectra (within the spectrum of the mixture) with NMR spectra of the corresponding, well-characterized adducts of **A** and **FMI**. The mixture contains 24% 1,3-*exo*; 2% 2,4-*exo*; 13% 1,3-*endo*; 17% 1,4-*endo* and 46% 2,4-*endo* isomers (Chart 1), a distribution not dissimilar to those of the small molecule models presented in Chapter 3 (**3c**, **3a**, **3d**, **3f**, and **3b**, respectively, are the corresponding compound numbers in that chapter). The complexity of the mixture is demonstrated in Figure 5-2; the inset shows the region of the ^{19}F NMR spectrum corresponding to the 4-fluorophenyl substituent on the maleimide, which has four distinct signals for the five adduct isomers (the 1,3-*endo* and 1,4-*endo* isomers give overlapping signals in both proton and fluorine spectra, yet one vinyl signal in the 1,4-*endo* adduct is well-resolved and therefore the ratios of 1,3-*endo* to 1,4-*endo* can be determined). Moreover, even though **9** could have up to 30 possible isomers if the two cyclopentadienes vary in structure independently, luckily one chromatographic fraction afforded an 8% yield of the single isomer that is depicted in Scheme 5-4 (both adducts are 2,4-*endo*). As shown below, the microstructures of DA polymers were assigned in like fashion.

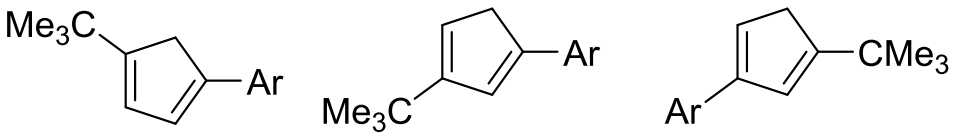

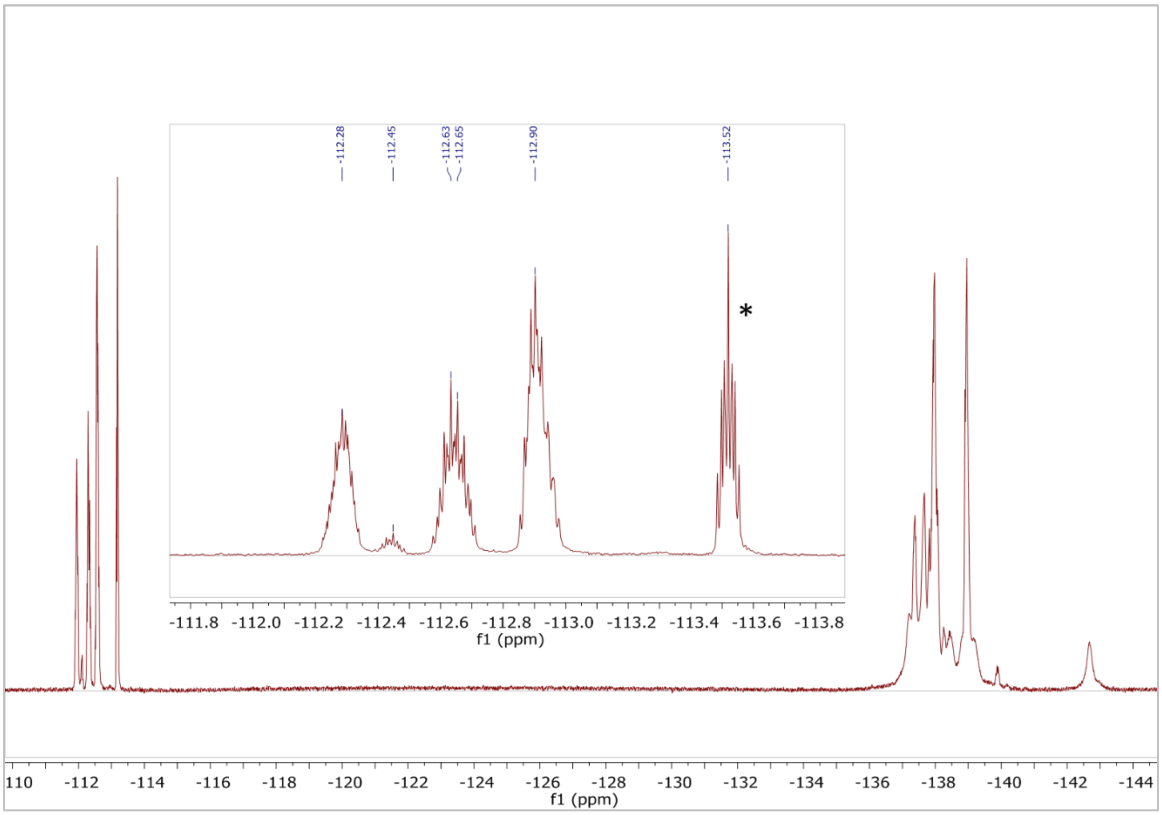

Figure 5-2. ^{19}F (376 MHz, $CDCl_3$) NMR spectrum of the crude mixture of adducts (**9**) arising from the reaction of bis(diene) **1** with **2** equiv of **FMI**. The inset shows the region of the spectrum assigned to the 4-fluorophenyl group on the maleimide moiety. The signal at −113.5 ppm corresponds to unreacted **FMI**. The other signals are assigned as follows: −112.3, 1,3-*exo*; −112.4, 2,4-*exo*; −112.6, 1,3-*endo* and 1,4-*endo*; and −112.9 (2,4-*endo*).

5.4.4 Polymer Synthesis

Polymers were prepared by the reaction of bis-dienes **1**, **2,** and **3** with bis-maleimides **4, 5, 6,** or **7** in rigorously (dried monomers massed to 0.0001 g) equimolar ratios as 33 wt. % solutions in toluene at 80 or 100 °C, or in *o*-dichlorobenzene at 150 °C, under anhydrous and anaerobic conditions as a precaution. Polymers were precipitated into saturated NaCl/methanol and dried under vacuum. Dried polymers were generally white to light tan with the exception of those derived from maleimide **4**, which were yellow.

Scheme 5-5

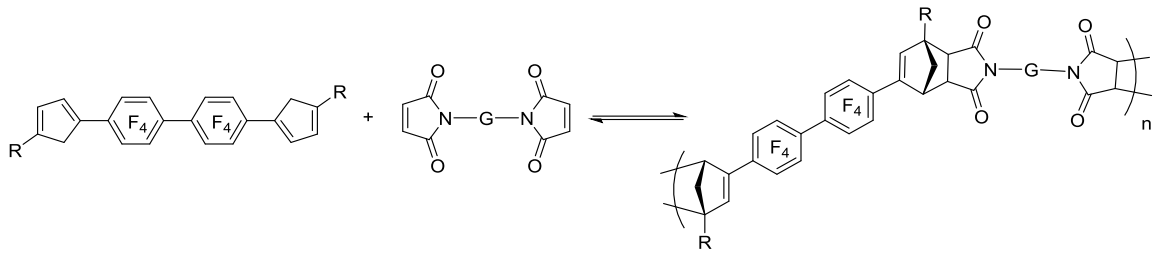

General polymerization of a bis-cyclopentadiene and a bis-maleimide

Since our prior NMR studies (described above for compound **9** and for single-ring models in Chapter 3) involved cyclopentadienes bearing *tert*-butyl substituents, we used a sample of polymer **P2** for detailed characterization of the microstructure by NMR spectrometry. The NMR spectrum of polymer **P2** is shown in Figure 5-3 along with the corresponding spectrum of the mixture of DA adducts arising from the reaction of **A** with **FMI** at the same reaction temperature (80 °C). We presume that the other polymers will have similar structural distributions, although the steric and electronic effects of the three alkyl substituents (*tert*-butyl, *iso*-propyl, and cumyl) obviously vary as will be demonstrated below in their effects on the glass transition.

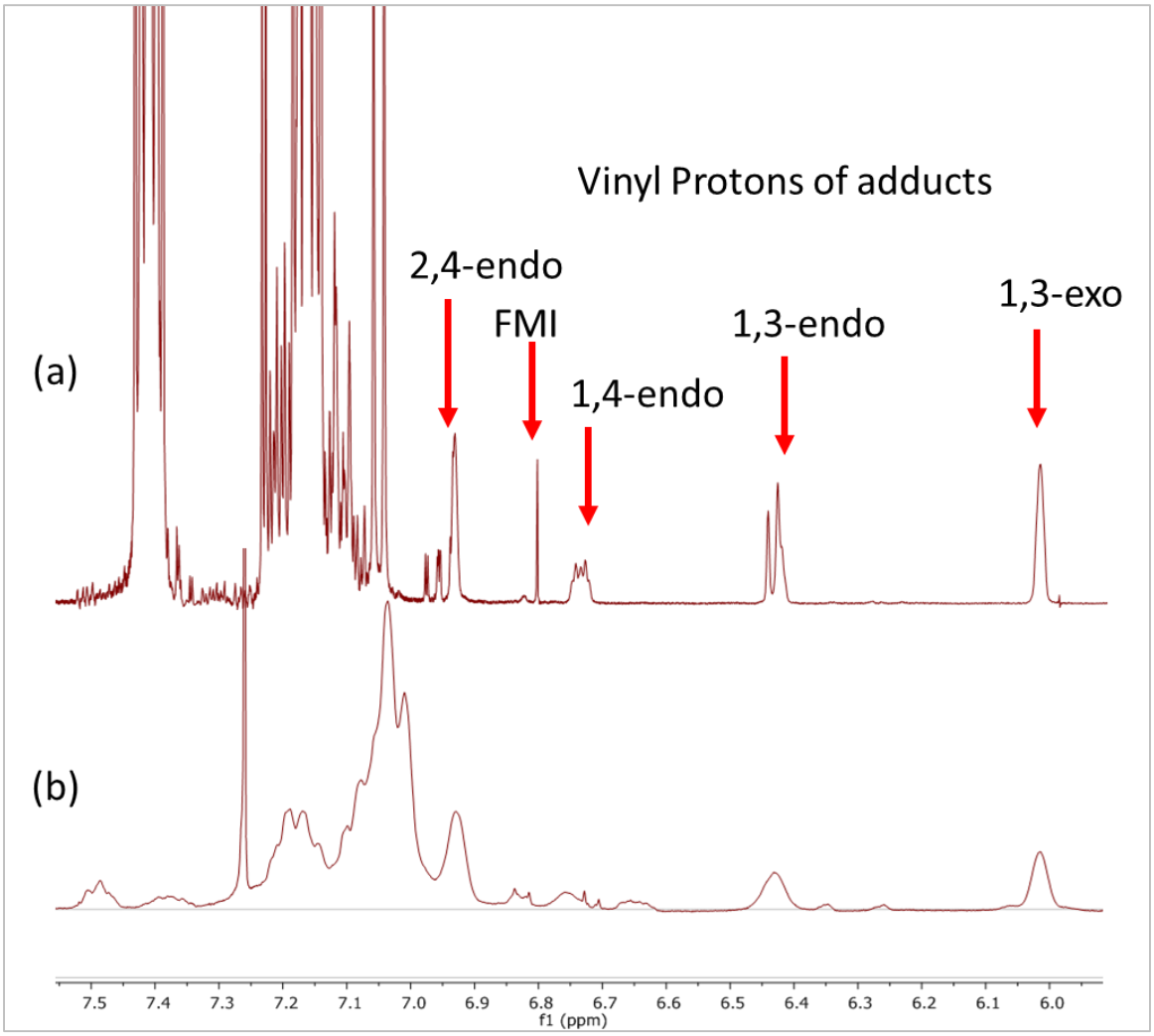

Figure 5-3. Comparison of the ^{1}H (400 MHz, $CDCl_3$) NMR spectra (vinyl and aromatic region only) for (a) model CPD-MI adducts prepared at 80 °C described in Chapter 3 and (b) polymer **P2** prepared at 80 °C. Vinyl signals for 1,3-*endo* overlap with a vinyl signal for the 1,4-*endo* compound.

The model and polymer NMR spectra correspond reasonably well. Table 5-2 shows the NMR chemical shifts that are predicted on the basis of these model studies. The vinyl CH region of the spectrum is the best resolved and the most diagnostic of the distribution of adduct isomers. While the chemical shifts observed for **P2** are not identical (at least partly due to the difference in maleimide substituent and perhaps also to solvation), we were able to correlate the model and polymer spectra fairly closely.

Table 5-2. Vinyl CH and tert-butyl NMR chemical shifts from small-molecule models and corresponding chemical shifts from polymer **P2**.

Model Compound	**Vinyl CH, model**	**Vinyl CH, polymer**	***t*-butyl CH_3, model**	***t*-butyl CH_3, polymer**
2,4-*endo*	6.9	6.7	1.2	1.3
2,4-*exo*	6.8	6.6	1.2	1.3
1,3-*endo*	6.4	6.3	1.1	1.0
1,3-*exo*	6.0	6.0	1.2	1.2
1,4-*endo*	6.7, 6.4	6.3, 6.3	--	1.1

5.4.5 Molecular Weight Determination

Size exclusion chromatography (SEC) was performed on the polymers to determine their molecular weight distributions. Absolute molecular weights were calculated using a light scattering detector, together with $d\eta/dc$ values measured for each polymer in THF solutions. This specific refractive index increment allows for the concentration of eluting sample to be known and then related to molecular weight based on the light scattering signal so that a distribution can be obtained. In all cases except two (see below), we were able to obtain a monomodal SEC trace for each polymer sample. In a few cases, initial SEC traces showed strong bimodality, but preparation of a fresh polymer sample under carefully controlled conditions, or reprecipitation of the polymer sample, afforded monomodal SEC traces. In the cases of Polymers **3** and **4** bimodality in the light scattering SEC traces is most likely caused by some aggregation of the polymer sample in THF solution. Refractive index traces were consistently monomodal with PDIs ~2, further supporting the possibility of aggregation and not cross-linking. Molecular weight and PDI did not seem to trend with monomer structure. Factors influencing molecular weight could include: stoichiometric imbalance (as a result of monomer purity and relatively small scale polymerizations); competitive rDA as a low binding constant will decrease DP according to the following relationship:[10,118]

$$\bar{X}_n = \sqrt{[M]_o K} \qquad [11]$$

5.4.6 Thermal Analysis

Differential scanning calorimetry (DSC) was performed on the polymers **P1** – **P15** to determine their glass transition temperatures (T_g). A typical thermogram obtained using polymer **P7** is shown in Figure 5-4. A relatively sharp transition is indicated at 166 °C. Strikingly absent from the thermogram is any transition at lower temperature that might be assigned to an rDA event. However, as these polymers are glassy, we conclude that there is insufficient mobility within the polymer for an rDA event to occur at temperatures below T_g. We recall from Chapter 3 that a crystalline sample of a corresponding model DA adduct that was heated to just below its melting point did not isomerize, whereas just a few degrees higher, in the molten state, isomerization was rapid. It is possible, therefore, that the transition shown in Figure 5-4 represents a combination of the glass transition and rDA events that may become possible with the onset of segmental mobitiliy.

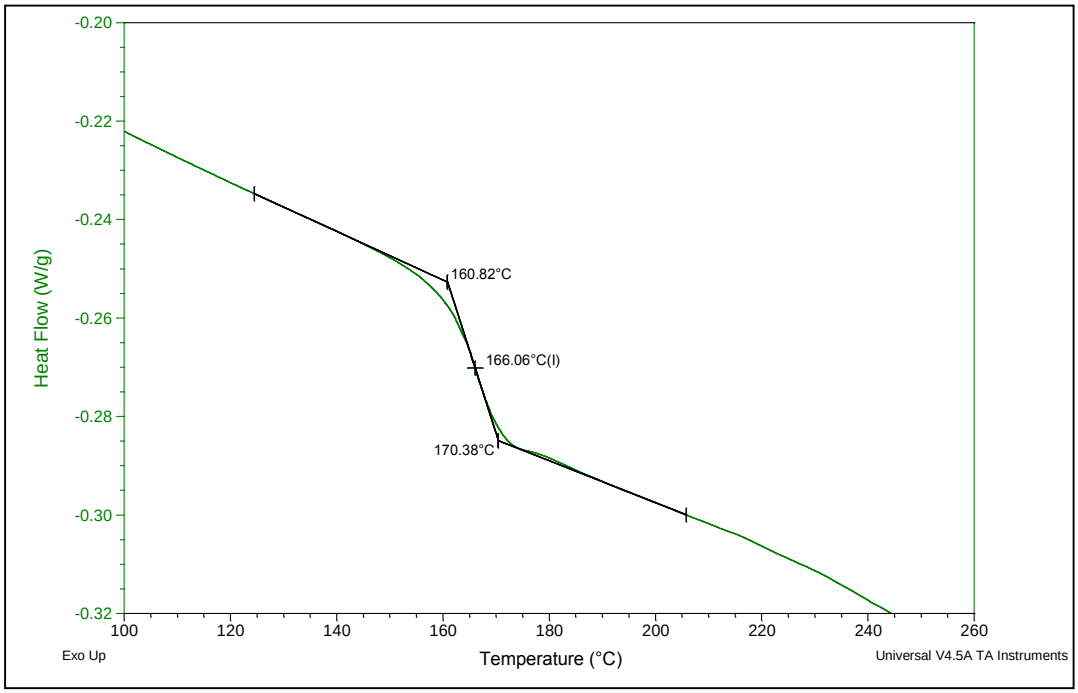

Figure 5-4. DSC thermogram (second heating cycle of a heat-cool-heat regime) of Diels-Alder polymer **P7**. The endotherm at 166 °C is assigned to the glass transition (T_g) although possible rDA events occurring concurrently with the onset of segmental mobility cannot be excluded.

The glass transition temperatures of polymers **P1** – **P15** showed interesting variations with monomer structure (Table 5-3). A strong trend is observed in the influence of the bis(MI) linker on the glass transition. We infer that the segmental motion that is beginning to occur at the T_g is arising mostly if not entirely from the linker. Thus the stiff aromatic linker gives a very high T_g, while the trend among the aliphatic linkers is toward lower T_g with increased linker length and flexibility.

Table 5-3. Glass transition temperatures (T_g) for Diels-Alder polymers as a function of monomer cyclopentadiene substituent (R) and bis(maleimide) linking group (G) defined in Scheme 5-3.

Polymer	R	G	T_g, °C	T_d, °C
1	$-C(CH_3)_3$	$-C_6H_4OC_6H_4-$	257	250
2	$-C(CH_3)_3$	$-(CH_2)_6-$	214	292
3	$-C(CH_3)_3$	$-CH_2CH_2(OCH_2CH_2)_2-$	187	283
4	$-C(CH_3)_3$	$-(CH_2)_{12}-$	163	293
5	$-CH(CH_3)_2$	$-C_6H_4OC_6H_4-$	273	315
6	$-CH(CH_3)_2$	$-(CH_2)_6-$	191	--
7	$-CH(CH_3)_2$	$-CH_2CH_2-(OCH_2CH_2)_2-$	166	295
8	$-CH(CH_3)_2$	$-(CH_2)_{12}-$	139	302
9	$-C(CH_3)_2Ph$	$-C_6H_4OC_6H_4-$	252	298
10	$-C(CH_3)_2Ph$	$-(CH_2)_6-$	203	--
11	$-C(CH_3)_2Ph$	$-CH_2CH_2(OCH_2CH_2)_2-$	171	314
12	$-C(CH_3)_2Ph$	$-(CH_2)_{12}-$	153	--
13	$-C(CH_3)_3$	$-(CH_2)_{12}-$	163	--
14	$-C(CH_3)_3$	$-C_6H_4OC_6H_4-$	263	--
15	$-C(CH_3)_3$	$-(CH_2)_6-$	211	--

A more subtle effect is observed in the trend arising from the cyclopentadiene substituent. The least "flexible" substituent is arguably the *tert*-butyl group because its structure is isotropic. That is, the *t*-butyl group may rotate, but each rotation results in the same conformation. The other groups can adjust their torsional angles with respect to the adduct norbornene moiety possibly to accommodate the onset of segmental motion elsewhere in the bulk polymer. Our speculative interpretation of this trend is that the size and symmetry of the Cp substituent influences the local free volume near the most mobile components of adjacent polymer chains, which almost certainly

are the bis(MI) linkers. As the Cp substituent rotates, it carves out or vacates small local volumes depending on the orientation of its largest substituent. The tert-butyl group is isotropic and therefore exhibits the smallest plasticizing effect.

Polymers prepared at T = 150 °C exhibited similar T_g values despite the differences in repeat unit microstructure (isomerism and stereochemistry).

Thermo-gravimetric analysis (TGA) was performed on representative polymers selected from **P1** – **P15**. A typical TGA trace is shown in Figure 5-5. All polymers were thermally stable under nitrogen up to at least 250 °C. Decomposition of the polymer appears to be independent of T_g. Moreover, the polymers do not display any degradation by TGA that can be assigned to rDA which should become available as a decomposition mechanism at $T > T_g$. We surmise that at temperatures below T_d, the DA/rDA equilibrium does not lie sufficiently in favor of rDA and therefore there is not an appreciable likelihood of *adjacent* adducts uncoupling simultaneously for enough time that the disconnected monomer can escape. It is unclear whether the decomposition observed in the TGA is primarily occurring by rDA and volatization of the uncoupled monomers, but samples recovered from the TGA at 300 °C are intractable solids, suggesting that other general decomposition pathways are involved.

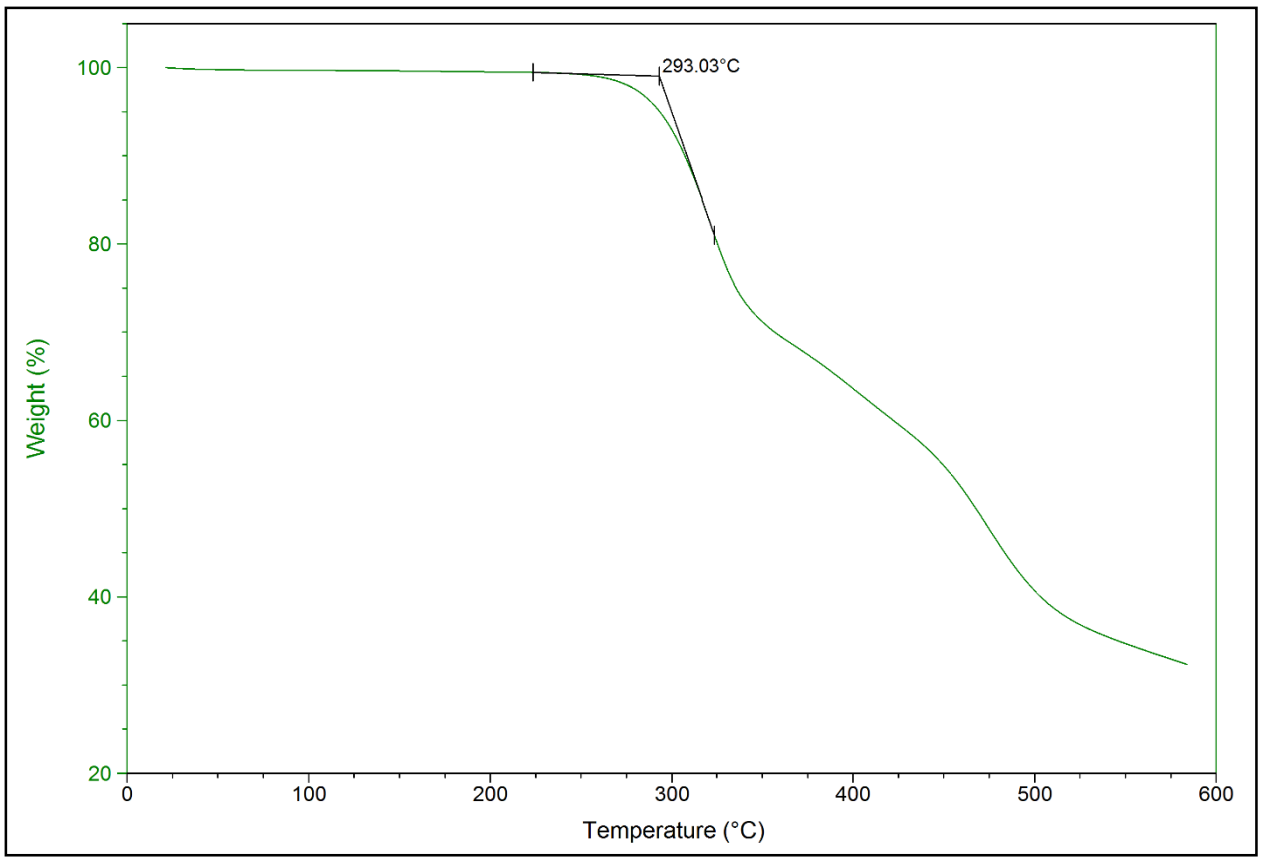

Figure 5-5. TGA trace of polymer **P4** showing thermal stability to ca. 290 °C, with a T_d of 293° C. The broad feature at ca. 425 °C is not assigned.

5.4.7 Depolymerization Studies

Next we studied the thermal depolymerization of our CPD-MI polymers. In **solution method 1**, as sample of a representative polymer (**P4**) was dissolved in *o*-dichlorobenzene at the same concentration at which polymerization was carried out, heated to 140 °C for 1 h, and then quenched. SEC analysis of the polymer before and after thermolysis is shown in Figure 5-6. The decrease in molecular weight suggests that at the temperature of the thermolysis experiment, the equilibrium for the DA reaction shift slightly in favor of rDA such that the number of linkages and therefore the overall average degree of polymerization (DP) decreases.

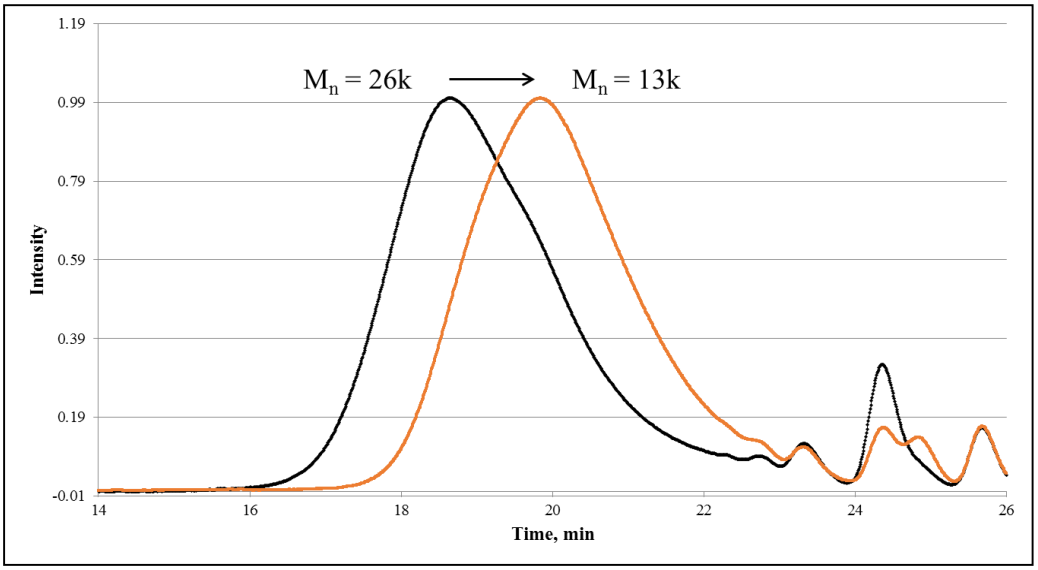

Figure 5-6. Size exclusion chromatograms of polymer **P4** as prepared (T_p = 80 °C, black trace) and after thermolysis at 140 °C in *o*-dichlorobenzene solution (orange trace)

In **solution method 2**, a sample of a representative polymer (**P4**) was thermolyzed in solution (1,2-dichlorobenzene, 110-140 °C) with an excess of **FMI** to trap transient CPD end groups exposed by rDA events (Scheme 5-6).

Scheme 5-6

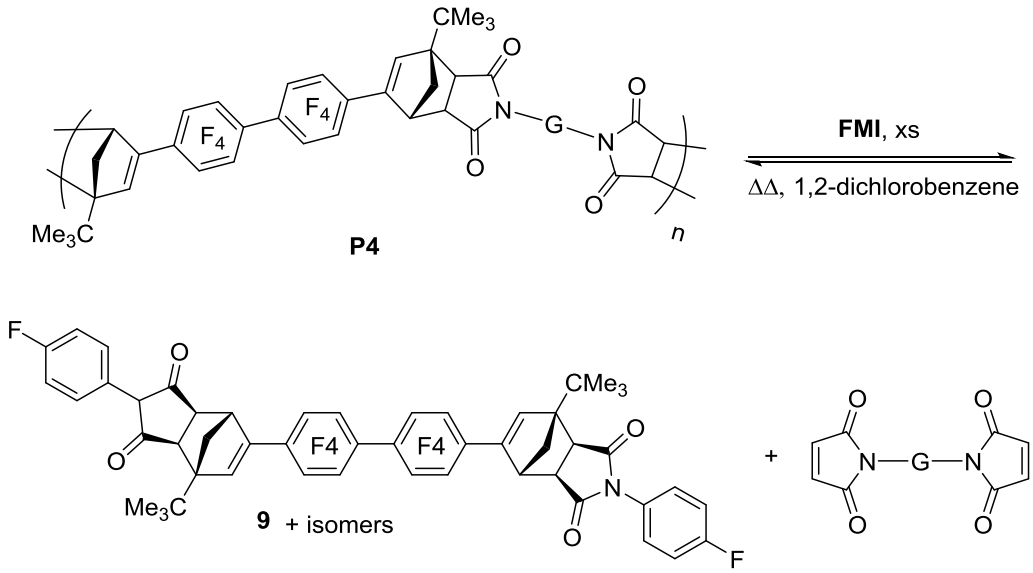

Depolymerization through maleimide exchange

The **FMI**-trapped bis(diene) monomer was recovered as an isomeric adduct mixture, similar to compound mixture **9** (please see Scheme 5-4 and Figure 5-2). A comparison of the spectrum

of **9** prepared directly from the purified monomer and recovered from the thermolysis of the polymer in the presence of excess **FMI** is shown in Figure 5-7.

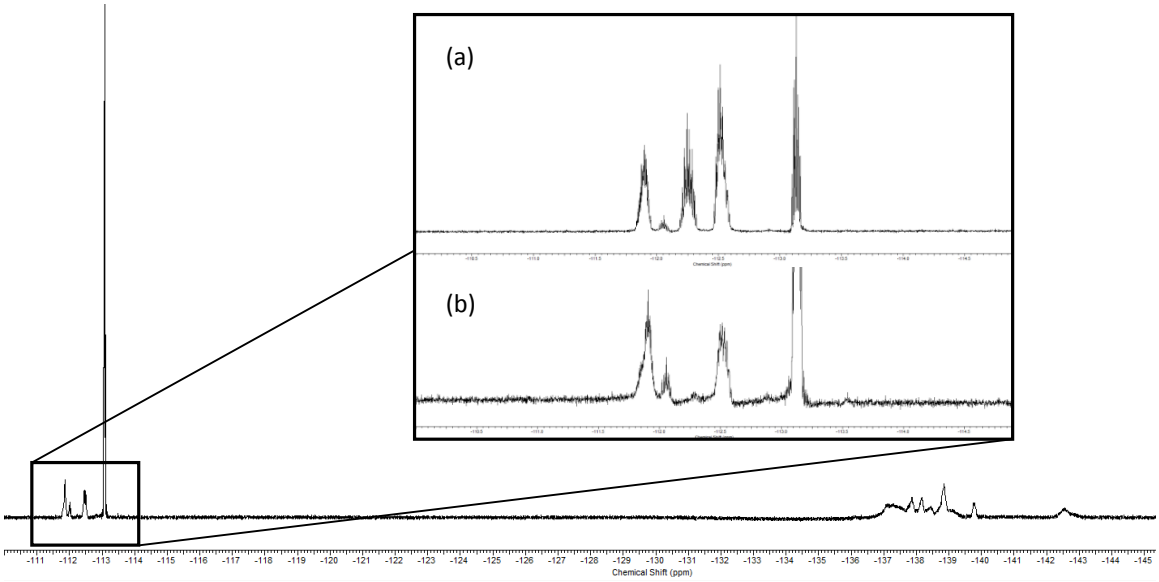

Figure 5-7. ^{19}F (376 MHz, $CDCl_3$) NMR spectra in $CDCl_3$. (a) Spectrum of the bis-adduct **9** prepared from purified monomer **1** and **FMI**. (b) Spectrum of **FMI**-trapped monomer obtained by the thermolysis of polymer **P4** in the presences of excess **FMI**.

In **bulk method 1**, a film prepared by solution casting onto glass-supported Mylar did not show an appreciable decrease in molecular weight or change in polydispersity when heated at 200 °C in a vacuum oven for 2 hours and then analyzed by SEC. A powder sample treated and analyzed in the same manner likewise did not show any change in M_n or PDI. However, as we have described above, rDA is expected to be structurally frustrated below the glass transition temperature and may still be slow at temperatures somewhat above T_g.

In **bulk method 2**, the diene monomer was captured by brute-force sublimation at a temperature (250 °C) that corresponds roughly to onset of decomposition observed in the TGA. The use of a high vacuum allowed the capture of a residue, which was found to contain monomer **1** in addition to other, unidentified products. The NMR spectra comparing the purified monomer **1** and the sample recovered from the thermolysis of polymer **P4** are shown in Figure 5-8. The

quantity of **1** recovered corresponds roughly to a 40% NMR yield (after accounting for solvent and other unidentified signals in the ^{1}H spectrum). This result tends to suggest that the decomposition observed in the TGA probably includes a substantial rDA component. TGA-MS might illuminate this question further.

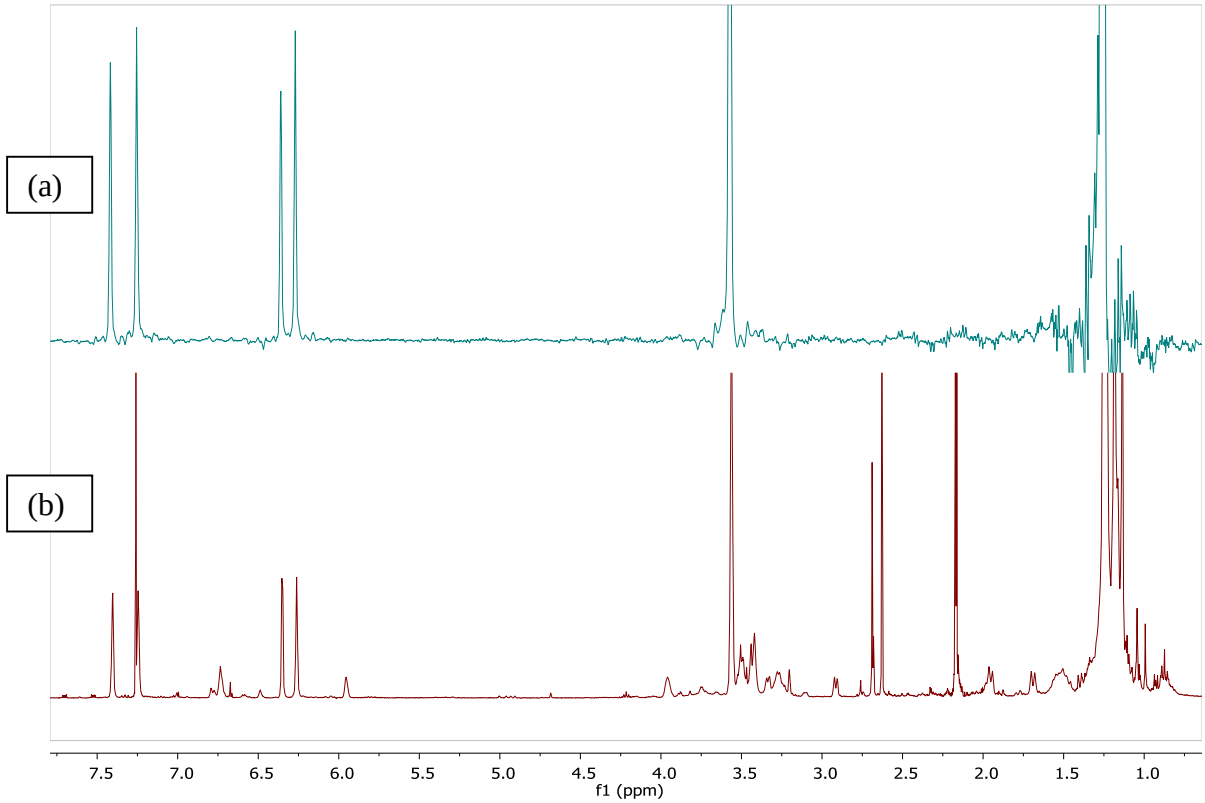

Figure 5-8. ^{1}H (400 MHz, $CDCl_3$) NMR spectra of monomer **1**. (a) Pure bis-diene **1**. (b) Bis-diene **1** recovered from the thermolysis of polymer **P4** under high vacuum sublimation at 250 °C. The signals in the region from ca. 6.0 to 7.5 ppm are vinyl CH signals representing a fingerprint compound **1**. $CHCl_3$ is also present at 7.26 ppm.

Chapter 6 Overall conclusions and future work

This dissertation has described the Diels-Alder reaction and its use in synthetic macromolecular chemistry. As described in Chapter 1, the strengths and limitations of existing approaches are fairly clear, even though many of the underlying fundamental details have not been brought into focus. Furan-maleimide chemistry has the appeal of being the easiest system to use synthetically and the most facile in terms of its reversibility. However the onset of rDA being so close to optimum polymerization temperatures leaves a narrow window of stability at best, such that polymers with DP > 20 are rare. At the same time, "single-component" CPD-CPDs polymers are too stable. Mindful of these approaches, the aim of this work was to develop a synthetically accessible CPD-MI polymerization system with intermediate thermal behavior. After establishing some fundamental trends in the DA reaction (Chapter 2), a path to filling this gap with an optimized CPD-MI DA reaction was realized (Chapter 3). Substituted cyclopentadienes, specifically those substituted with both sterically cumbersome and electron withdrawing groups arrested CPD self-dimerization, while destabilizing the CPD-MI adduct substantially compared to less substituted congeners. The CPD-MI chemistry is complicated, but thanks to NMR spectrometry, liquid chromatography, and X-ray crystallography, not intractable. Meanwhile I attained a better understanding of purely electronic effects on the Diels Alder reaction using a series of triarylated cyclopentadienes (Chapter 4), while demonstrating that with appropriate substitution the tenacious reactivity of cyclopentadiene toward maleic acid derivatives can be tamed to the point where adduct formation is in dynamic equilibrium. Finally, Chapter 5 described the development of a CPD-MI polymer based on a bis-CPD monomer closely related to the synthetic model developed in Chapter 3. The polymers prepared had molecular weights of 10 to 50 kDa, but were quite brittle when cast into films. Reversibility of the polymerization was clearly demonstrated in solution starting at 120 °C and even in the bulk at 250 °C.

There certainly is much left to develop in this area. A closely related monomer design (Scheme 6-1) starts from dicyclopentadienylpropane, a known compound prepared from 6,6-dimethylfulvene. This monomer has the advantage that the *para* fluorines of the perfluoroaryl groups are still available for further functionalization.

Scheme 6-1

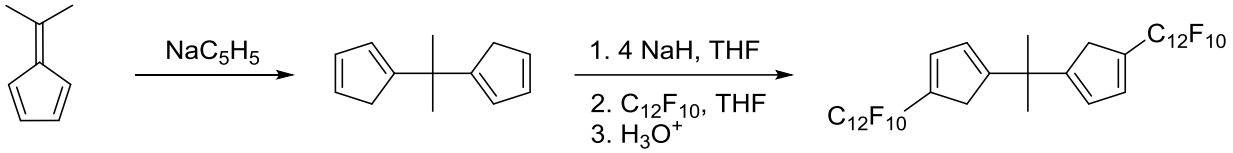

Synthesis of a bis-diene monomer bearing reactive *para* flourines

One challenge the present two-component DA polymers face is the molecular weight limitation. This obstacle may be overcome by the use of telechelics to "build-in" the molecular weight prior to DA chain extension as Watanabe showed (see Chapter 1).[12] As telomers are developed, however, it is critical to ensure 1:1 stoichiometry when chain extending. To better understand the influence of T_g on retro-DA, a telomer having a low T_g, < 100 °C, such as a poly(dimethysiloxane) might enable enough motion at 120 °C to allow rDA to occur normally.

A second development strategy, which has been explored briefly, is to combine furan and CPD chemistry to build a macromolecule with two distinct temperature regimes for response. The proposed strategy involves having the three species present in a macromolecular structure. At low temperatures furans and maleimides will react to form adducts while the substituted CPD moieties spectate. From other research in our group, a CPD moiety is known in which the DA reaction is not realized until temperatures exceeding 120 °C. At this temperature the furan/MI adducts have dissociated by retro-DA and free maleimide may then react with the CPD moiety. At this point the CPD will act as a sink for MI and drive the reaction to the right. Furthermore, at even higher

temperatures the CPD/MI adduct will decompose by retro-DA. The reaction may then be quenched resulting in once again free MI.

In a preliminary study a bis-furan was reacted with *N*-4-fluorophenylmaleimide to form an adduct. At 60 °C the reaction reached approximately 5% conversion to adduct. Upon cooling to 5 °C for 12 hours, the conversion increased to 8%. Heating the sample to 100 °C reduced conversion to ~3% over 240 hours. The sample was then quenched to room temperature and was allowed to stand for 36 hours. Conversion at this point was in excess of 15%. This experiment showed that furan/maleimide adducts are thermally dynamic, as expected. What it also showed was the temperature regime for reversal was below that for adduct formation with a CPD moiety such as **4**.

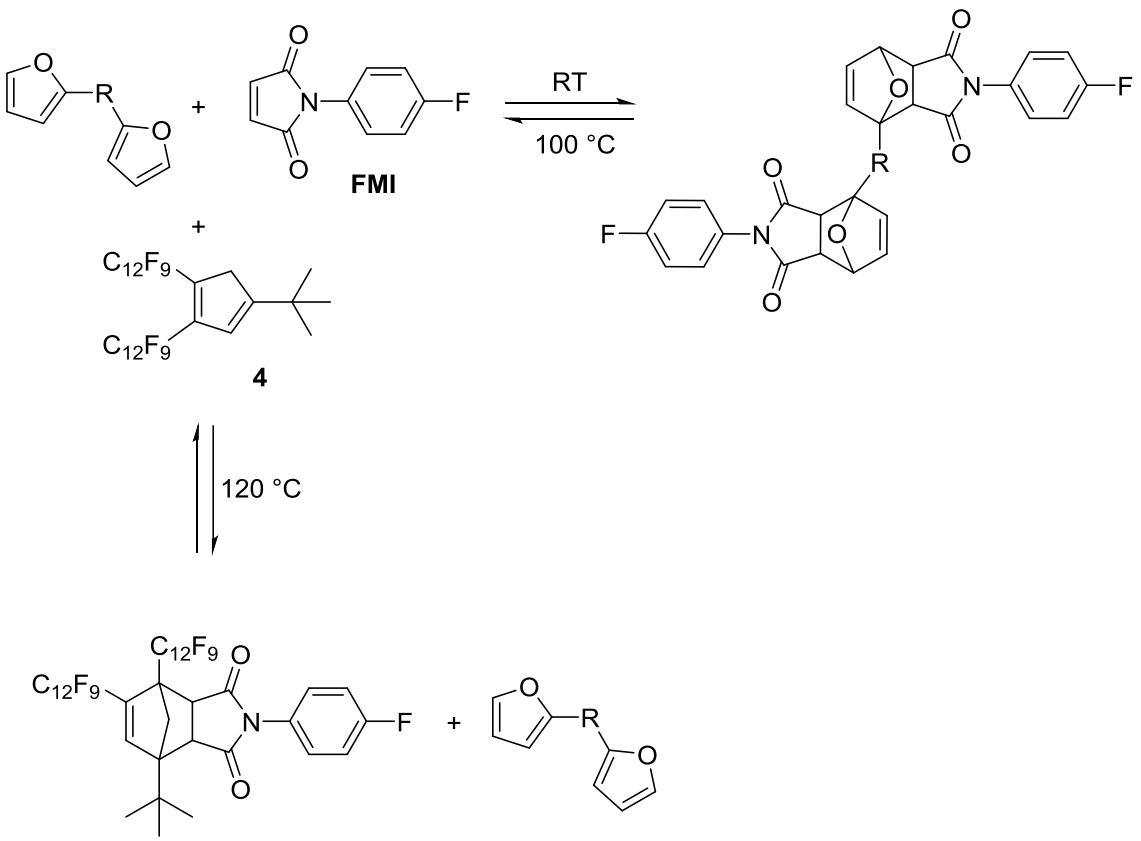

Figure 6-1. Proposed coupling-decoupling maleimide exchange between furan and CPD moieties.

Appendix A Supporting information for Chapter 2

NMR Spectra

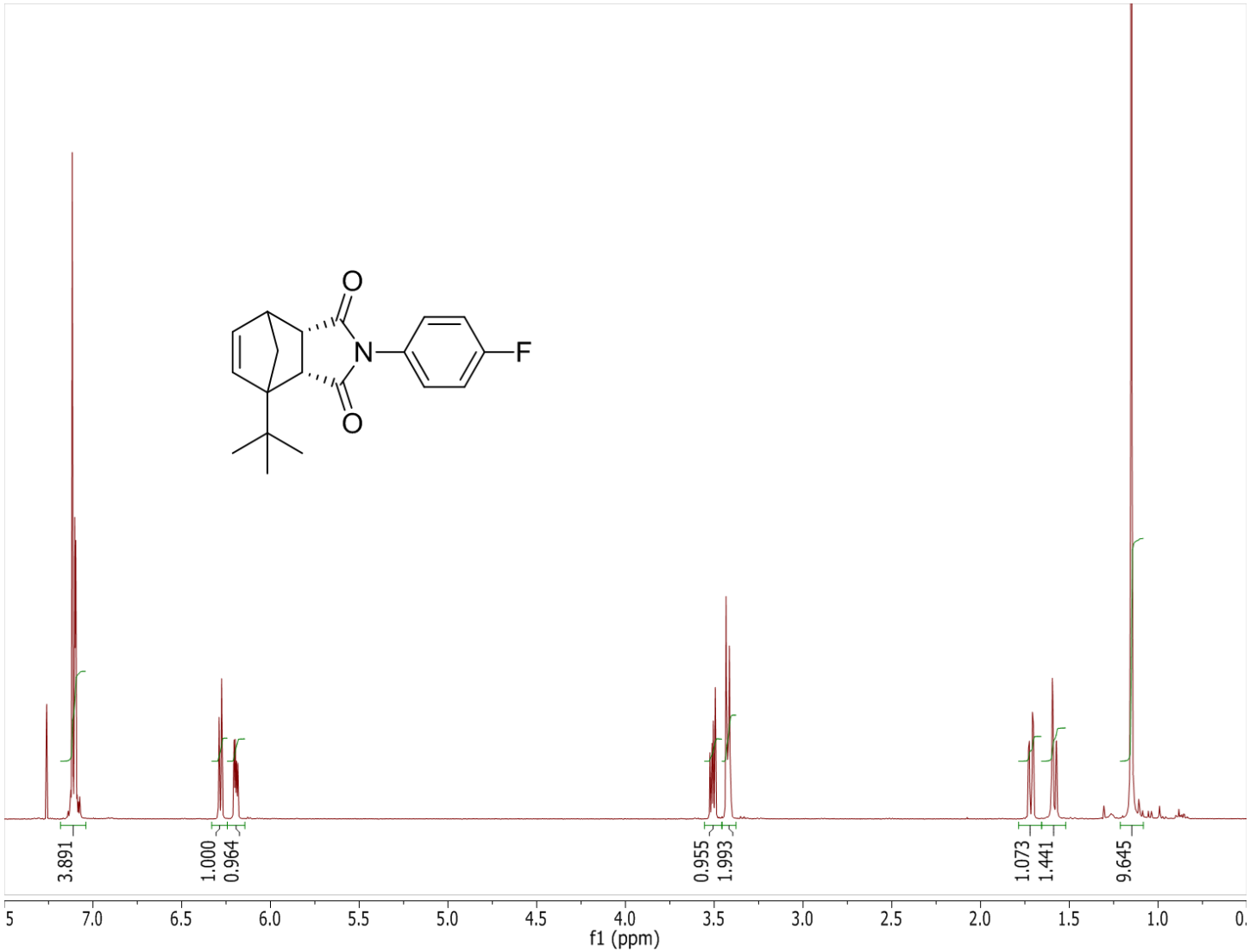

Figure A1. ^{1}H (400 MHz, $CDCl_3$) NMR spectrum of compound **1a**.

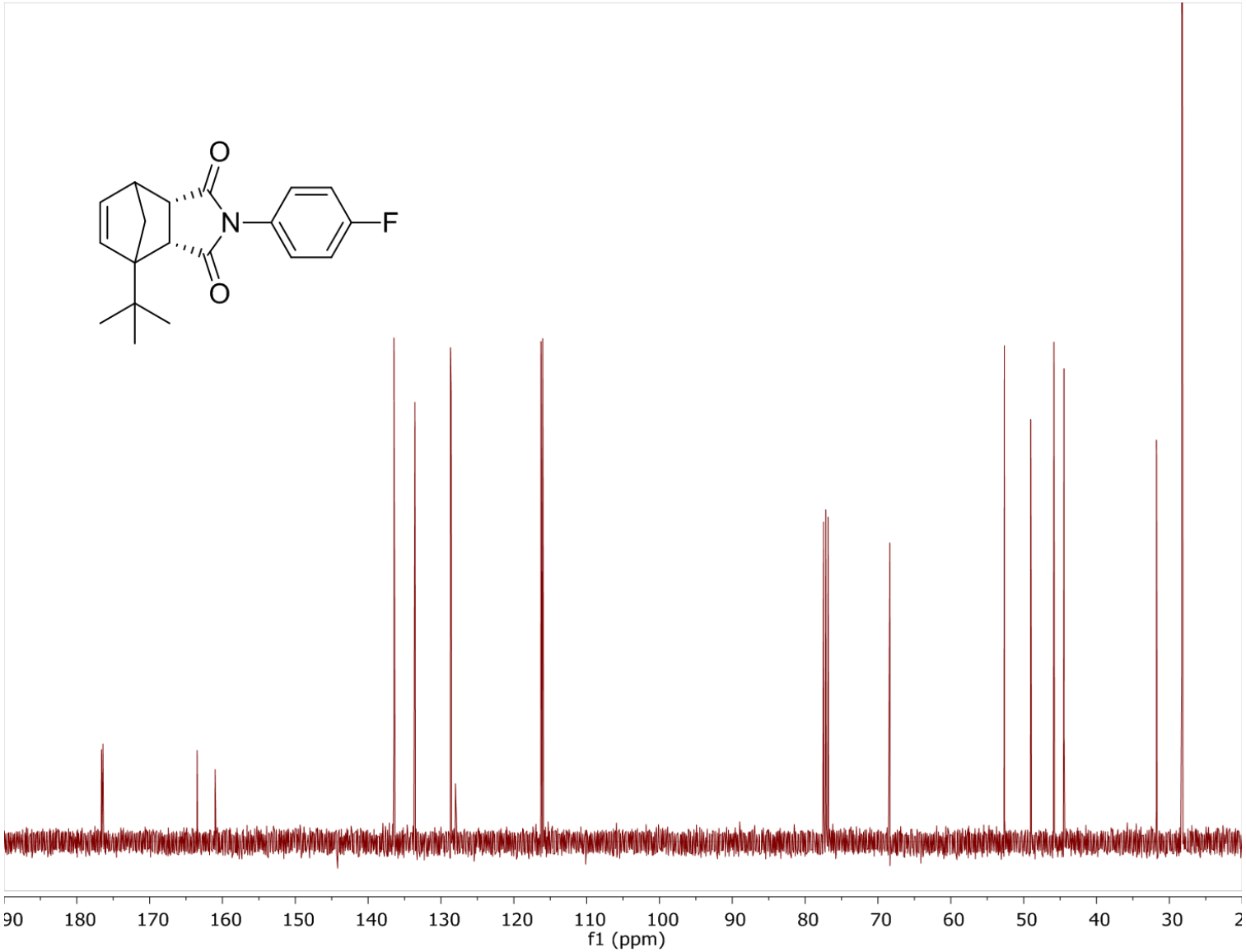

Figure A2. ^{13}C (100 MHz, $CDCl_3$) NMR spectrum of compound **1a**.

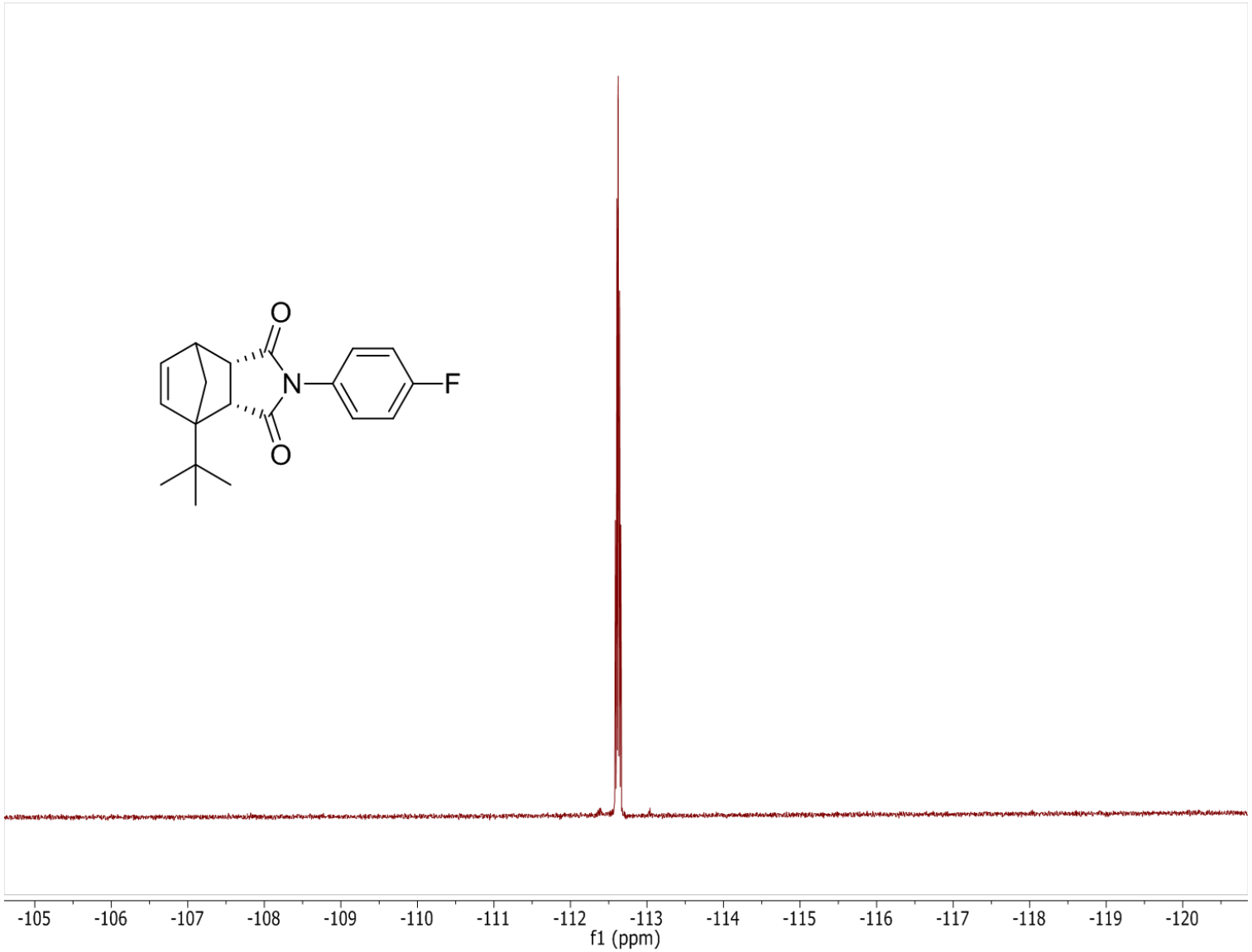

Figure A3. ^{19}F (376 MHz, $CDCl_3$) NMR of compound **1a**.

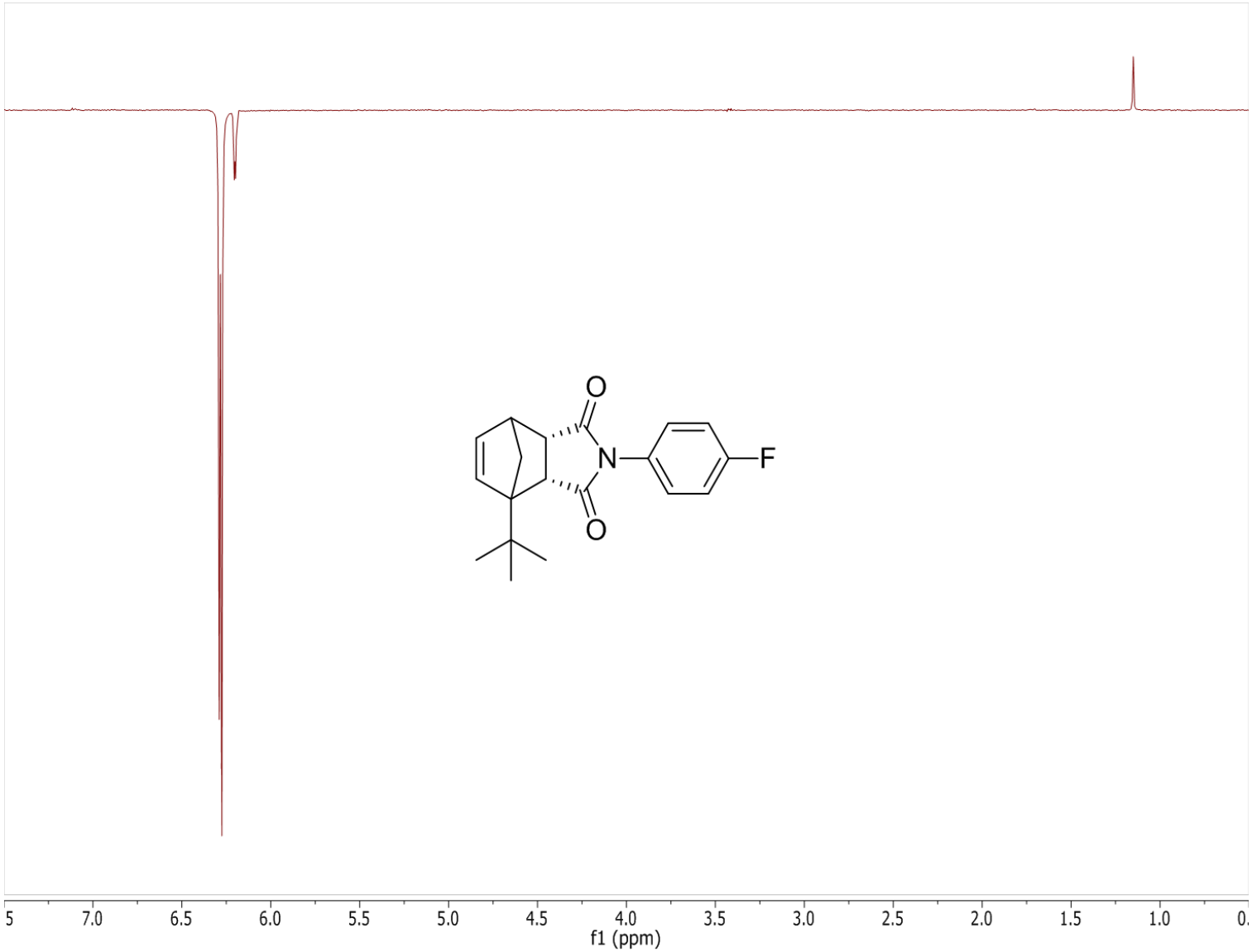

Figure A4. ^{1}H 1D NOE spectrum of compound **1a** in $CDCl_3$.

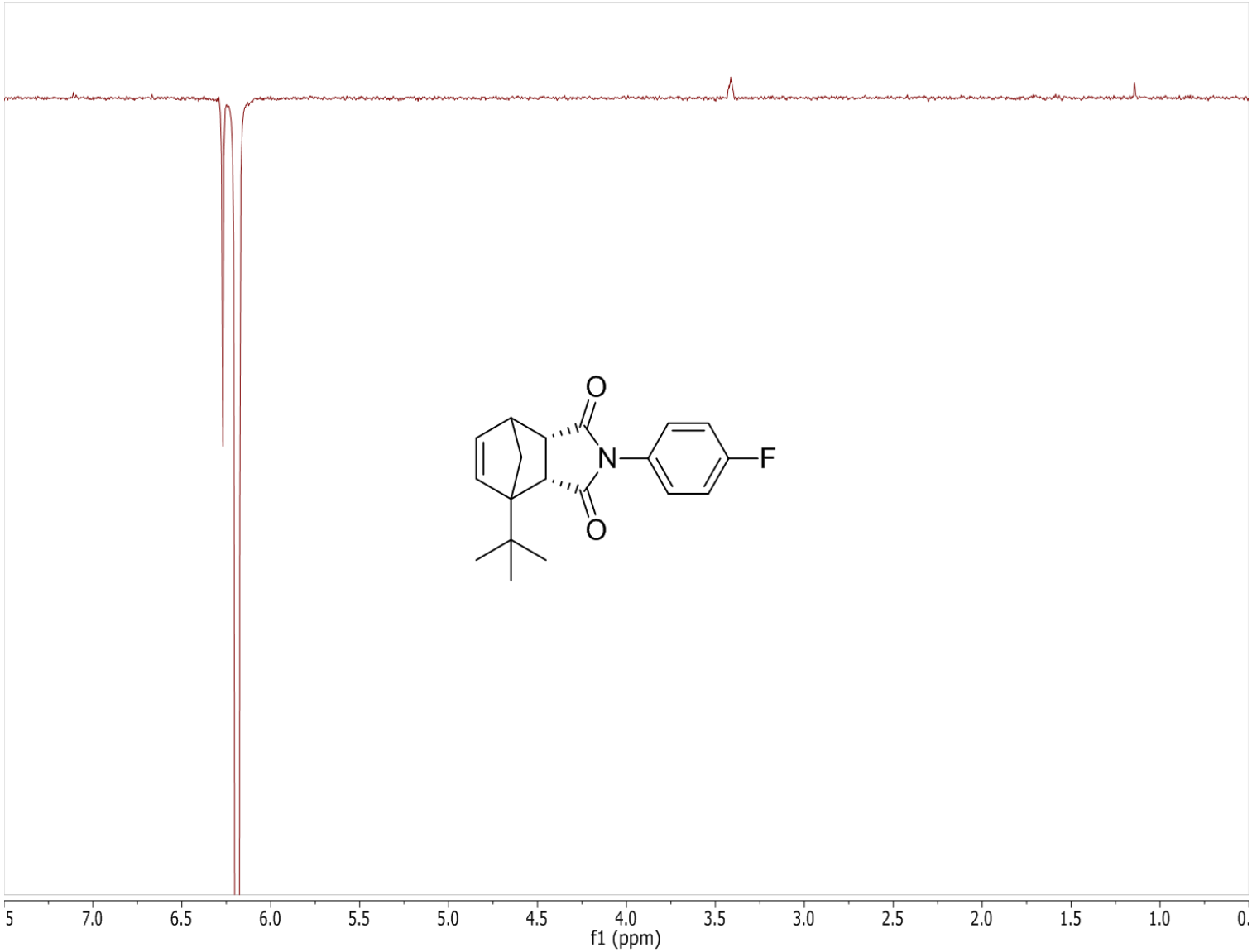

Figure A5. ^{1}H 1D NOE spectrum of compound **1a** in $CDCl_3$.

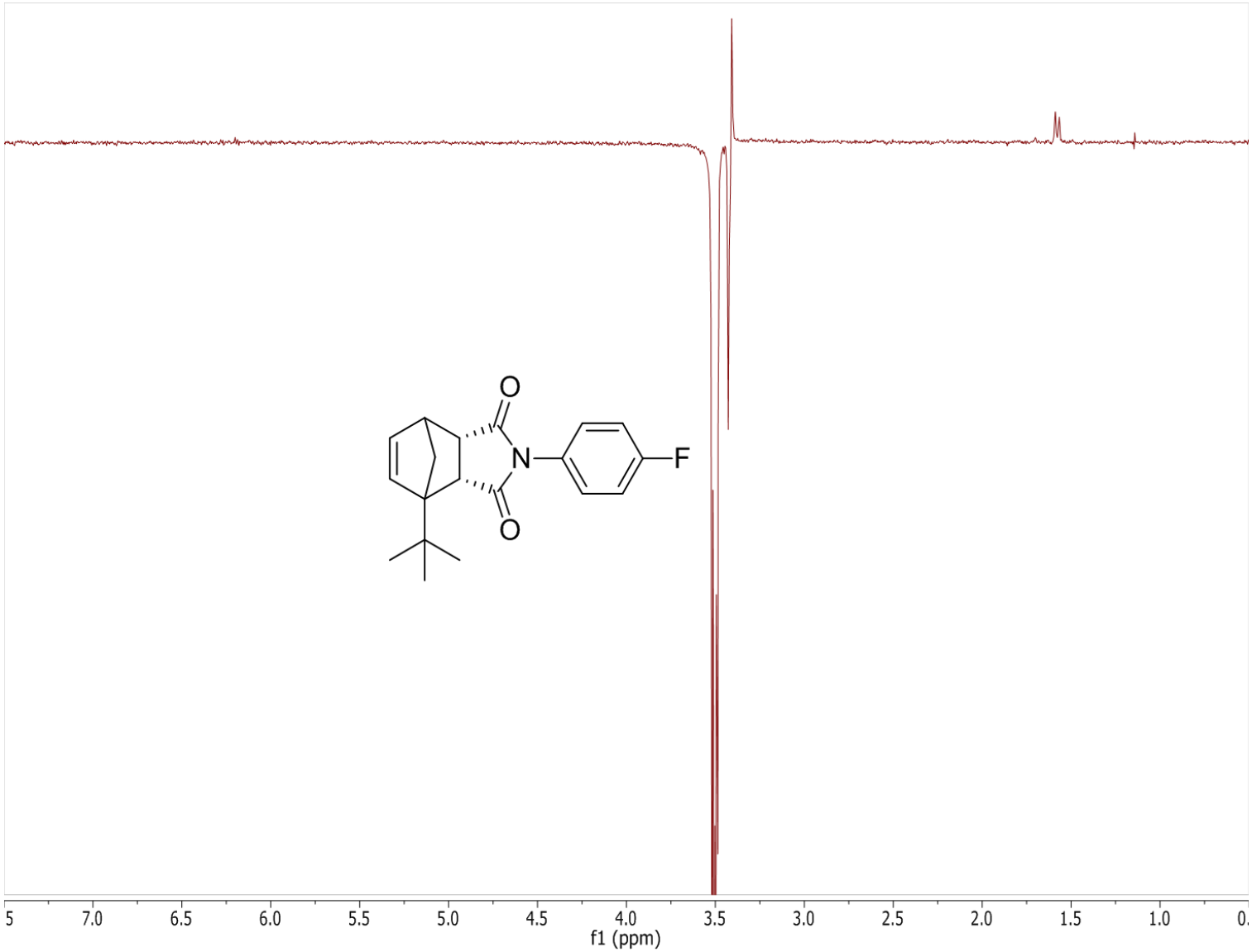

Figure A6. ^{1}H 1D NOE spectrum of compound **1a** in $CDCl_3$.

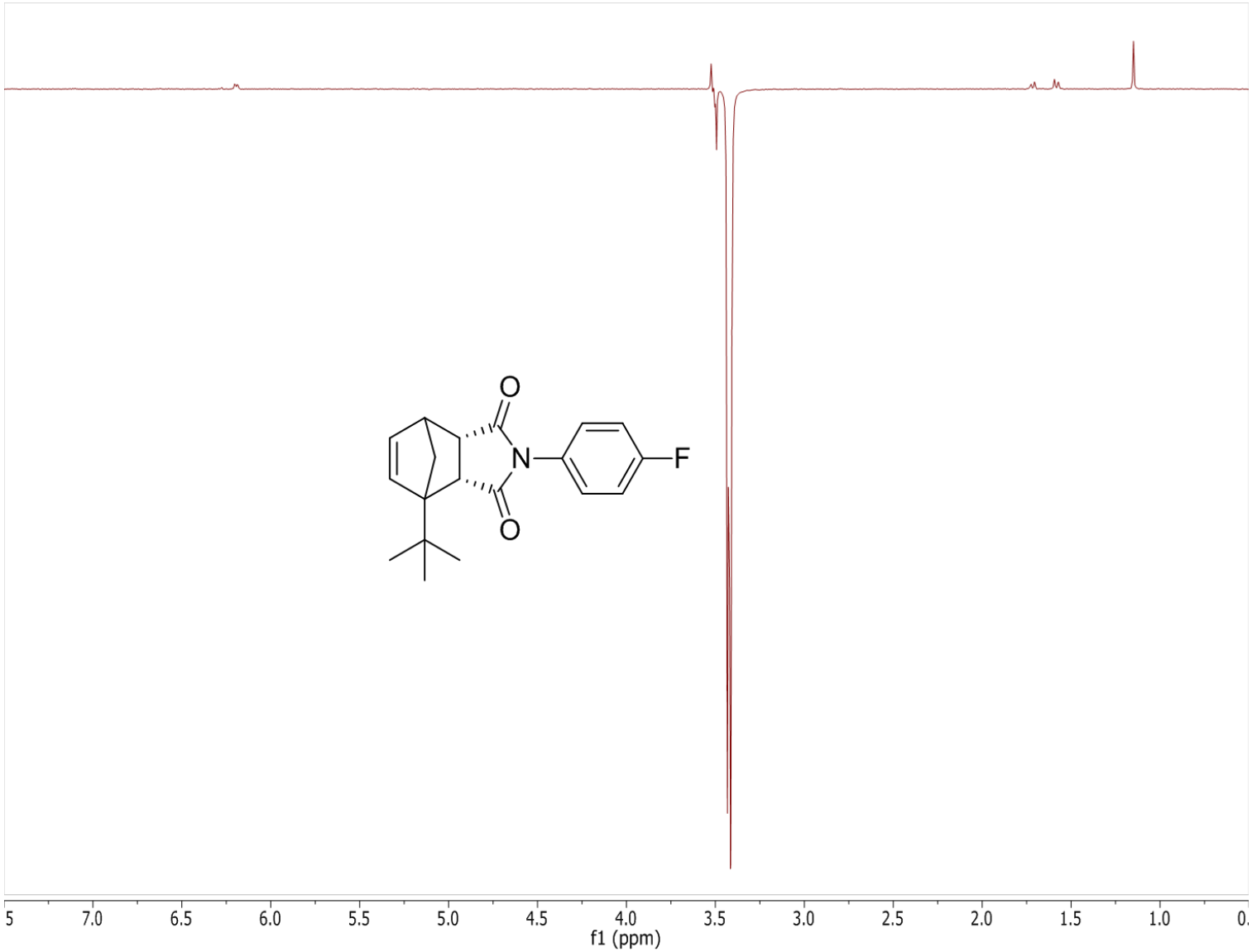

Figure A7. ^{1}H 1D NOE spectrum of compound **1a** in $CDCl_3$.

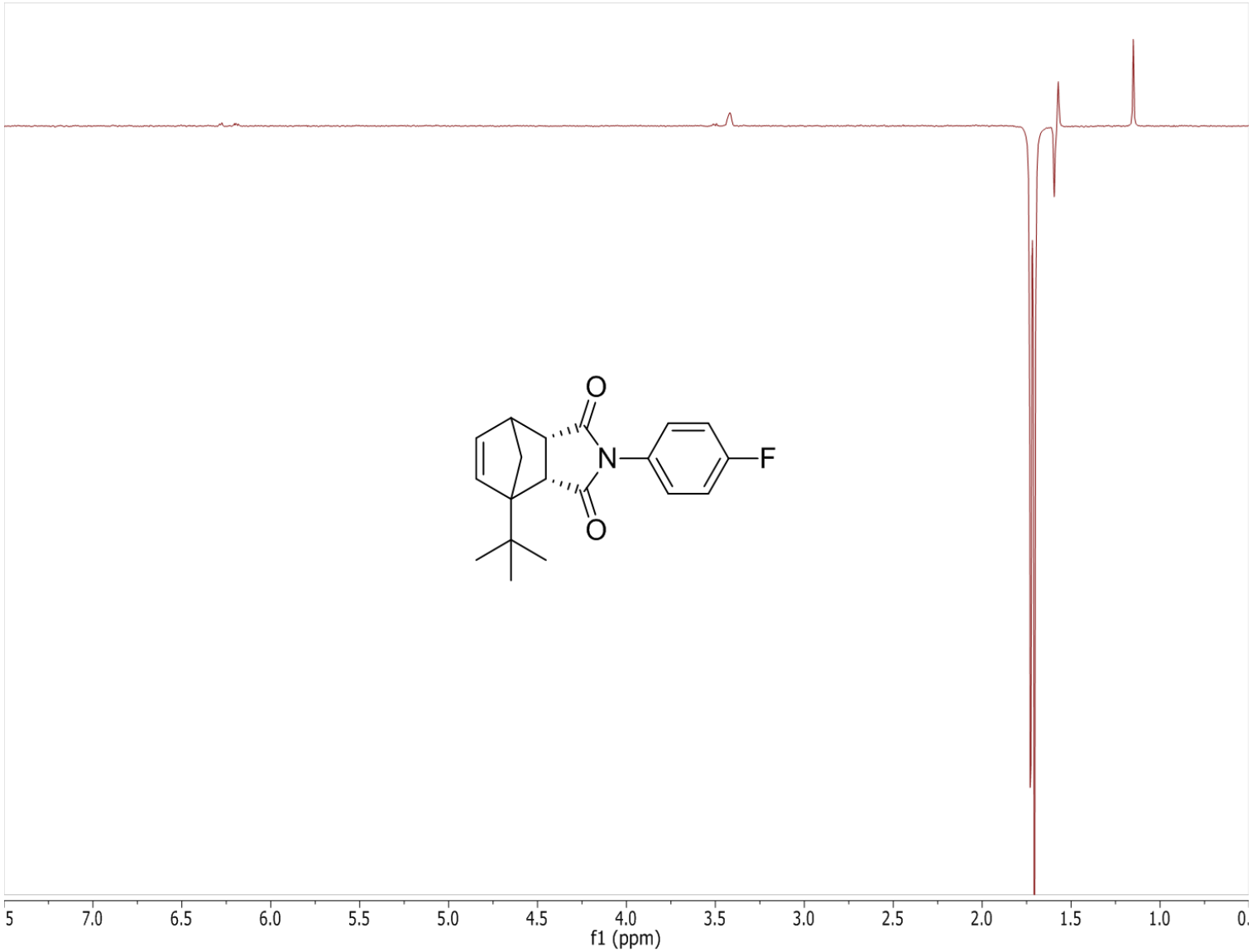

Figure A8. ^{1}H 1D NOE spectrum of compound **1a** in $CDCl_3$.

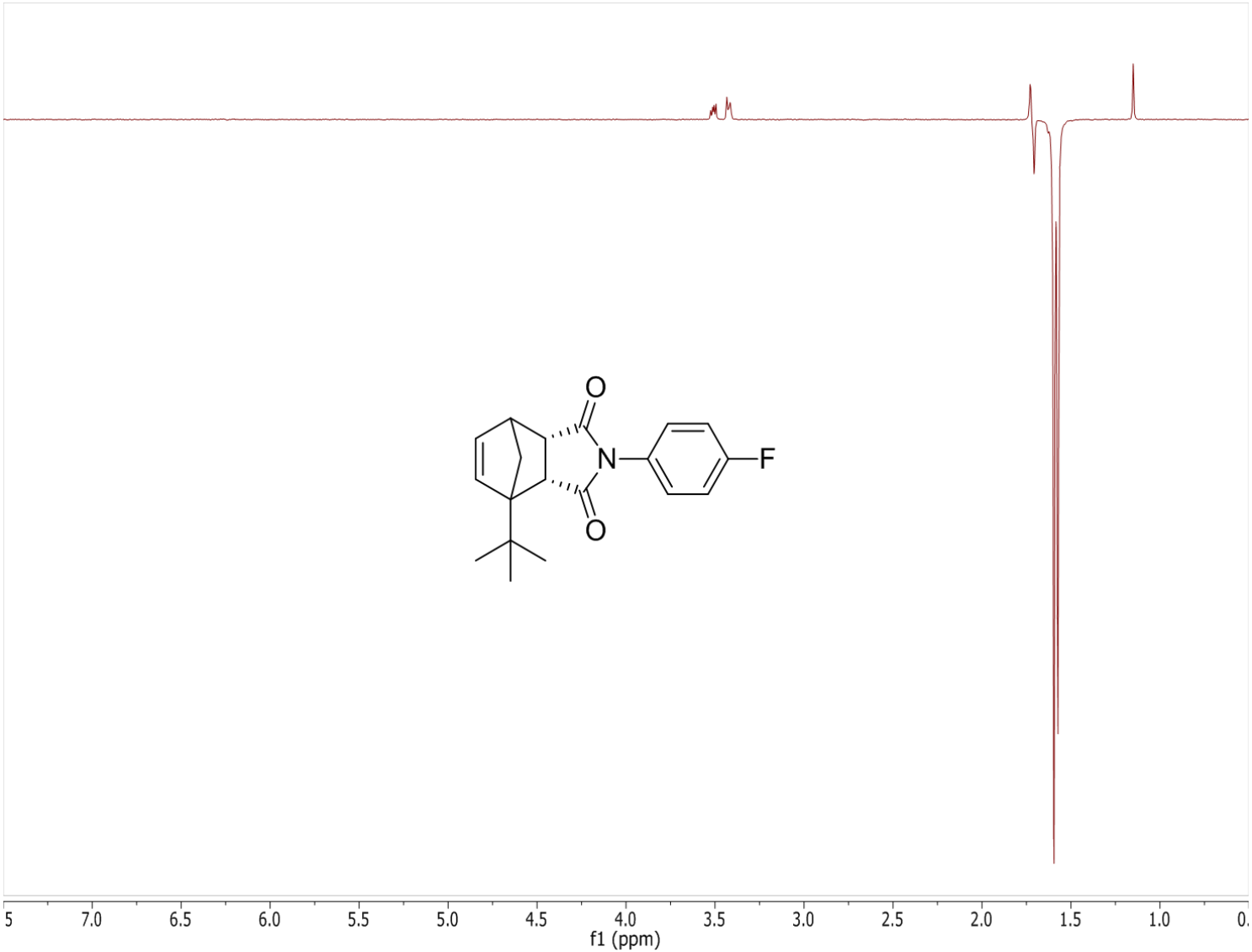

Figure A9. ^{1}H 1D NOE spectrum of compound **1a** in $CDCl_3$ shows through space spin relaxation from bridging protons at δ 1.58 ppm to methine protons at δ 3.50 and 3.42 ppm, indicating the molecule has *endo* stereochemistry.

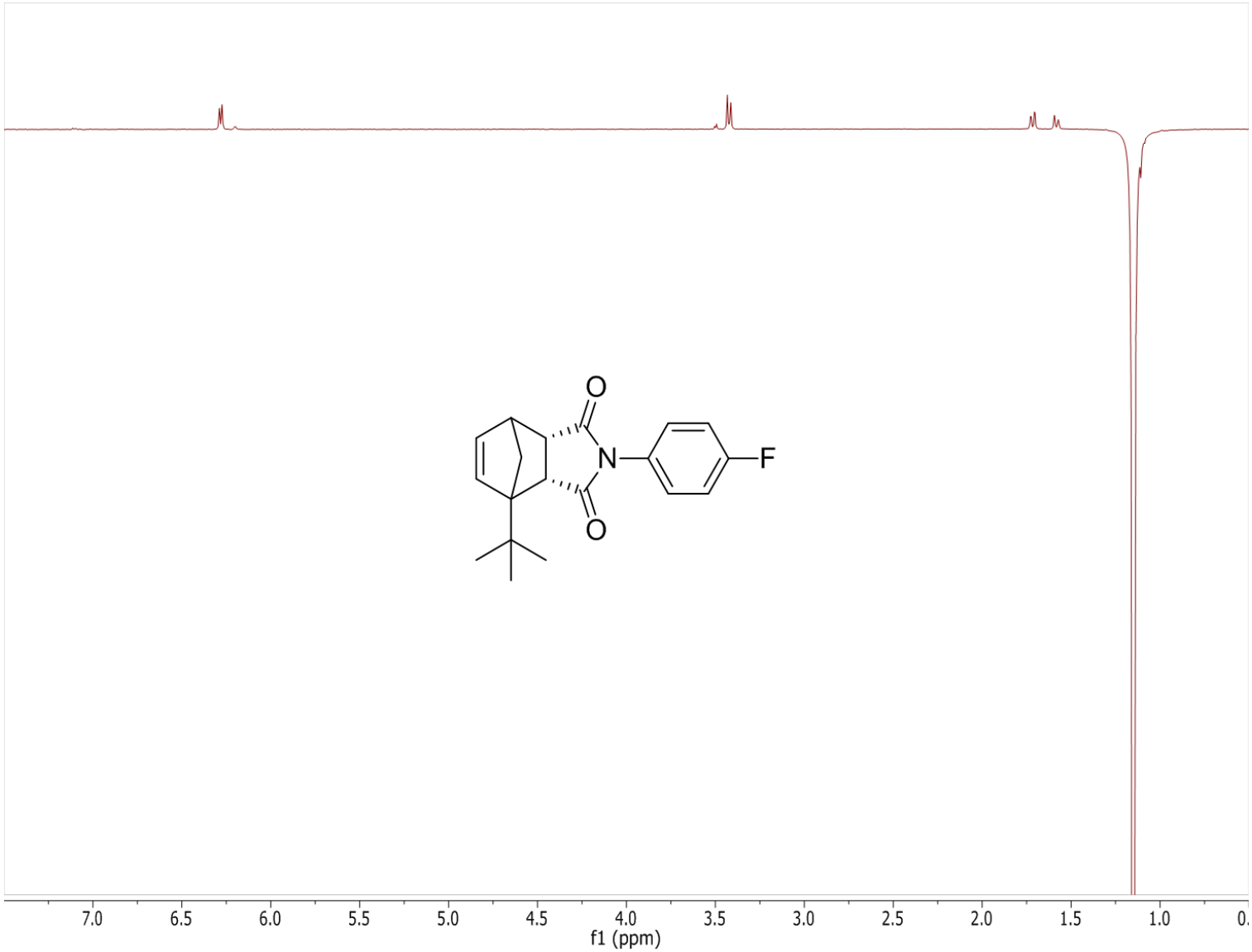

Figure A10. ^{1}H 1D NOE spectrum of compound **1a** in $CDCl_3$.

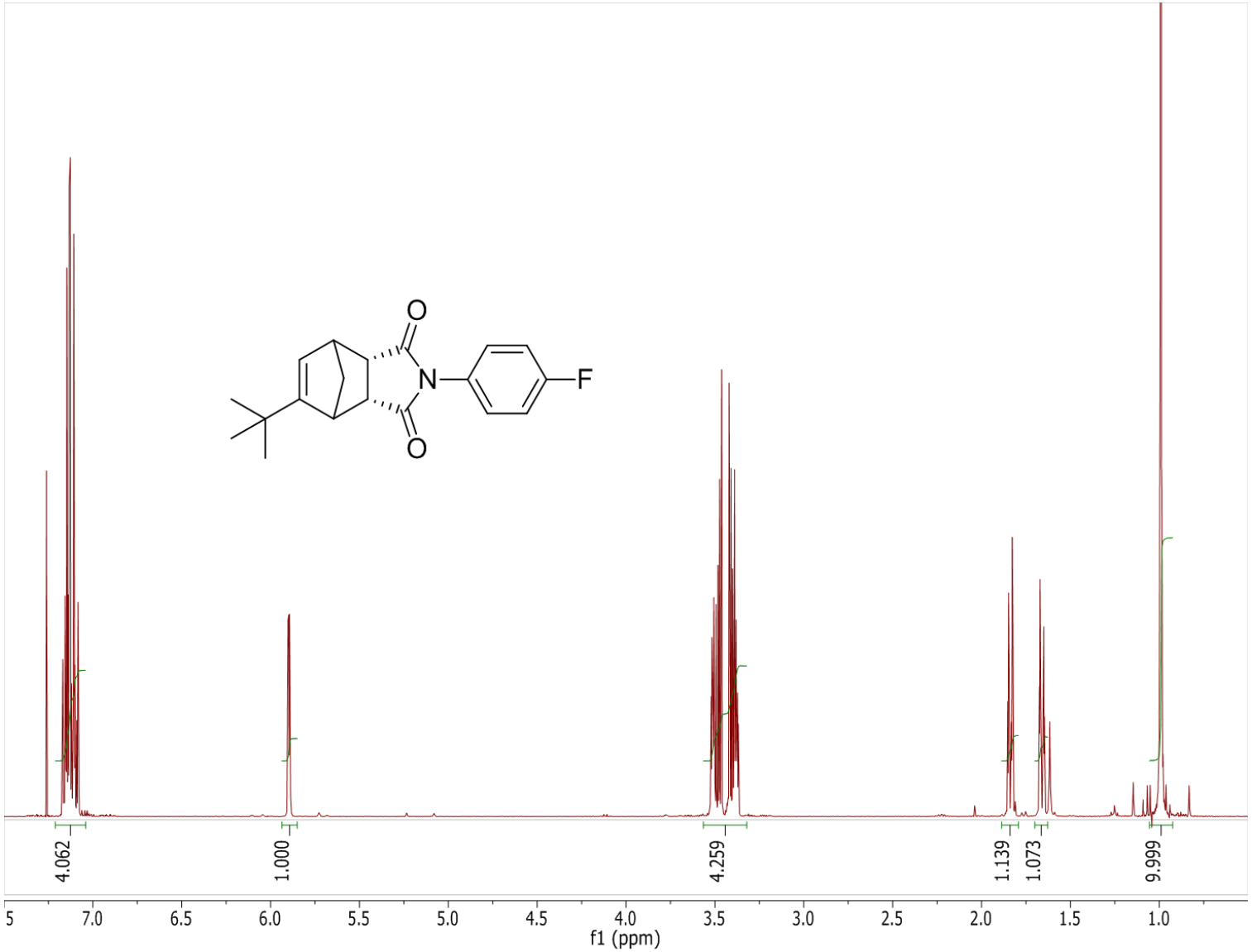

Figure A11. ^{1}H (400 MHz, $CDCl_3$) NMR of compound **3a**.

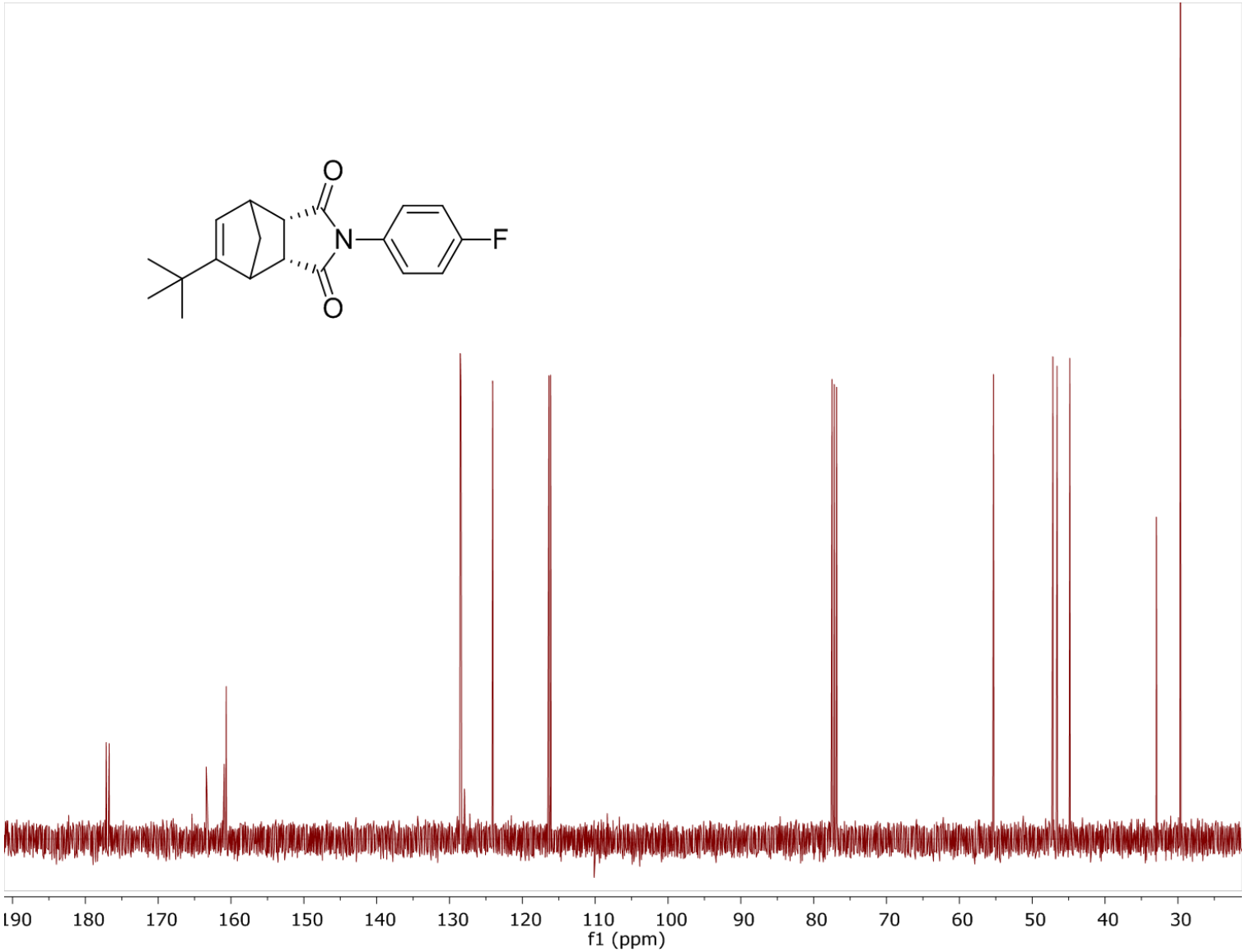

Figure A12. ^{13}C (100 MHz, $CDCl_3$) NMR of compound **3a**.

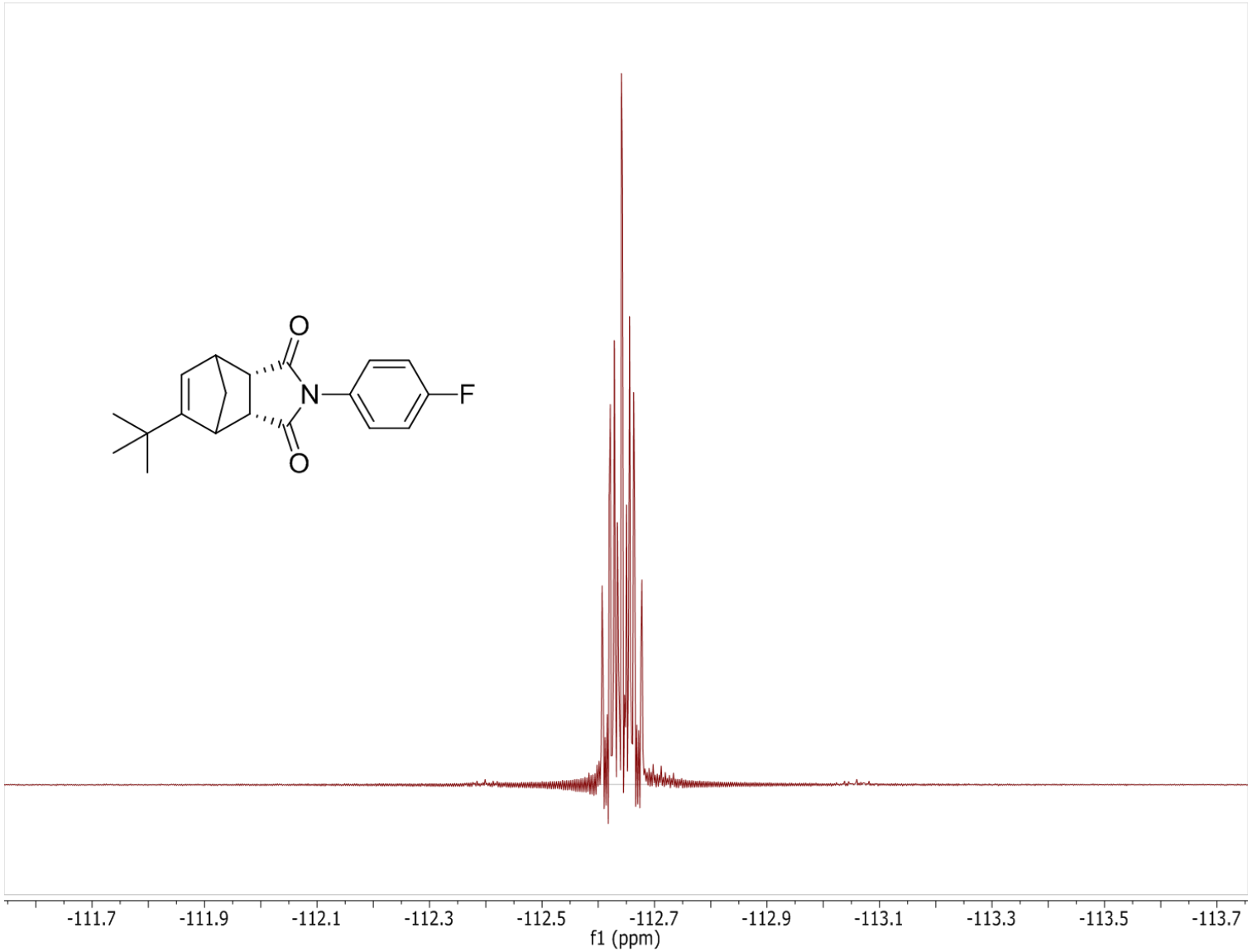

Figure A13. ^{19}F (376 MHz, $CDCl_3$) NMR of compound **3a**.

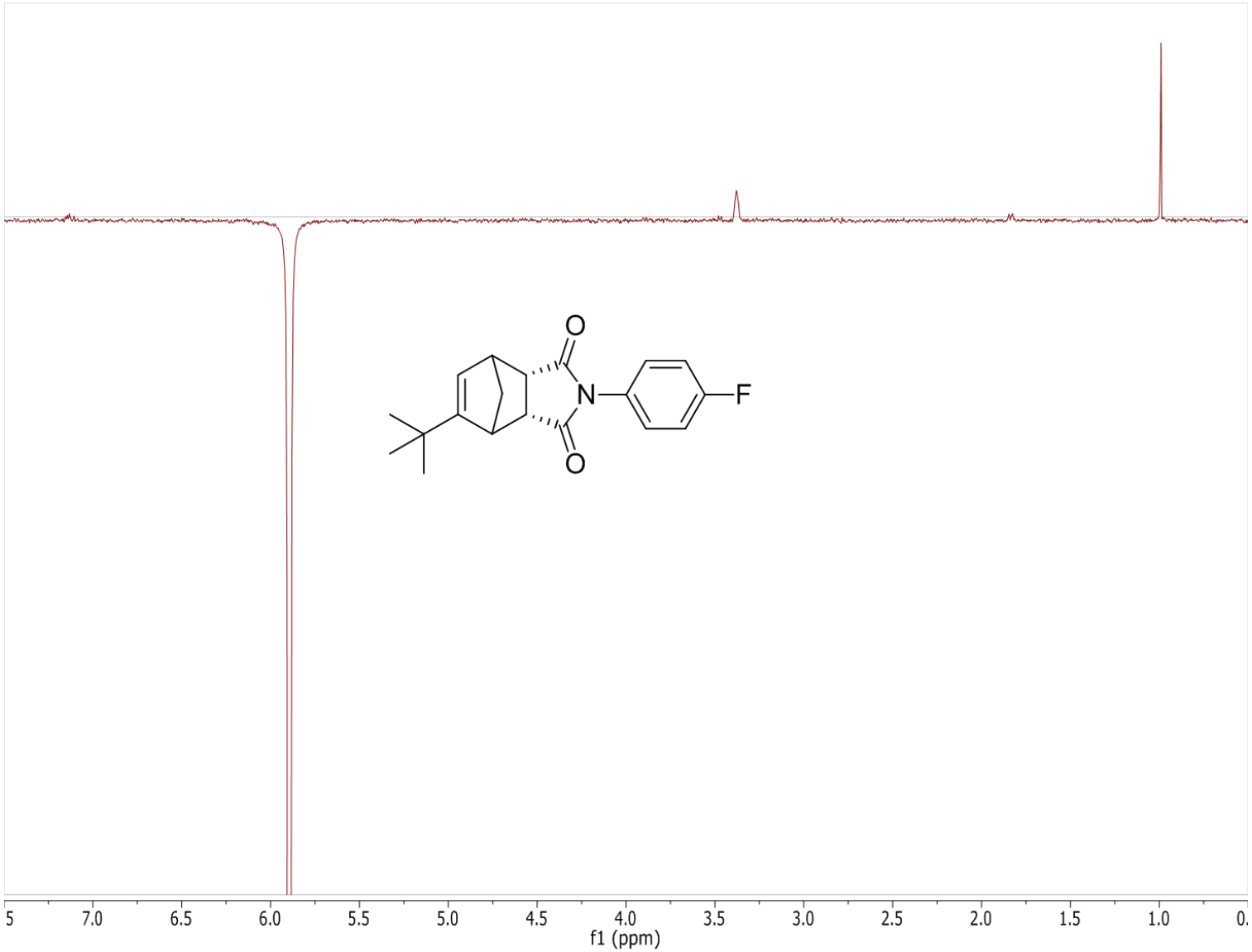

Figure A14. ^{1}H 1D NOE spectrum of compound **3a** in $CDCl_3$.

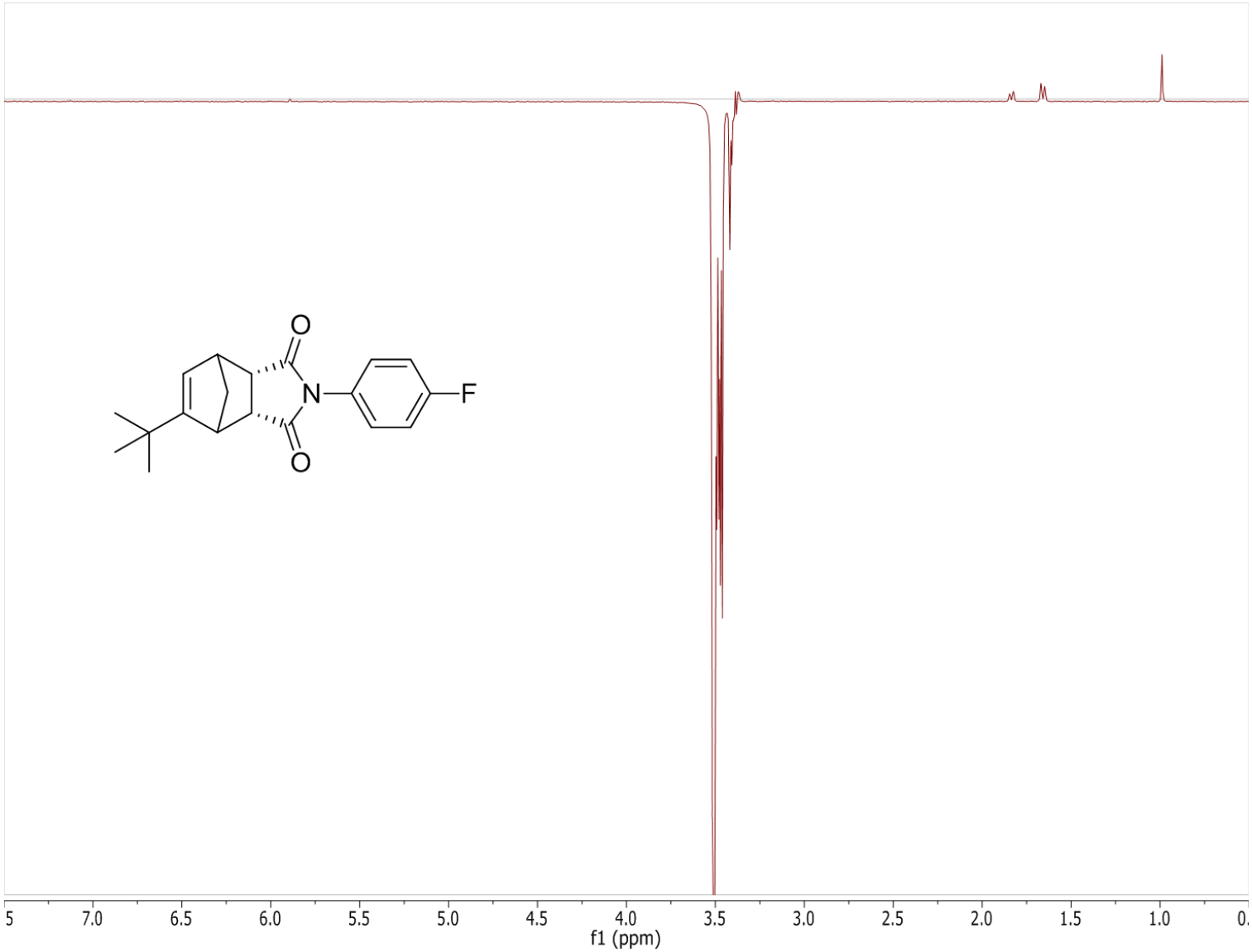

Figure A15. ^{1}H 1D NOE spectrum of compound **3a** in $CDCl_3$.

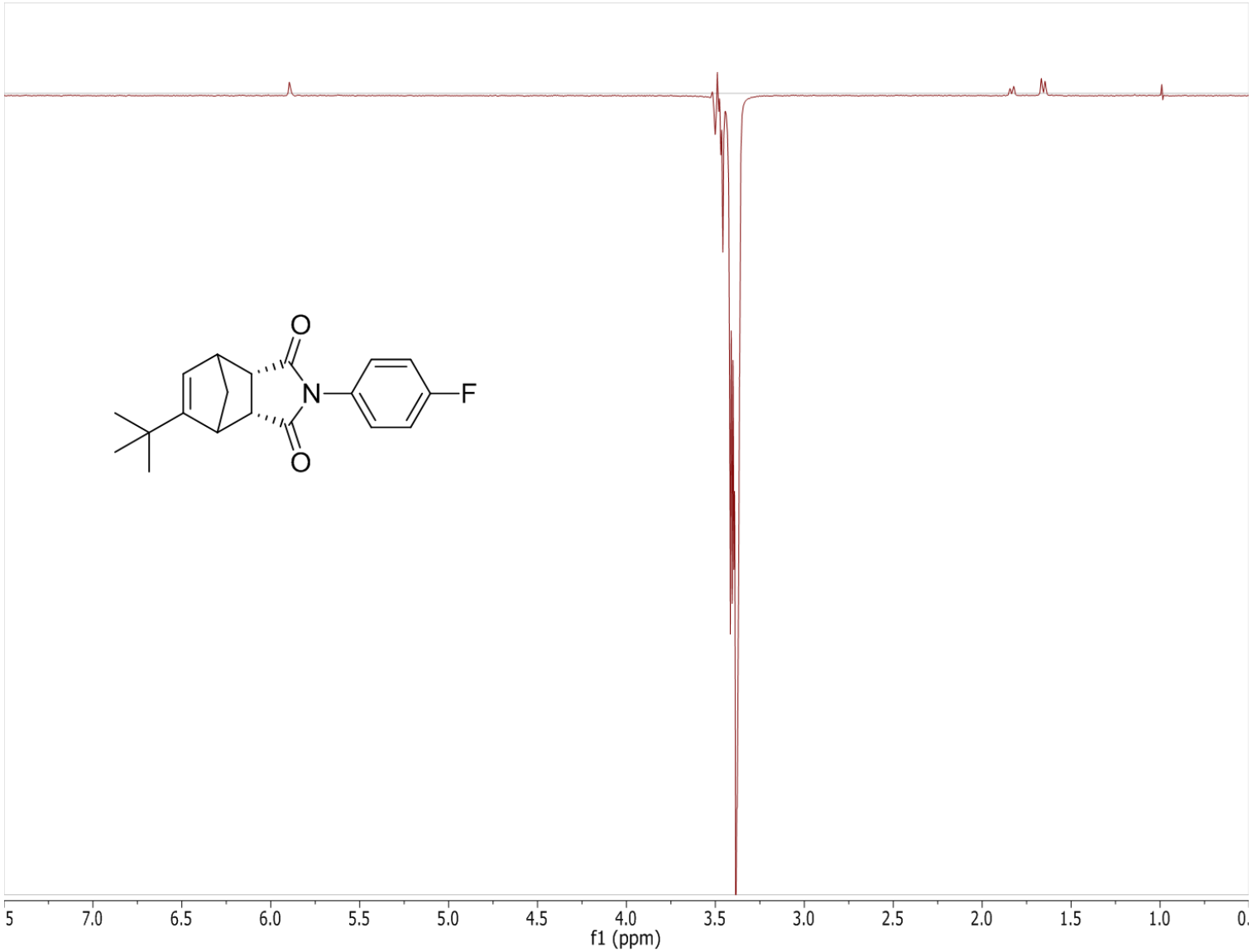

Figure A16. ^{1}H 1D NOE spectrum of compound **3a** in $CDCl_3$.

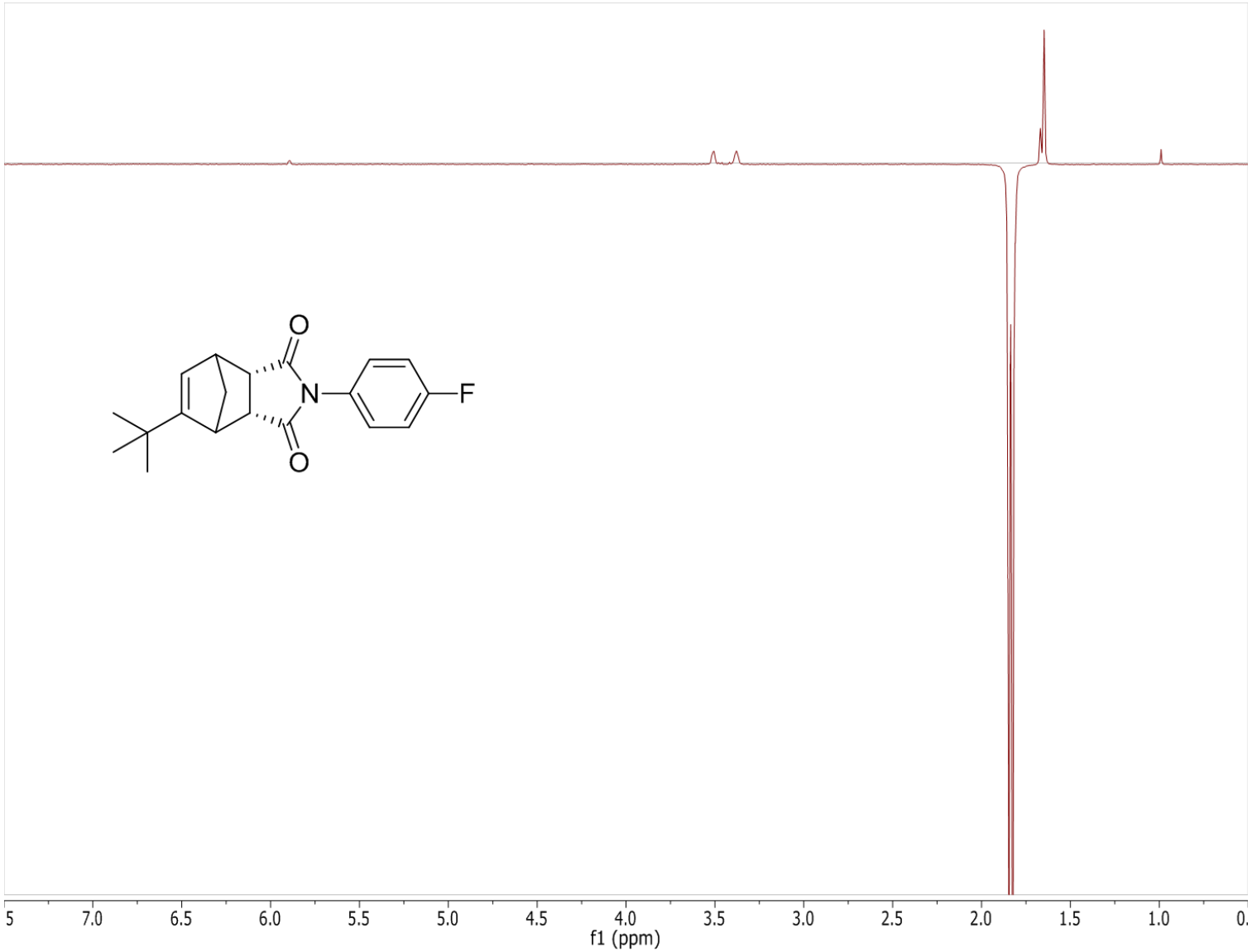

Figure A17. ^{1}H 1D NOE spectrum of compound **3a** in $CDCl_3$.

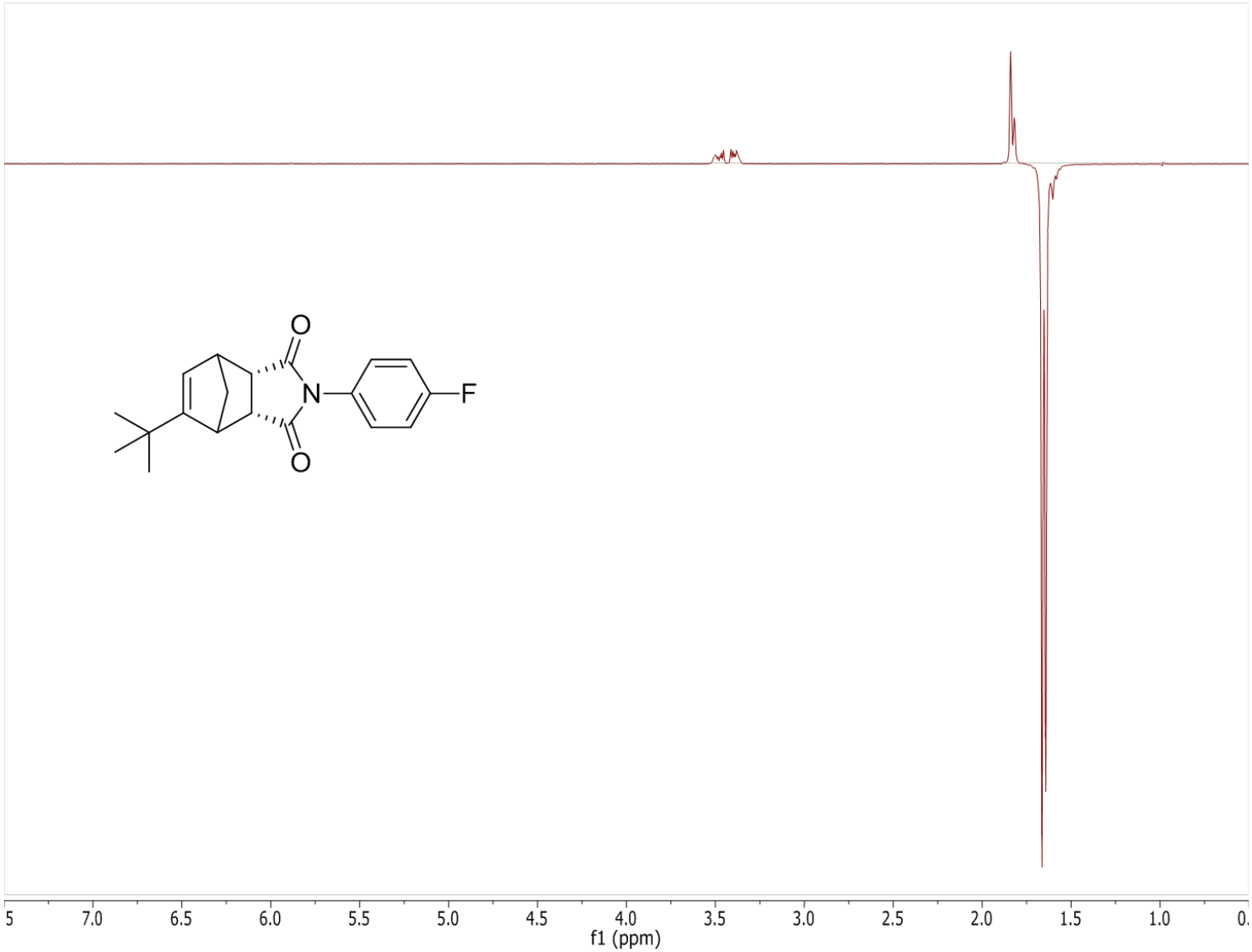

Figure A18. ^{1}H 1D NOE spectrum of compound **3a** in $CDCl_3$.

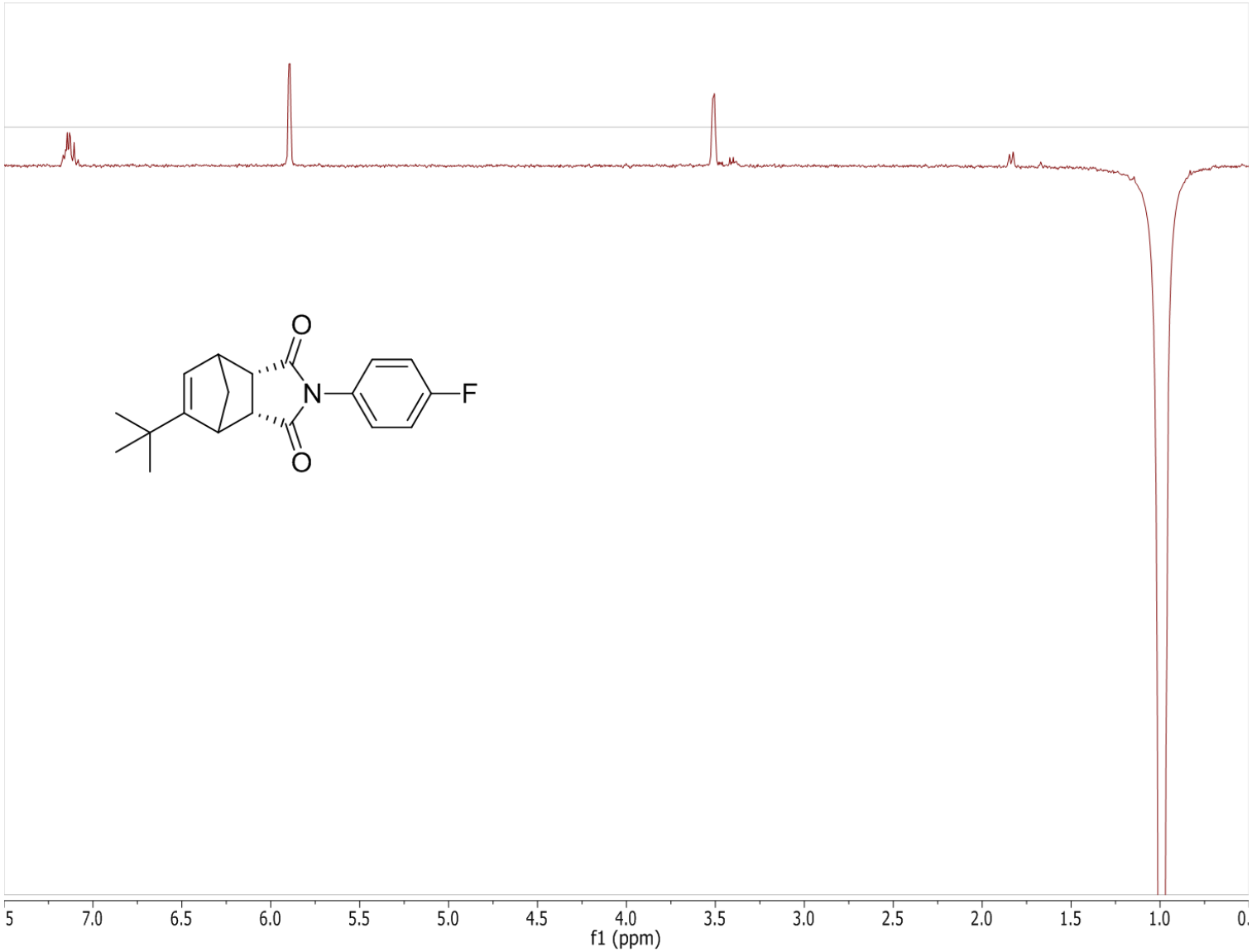

Figure A19. ^{1}H 1D NOE spectrum of compound **3a** in $CDCl_3$.

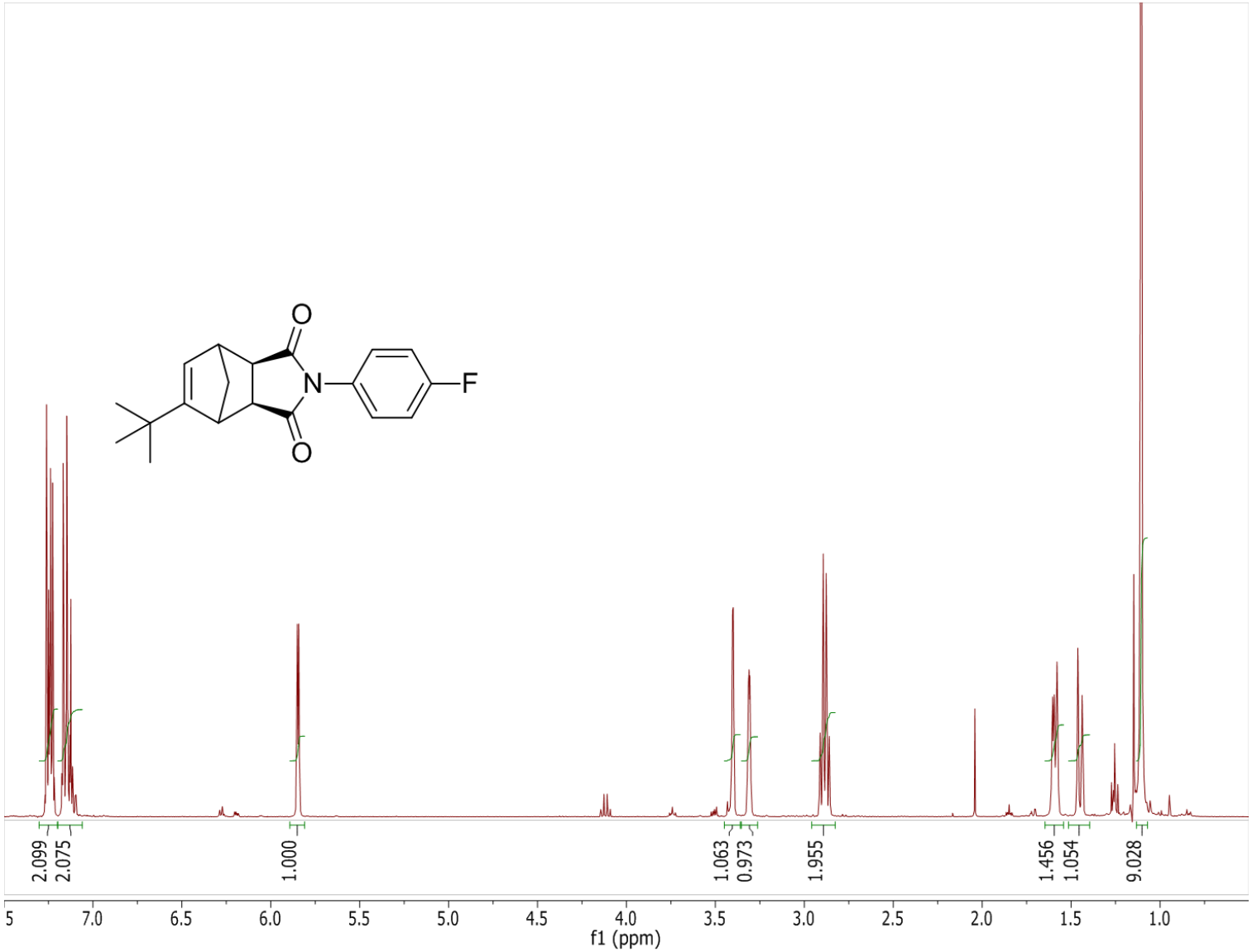

Figure A20. ^{1}H (400 MHz, $CDCl_3$) NMR spectrum of compound **4a**.

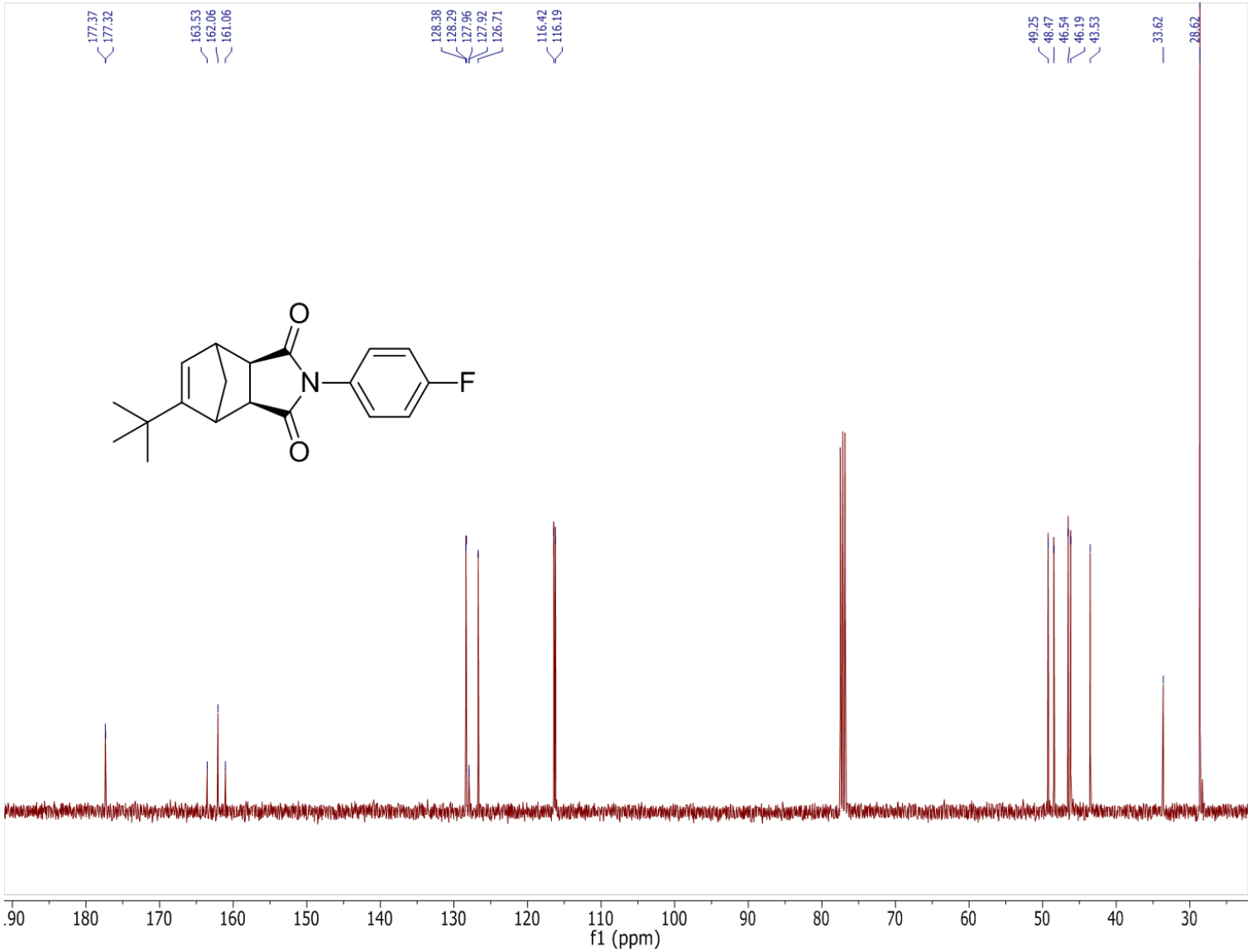

Figure A21. ^{13}C (100 MHz, $CDCl_3$) NMR spectrum of compound **4a**.

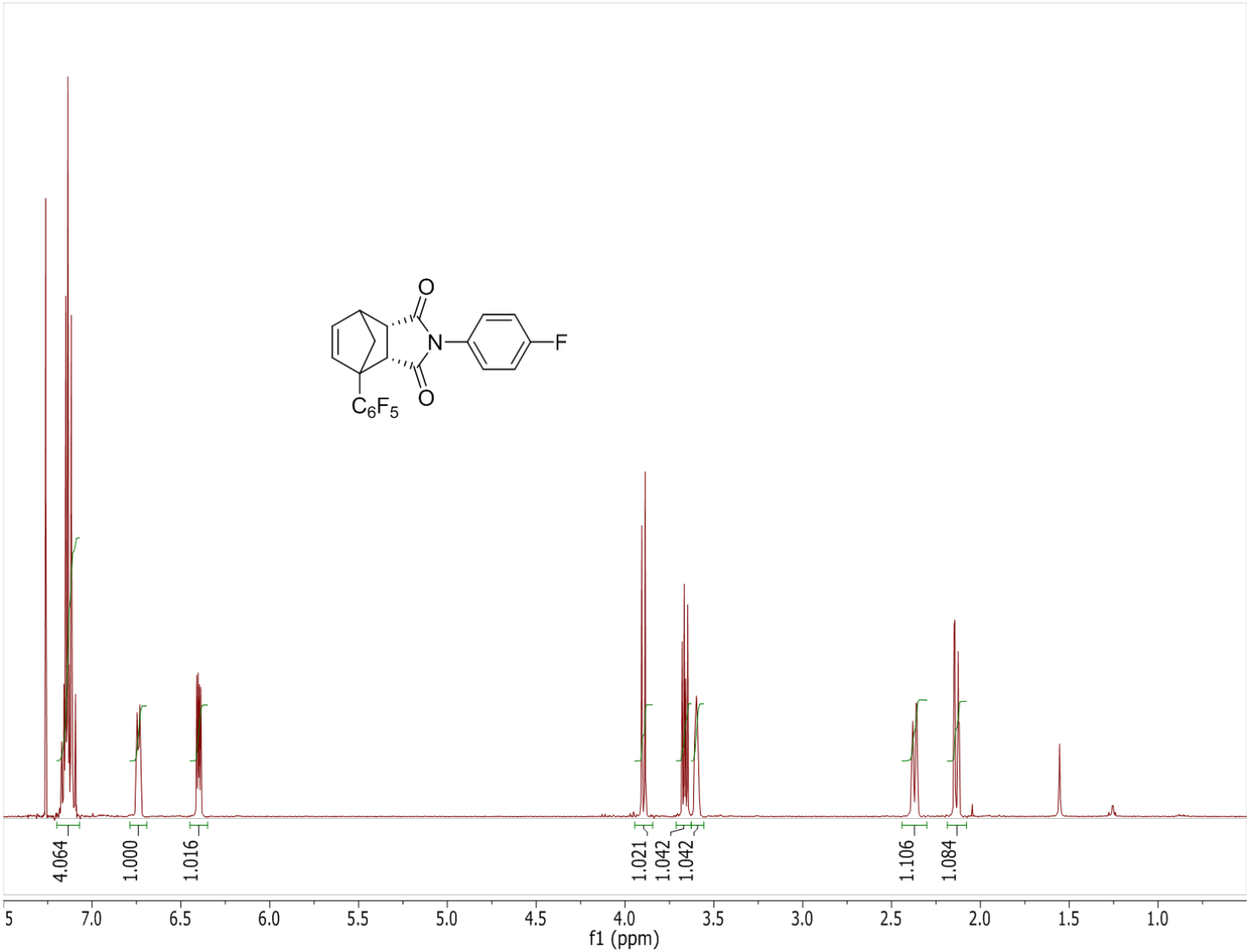

Figure A22. ^{1}H (400 MHz, $CDCl_3$) NMR spectrum of **1b**.

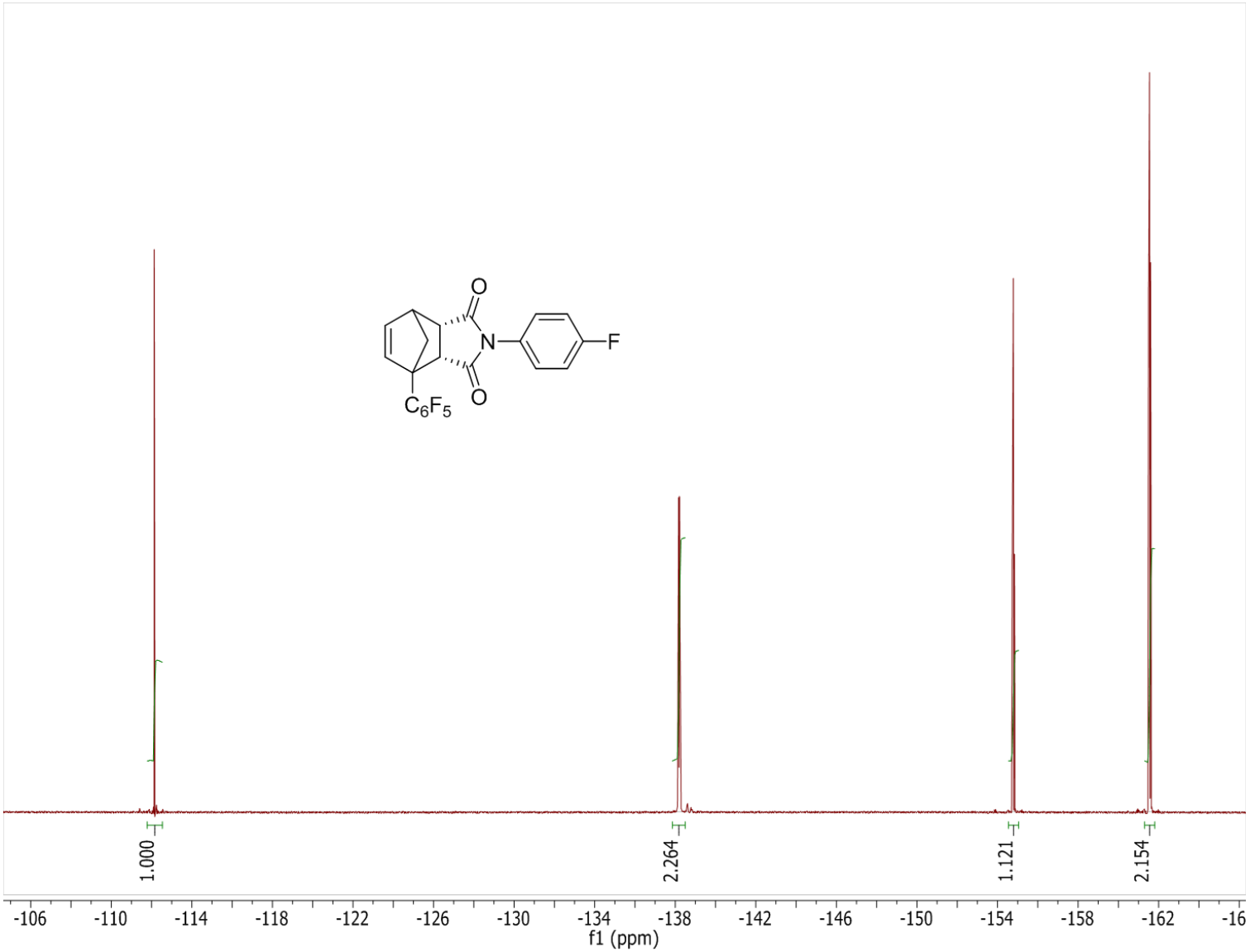

Figure A23. ^{19}F (376 MHz, $CDCl_3$) NMR spectrum of **1b** in.

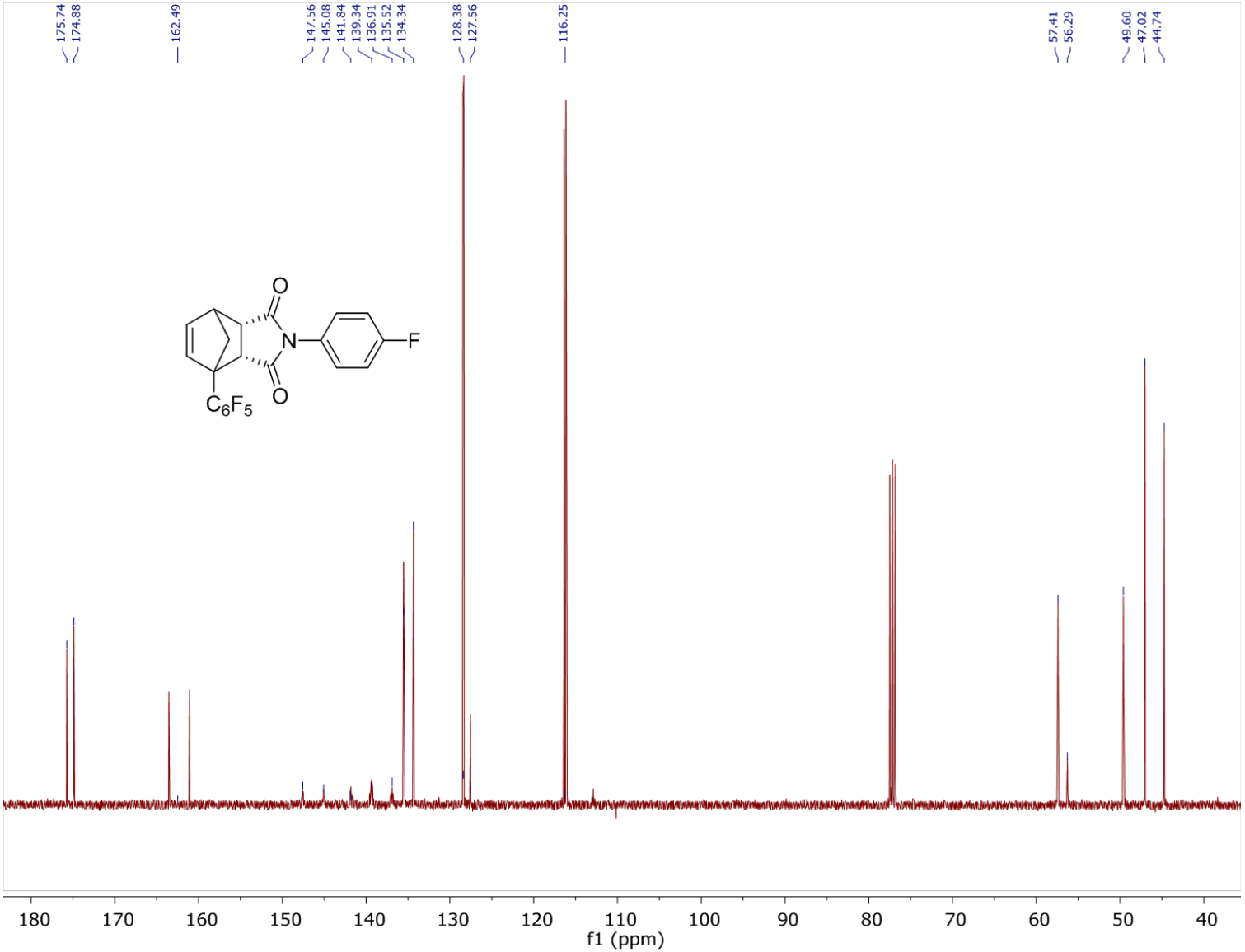

Figure A24. ^{13}C (100 MHz, $CDCl_3$) NMR spectrum of **1b**.

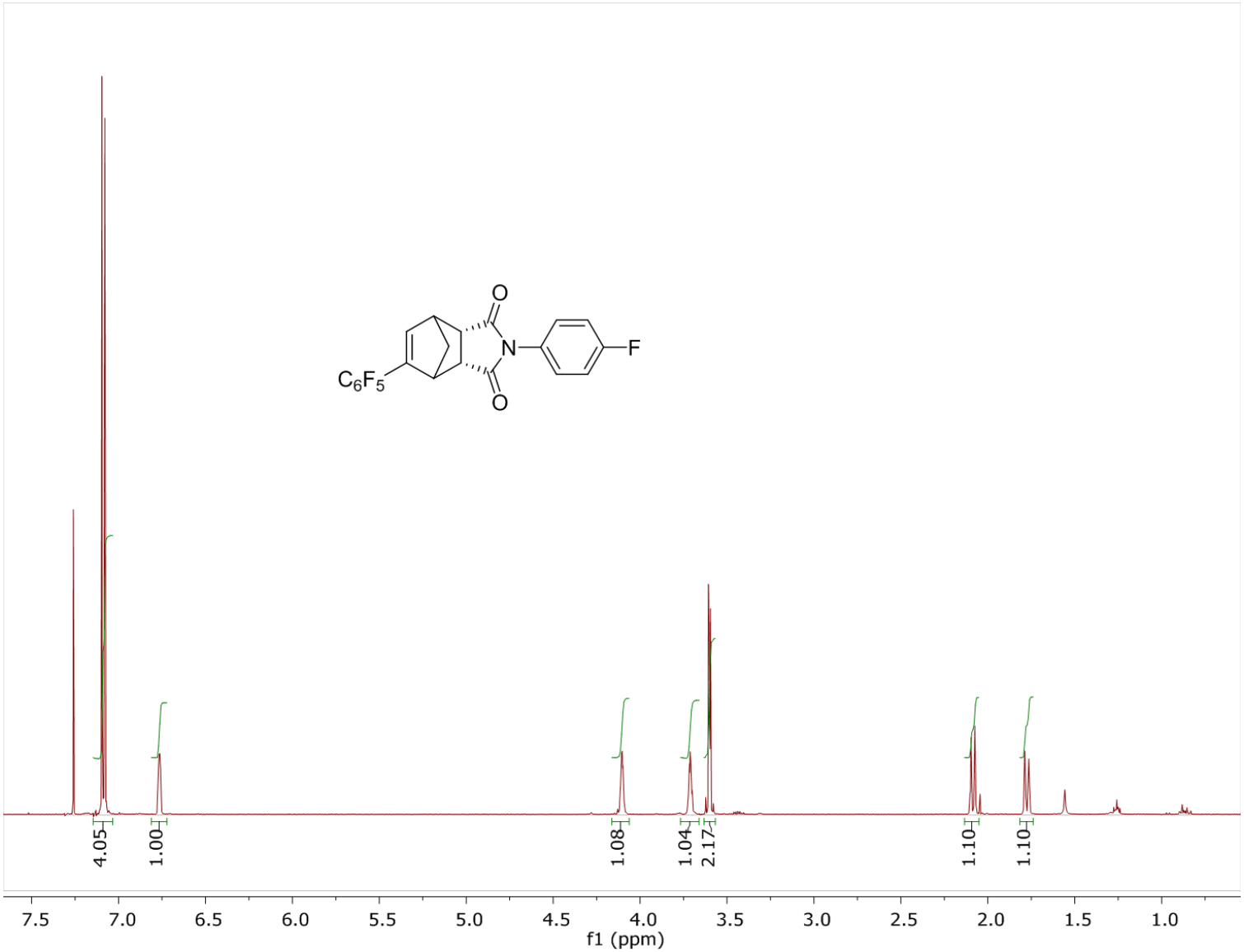

Figure A25. ^{1}H (400 MHz, $CDCl_3$) NMR spectrum of **3b**.

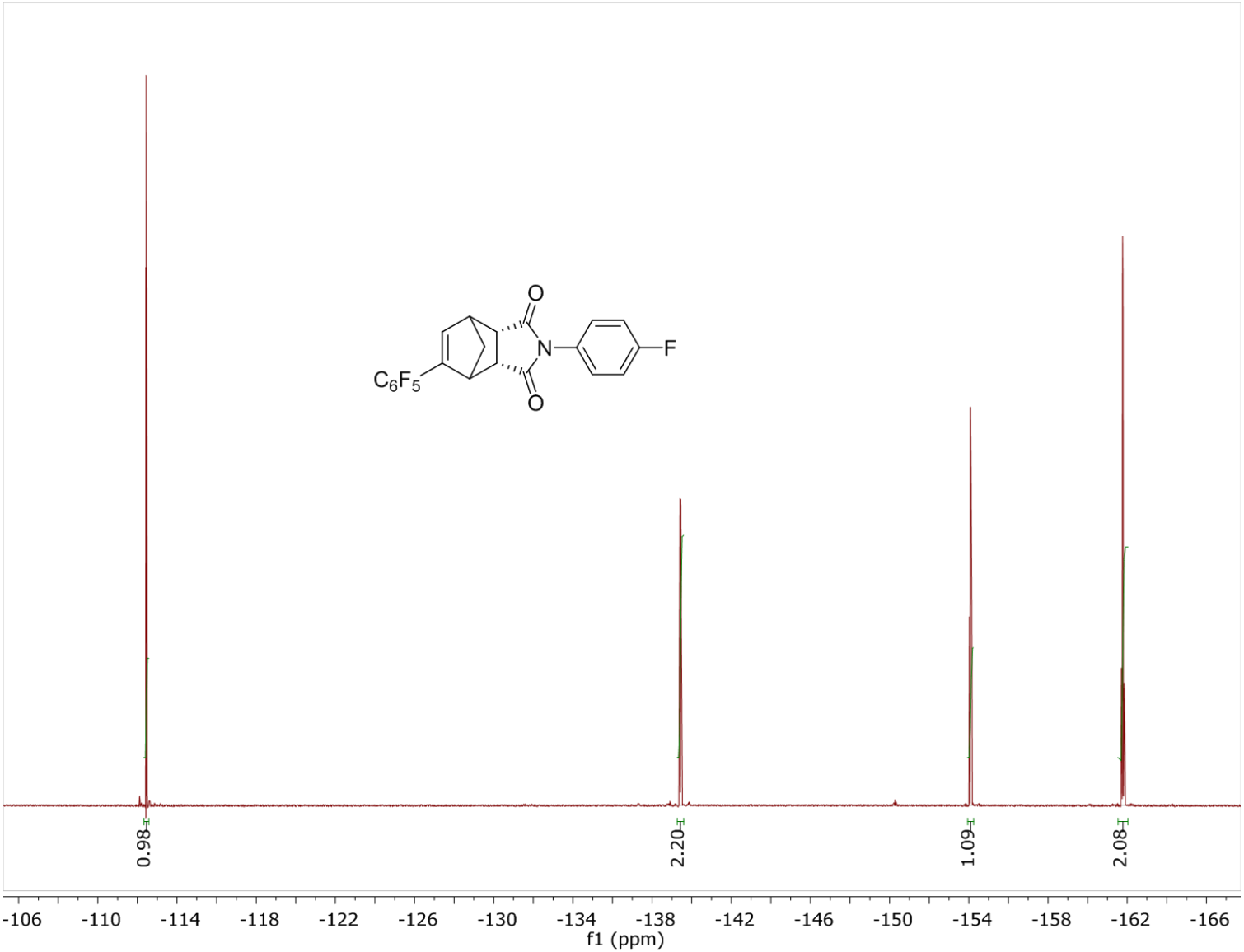

Figure A26. ^{19}F (376 MHz, $CDCl_3$) NMR spectrum of **3b**.

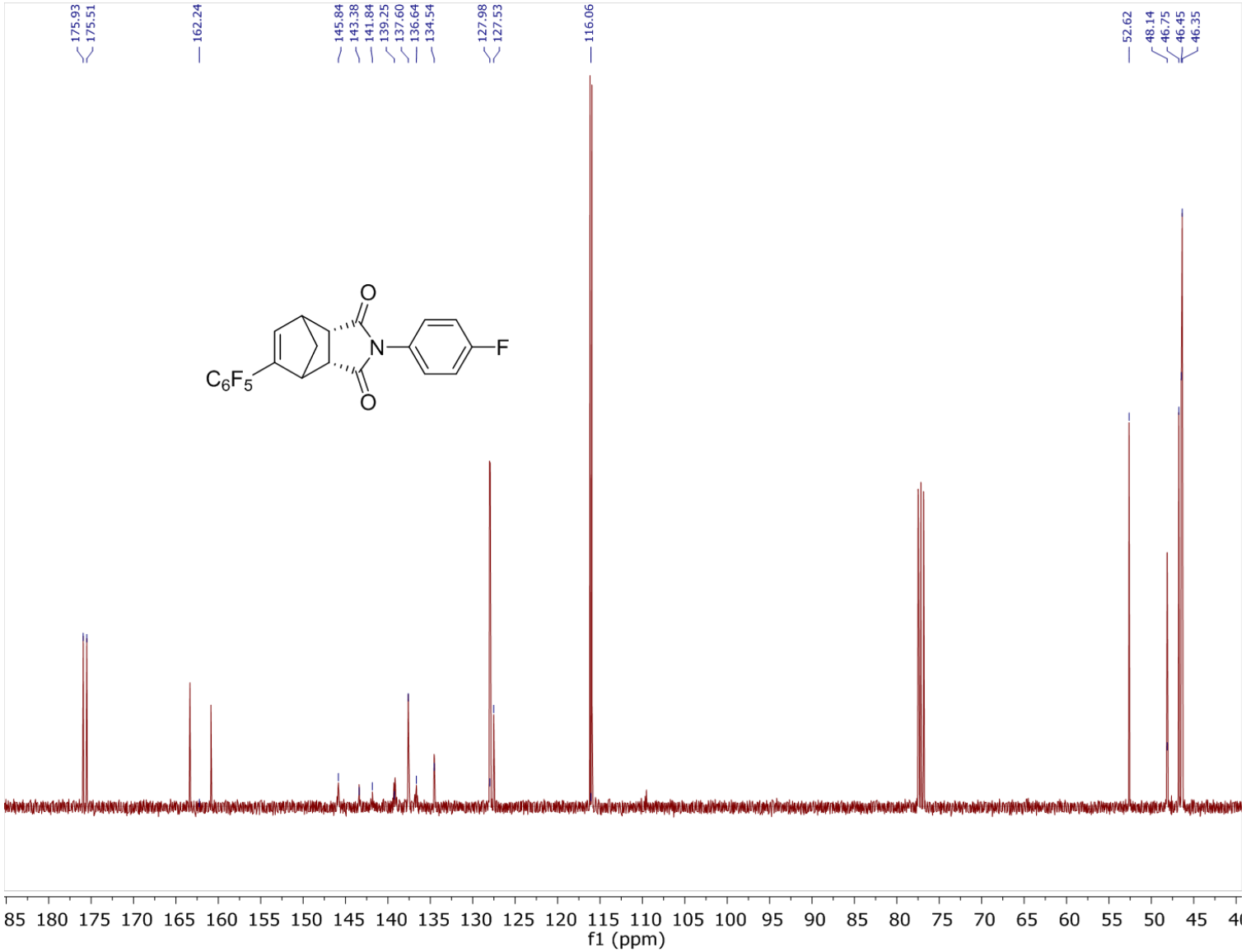

Figure A27. ^{13}C (100 MHz, $CDCl_3$) NMR spectrum of **3b**.

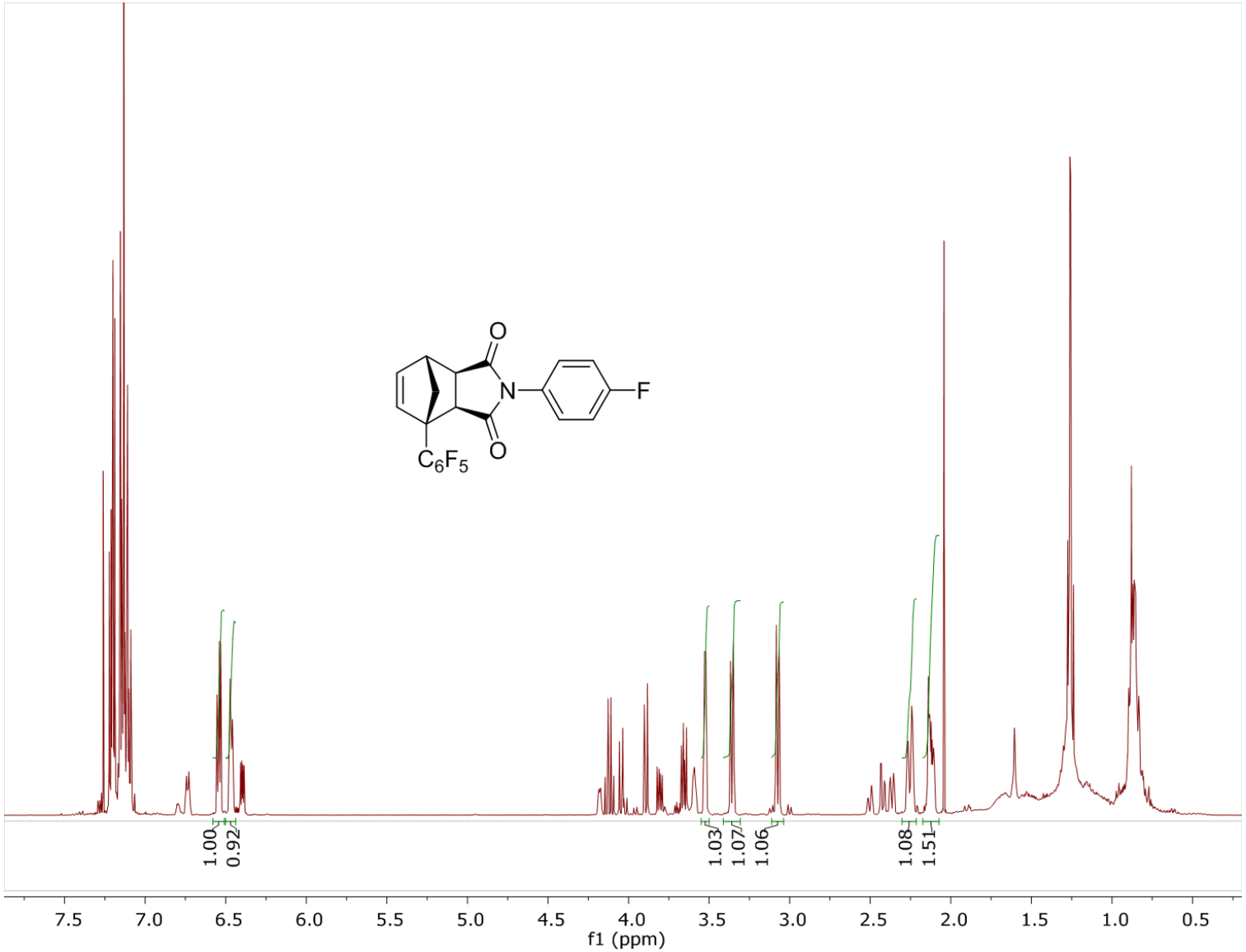

Figure A28. ^{1}H (400 MHz, $CDCl_3$) NMR spectrum of **2b**. Integrated signals are assigned to **2b**.

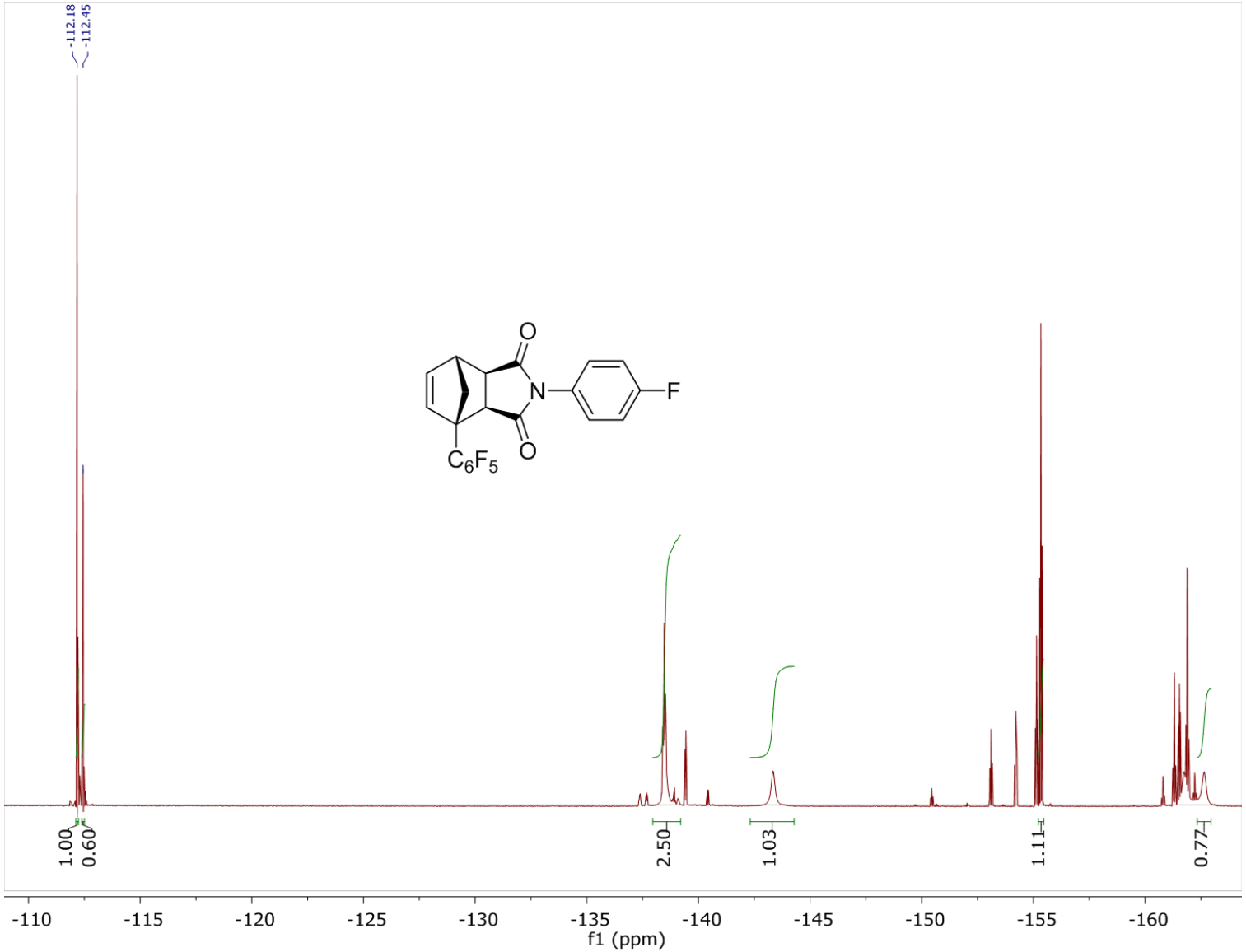

Figure A29. ^{19}F (376 MHz, $CDCl_3$) NMR spectrum of **2b**.

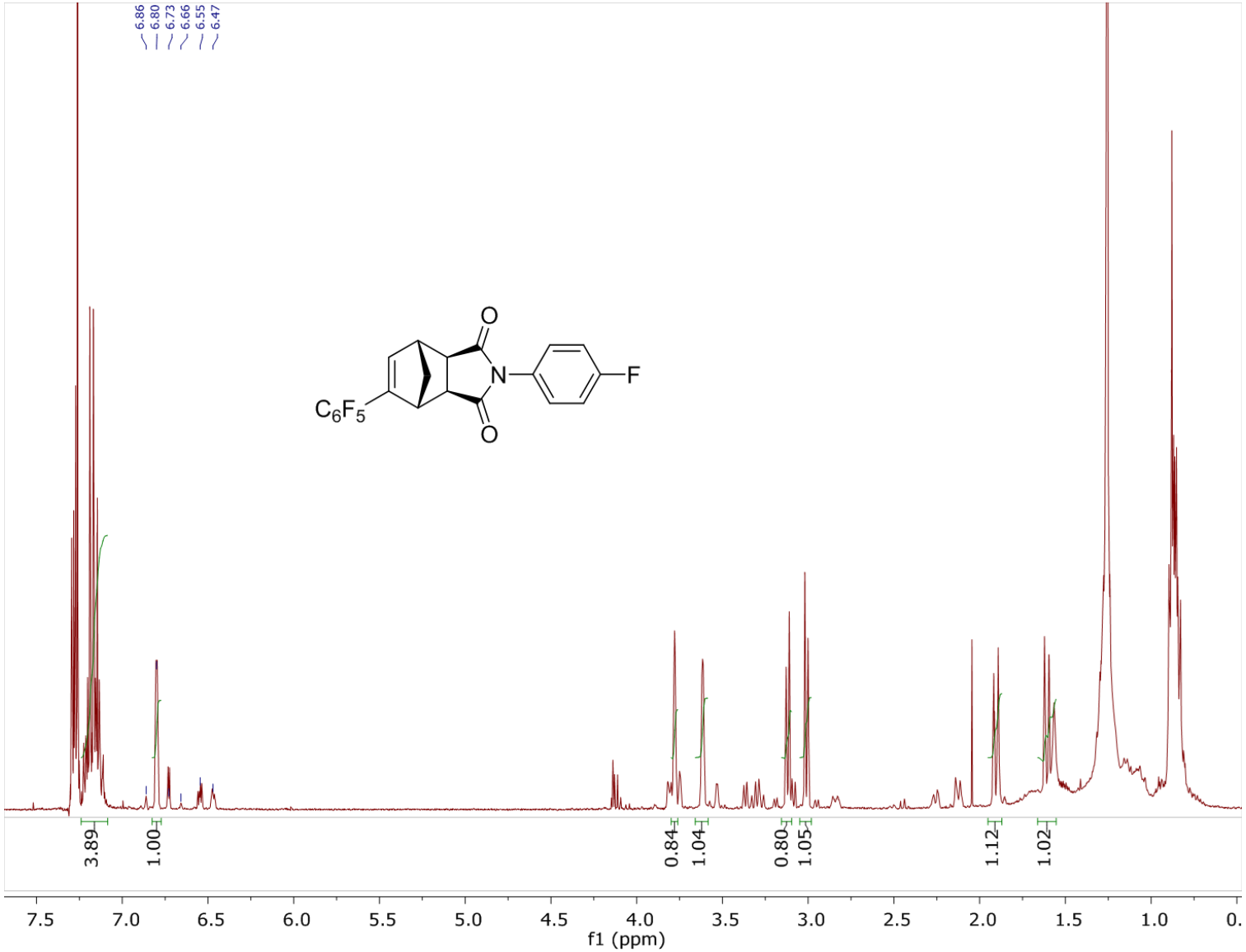

Figure A30. ^{1}H (400 MHz, $CDCl_3$) NMR spectrum of **4b**.

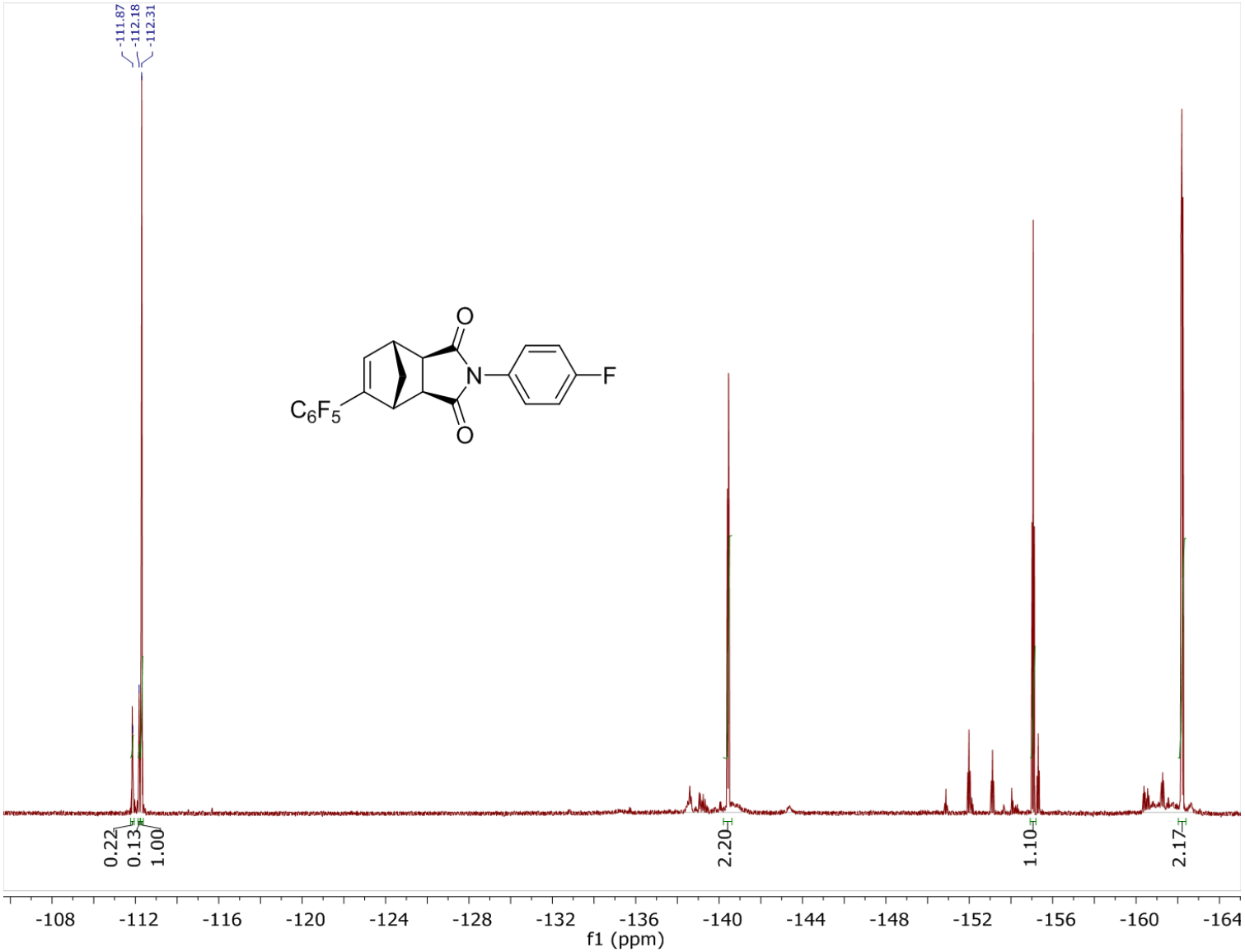

Figure A31. ^{19}F (376 MHz, $CDCl_3$) NMR spectrum of **4b**.

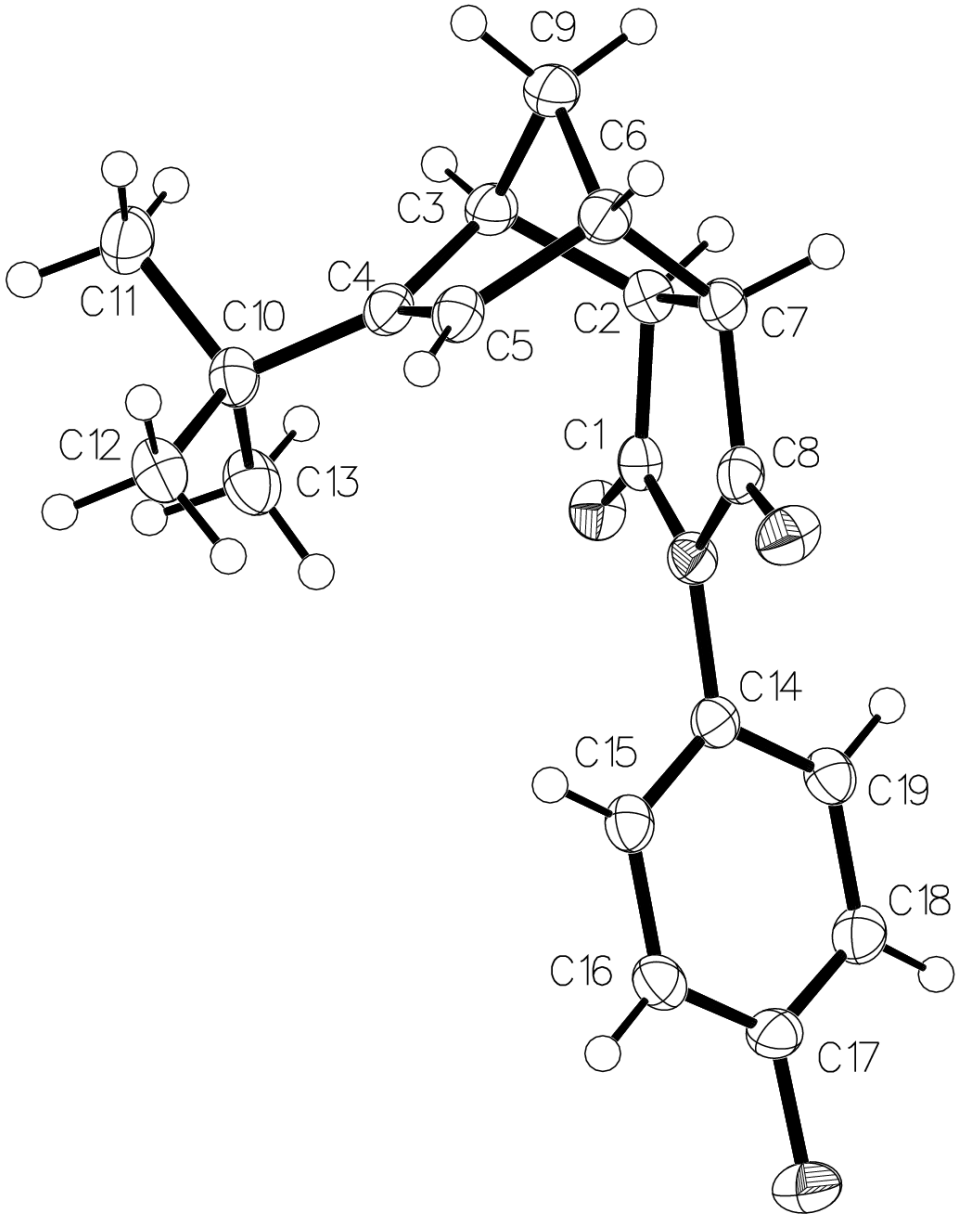

Figure A32. Ellipsoid plot (50% probability) of the molecular structure of crystalline adduct **3a** showing *endo* stereochemistry and attachment of *t*Bu group at the 2-carbon (C=C double bond) of the norbornene. The atom attached to C17 is F17. Hydrogen atoms are numbered according to the carbon atoms to which they are attached.

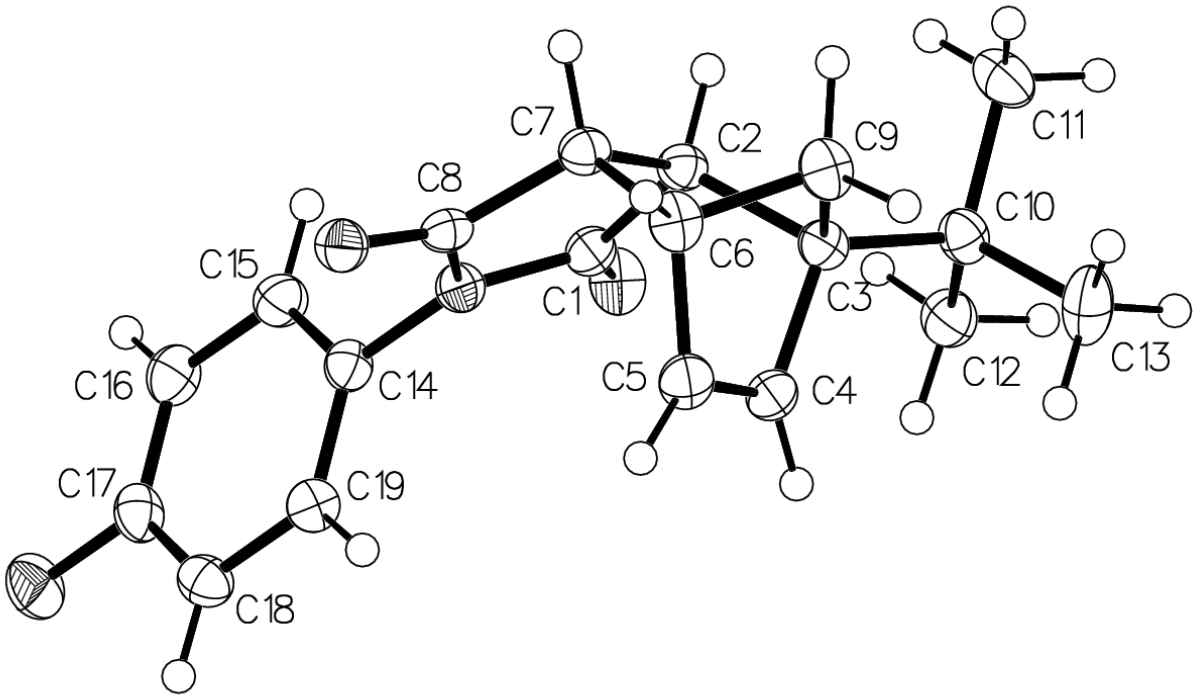

Figure A33. Ellipsoid plot (50% probability) of the molecular structure of crystalline adduct **1a** showing *endo* stereochemistry and attachment of *t*Bu group at the 1-carbon (C-C bridgehead) of the norbornene. The atom attached to C17 is F17. Hydrogen atoms are numbered according to the carbon atoms to which they are attached.

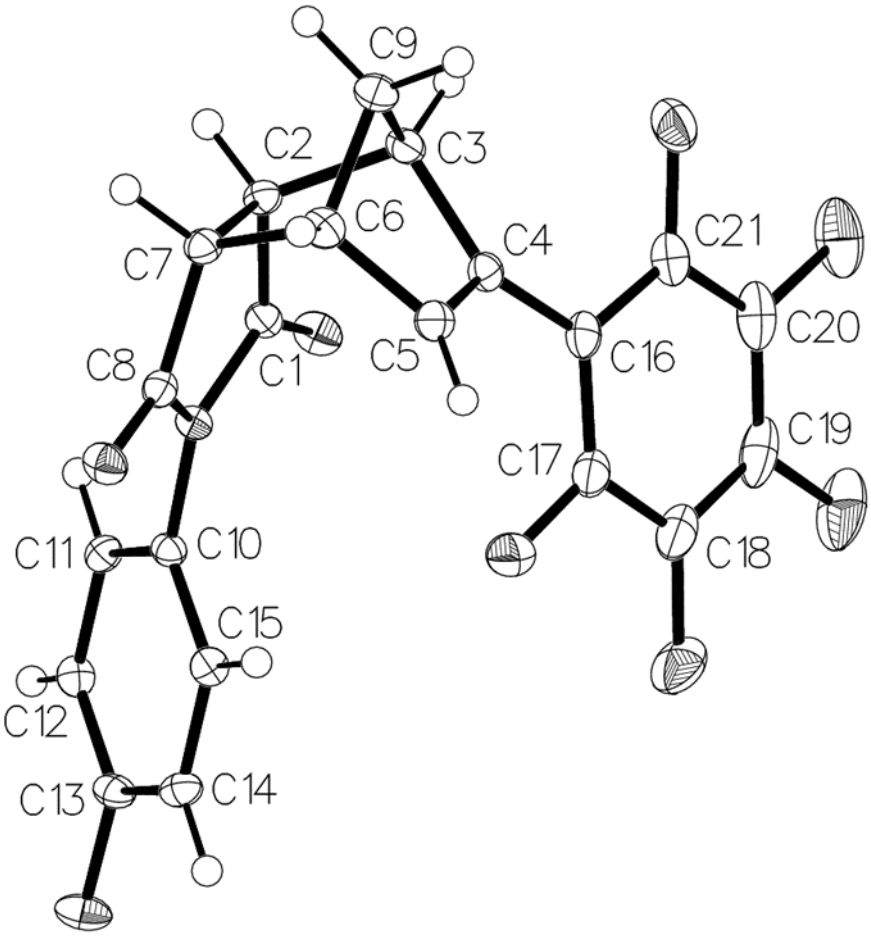

Figure A34. Ellipsoid plot (50% probability) of the molecular structure of crystalline adduct **3b** showing *endo* stereochemistry and attachment of C_6F_5 group at the 2-carbon (C=C double bond) of the norbornene. Hydrogen and Fluorine atoms are numbered according to the carbon atoms to which they are attached.

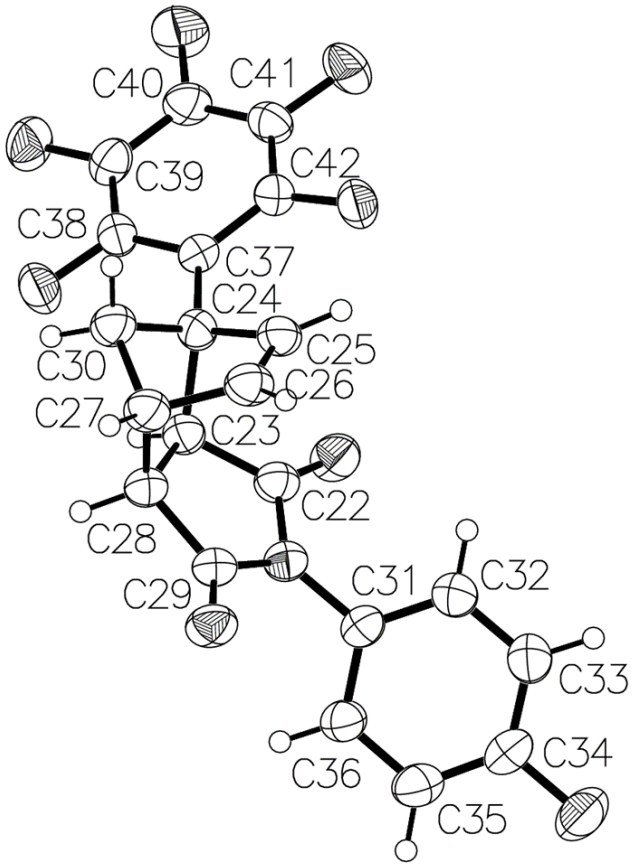

Figure A35. Ellipsoid plot (50% probability) of the molecular structure of crystalline adduct **1b** showing *endo* stereochemistry and attachment of C_6F_5 group at the 1-carbon (bridgehead) of the norbornene. Hydrogen and Fluorine atoms are numbered according to the carbon atoms to which they are attached.

Crystallographic data table

Compound	1a	3b	3a	1b
Empirical formula	$C_{19}H_{20}FNO_2$	$C_{21}H_{11}F_6NO_2$	$C_{19}H_{20}FNO_2$	$C_{21}H_{11}F_6NO_2$
Formula weight	313.36	423.31	313.36	423.31
Crystal system	Monoclinic	Monlclinic	Monoclinic	Monoclinic
Space group	*P* 1 2_1/*n* 1	*P* 1 2_1/*c* 1	*P* 1 21/*n* 1	*P* 1 2_1/*c* 1
a (Å)	a = 14.3547(2) Å	10.5250(3)	12.47085(16)	*a* = 13.6756(6) Å
b (Å)	b = 6.67226(10) Å	6.63208(19)	6.50860(10)	*b* = 25.8429(7) Å
c (Å)	c = 17.3887(3) Å	24.8502(8)	19.5534(3)	*c* = 10.1676(3) Å
α =	90	90	1586.08(4)	3529.7(2) Å3
β =	104.5312(16)	91.79(3)	90	90
γ =	90	90	92.0565(13)	100.807(4)
Volume ($Å^3$)	1612.17(5)	1733.76(9)	90	90
Z	4	4	4	8
Density (calc) (Mg/m^3)	1.291	1.622	1.312	1.593
Absorption coefficient (mm^{-1})	0.744	0.148	0.757	1.284
F(000)	664	856	664	1712
Temp (K)	99.95(10)	99.9(3)	99.95(10)	200.0(3)
Crystal size (mm^3)	0.3363 x 0.184 x 0.0411	0.3857 x 0.3582 x 0.21	0.46 x 0.14 x 0.05	0.5848 x 0.3007 x 0.014
Theta range for data collection	3.581 to 74.828°	3.632 to 31.385°	4.138 to 74.816	3.290 to 75.242
Index ranges	-17<=h<=17, -8<=k<=8, -21<=l<=21	-14<=h<=15, -9<=k<=9, -35<=l<=35	-15<=h<=15, -7<=k<=8, -24<=l<=24	-16<=h<=17, -32<=k<=32, -12<=l<=11
Reflections collected	21456	21807	19987	42680
Independent reflections	3311 [R(int) = 0.0404]	5361 [R(int) = 0.0448]	3258 [R(int) = 0.0455]	7229 [R(int) = 0.1061]
Completeness to theta	(67.684°) 99.90%	(25.242°) 99.80%	(67.684°) 99.90%	(67.684°) 100.00%
Absorption correction	Gaussian	Analytical	Gaussian	Analytical
Max. and min. transmission	1.414 and 0.851	0.971 and 0.952	1.408 and 0.821	0.982 and 0.687
Refinement method	Full-matrix least-squares on F2	Full-matrix least-squares on F2	Full-matrix least-squares on F2	Full-matrix least-squares on F2
Data / restraints / parameters	3311 / 0 / 211	5361 / 0 / 271	3258 / 0 / 211	7229 / 0 / 541
Goodness-of-fit on F^2	1.031	1.038	1.029	1.025
Final R indices [I>2sigma(I)]	R1 = 0.0391, wR2 = 0.1050	R1 = 0.0464, wR2 = 0.1056	R1 = 0.0411, wR2 = 0.1119	R1 = 0.0803, wR2 = 0.2142
R indices (all data)	R1 = 0.0442, wR2 = 0.1098	R1 = 0.0675, wR2 = 0.1198	R1 = 0.0460, wR2 = 0.1177	R1 = 0.1044, wR2 = 0.2477
Largest diff. peak and hole ($e/Å^3$)	0.281 and -0.214	0.399 and -0.263	0.305 and -0.273	0.411 and -0.471 e.Å-3

Appendix B Supporting information for: Models for Diels-Alder Adduct Formation in Cyclopentadiene-Maleimide Polymers

Jeremy B. Stegall, Carla Slebodnick, and Paul A. Deck*

Department of Chemistry, Virginia Tech, Blacksburg, VA 24061

NMR Spectra

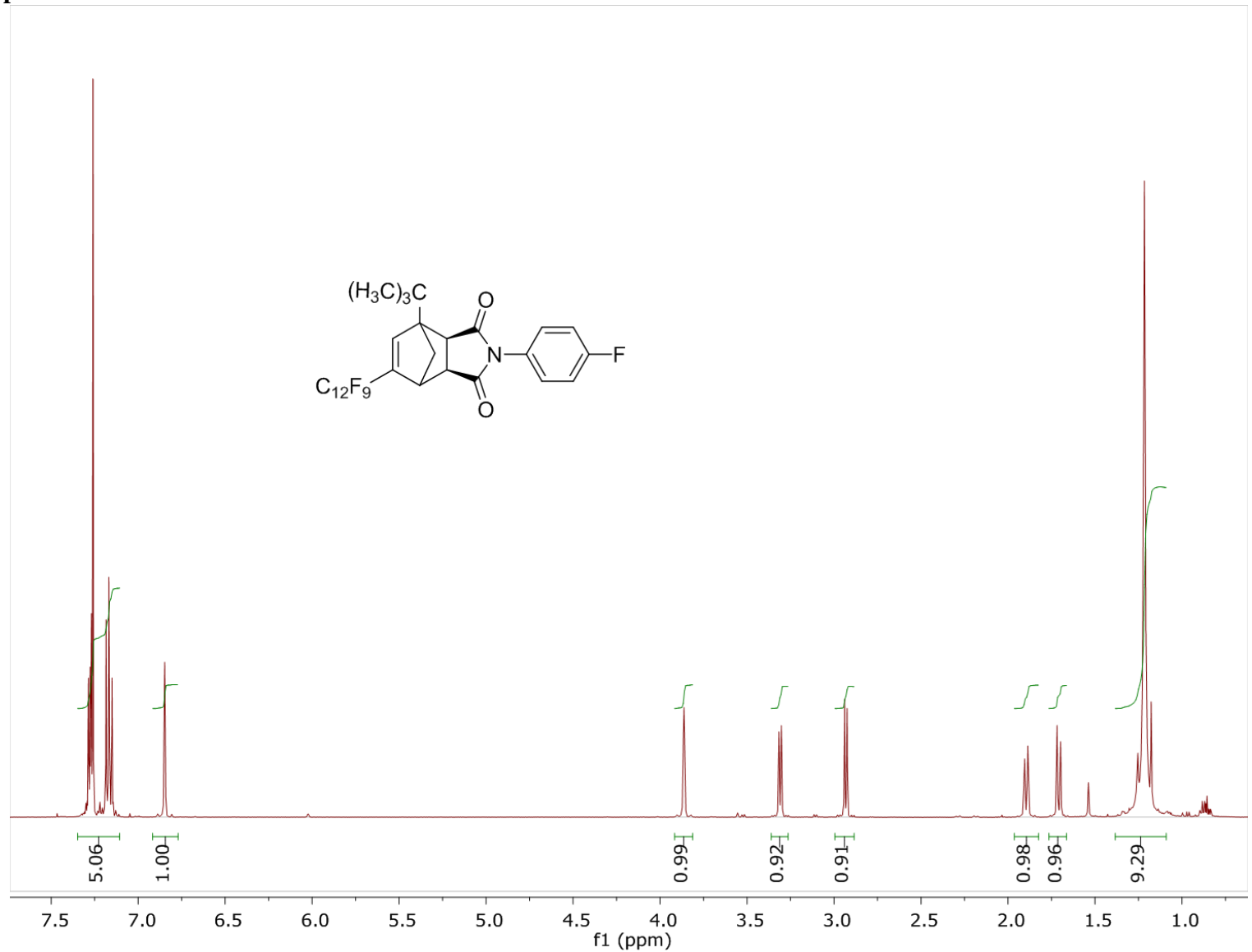

Figure B1. ^{1}H (400 MHz, $CDCl_3$) NMR spectrum of compound **3a**.

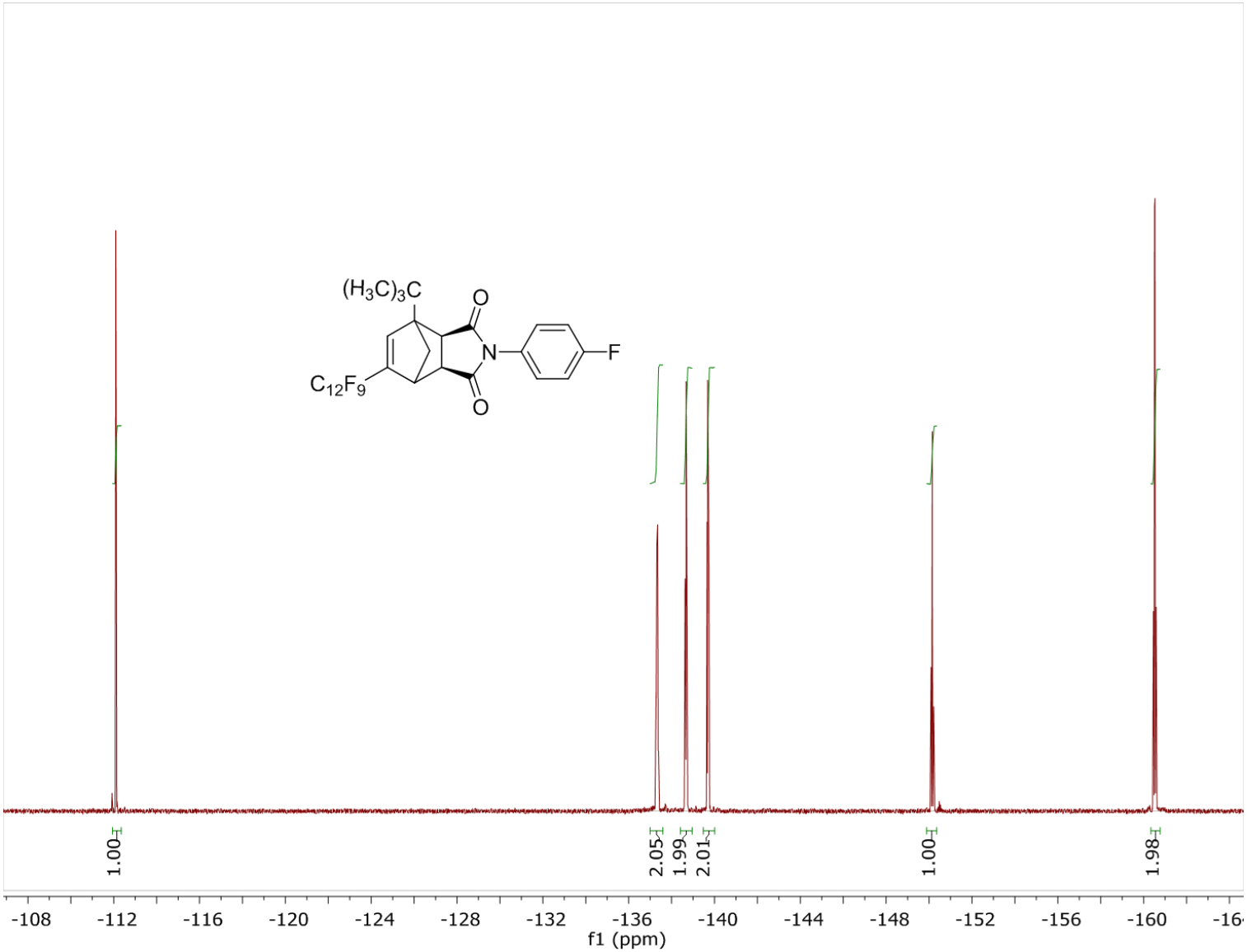

Figure B2. ^{19}F (376 MHz, $CDCl_3$) NMR spectrum of compound **3a**.

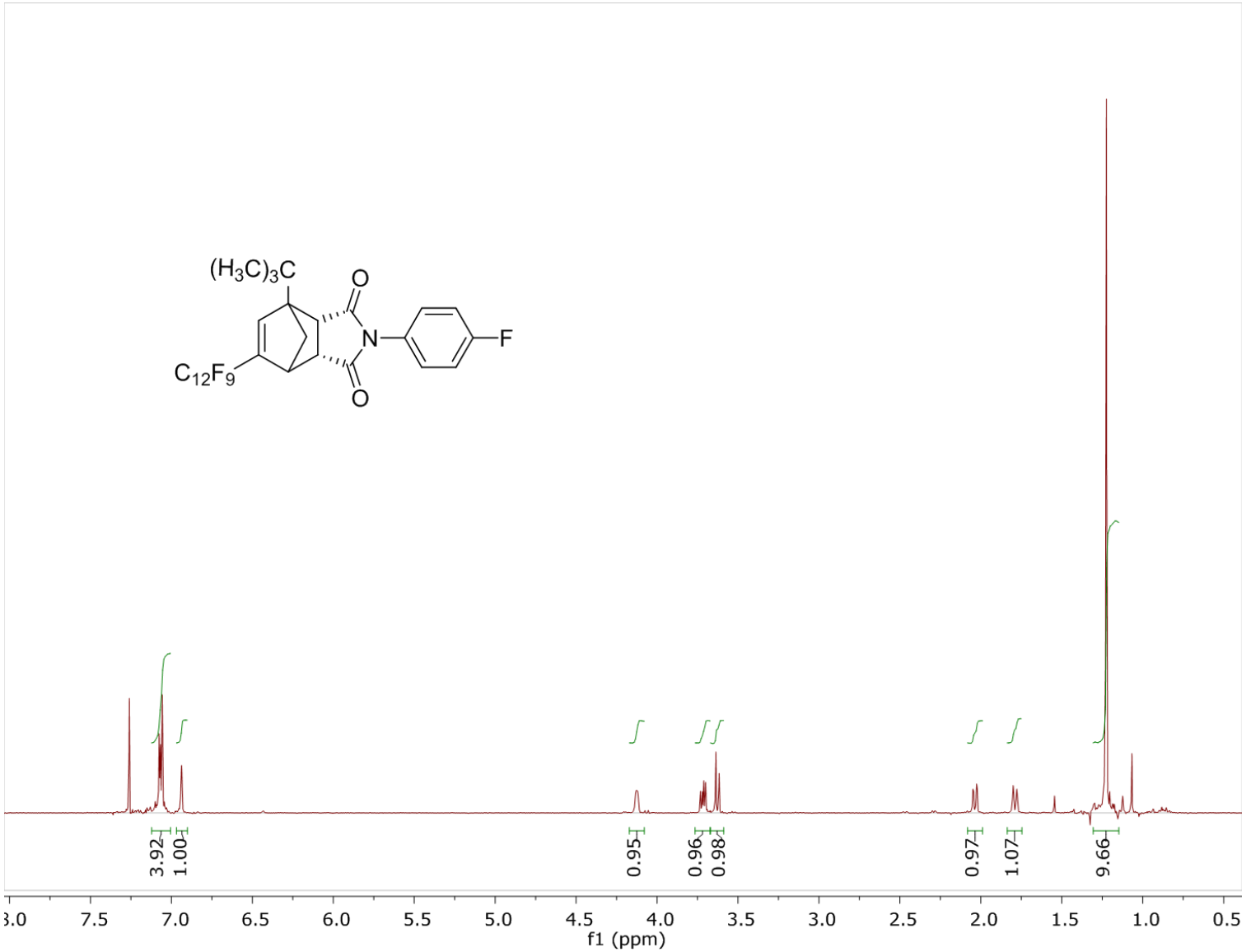

Figure B3. ^{1}H (400 MHz, $CDCl_3$) NMR spectrum of compound **3b**.

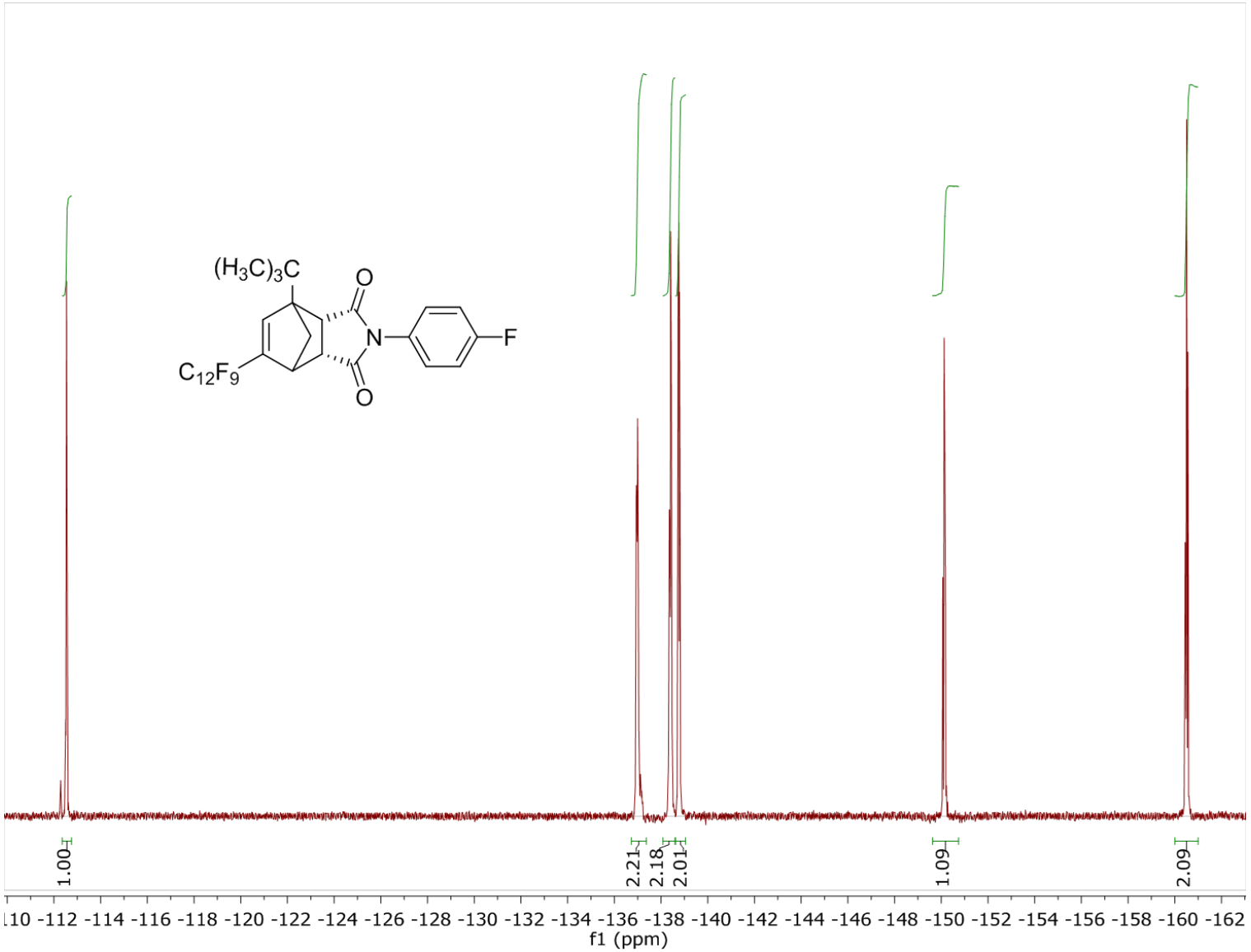

Figure B4. ^{19}F (376 MHz, $CDCl_3$) NMR spectrum of compound **3b**.

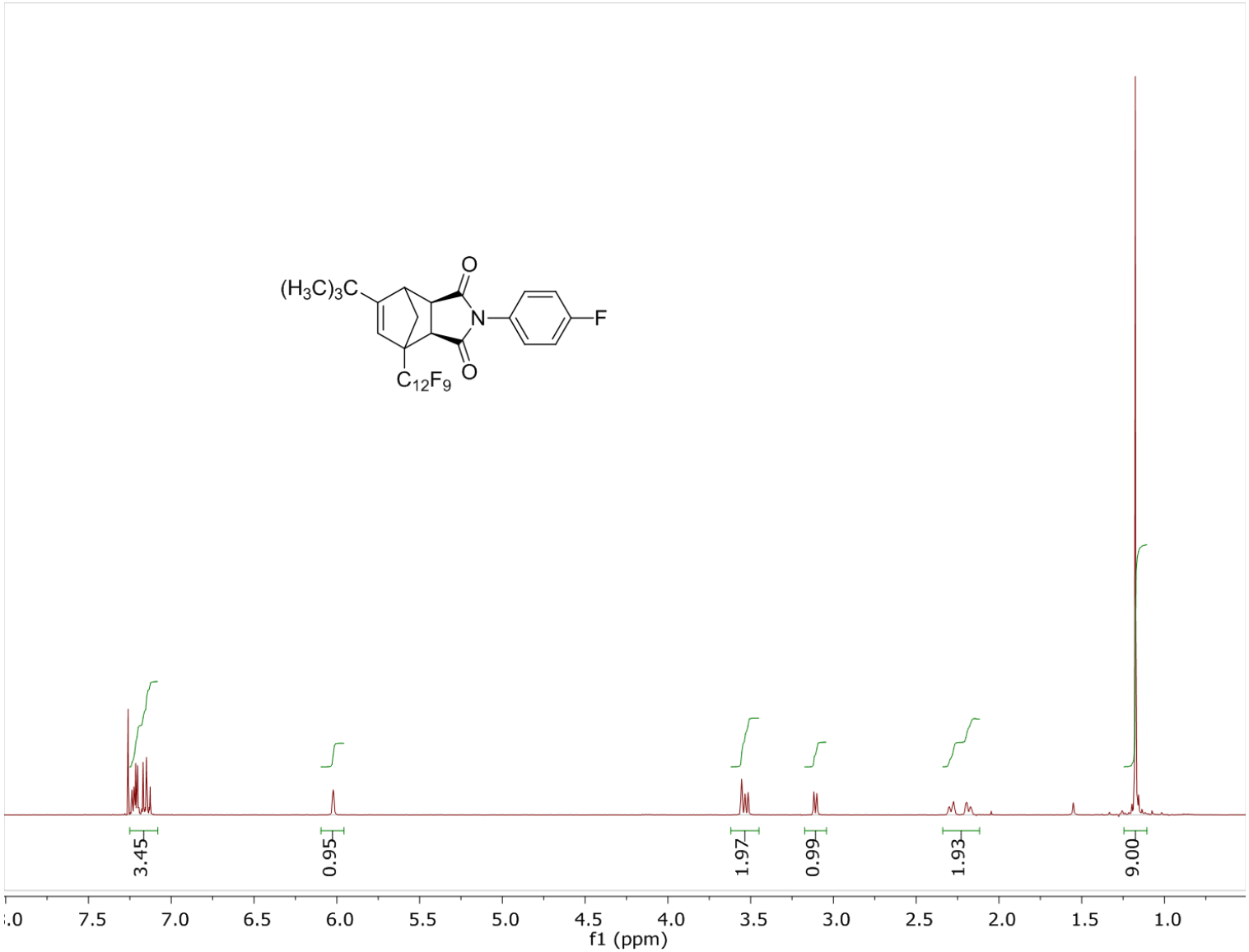

Figure B5. ^{1}H (400 MHz, $CDCl_3$) NMR spectrum of compound **3c**.

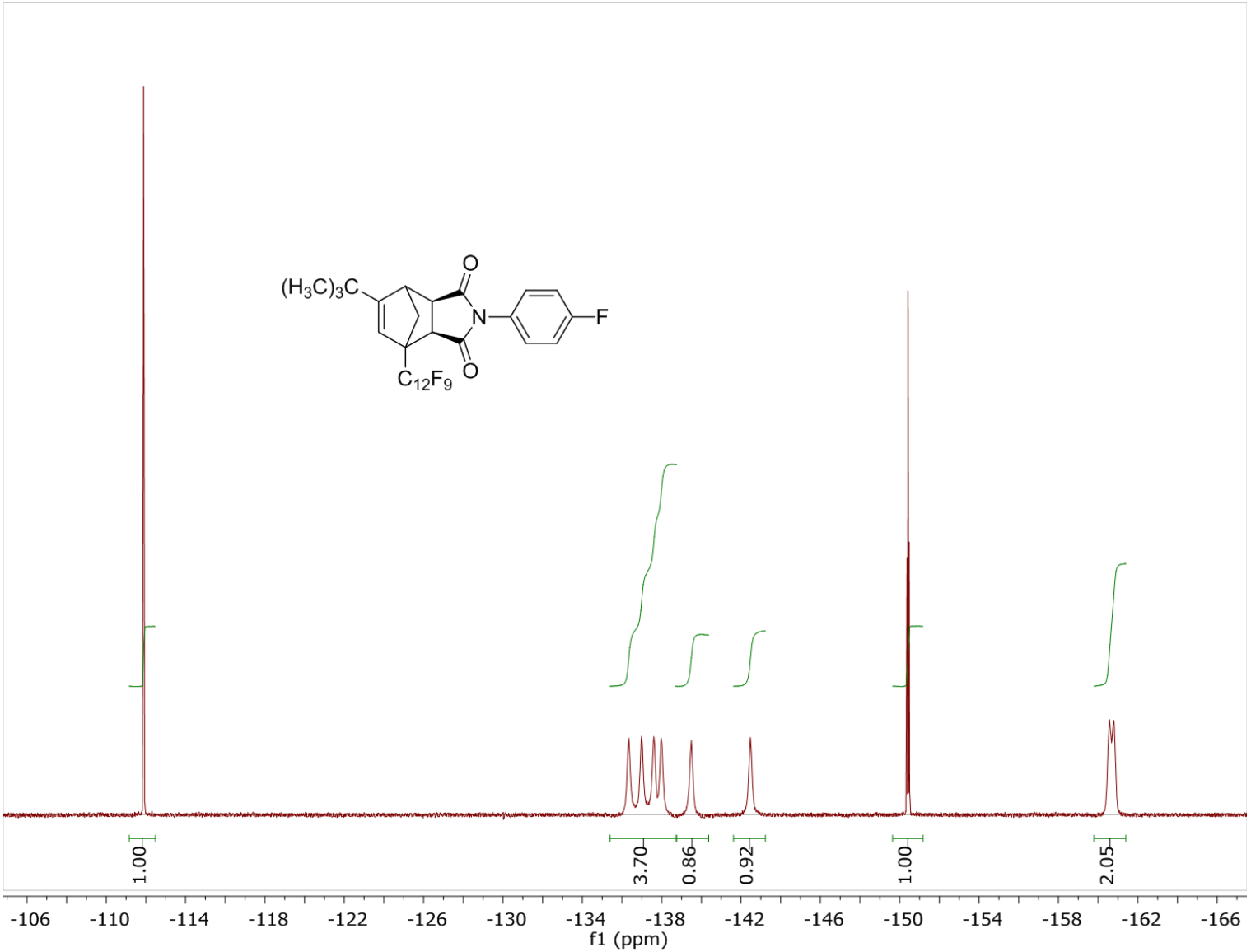

Figure B6. ^{19}F (376 MHz, $CDCl_3$) NMR spectrum of compound **3c**.

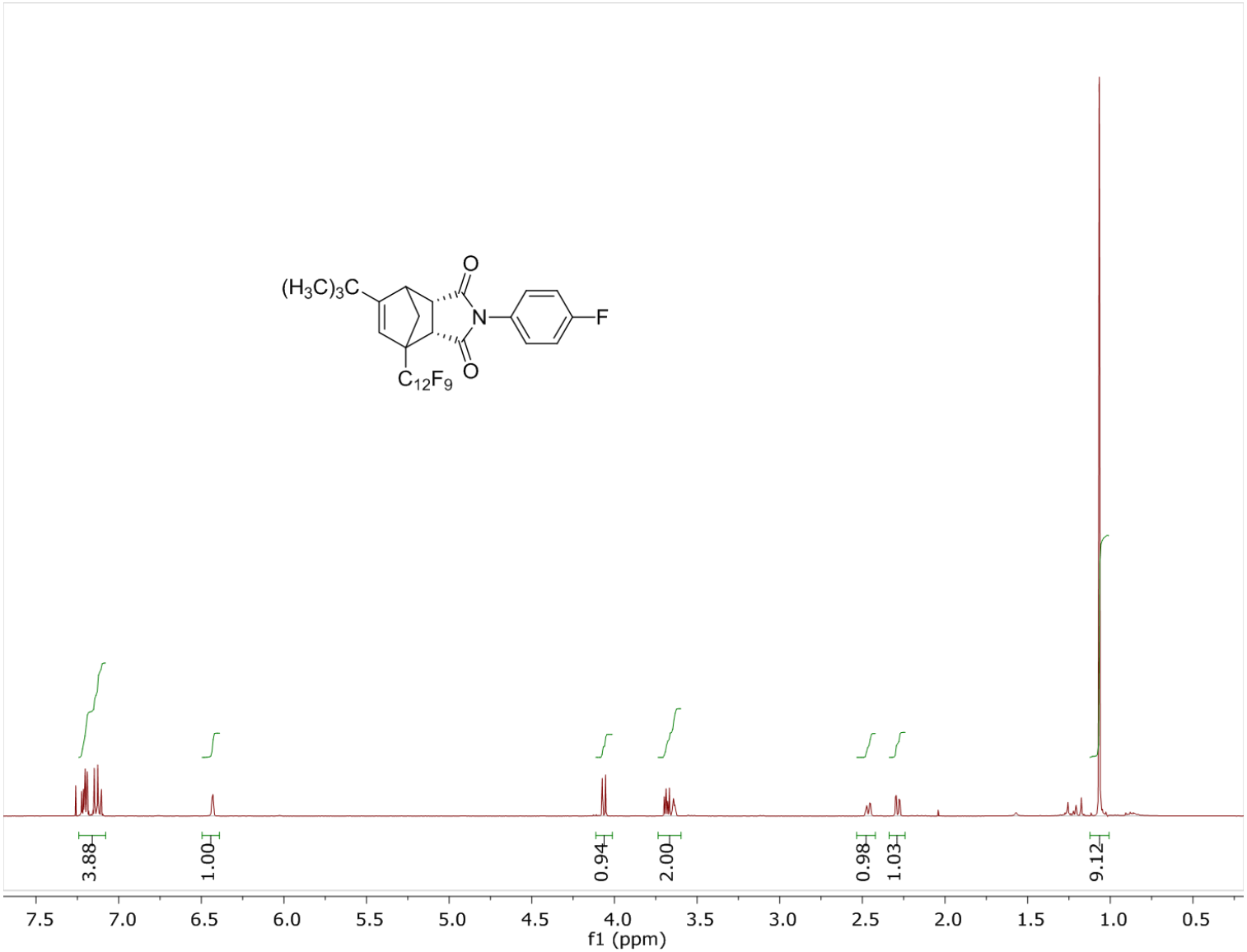

Figure B7. ^{1}H (400 MHz, $CDCl_3$) NMR spectrum of compound **3d**.

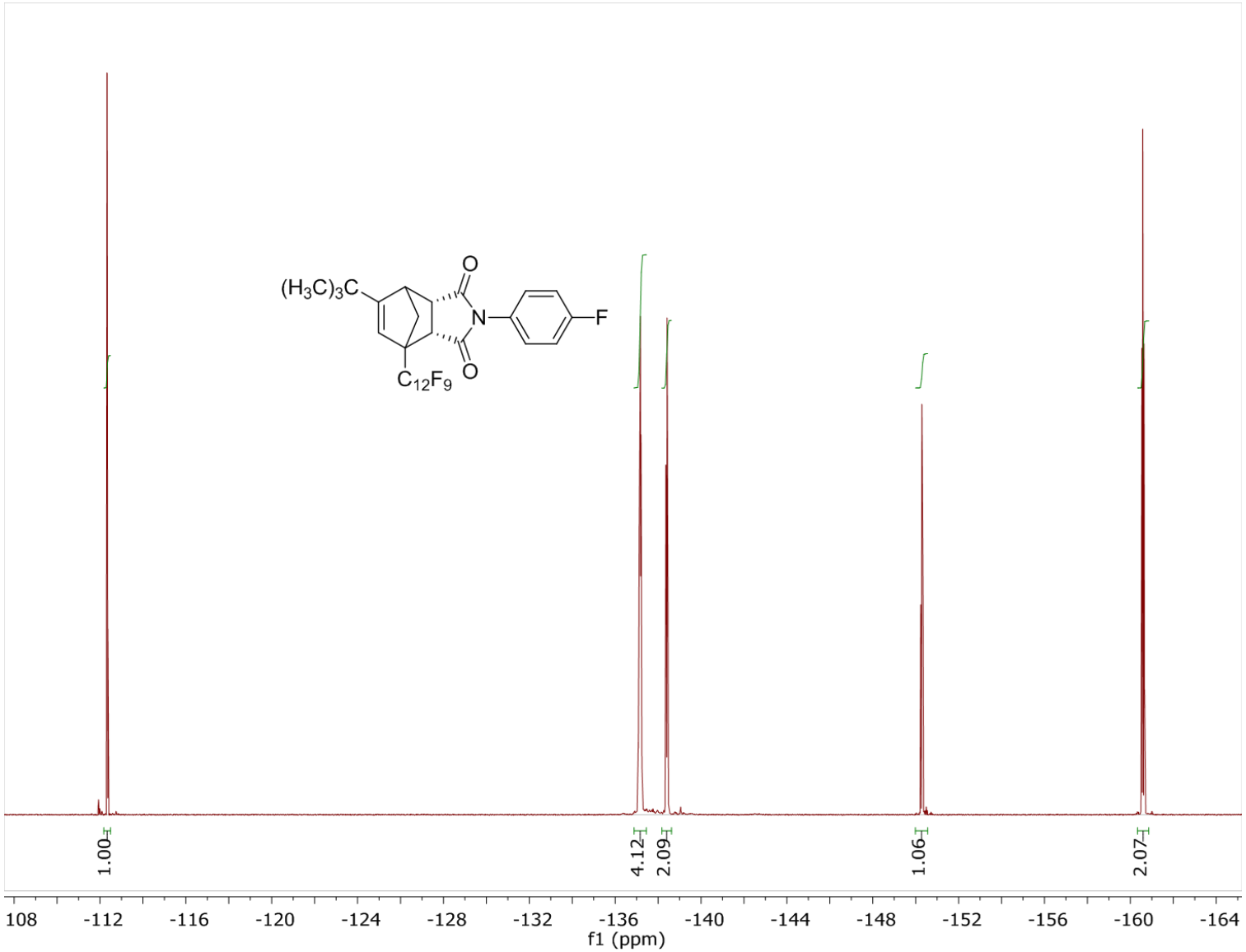

Figure B8. ^{19}F (376 MHz, $CDCl_3$) NMR spectrum of compound **3d**.

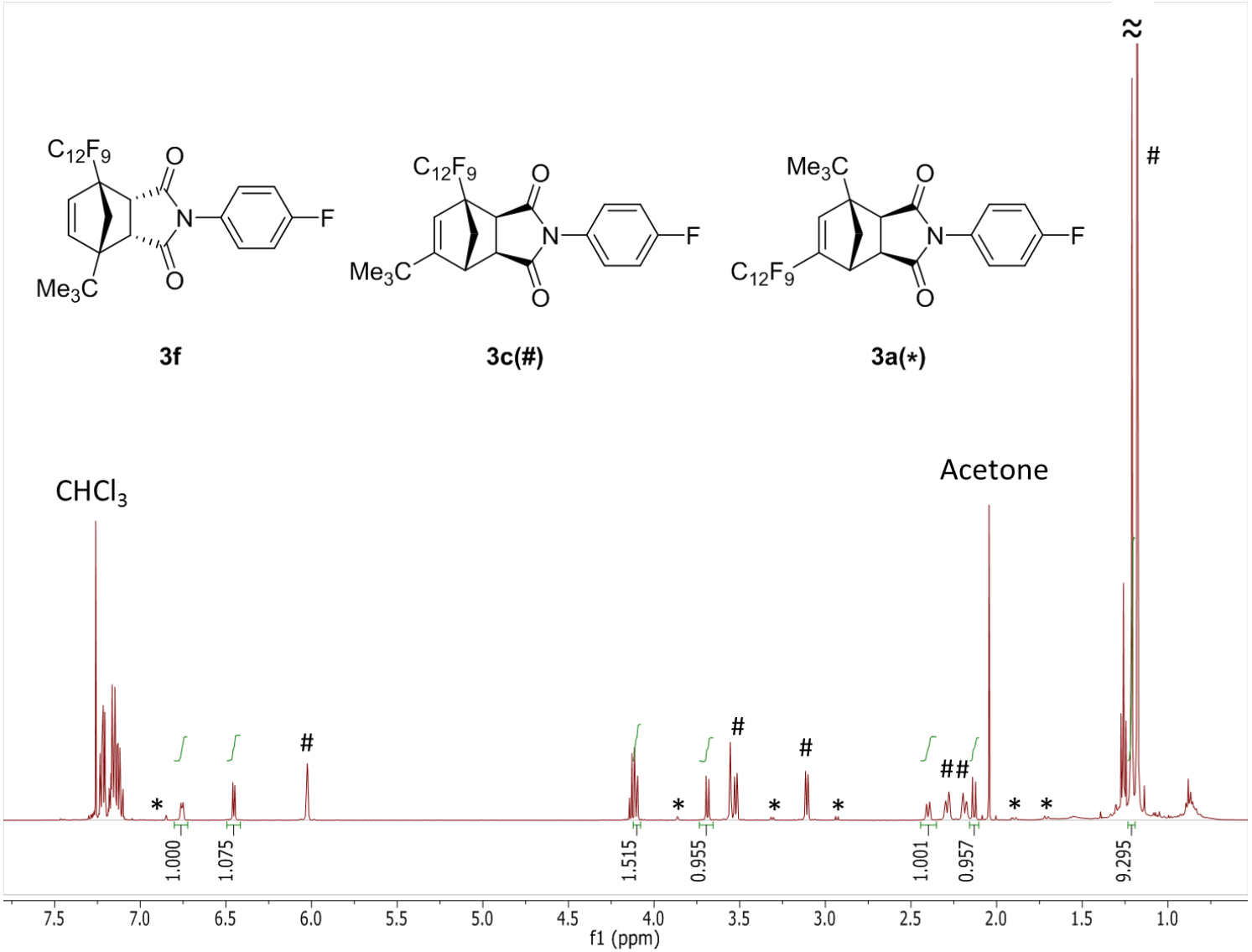

Figure B9. ^{1}H (400 MHz, $CDCl_3$) NMR spectrum of compound **3f** (with **3c** and **3a**).

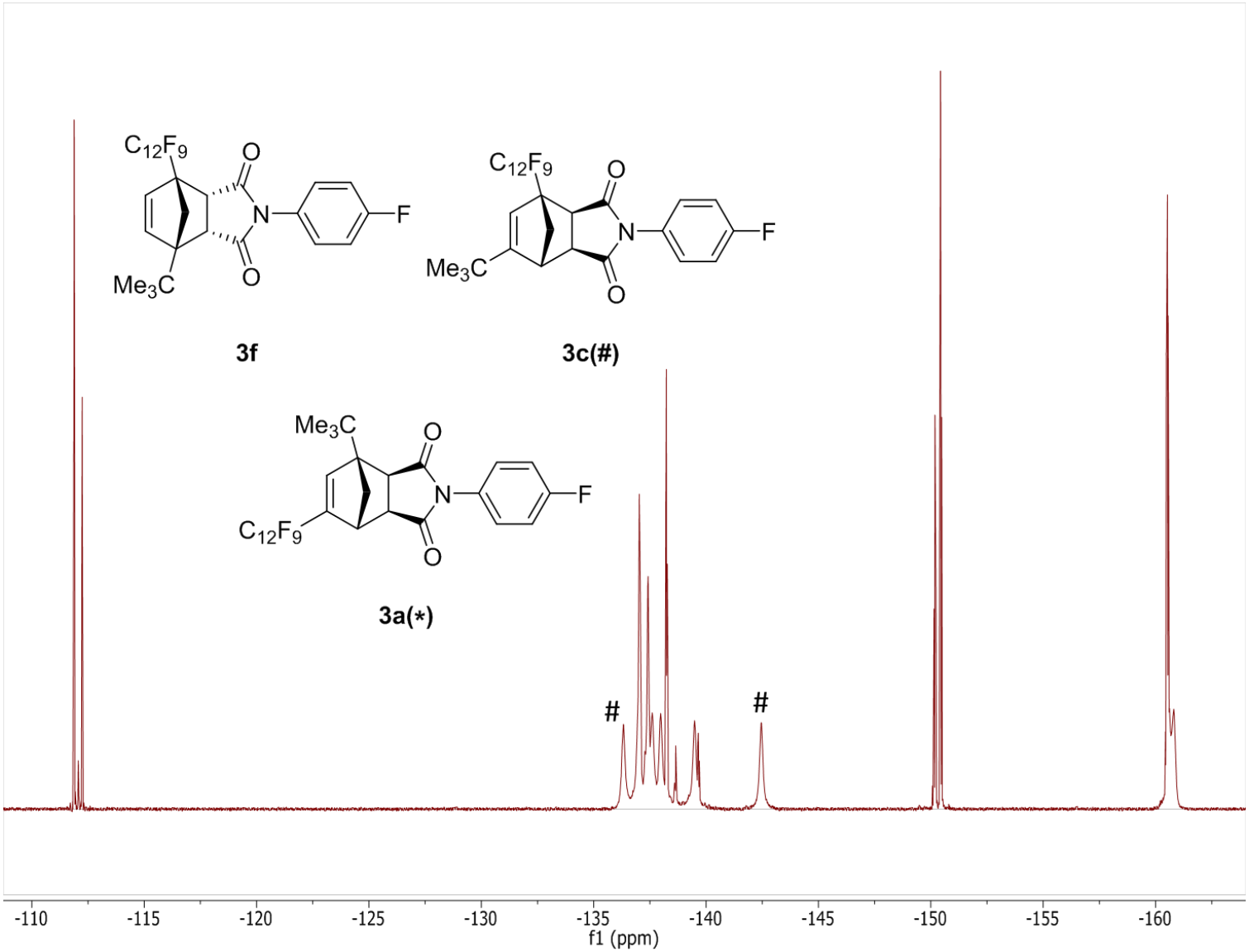

Figure B10. ^{19}F (376 MHz, $CDCl_3$) NMR spectrum of compound **3f** (with **3c** and **3a**).

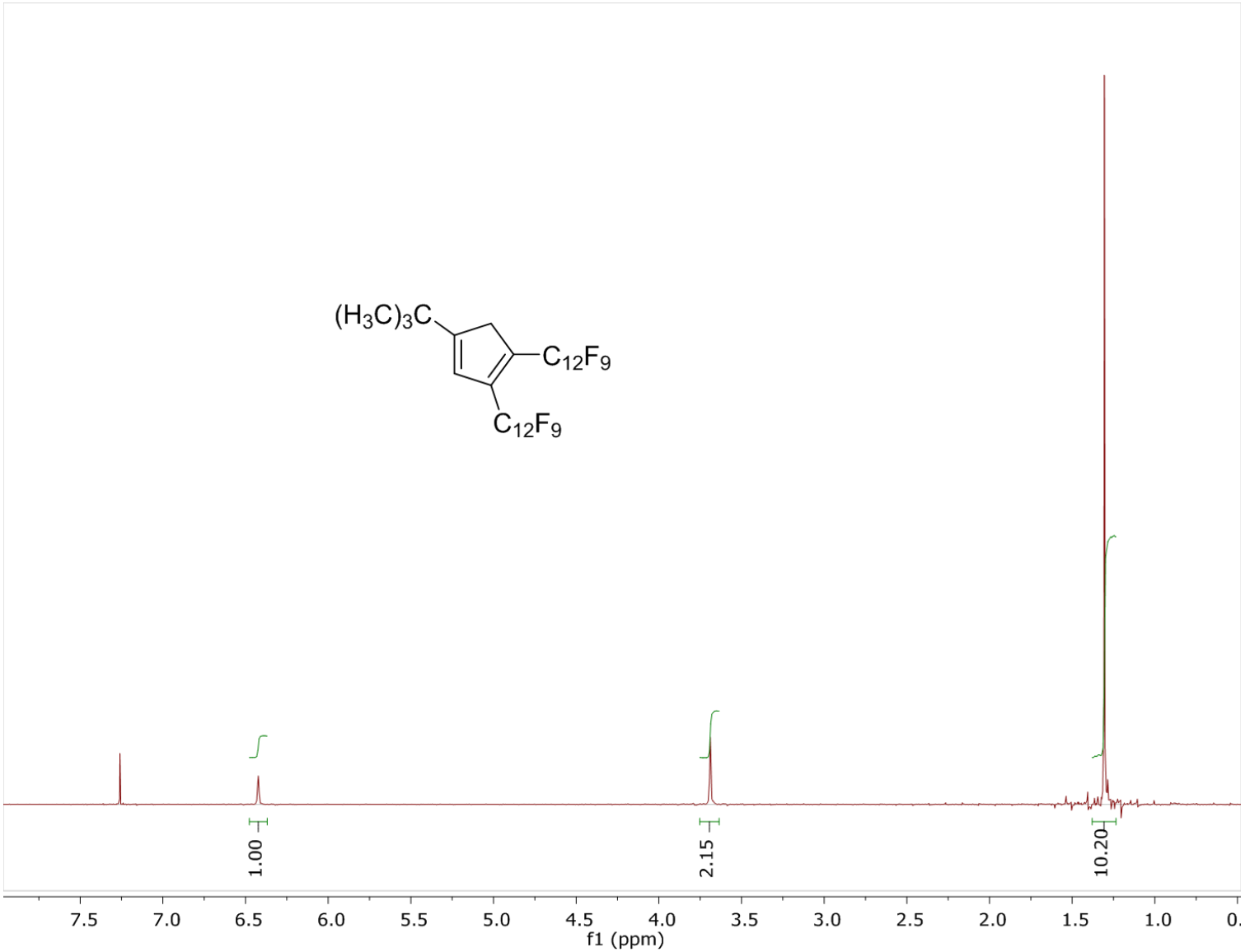

Figure B11. ^{1}H (400 MHz, $CDCl_3$) NMR spectrum of compound **4**.

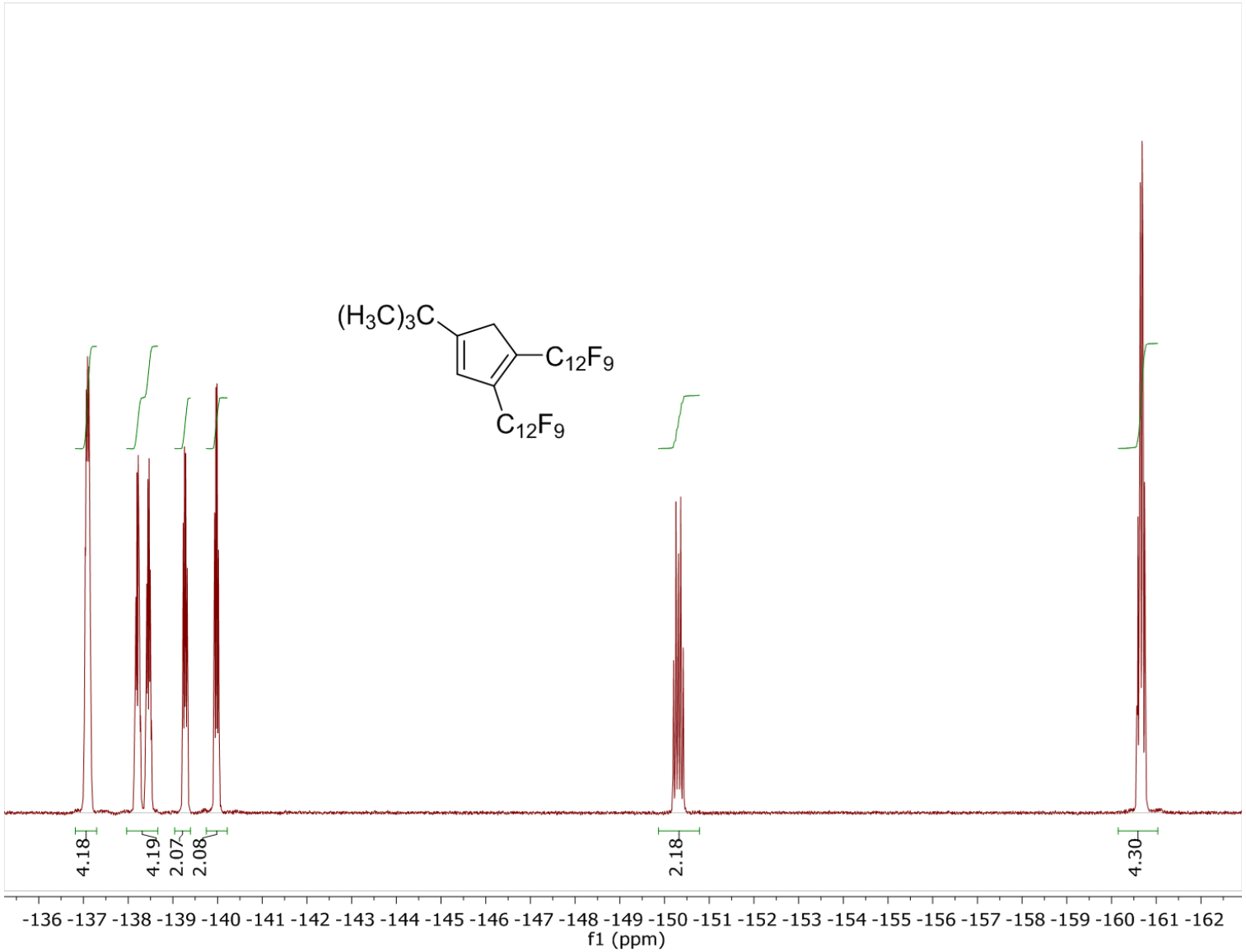

Figure B12. ^{19}F (376 MHz, $CDCl_3$) NMR spectrum of compound **4**.

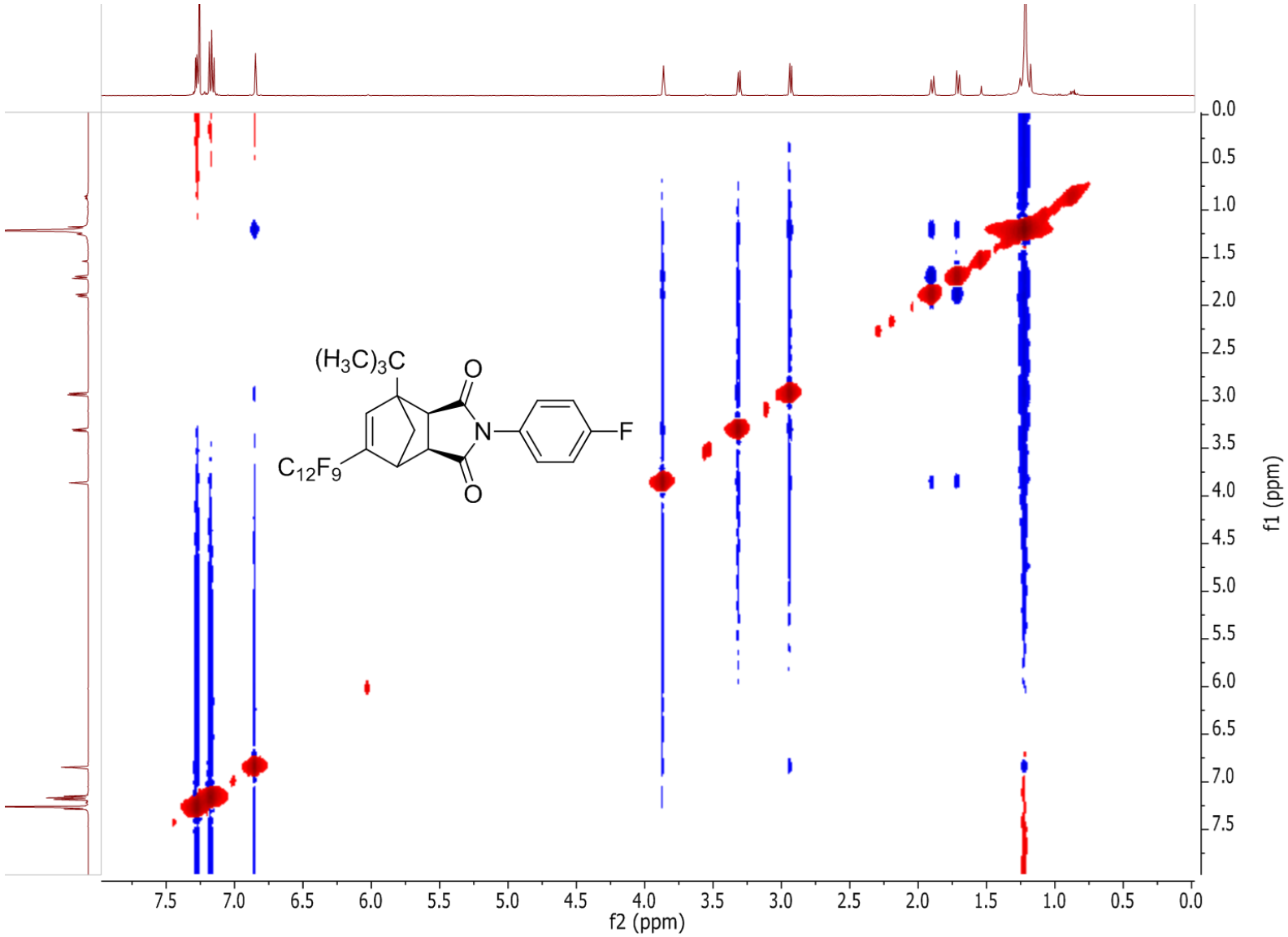

Figure B13. 2D NOE spectrum of compound **3a** in $CDCl_3$.

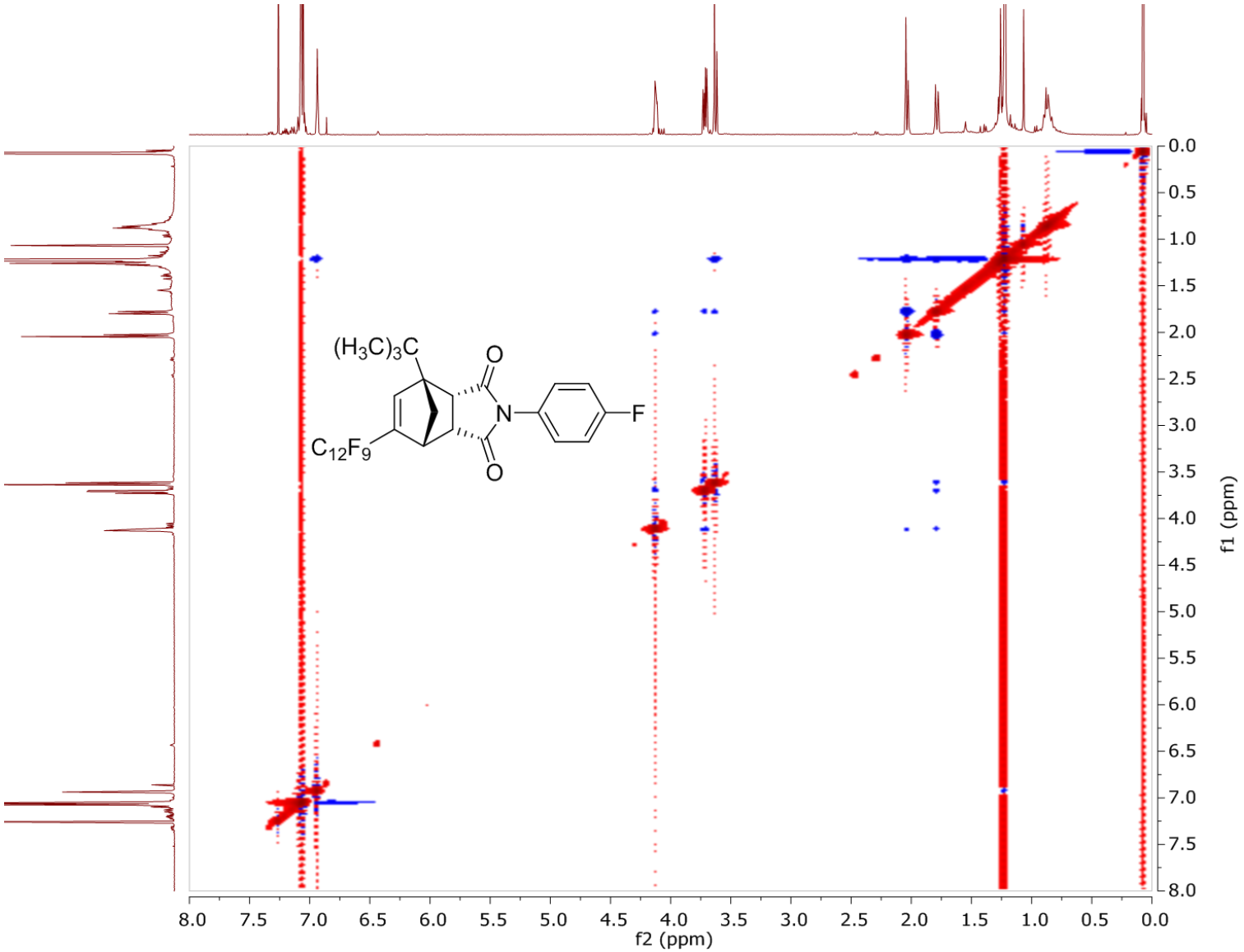

Figure B14. 2D NOE spectrum of compound **3b** in $CDCl_3$.

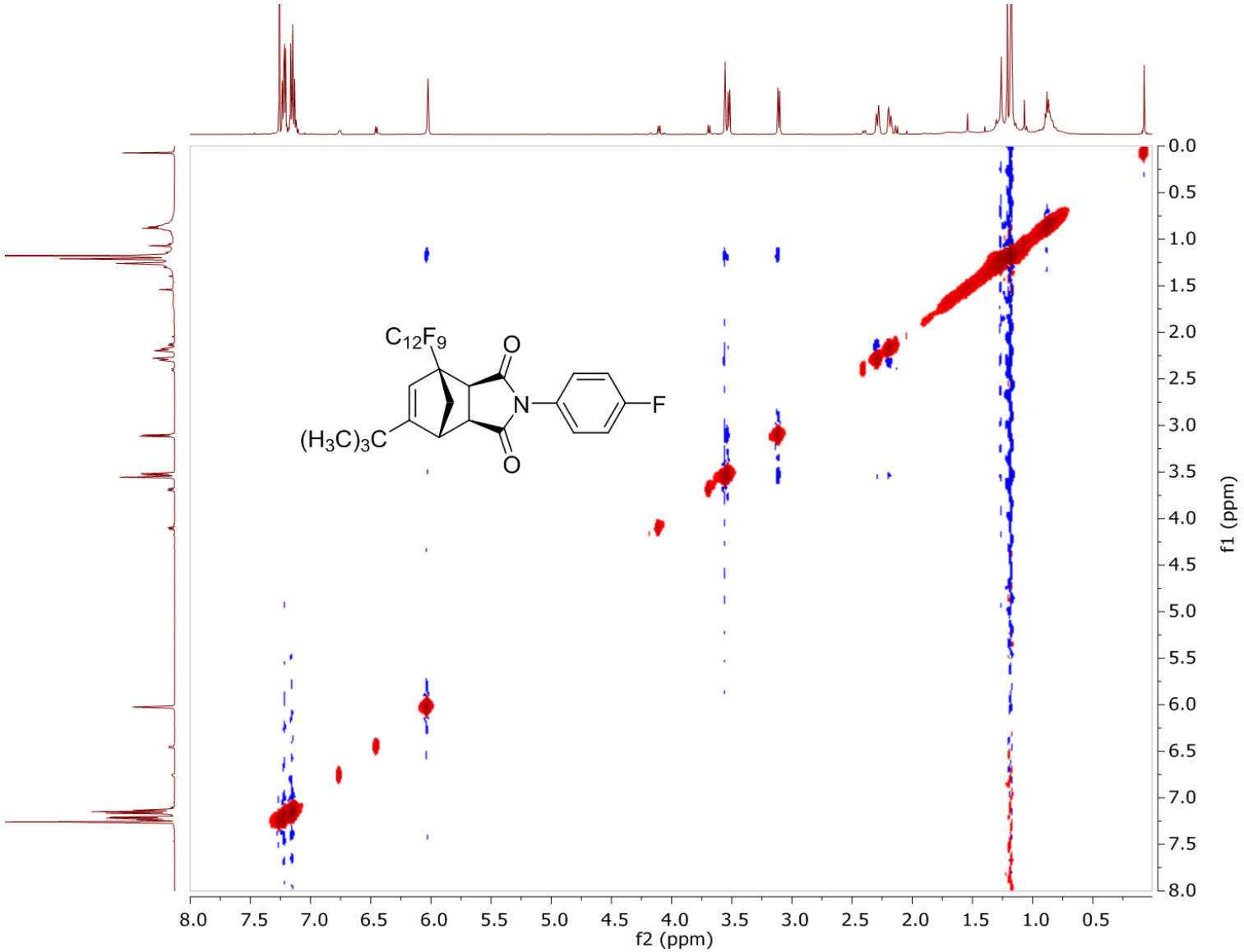

Figure B15. 2D NOE spectrum of compound **3c** in $CDCl_3$.

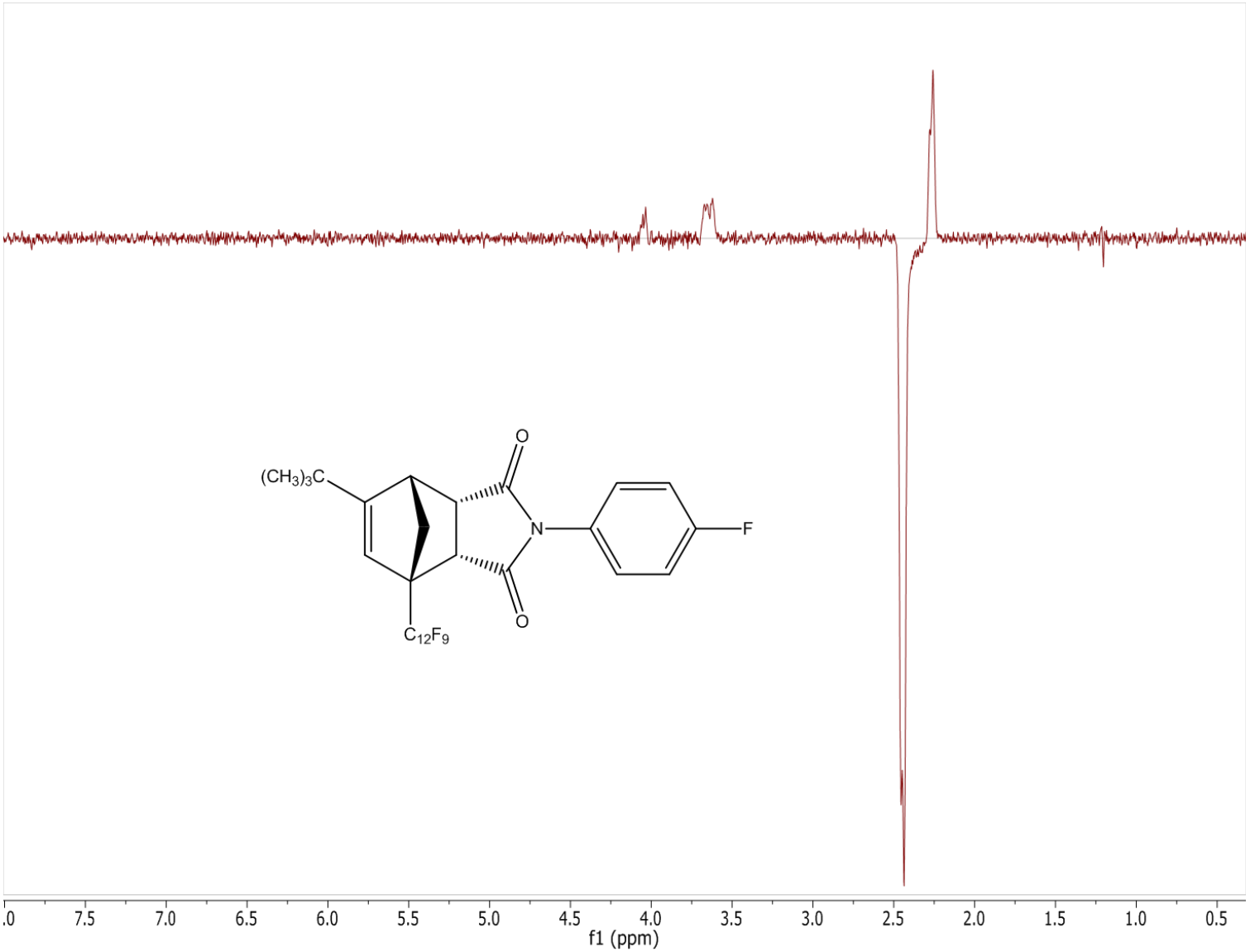

Figure B16. 1D ^{1}H NOE spectrum of **3d**.

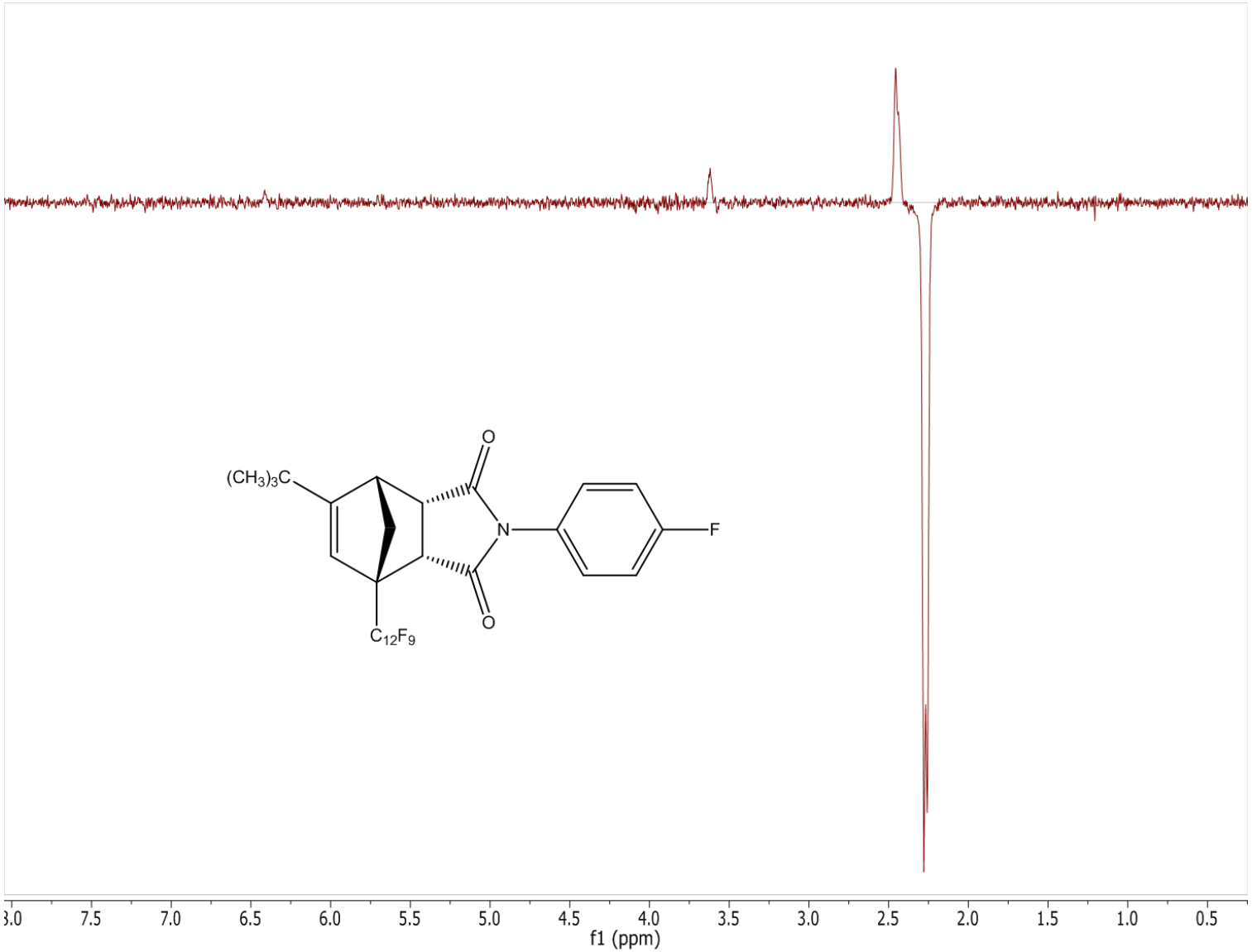

Figure B17. 1D ^{1}H NOE spectrum of **3d**.

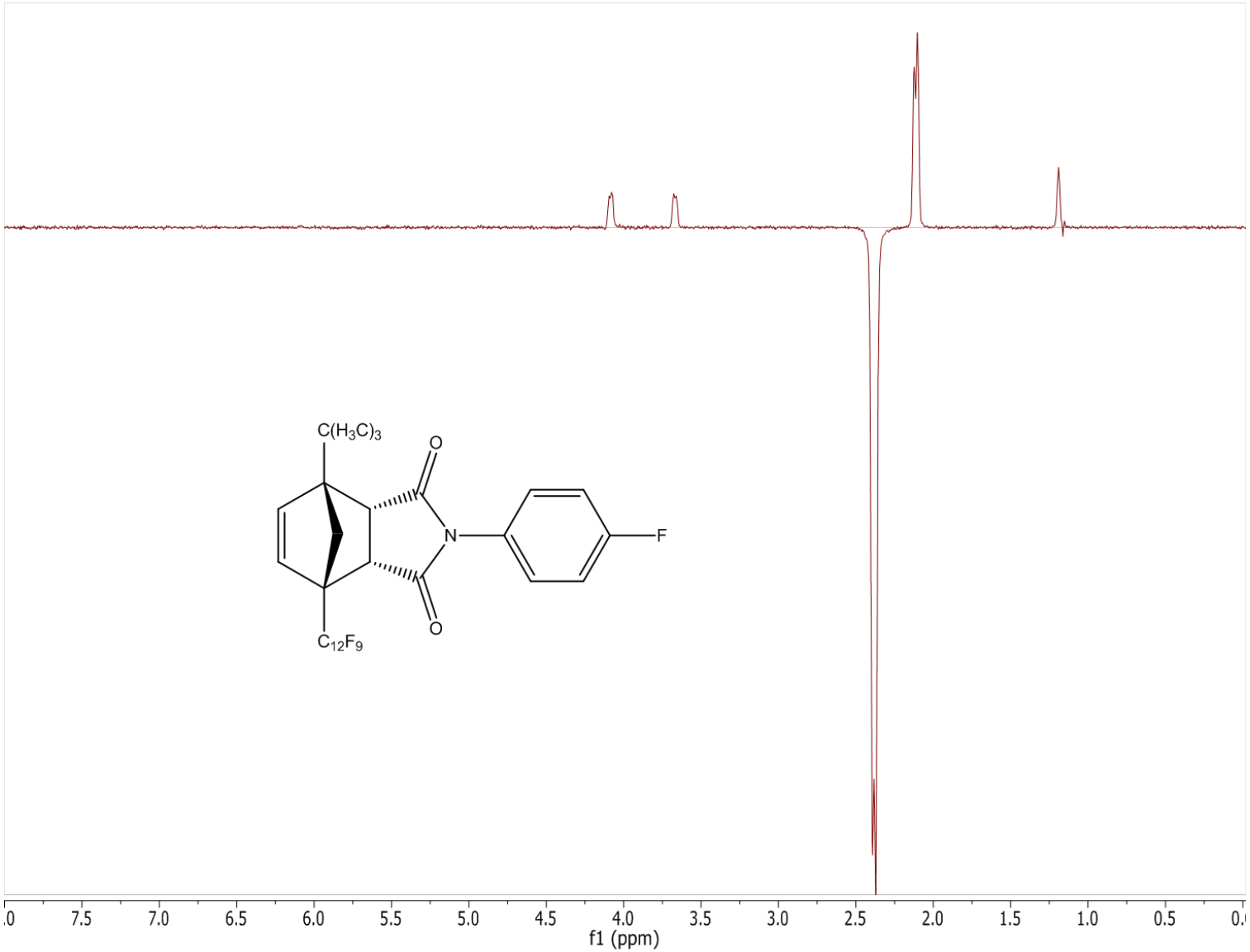

Figure B18. 1D ^{1}H NOE spectrum of **3f**.

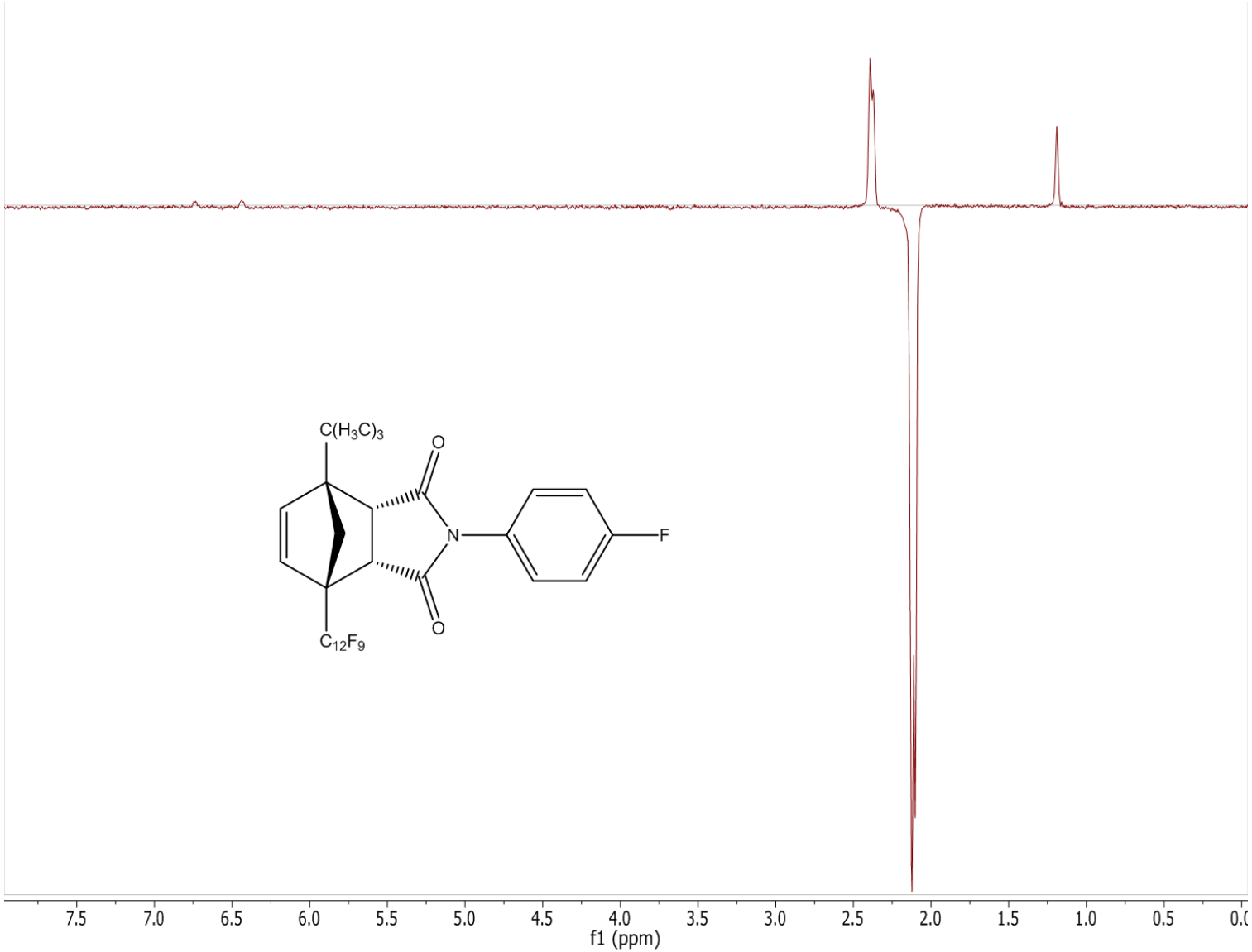

Figure B19. 1D ^{1}H NOE spectrum of **3f**.

Structures

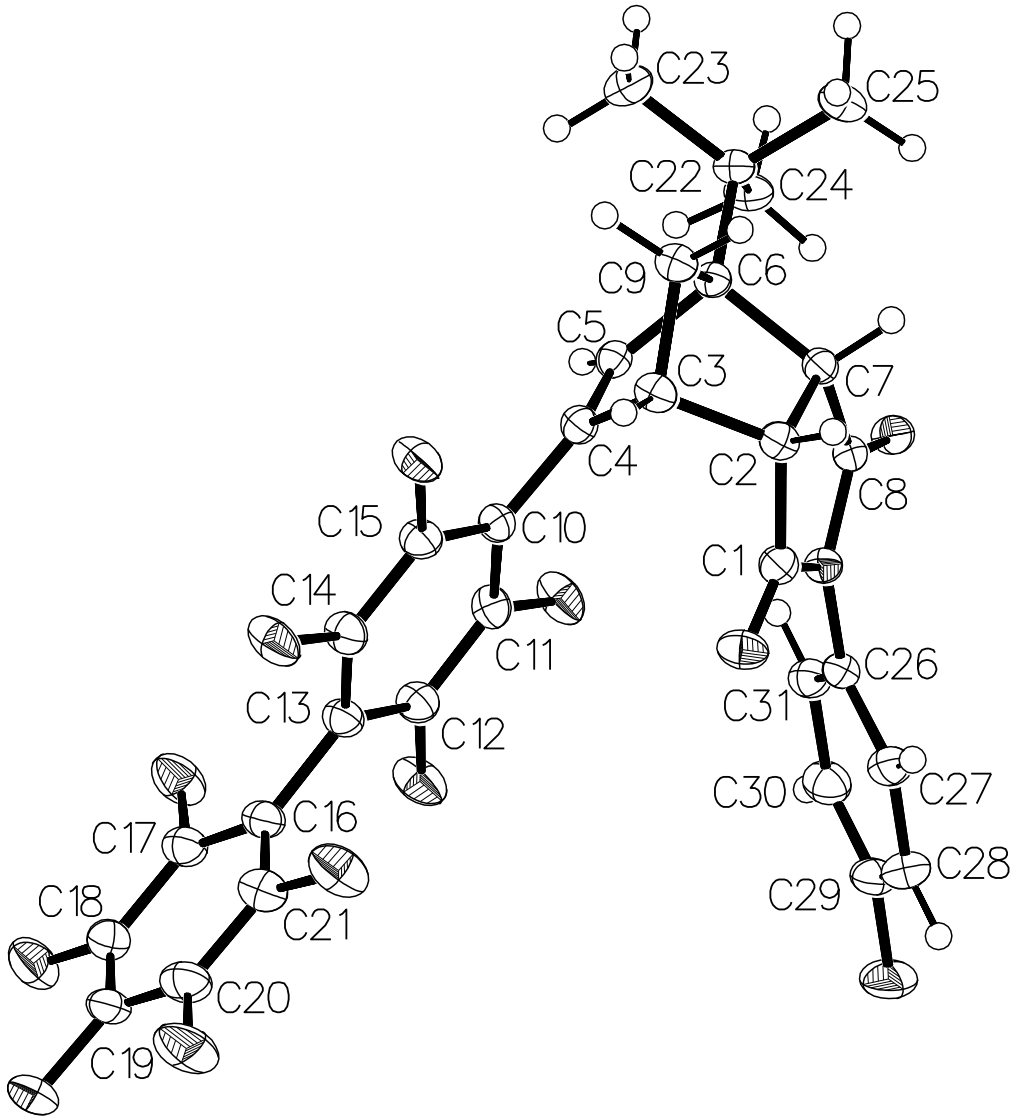

Figure B20. Ellipsoid plot (50% probability) of the molecular structure of crystalline adduct **3b** showing *endo* stereochemistry and attachment of $C_{12}F_9$ group at the 2-carbon (C=C double bond) of the norbornene and a *t*Bu group at the 1-carbon (bridgehead) of the norbornene. Hydrogen and Fluorine atoms are numbered according to the carbon atoms to which they are attached.

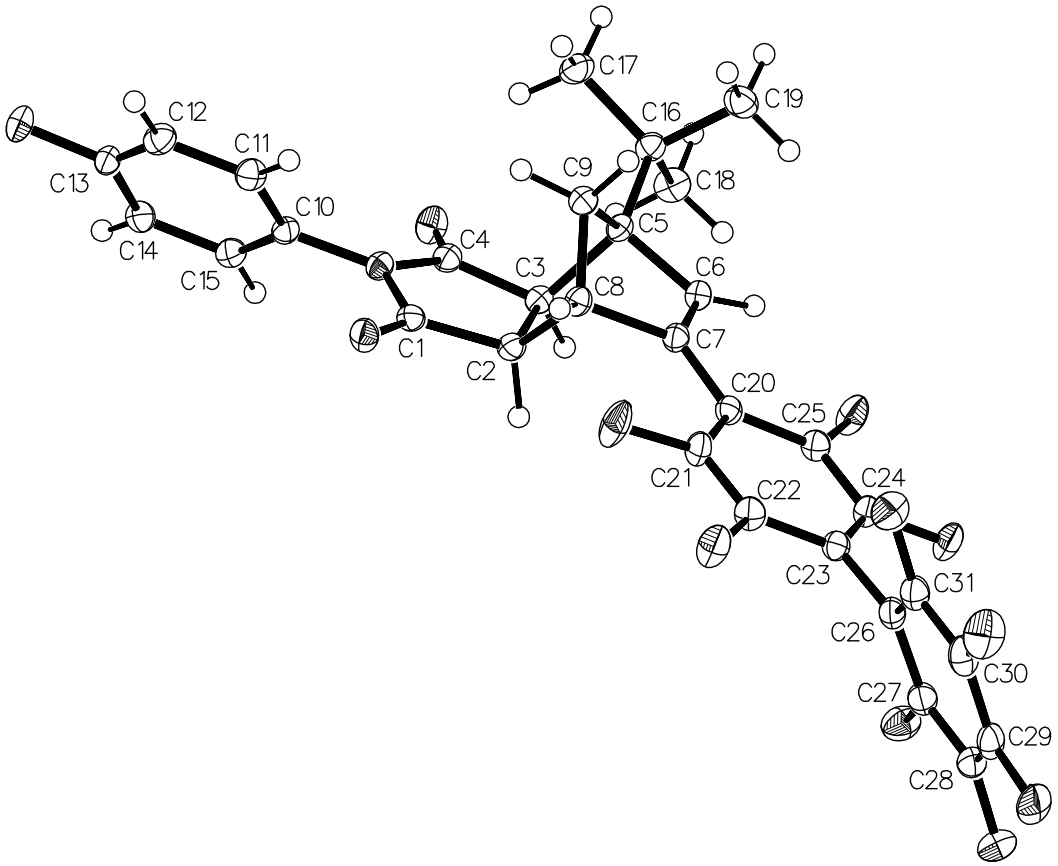

Figure B21. Ellipsoid plot (50% probability) of the molecular structure of crystalline adduct **3a** showing *exo* stereochemistry and attachment of $C_{12}F_9$ group at the 2-carbon (C=C double bond) of the norbornene and a *t*Bu group at the 1-carbon (bridgehead) of the norbornene. Hydrogen and Fluorine atoms are numbered according to the carbon atoms to which they are attached.

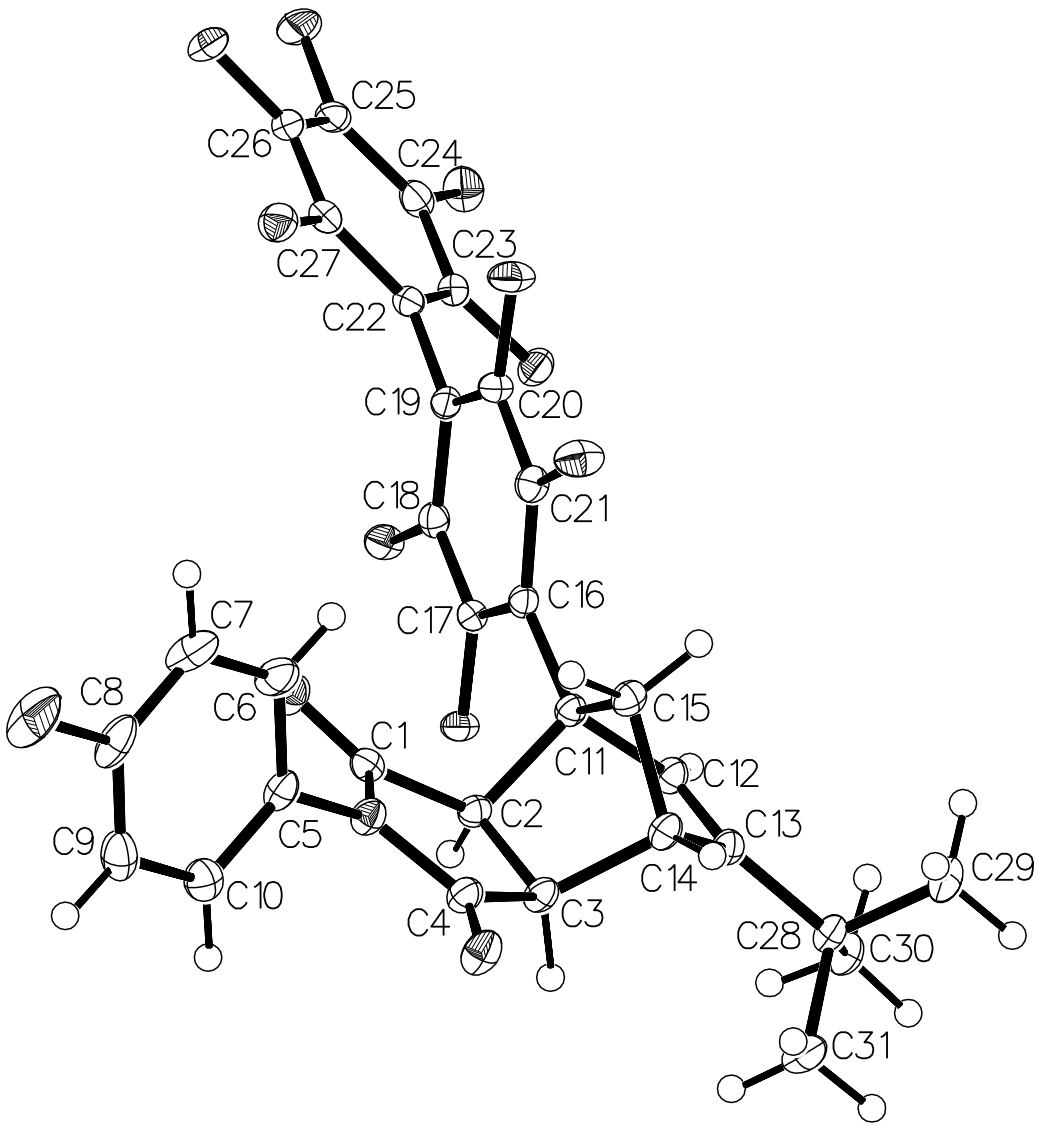

Figure B21. Ellipsoid plot (50% probability) of the molecular structure of crystalline adduct **3c** showing *exo* stereochemistry and attachment of the *t*Bu group at the 2-carbon (C=C double bond) of the norbornene and the $C_{12}F_9$ group at the 1-carbon (bridgehead) of the norbornene. Hydrogen and Fluorine atoms are numbered according to the carbon atoms to which they are attached.

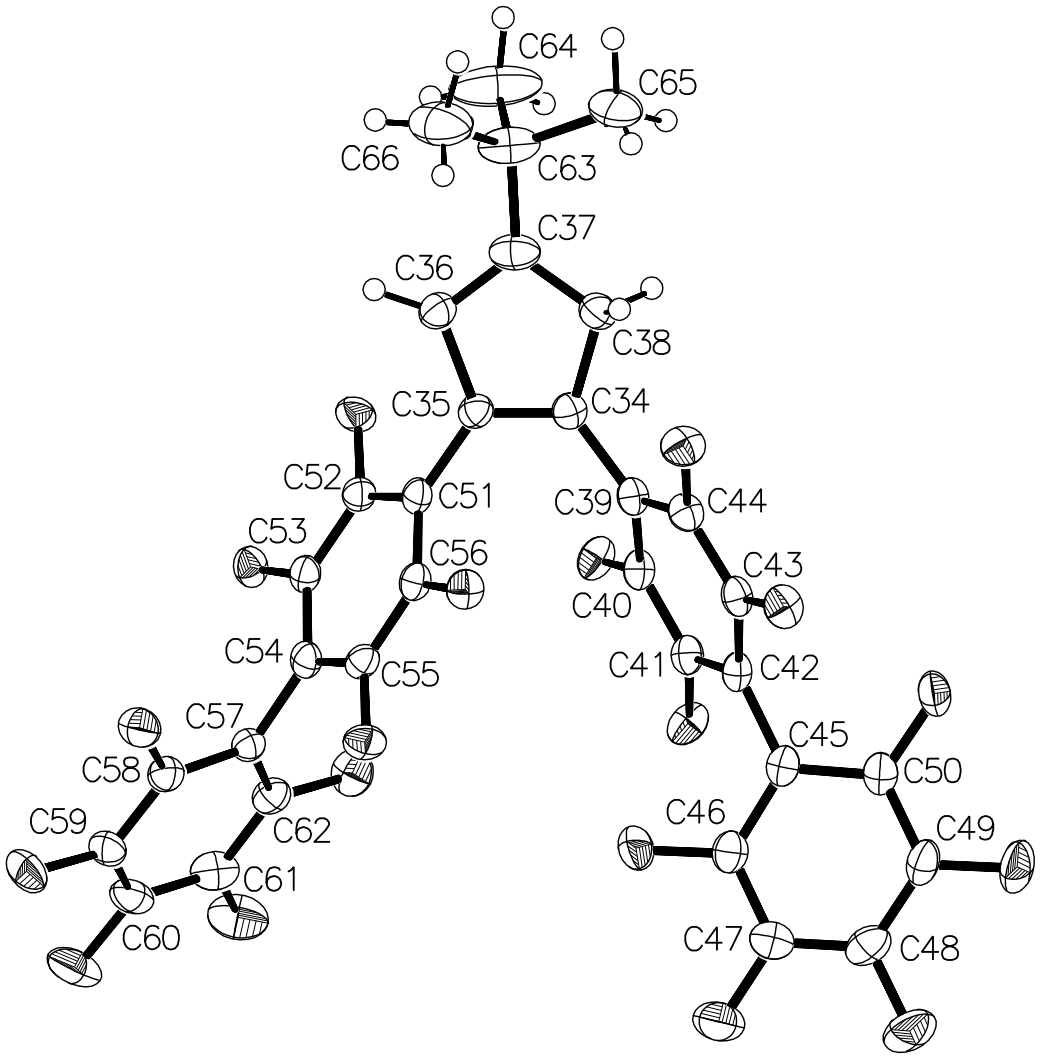

Figure B22. Ellipsoid plot (50% probability) of the molecular structure of crystalline adduct **4**. Hydrogen and Fluorine atoms are numbered according to the carbon atoms to which they are attached.

Crystallographic data table

Compound	3c	3b	3a	4
Empirical formula	$C_{31}H_{19}F_{10}NO_2$	$C_{31}H_{19}F_{10}NO_2 \cdot 0.29(C_6H_{14})$	$C_{31}H_{19}F_{10}NO_2$	$C_{33}H_{12}F_{18}$
Formula weight	627.47	652.46	627.47	750.43
Diffractometer	Oxford Diffraction SuperNova A	Oxford Diffraction SuperNova A	Oxford Diffraction SuperNova A	Oxford Diffraction SuperNova A
Crystal system	monoclinic	monoclinic	monoclinic	orthorhombic
Space group	*C*2/*c*	$P2_1/c$	*C*2/*c*	$Pca2_1$
a (Å)	26.5337(5)	15.5676(4)	34.9288(6)	11.50554(9)
b (Å)	8.87410(15)	7.1922(2)	7.03778(10)	22.27253(17)
c (Å)	23.2834(4)	26.4687(7)	21.2732(3)	23.1138(2)
Volume ($Å^3$)	5359.91(16)	2935.36(14)	5220.34(14)	5923.08(9)
Z	8	4	8	8
Density (calc) (Mg/m^3)	1.555	1.476	1.597	1.683
Absorption coefficient	1.278 mm^{-1}	1.188 mm^{-1}	1.312 mm^{-1}	1.612 mm^{-1}
F(000)	2544	1330	2544	2976
Temp (K)	100	100	100	100
Crystal size (mm^3)	0.2123 x 0.1596 x 0.0544	0.482 x 0.1236 x 0.0925	0.1927 x 0.1566 x 0.1338	0.5131 x 0.3567 x 0.2185
Theta range for data collection	3.88 to 76.42°	4.11 to 76.24°	4.16 to 76.22°	4.31 to 76.30°
Index ranges	−32<=h<=33, −11<=k<=9, −29<=l<=27	−19<=h<=19, −8<=k<=9, −33<=l<=30	−40<=h<=44, −8<=k<=8, −26<=l<=26	−14<=h<=14, −26<=k<=27, −28<=l<=26
Reflections collected	21858	30125	42733	38122
Independent reflections	5576 [R(int) = 0.0318]	6106 [R(int) = 0.0291]	5443 [R(int) = 0.0194]	11690 [R(int) = 0.0219]
Completeness to theta	99.0 %	99.5 %	99.6 %	99.50%
Absorption correction	Gaussian	Gaussian	Gaussian	Gaussian
Max. and min. transmission	1.114 and 0.825	1.364 and 0.870	0.858 and 0.810	1.053 and 0.673
Refinement method	Full-matrix least-squares on F^2	Full-matrix least-squares on F^2	Full-matrix least-squares on F^2	Full-matrix least-squares on F^2
Data / restraints / parameters	5576 / 0 / 400	6106 / 0 / 400	5443 / 0 / 400	11690 / 1 / 991
Goodness-of-fit on F^2	1.023	1.046	1.046	1.034
Final R indices [I>2sigma(I)]	R1 = 0.0341, wR2 = 0.0885	R1 = 0.0363, wR2 = 0.1032	R1 = 0.0325, wR2 = 0.0857	R1 = 0.0391, wR2 = 0.1056
R indices (all data)	R1 = 0.0375, wR2 = 0.0919	R1 = 0.0402, wR2 = 0.1068	R1 = 0.0337, wR2 = 0.0867	R1 = 0.0396, wR2 = 0.1063
Largest diff. peak and hole ($e/Å^3$)	0.353 and −0.265	0.323 and −0.208	0.327 and −0.213	0.459 and -0.223

Appendix C Supporting Information for: Electronic Effects of Isosteric Substituents on Diels-Alder Reactions of Substituted Cyclopentadienes and *N*-(4-Fluorophenyl)maleimide

Jeremy B. Stegall, Carla Slebodnick, Kimberly F. Tetterton,[3] and Paul A. Deck*

Department of Chemistry, Virginia Tech, Blacksburg, VA 24061

[3] Undergraduate research participant.

NMR Spectra

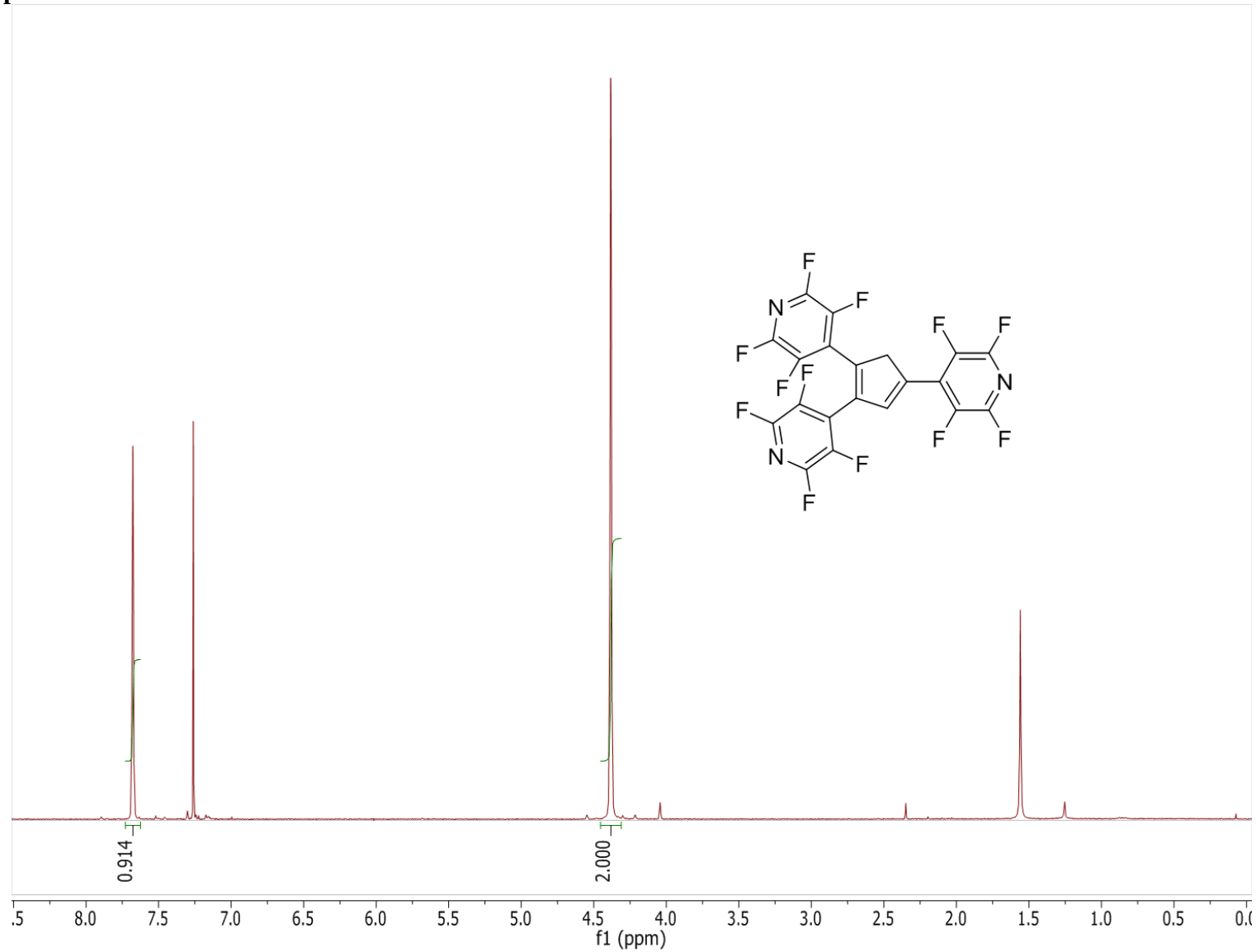

Figure C1. ^{1}H (400 MHz, $CDCl_3$) NMR spectrum of **1c**.

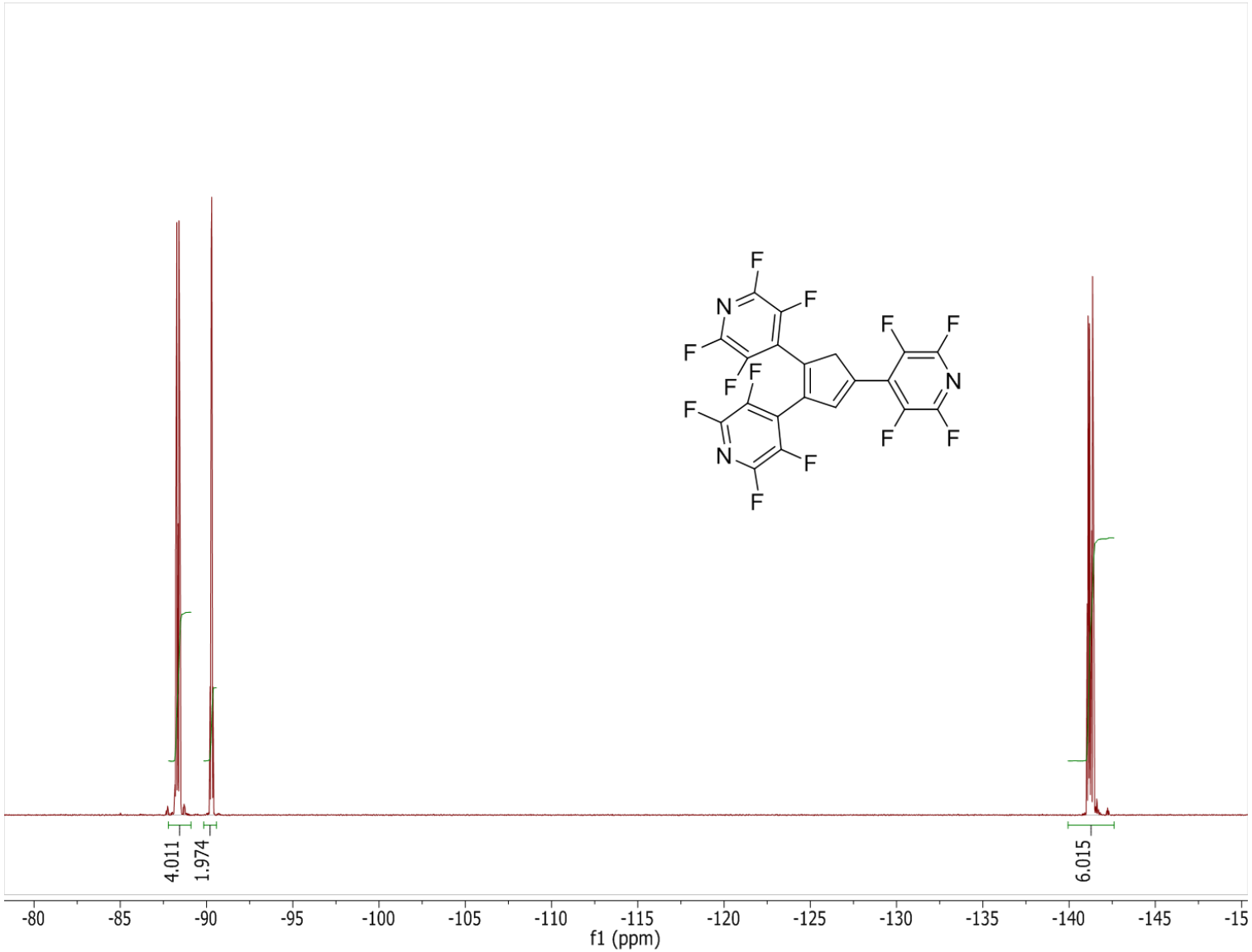

Figure C2. ^{19}F (376 MHz, $CDCl_3$) NMR spectrum of **1c**.

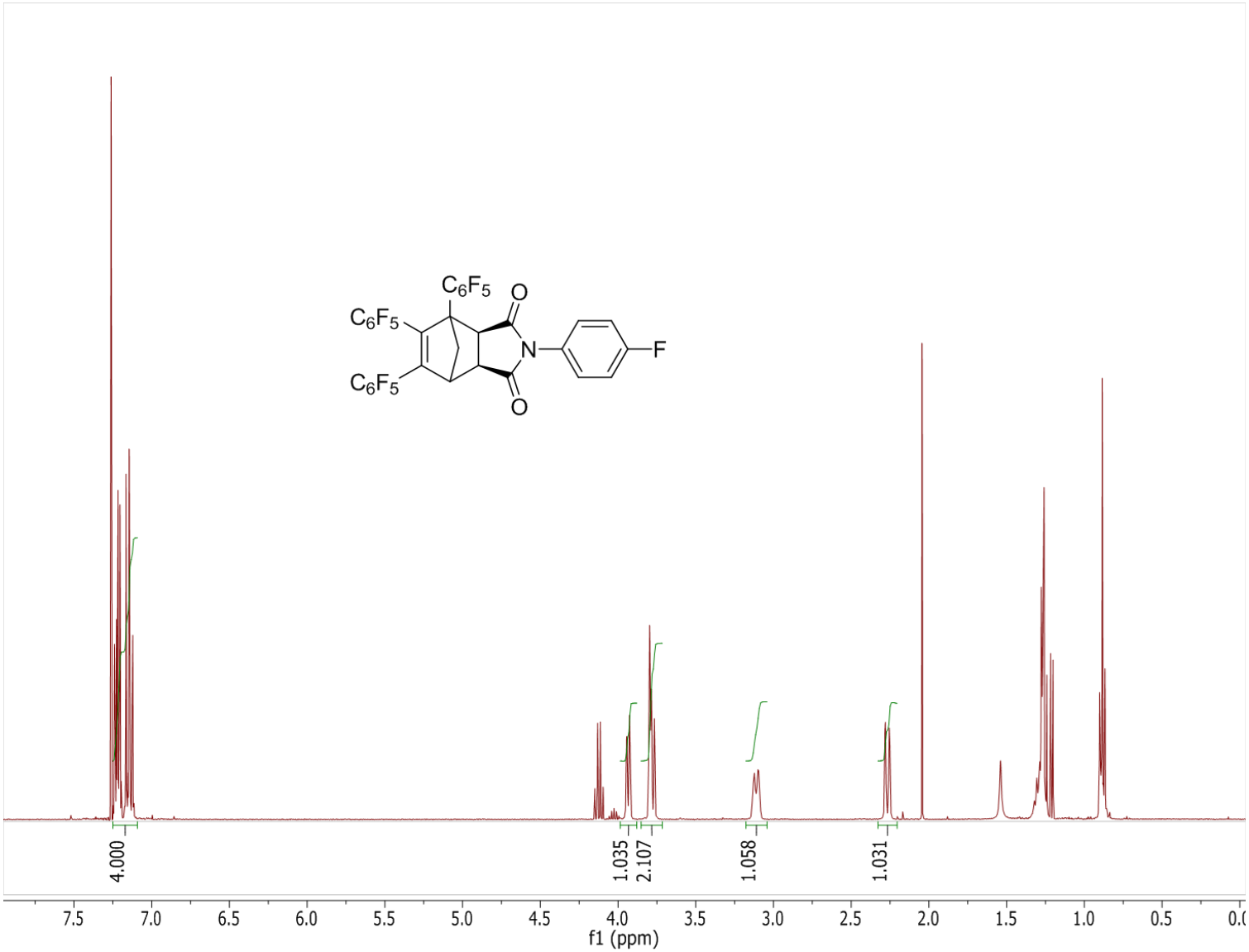

Figure C3. ^{1}H (400 MHz, $CDCl_3$) NMR spectrum of **6a**.

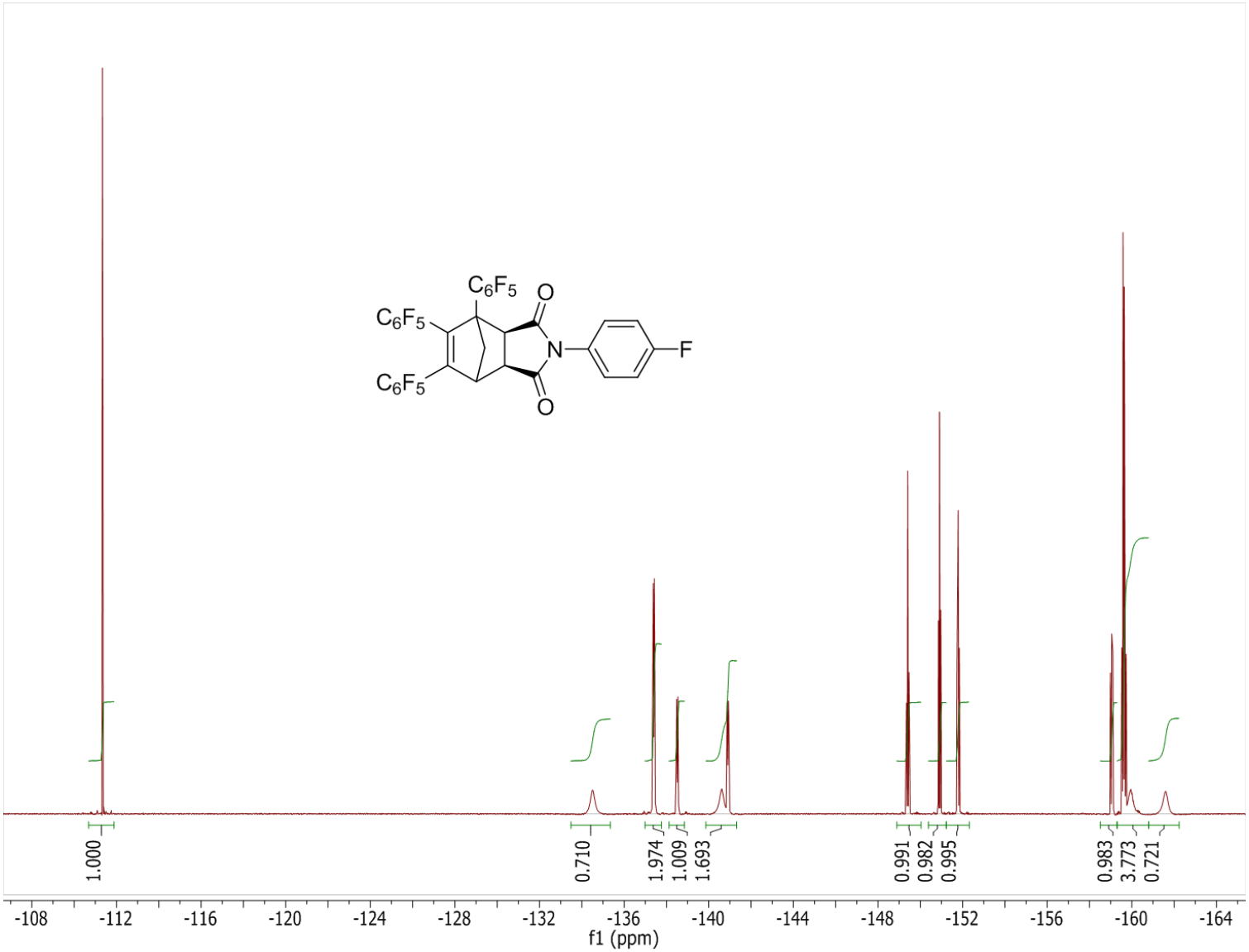

Figure C4. ^{19}F (376 MHz, $CDCl_3$) NMR spectrum of **6a**.

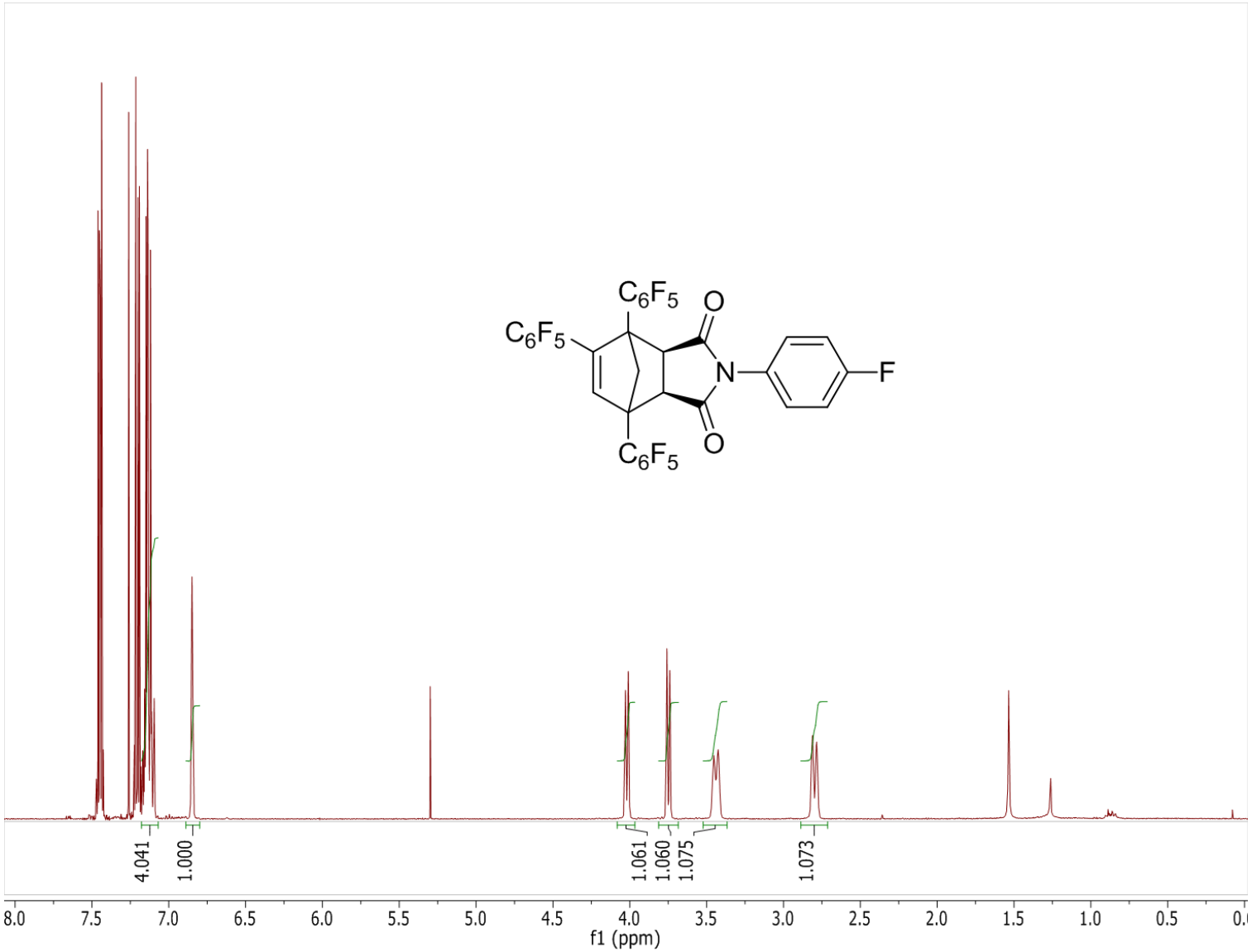

Figure C5. ^{1}H (400 MHz, $CDCl_3$) NMR spectrum of **5a**.

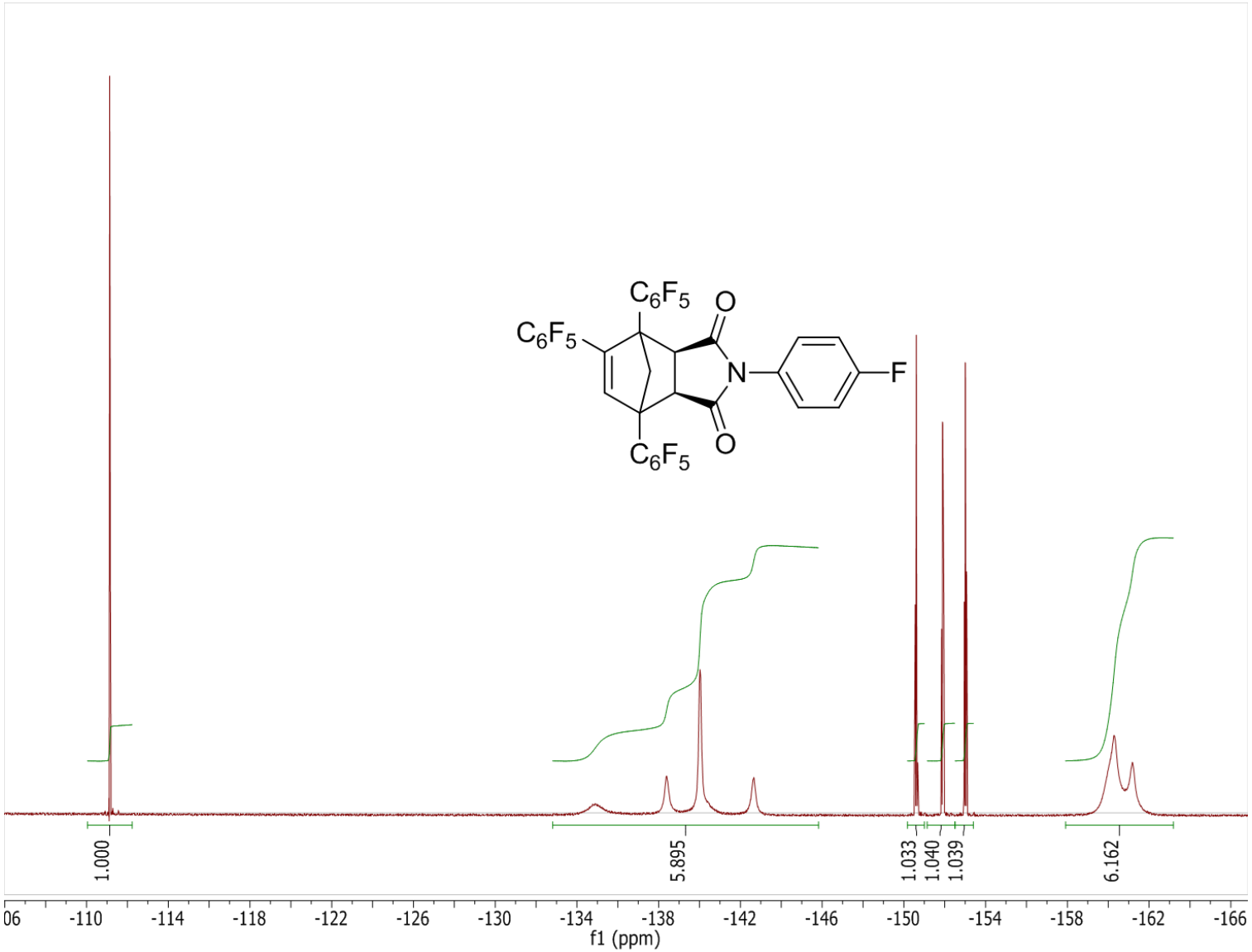

Figure C6. ^{19}F (376 MHz, $CDCl_3$) NMR spectrum of **5a**.

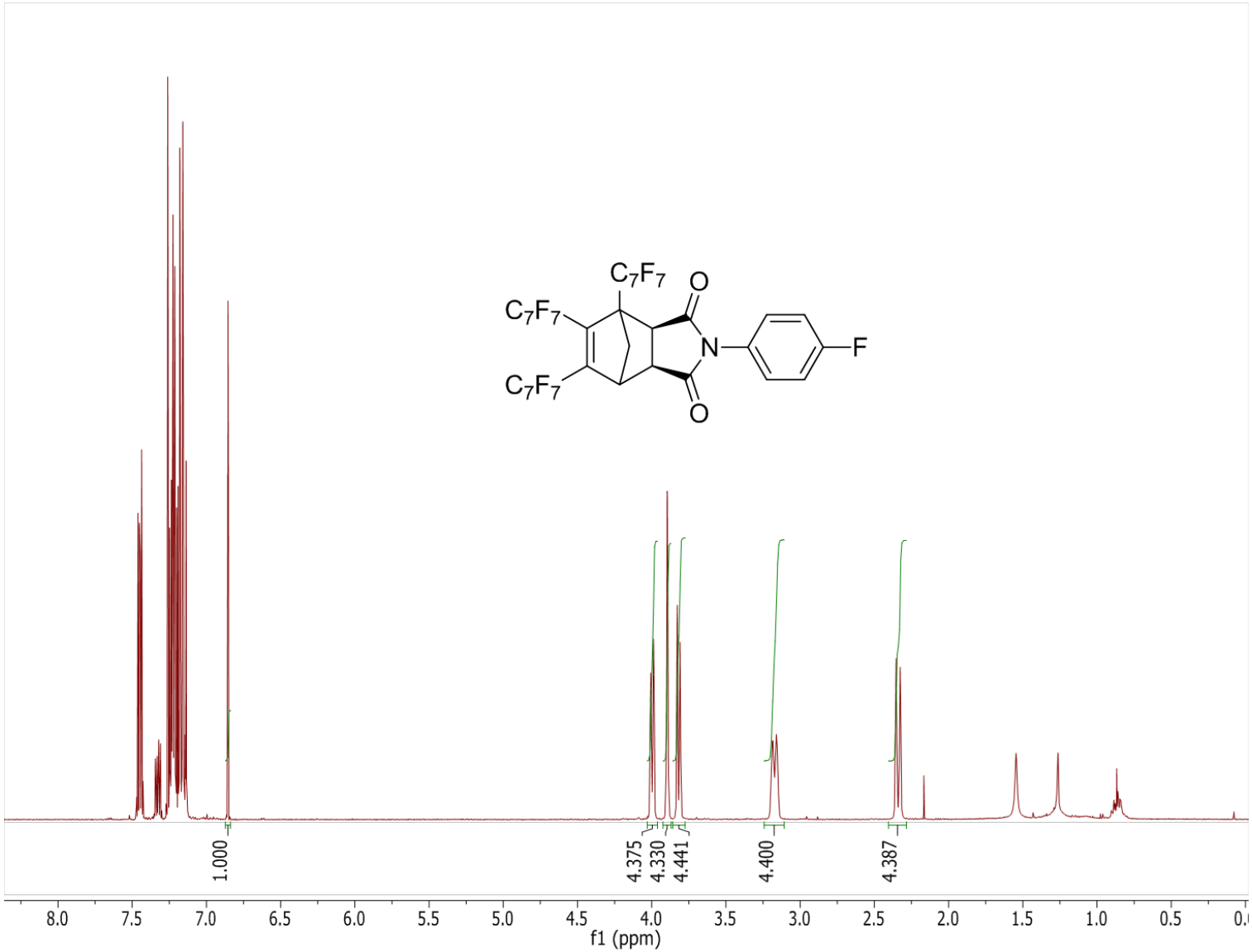

Figure C7. ^{1}H (400 MHz, $CDCl_3$) NMR spectrum of **6b**.

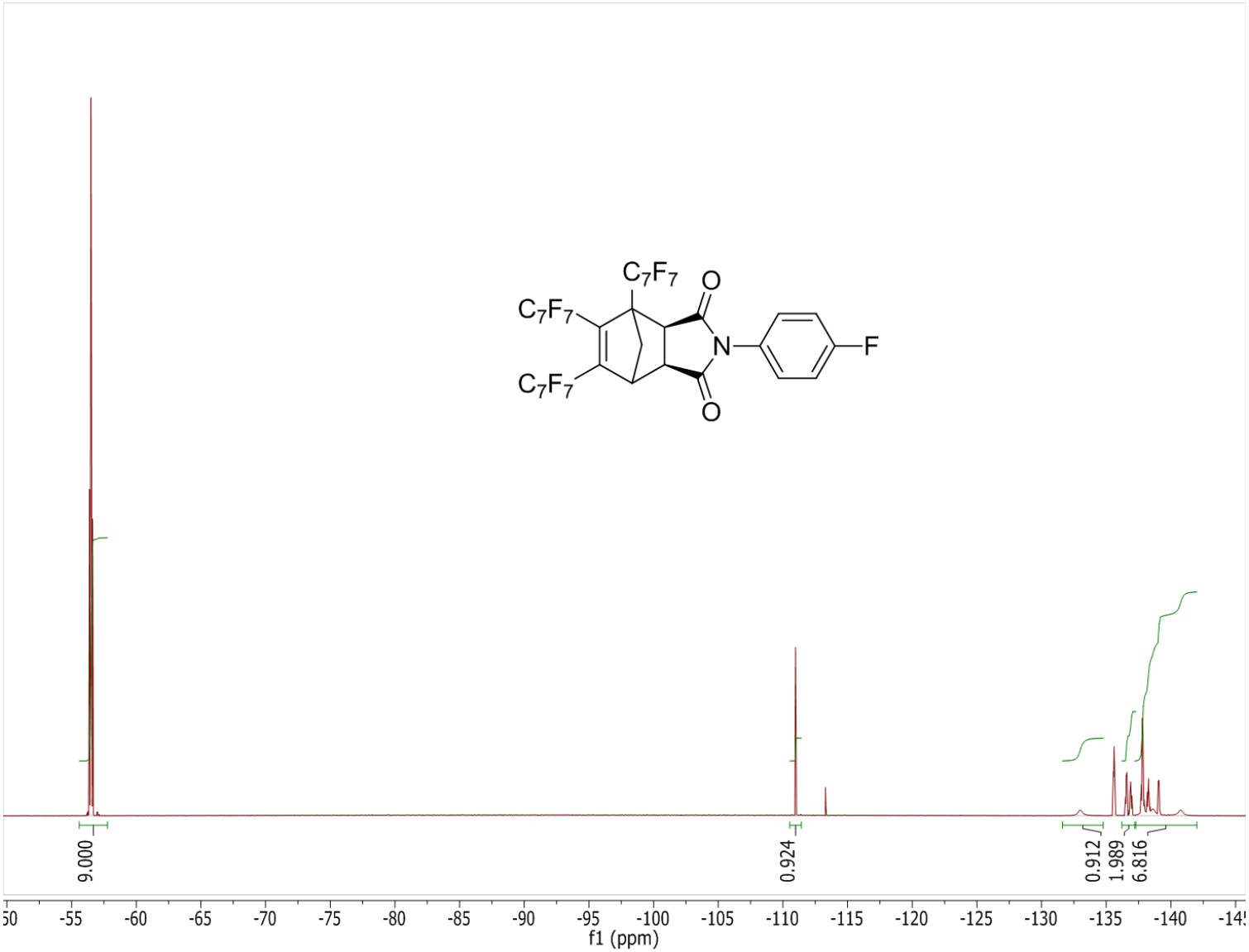

Figure C8. ^{19}F (376 MHz, $CDCl_3$) NMR spectrum of **6b**.

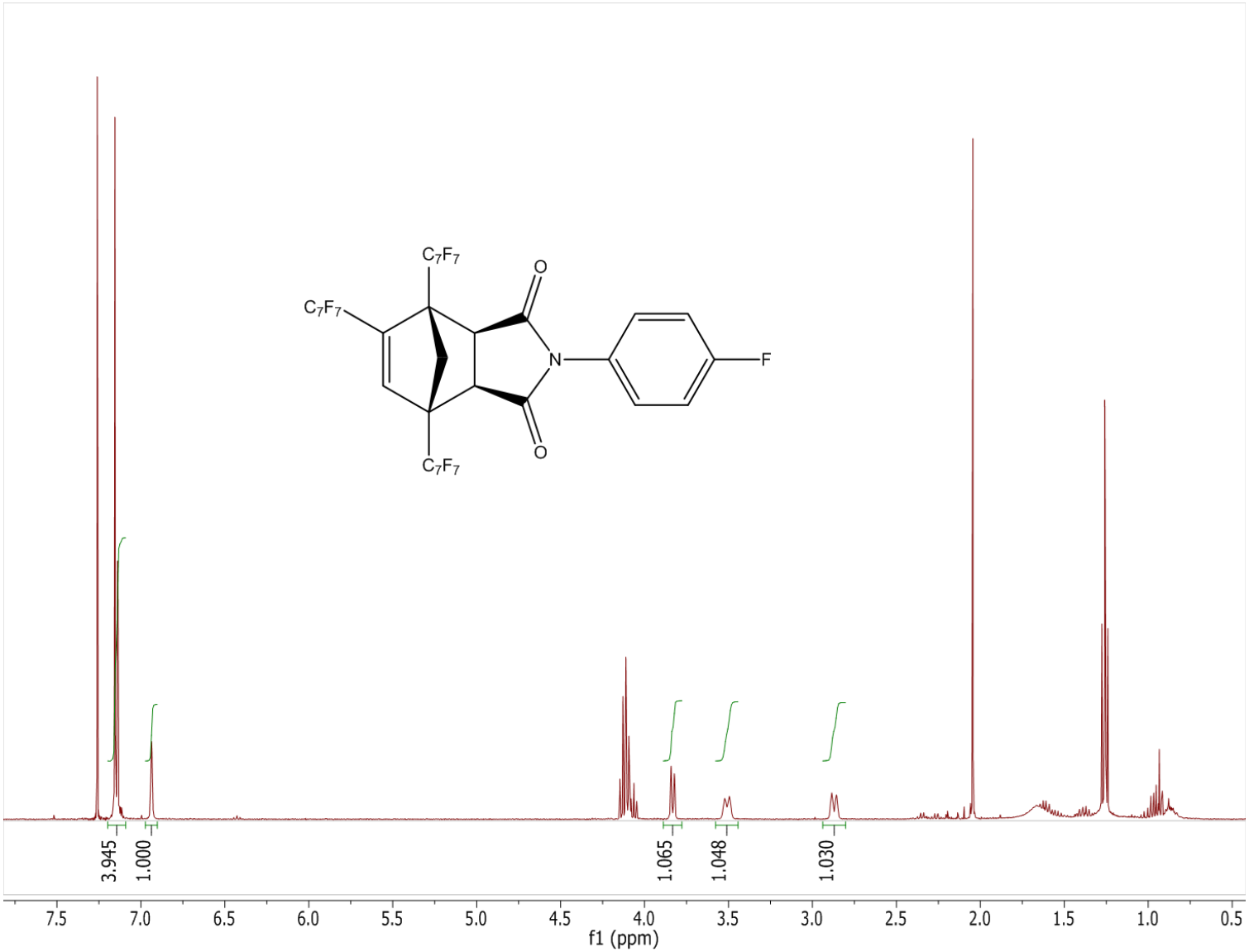

Figure C9. ^{1}H (400 MHz, $CDCl_3$) NMR spectrum of **5b**.

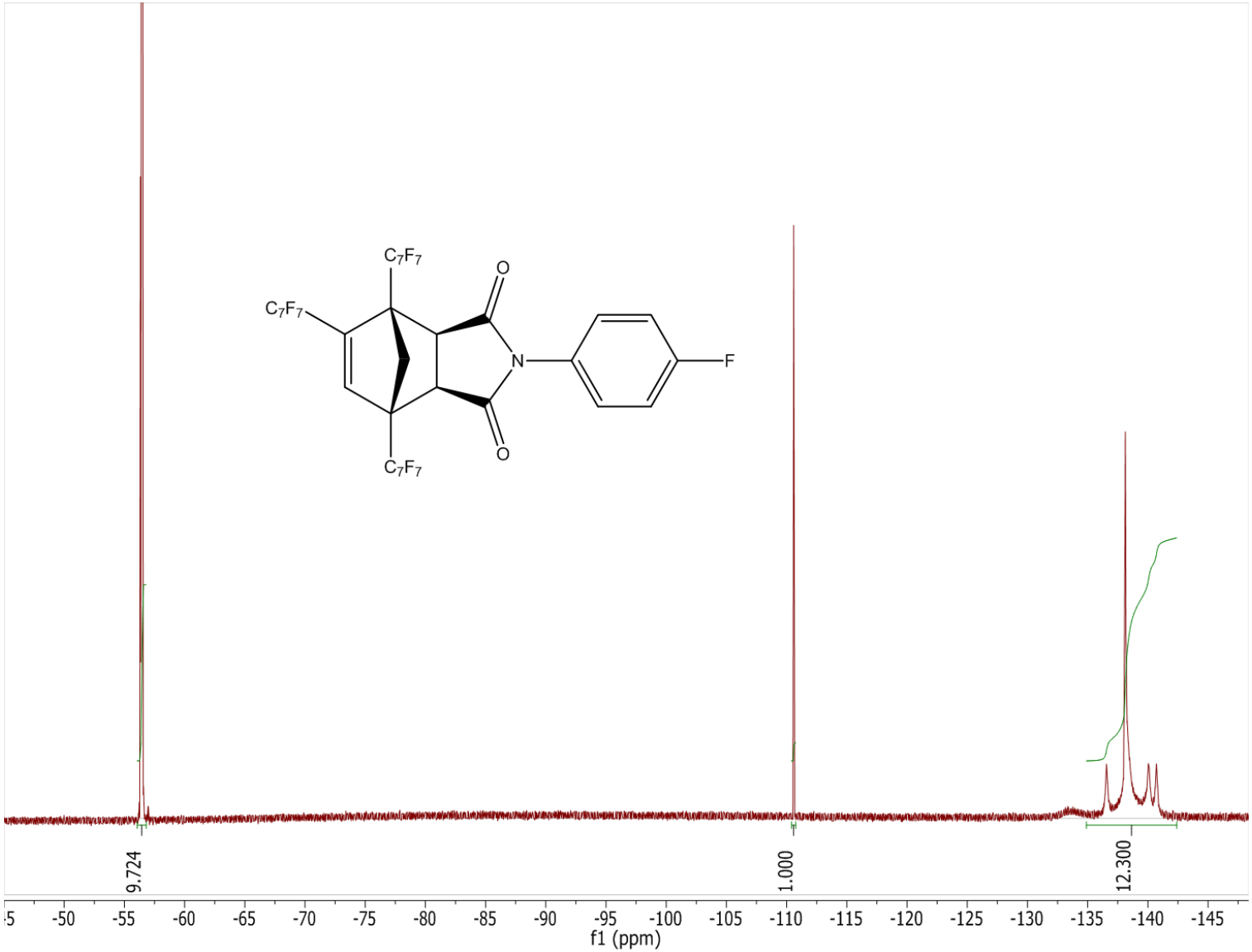

Figure C11. ^{19}F (376 MHz, $CDCl_3$) NMR spectrum of **5b**.

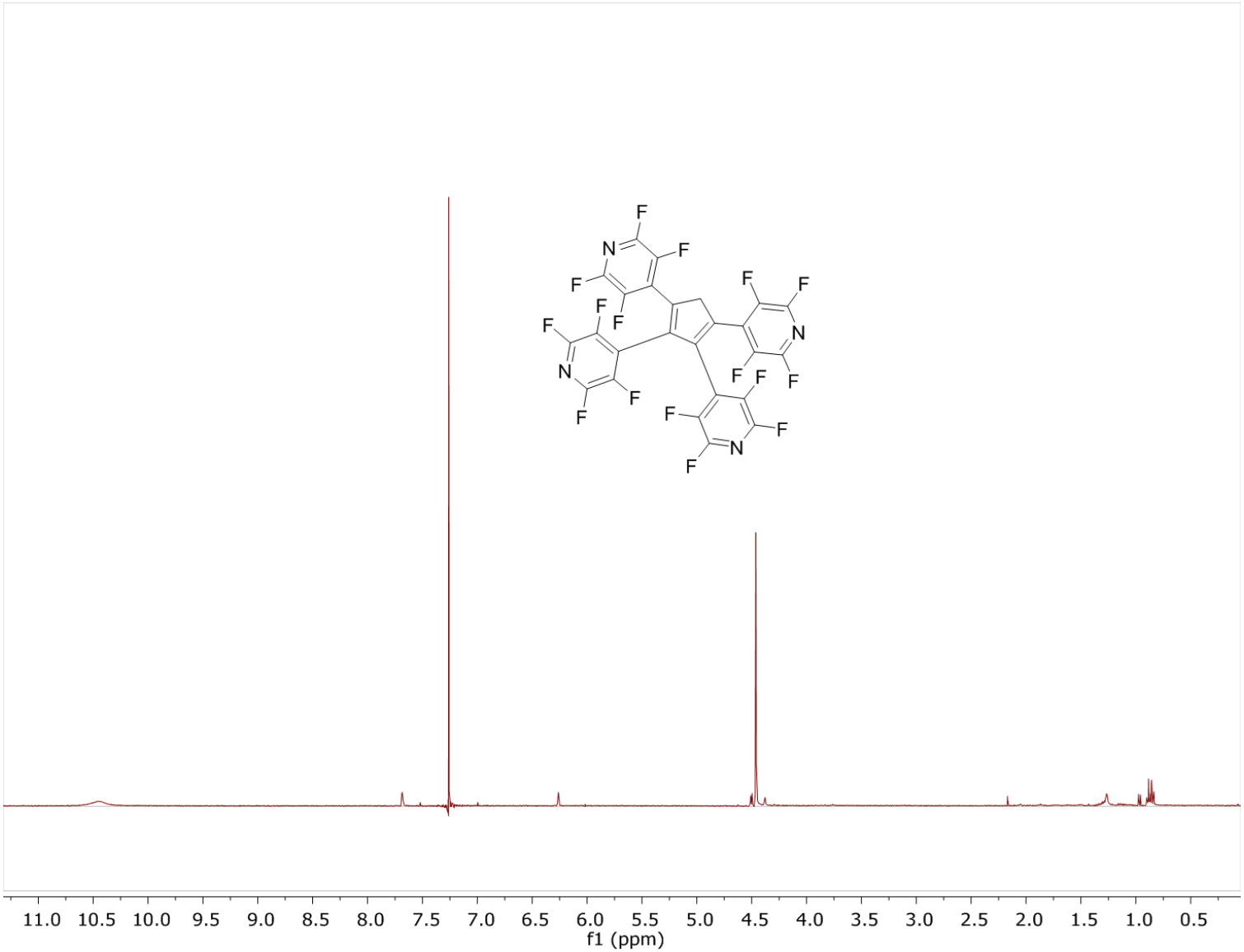

Figure C12. ^{1}H (400 MHz, $CDCl_3$) NMR spectrum of **7**.

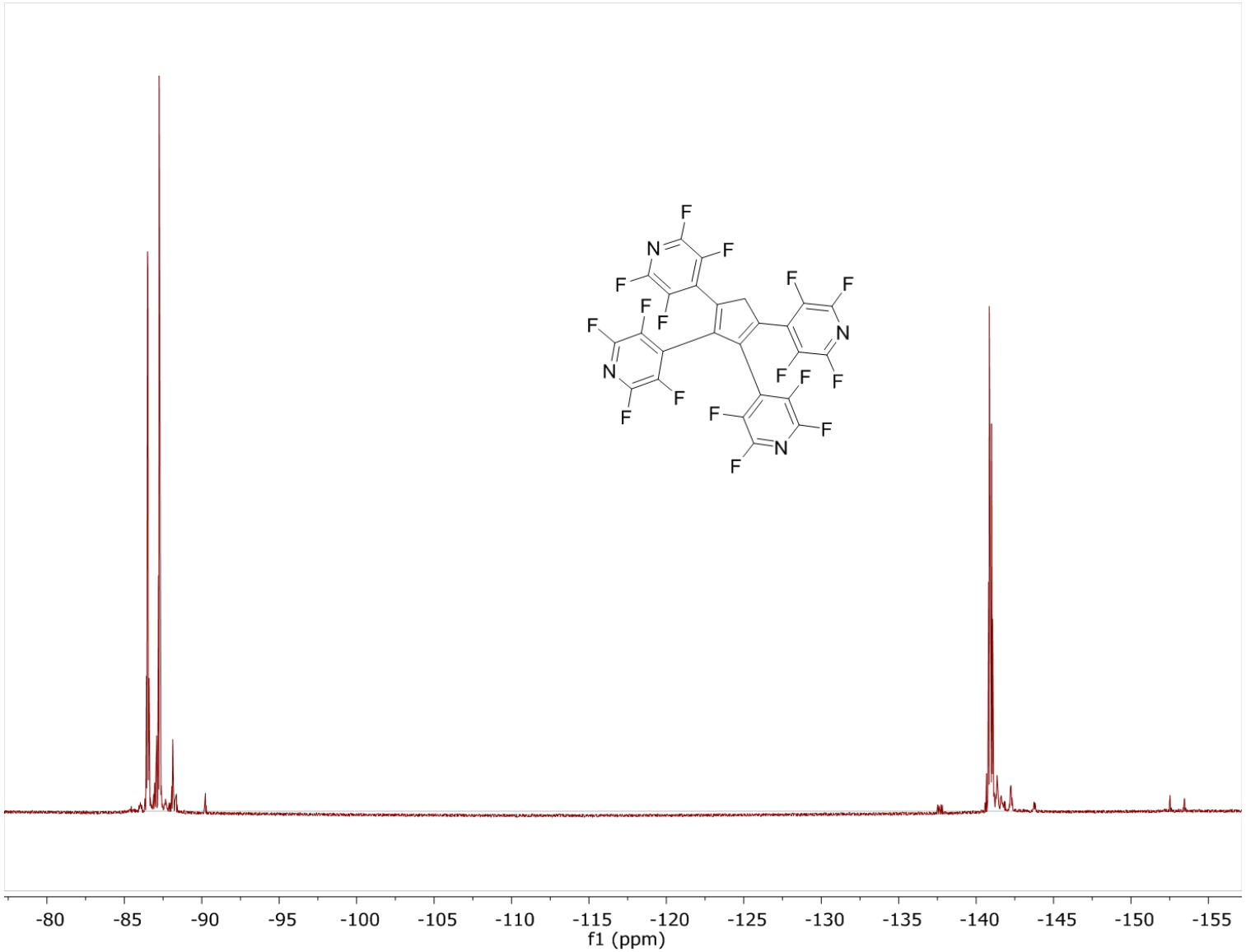

Figure C13. ^{19}F (376 MHz, $CDCl_3$) NMR spectrum of **7**.

Crystal Structures

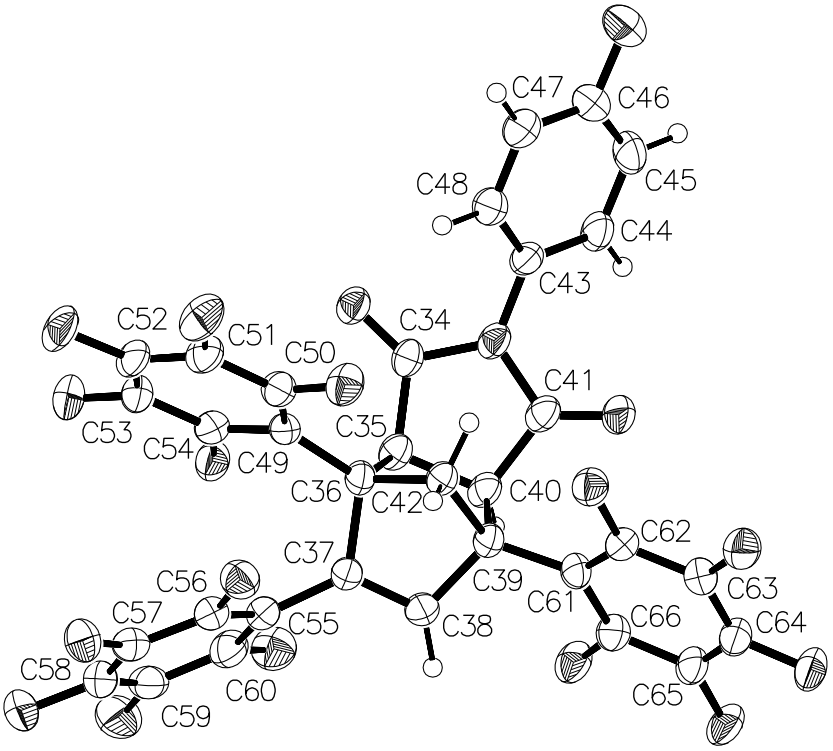

Figure C14. Ellipsoid plot (50% probability) of the molecular structure of crystalline adduct **5a** showing *exo* stereochemistry and attachment of a C_6F_5 group at the 2 carbon (C=C double bond) of the norbornene and the C_6F_5 groups at the 1 and 3-carbons (bridgehead) of the norbornene. Hydrogen and Fluorine atoms are numbered according to the carbon atoms to which they are attached.

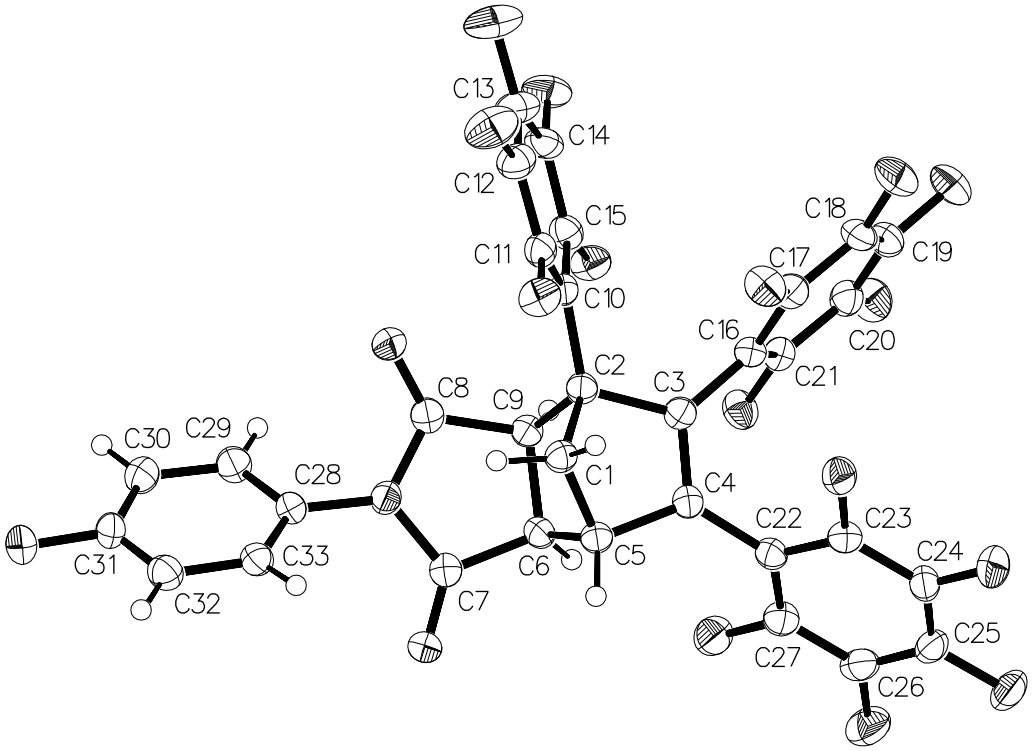

Figure C15. Ellipsoid plot (50% probability) of the molecular structure of crystalline adduct **6a** showing *exo* stereochemistry and attachment of C_6F_5 groups at the 2 and 3 carbons (C=C double bond) of the norbornene and the C_6F_5 groups at the 1-carbon (bridgehead) of the norbornene. Hydrogen and Fluorine atoms are numbered according to the carbon atoms to which they are attached.

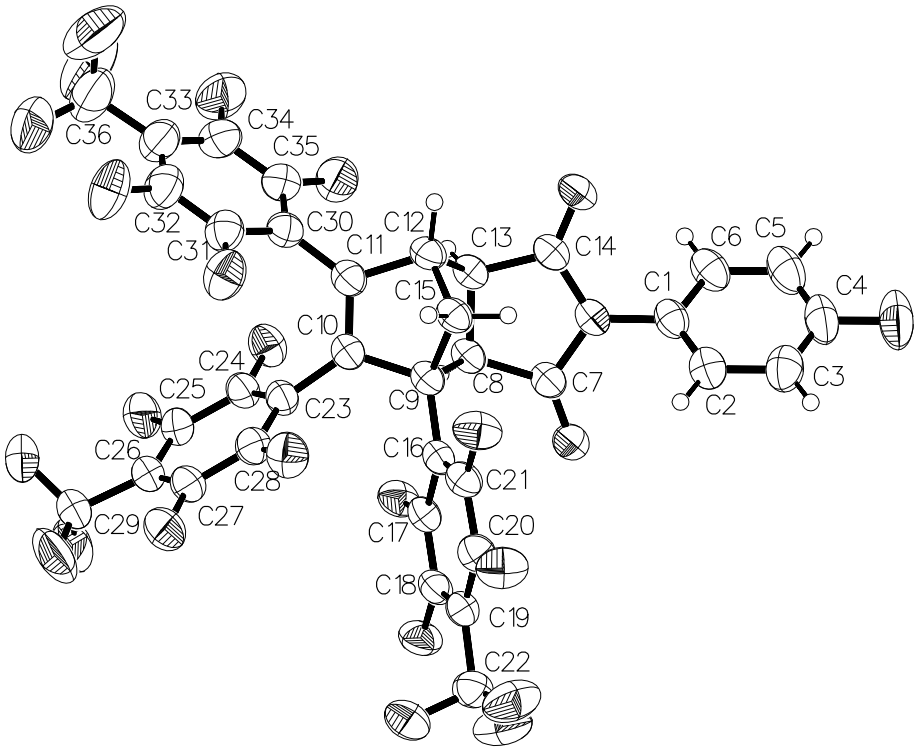

Figure C16. Ellipsoid plot (50% probability) of the molecular structure of crystalline adduct **6b** showing *exo* stereochemistry and attachment of C_7F_7 groups at the 2 and 3 carbons (C=C double bond) of the norbornene and the C_7F_7 groups at the 1-carbon (bridgehead) of the norbornene. Hydrogen and Fluorine atoms are numbered according to the carbon atoms to which they are attached.

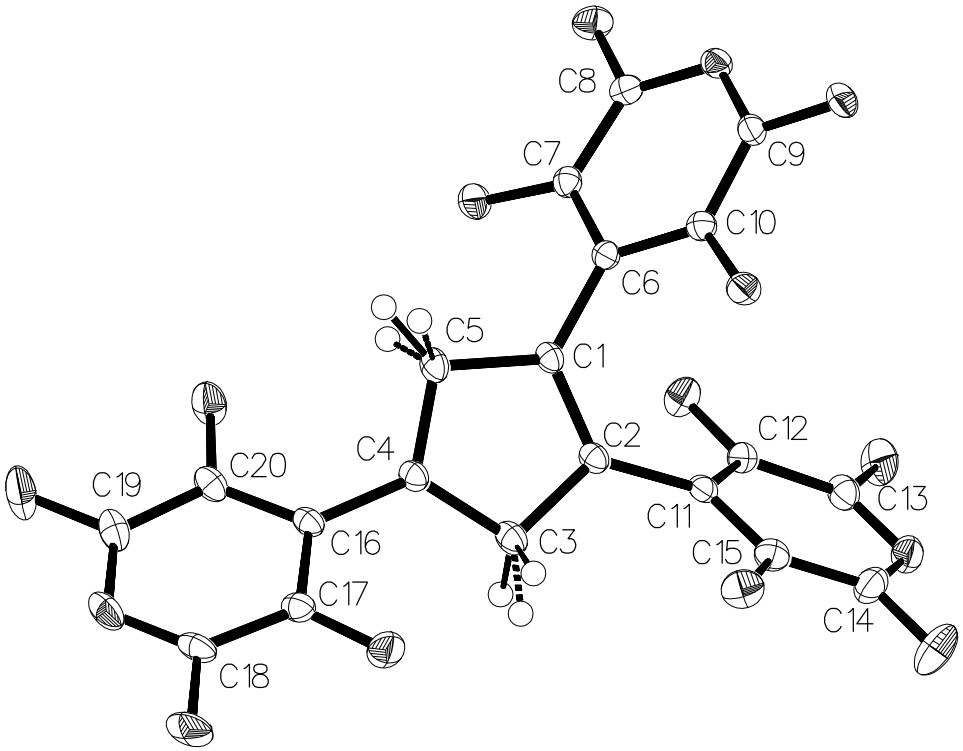

Figure C17. Ellipsoid plot (50% probability) of the molecular structure of crystalline diene **1c**. Fluorine atoms are numbered according to the carbon atoms to which they are attached. Selected bond distances (Å): C1−C2, 1.355; C2−C3, 1.485; C3−C4, 1.439; C4−C5, 1.417; C5−C1, 1.477. Selected torsional angles (deg): C1−C2−C11−C12, 52; C2−C1−C6−C10, 50; C3−C4−C6−C17, 38. **Inset**: Diagram showing positional disorder of CH_2 and CH carbons (C3 and C5).

Crystallographic Data Table

Compound	1c	6a	5a	6b
Empirical formula	$C_{20}H_3F_{12}N_3$	$2(C_{33}H_9F_{16}NO_2) \bullet CHCl_3$	$C_{33}H_9F_{16}NO_2$	$C_{36}H_9F_{22}NO_2$
Formula weight	513.25	1630.19	755.41	905.44
Temperature (K)	100.00(10)	100.00(10)	100.00(14)	150.00(14)
Wavelength (Å)	0.7107	1.5418	1.5418	1.5418
Crystal system	Monoclinic	Monoclinic	Triclinic	Orthorhombic
Space group	$P12_1/n1$	$P12_11$	P – 1	*Pbca*
a (Å)	12.2640(3)	18.2372(3)	11.9739(8)	12.62363(19)
b (Å)	11.8852(2)	7.68910(12)	14.2258(10)	21.7227(3)
c (Å)	13.0387(3)	23.0737(3)	16.7965(10)	24.7331(5)
α (°)	90	90	93.8	90
β (°)	110.239(3)	110.3832(17)	91.5	90
γ (°)	90	90	99.5	90
Volume ($Å^3$)	1783.18(6)	3032.97(8)	2813.7(3)	6782.28(19)
Z	4	2	4	8
D_{calc} ($Mg\ m^{-3}$)	1.912	1.785	1.783	1.773
Absorption coefficient (mm^{-1})	0.204	2.786	1.666	1.767
F(000)	1008	1612	1496	3568
Crystal size (mm^3)	0.6694 x 0.3528 x 0.1049	0.2505 x 0.0885 x 0.0538	0.1990 x 0.0359 x 0.0290	0.317 x 0.2066 x 0.0735
θ collection range (°)	3.62 to 32.40	3.814 to 74.641	3.158 to 75.239	3.574 to 75.386
Reflections collected	33453	36758	18718	70749
Independent reflections	6054 [R(int) = 0.0385]	12317 [R(int) = 0.0376]	18718 [R(int) = ?]	6931 [R(int) = 0.0467]
Completeness to theta	99.8 %	θ = 67.684°, 99.78 %	θ = 70.000°, 99.9%	θ = 67.684°, 99.9 %
Absorption correction	Gaussian	Gaussian	Semi-empirical from equivalents	Gaussian
Max. and min. transmission	1.399 and 0.916	1.067 and 0.706	1.0000 and 0.88562	0.886 and 0.731
Refinement method	Full-matrix least-squares on F^2	Full-matrix least-squares on F^2	Full-matrix least-squares on F^2	Full-matrix least-squares on F^2
Data / restraints / parameters	6054 / 0 / 317	12317 / 1 / 991	18718/0/398	6931 / 0 / 550
GoF on F^2	1.026	1.026	1.020	1.061
Final R indices [I>2sigma(I)]	R1 = 0.0402, wR2 = 0.0908	R1 = 0.0407, wR2 = 0.0973	R1 = 0.0751, wR2 = 0.1973	R1 = 0.0682, wR2 = 0.1978
R indices (all data)	R1 = 0.0566, wR2 = 0.1001	R1 = 0.0504, wR2 = 0.1054	R1 = 0.1180, wR2 =0.2339	R1 = 0.0779, wR2 = 0.2134
Peak and hole ($e\ Å^{-3}$)	0.797 and -0.358	0.471 and -0.275	0.415 and -0.438	1.872 and -0.642

Initial Rate Plots

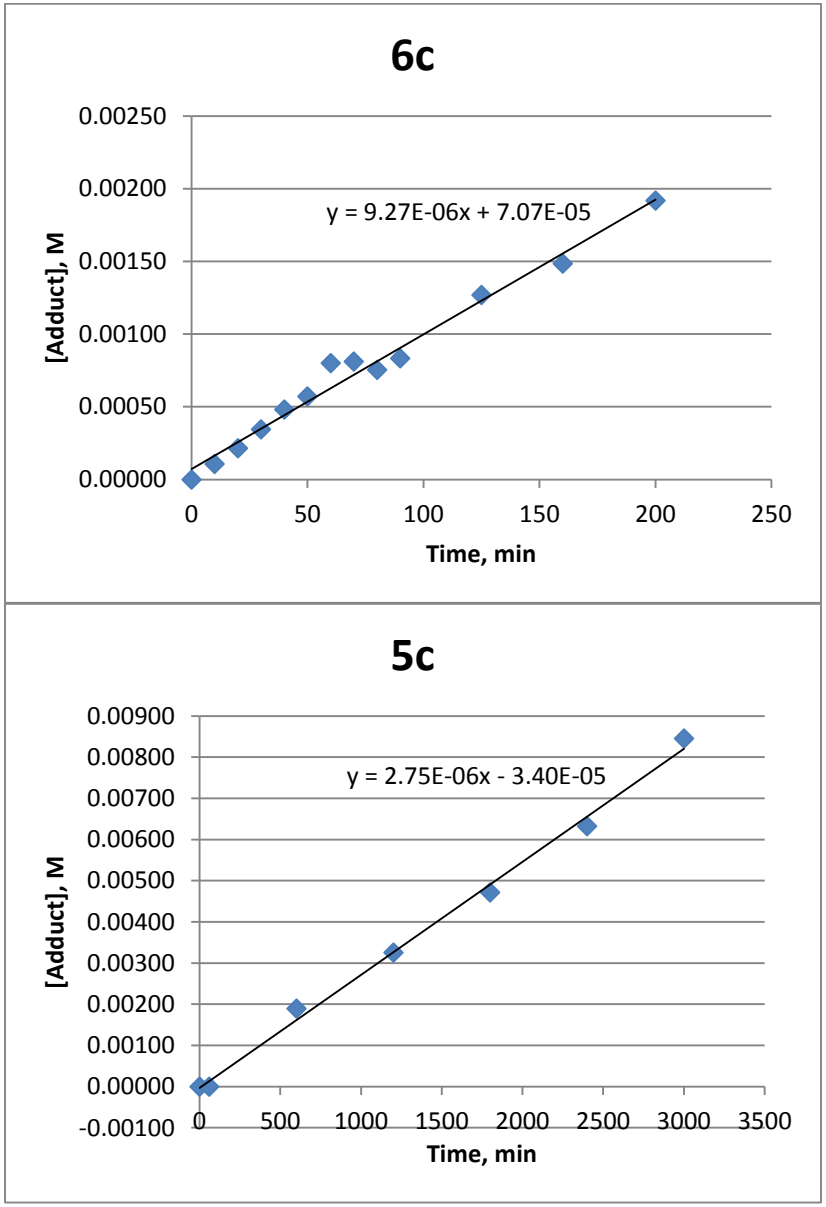

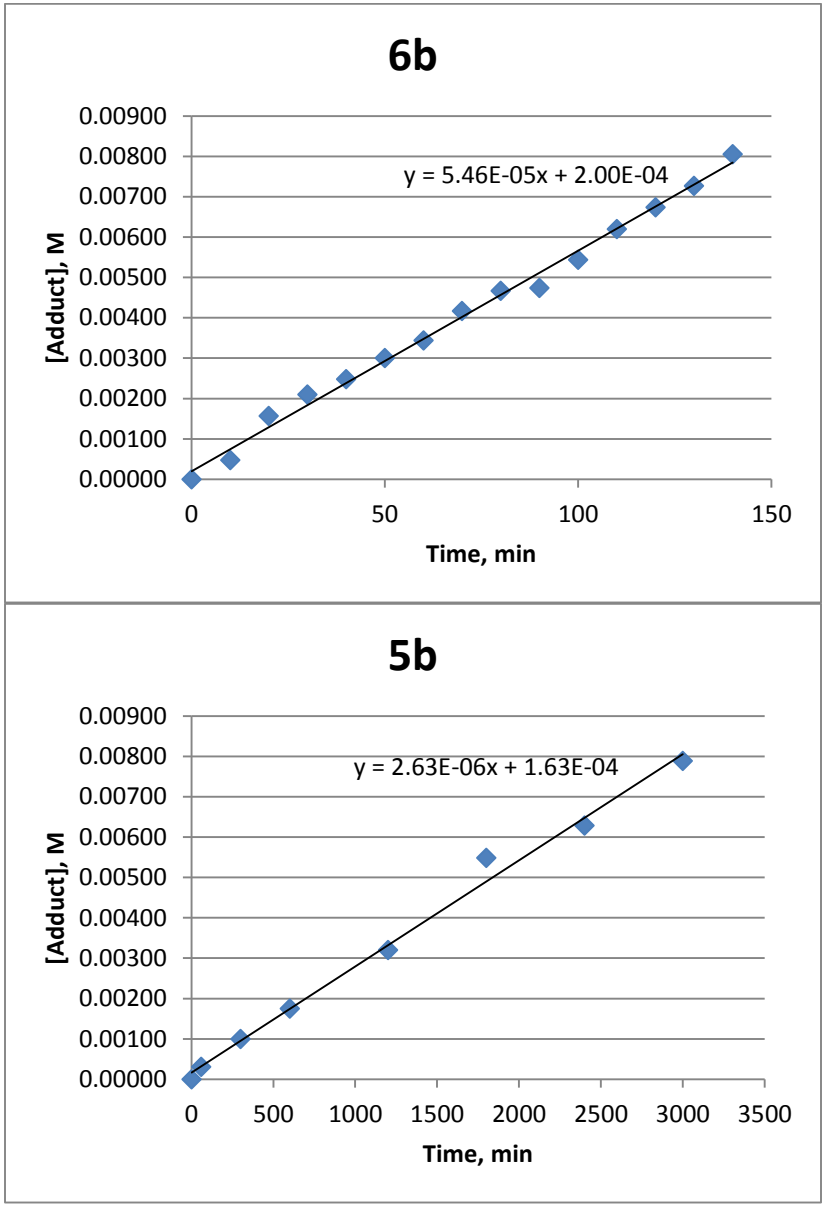

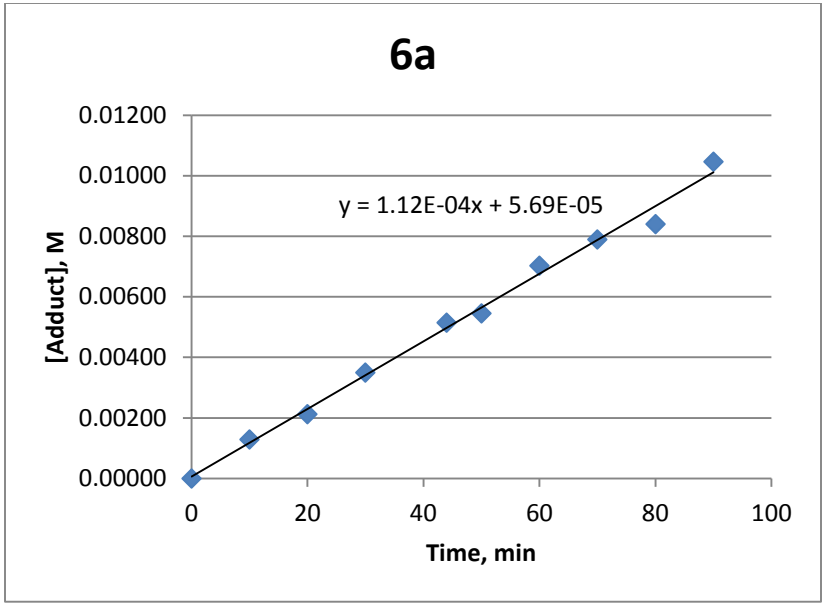
6a
y = 1.12E-04x + 5.69E-05
[Adduct], M
Time, min
0.01200
0.01000
0.00800
0.00600
0.00400
0.00200
0.00000
0
20
40
60
80
100

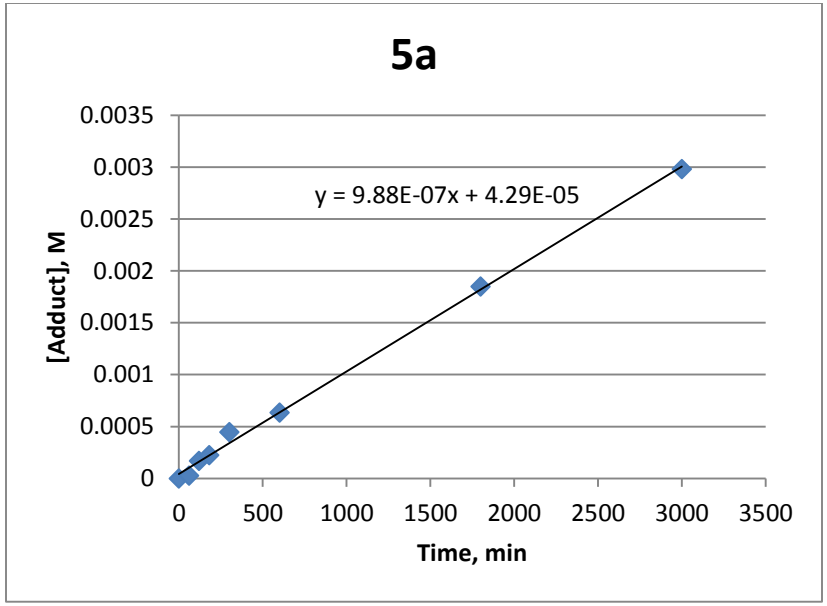
5a
y = 9.88E-07x + 4.29E-05
[Adduct], M
Time, min
0.0035
0.003
0.0025
0.002
0.0015
0.001
0.0005
0
0
500
1000
1500
2000
2500
3000
3500

Appendix D Supporting information for: Linear Polymers Based on the Diels-Alder reaction of bis(cyclopentadienes) and bis(maleimides)

Jeremy B. Stegall, Sanghamitra Sen, Carla Slebodnick, and Paul A. Deck*

Department of Chemistry, Virginia Tech, Blacksburg, VA 24061

Relationship of X_n, K and [M]

A general coupling reaction (such as the DA reaction) is shown in eq 1.

$$M1 + M2 = P \quad [1]$$

Next we can establish an equilibrium constant (eq 2) with the common assumption of unit activity coefficients.

$$K = \frac{[P]}{[M_1][M_2]} \quad [2]$$

If the two reactant concentrations are equal (eq 3), then the equilibrium constant simplifies in form *(eq 4).*

$$[M_1] = [M_2] = [M] \quad [3]$$

$$K = \frac{[P]}{[M]^2} \quad [4]$$

Next the total conversion (reaction progress, *p*) is defined as the ratio of product and *initial* reactant concentration (eq 5).

$$p = \frac{[P]}{[M]_o} \quad [5]$$

Both reactant and product concentrations can now be expressed in terms of the conversion (eq 6-7).

$$[M] = [M]_o 1 - p) \quad [6]$$

$$[P] = [M_o]p \quad [7]$$

Substitution gives the equilibrium constant in terms of M_o and p (eq 8).

$$K = \frac{[M]_o p}{[M]_o{}^2 (1-p)^2} \quad [8]$$

In the Carothers Equation the degree of polymerization is also expressed in terms of the conversion (eq 9).

$$\bar{X}_n = \frac{1}{1-p} \quad [9]$$

Substituting eq 9 into eq 8, simplifying, and rearranging gives us a relationship that includes our experimentally tunable quantities (eq 10).

$$[M]_o K = p \bar{X}_n{}^2 \quad [10]$$

Assuming high conversion (p ~ 1) gives the final relationship (eq 11).

$$\bar{X}_n = \sqrt{[M]_o K} \quad [11]$$

We find that the degree of polymerization depends on both the overall reaction concentration and the binding constant, but not in a linear fashion. To double the degree of polymerization, either the binding constant or the reaction concentration must be increased by a factor of four.

NMR Spectra

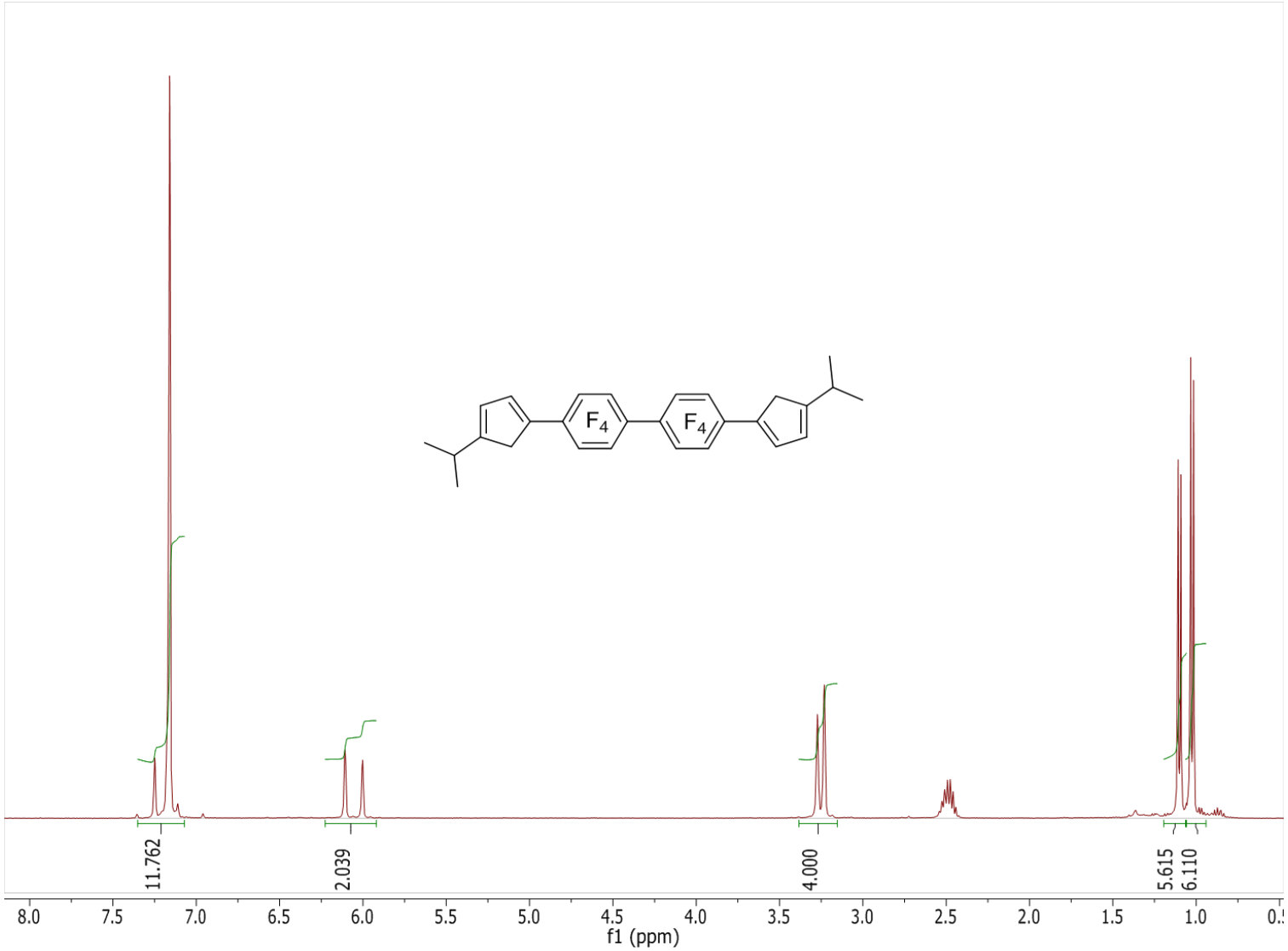

Figure D1. ^{1}H NMR spectrum of **1** in $CDCl_3$

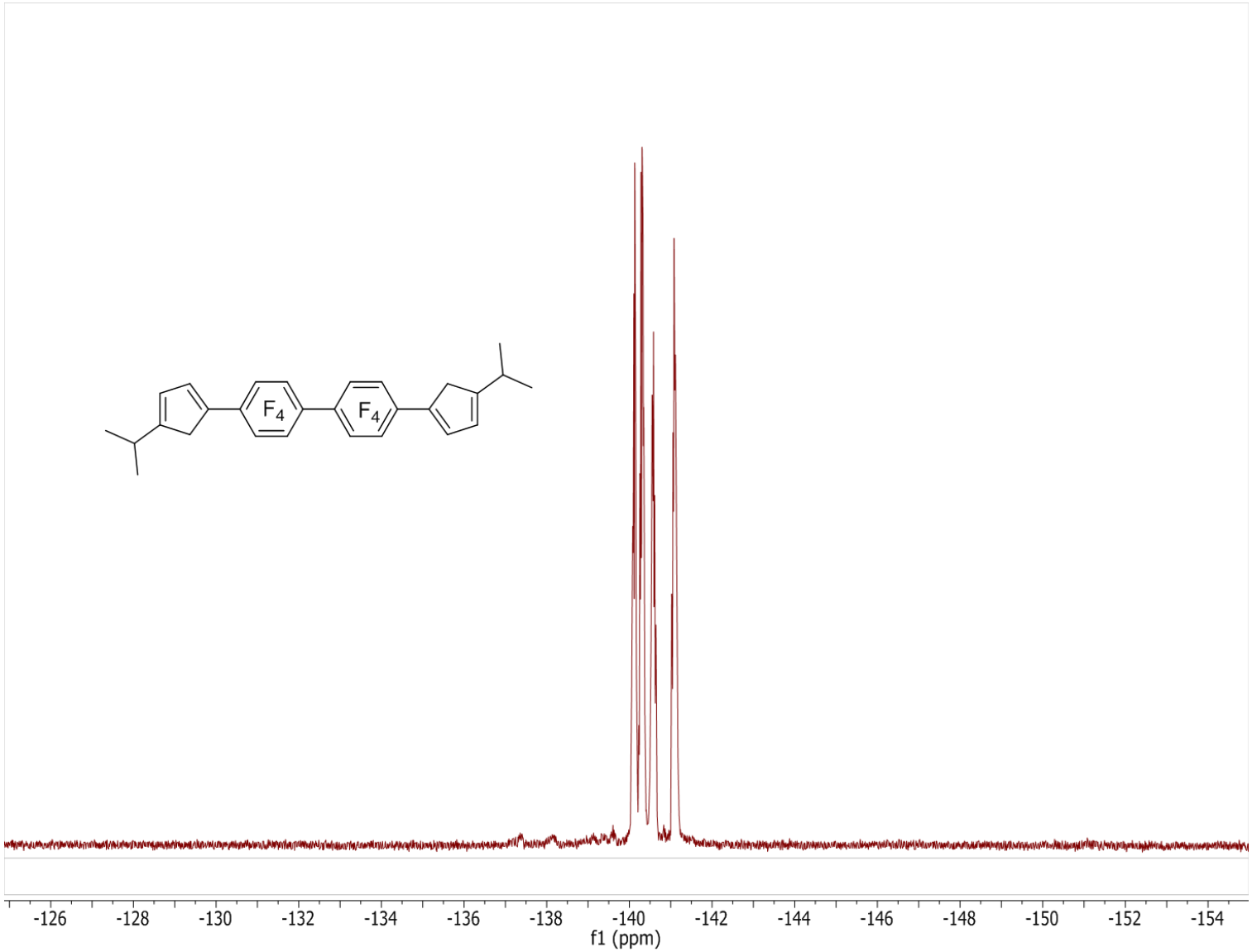

Figure D2. ^{19}F NMR spectrum of **1** in $CDCl_3$

Crystallographic Information

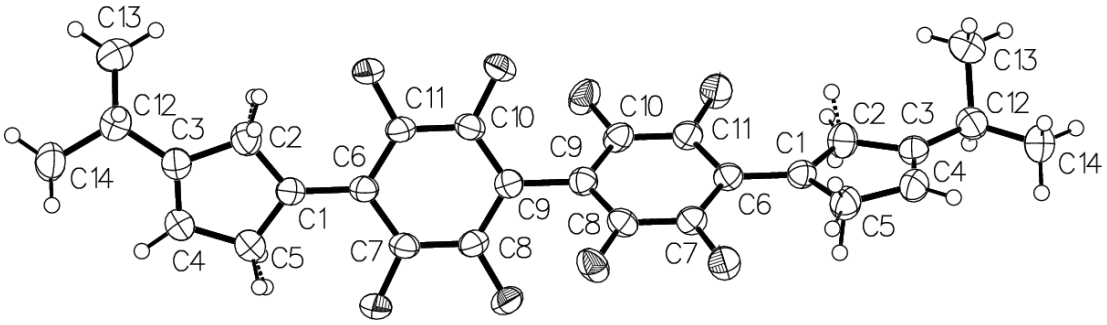

Figure D3. Ellipsoid plot (50% probability) of the molecular structure of crystalline adduct **2**. Fluorine and hydrogen atoms are numbered the same as the carbon atoms to which they are attached.

Crystallographic Data Table

Compound	2
Empirical formula	$C_{28}H_{22}F_8$
Formula weight	510.46
Crystal system	Monoclinic
Space group	C 12/c 1
a (Å)	24.9384(8)
b (Å)	6.40843(13)
c (Å)	16.3839(6)
α (°)	90
β (°)	118.508(5)
γ (°)	90
Volume ($Å^3$)	2300.94(12)
Z	4
Density (calc) (Mg/m^3)	1.474
Absorption coefficient (mm^{-1})	0.130
F(000)	1048
Temp (K)	199.95(10)
Crystal size (mm^3)	0.3931 x 0.206 x 0.0825
Theta range for data collection	3.31 to 30.51°
Index ranges	-35<=h<=35, -9<=k<=9, -23<=l<=23
Reflections collected	20236
Independent reflections	3508 [R(int) = 0.0289]
Completeness to theta = 30.51°	99.90%
Absorption correction	Semi-empirical from equivalents
Max. and min. transmission	1.00000 and 0.90624
Refinement method	Full-matrix least-squares on F2
Data / restraints / parameters	3508 / 0 / 168
Goodness-of-fit on F^2	1.067
Final R indices [I>2sigma(I)]	R1 = 0.0491, wR2 = 0.1257
R indices (all data)	R1 = 0.0671, wR2 = 0.1367
Largest diff. peak and hole ($e/Å^3$)	0.319 and -0.185 e.Å-3

SEC traces

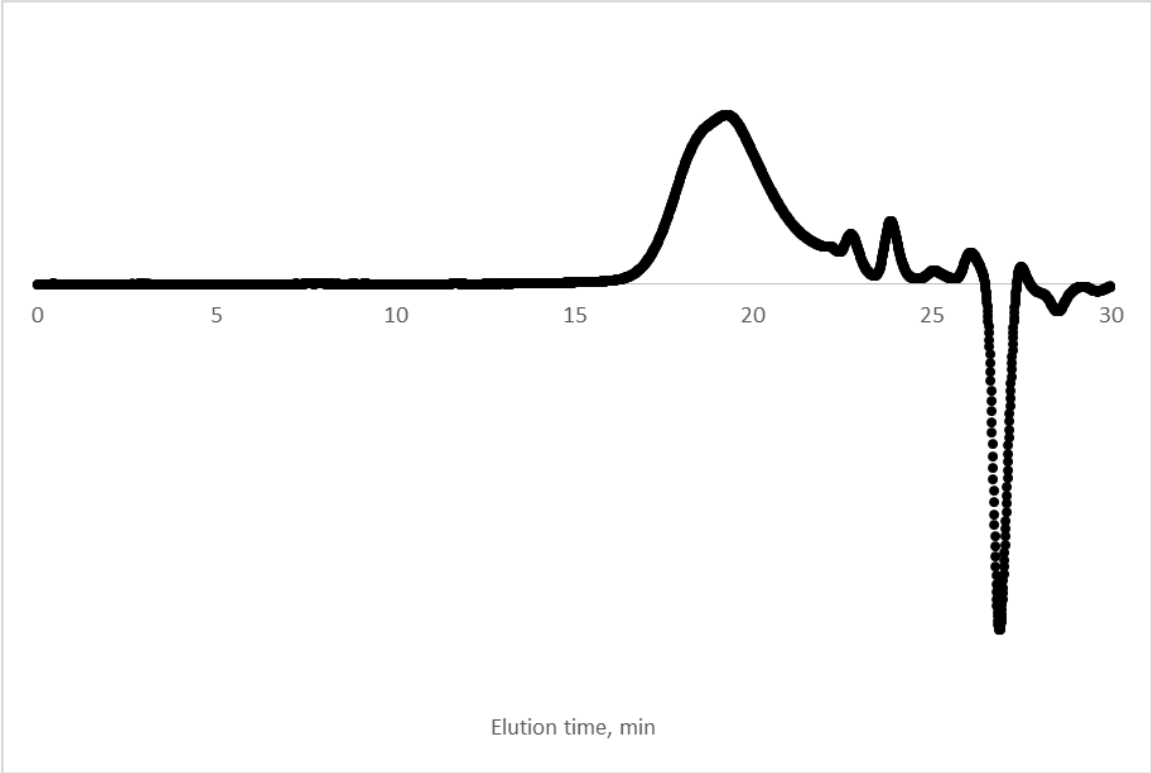

1-183-3 Polymer **1**, Refractive index

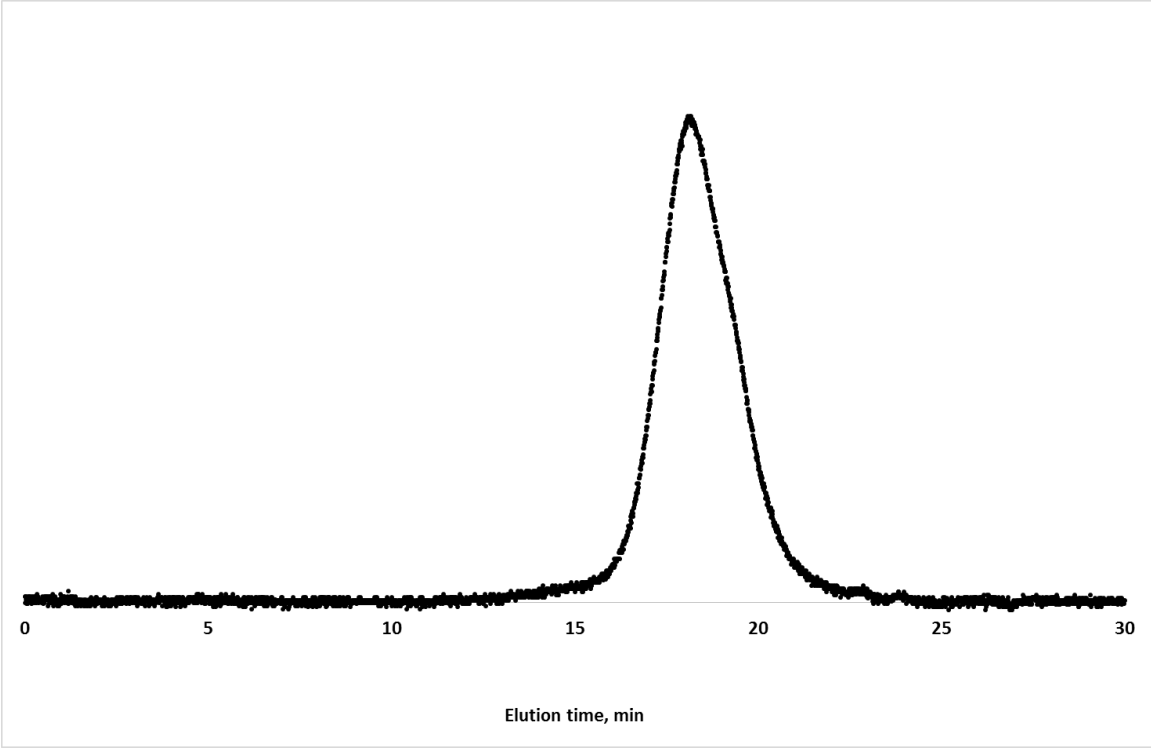

1-183-3 Polymer **1**, Light scattering

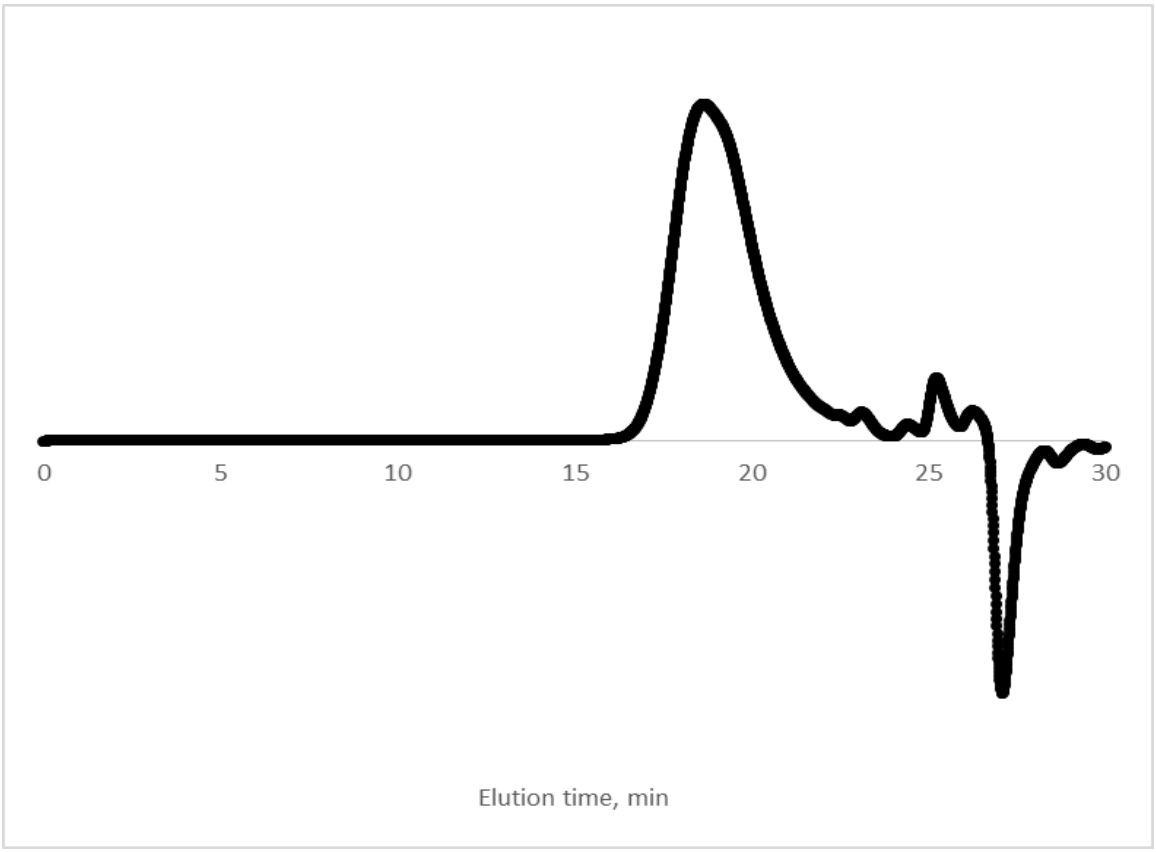

2-42-2 Polymer **2**, Refractive index

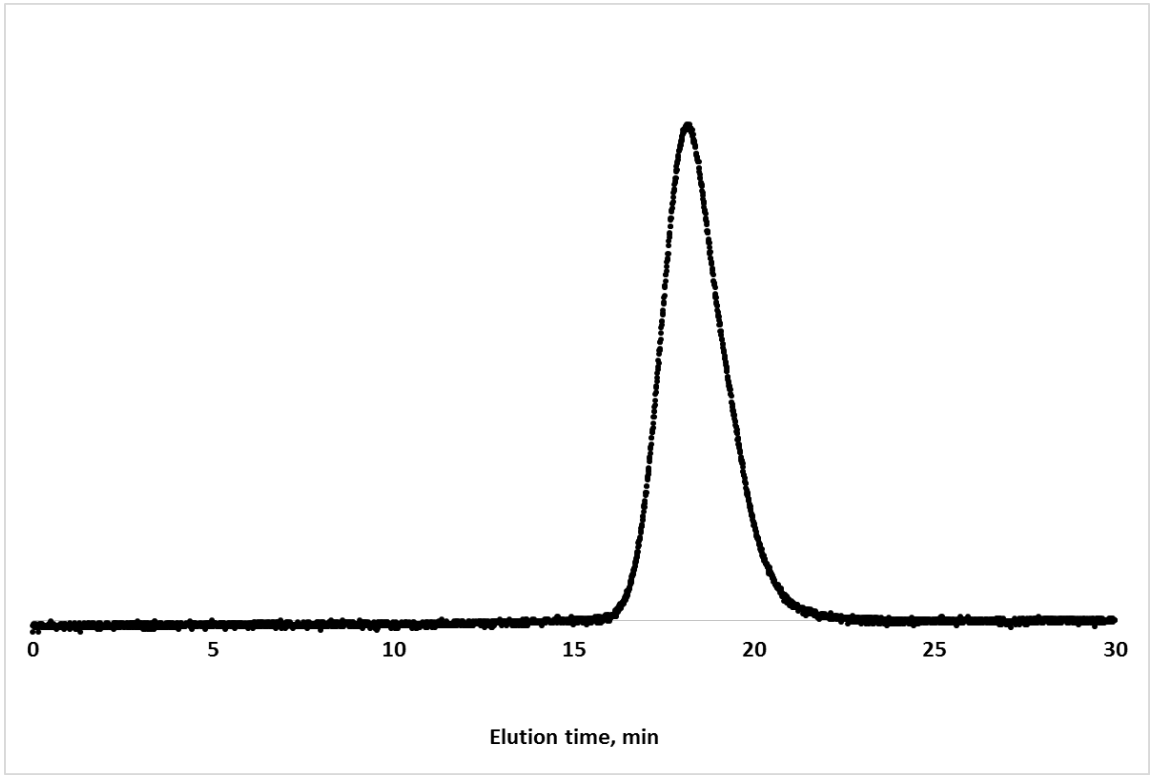

2-42-2 Polymer **2**, Light scattering

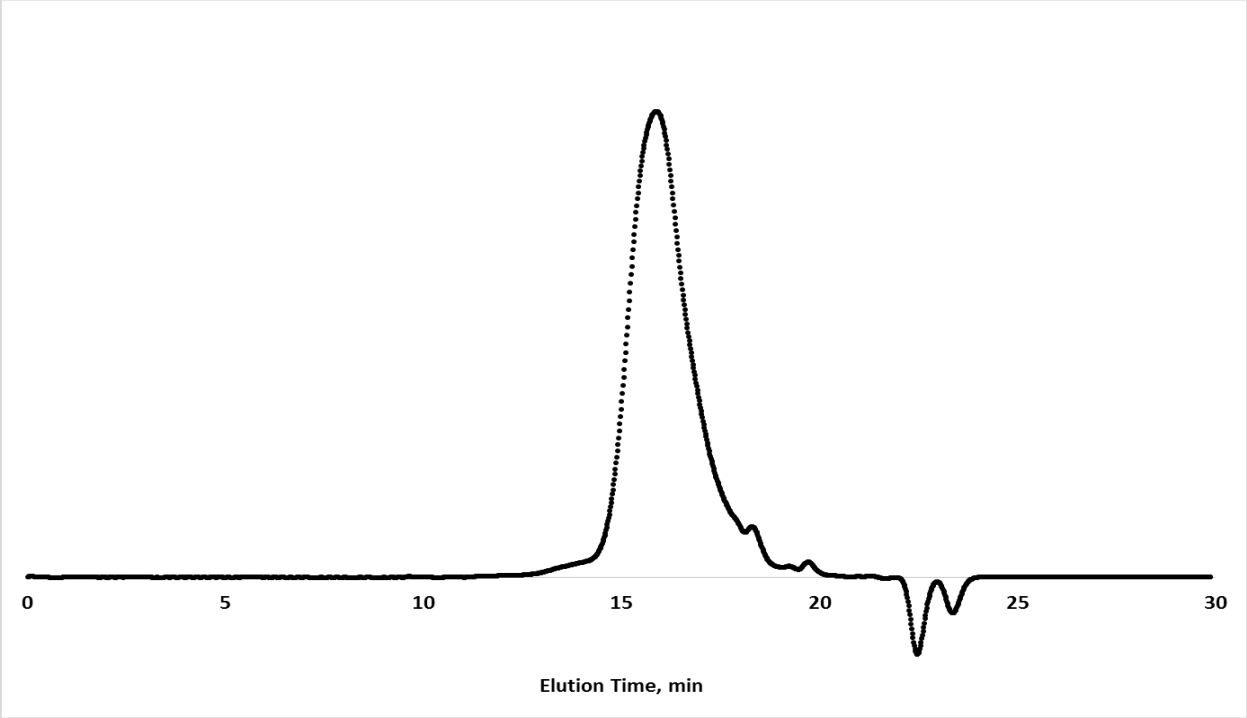

2-73-2 Polymer **3,** Refractive index

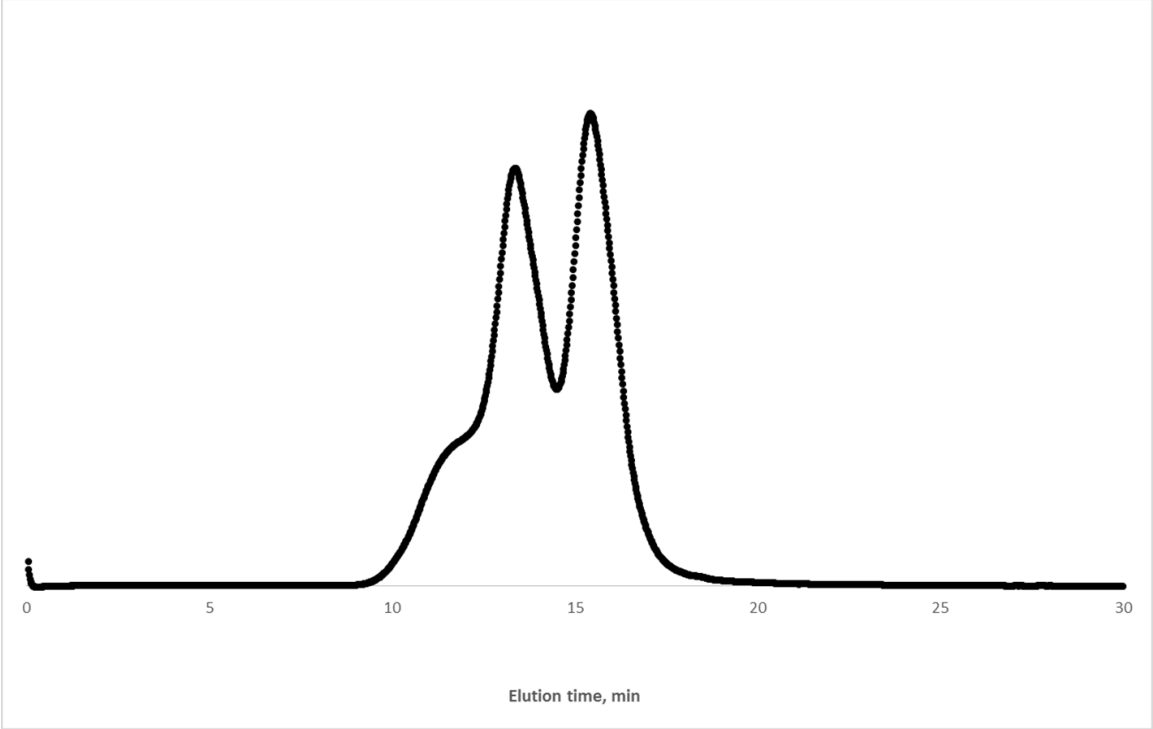

2-73-2 Polymer **3**, Light scattering

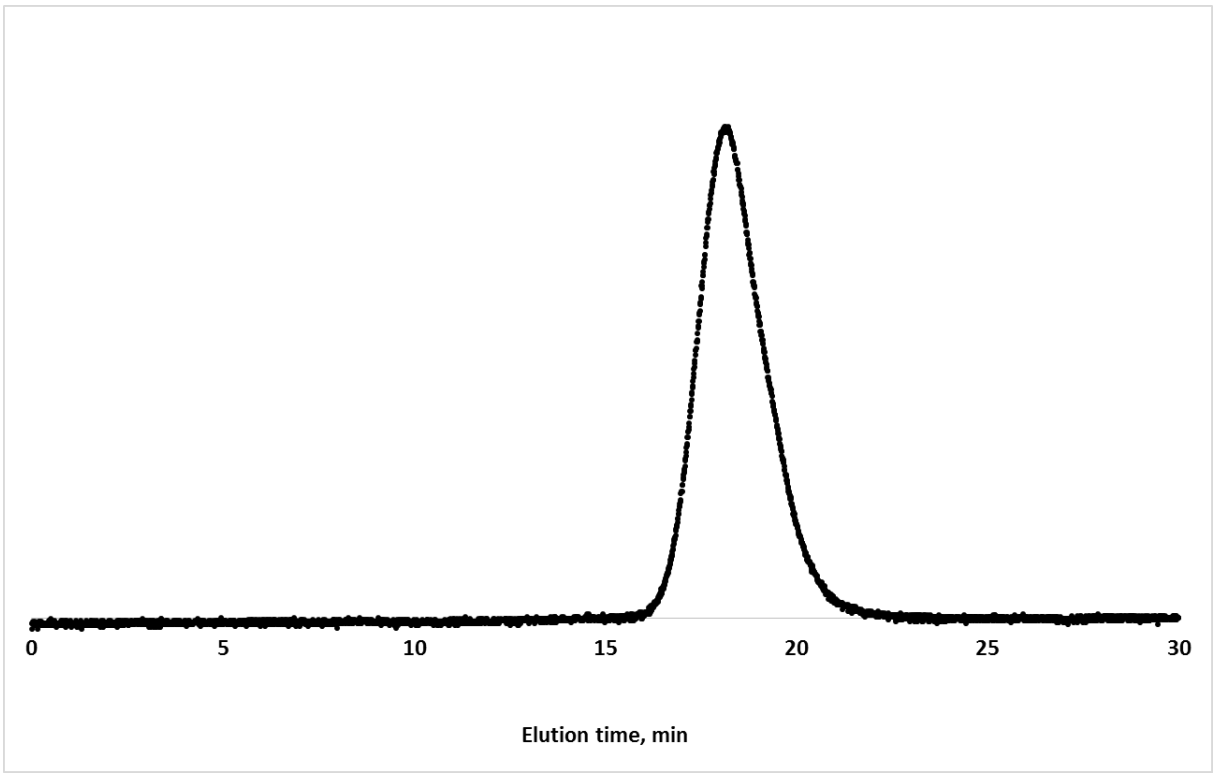

2-43-2 Polymer **4**, Refractive index

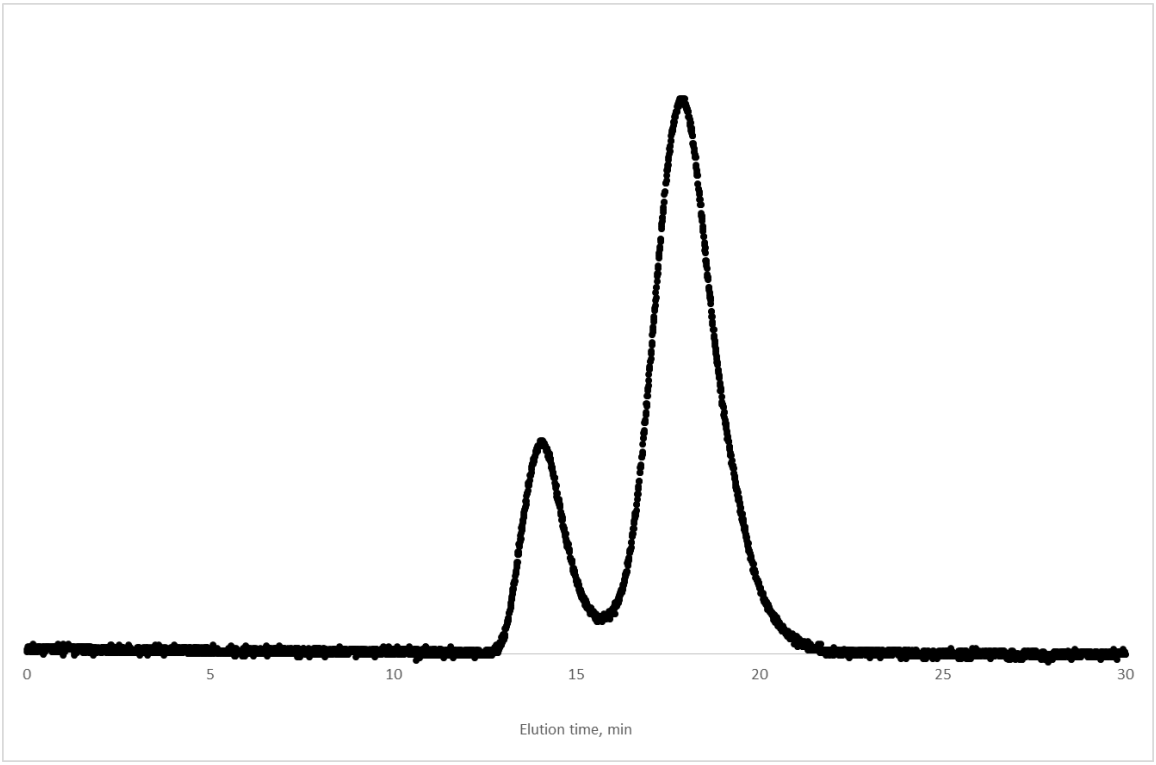

2-43-2 Polymer **4**, Light scattering

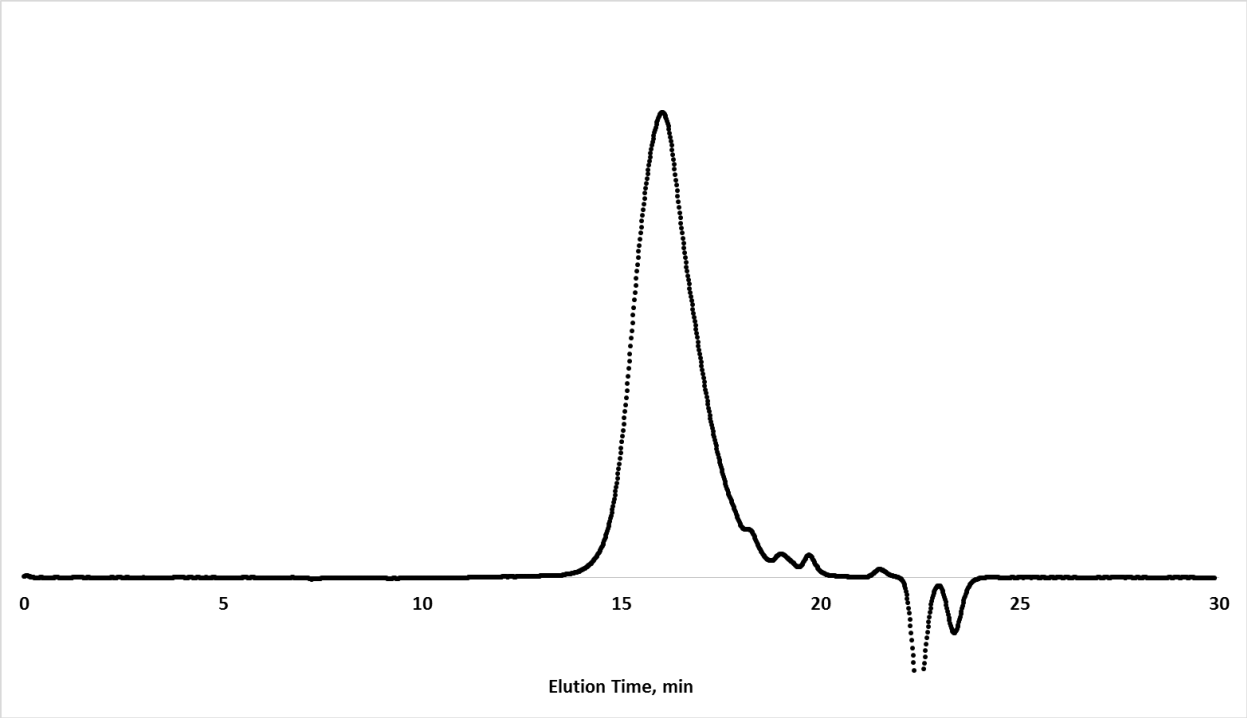

2-142A1 Polymer **5**, Refractive index

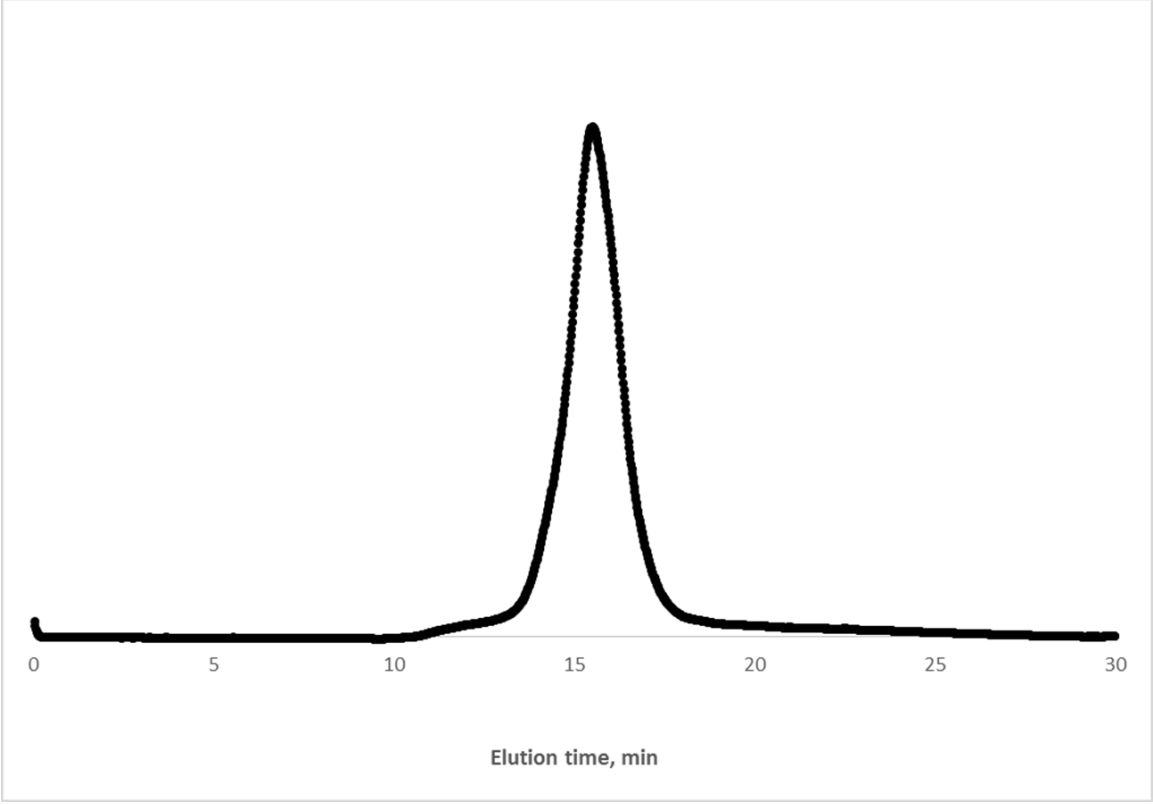

Polymer **5**, Light scattering

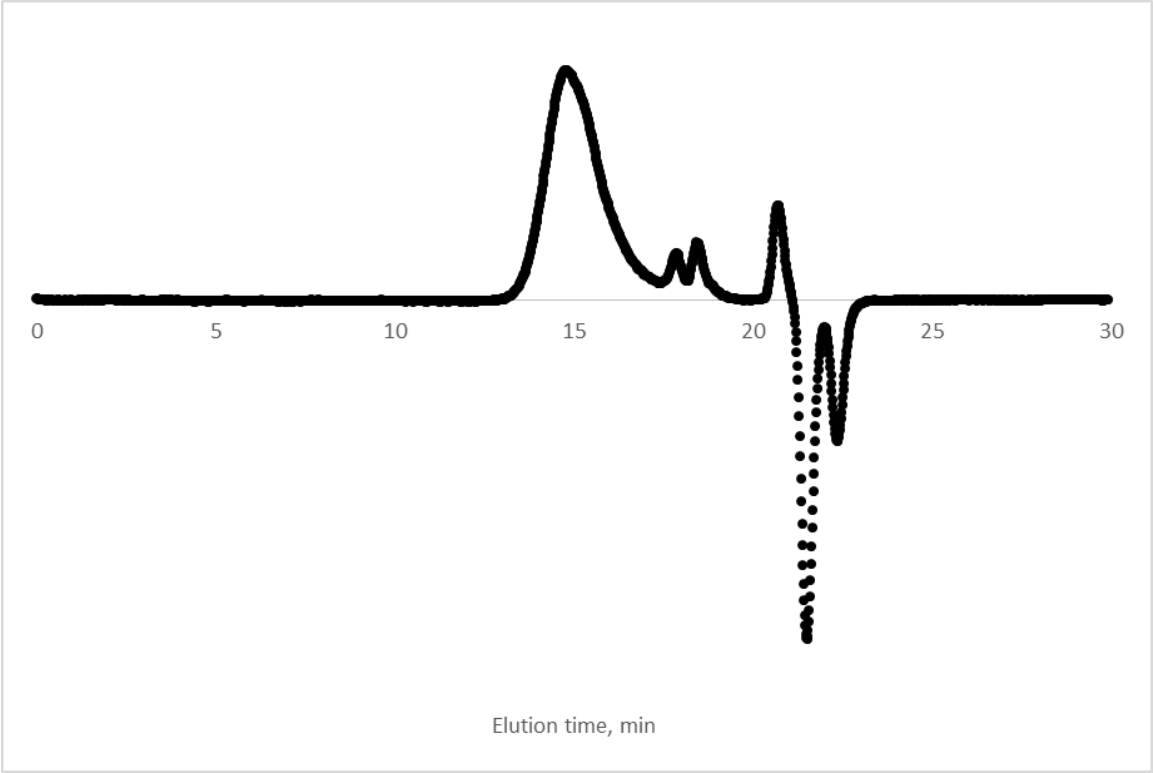

2-49-2A Polymer **6**, Refractive index

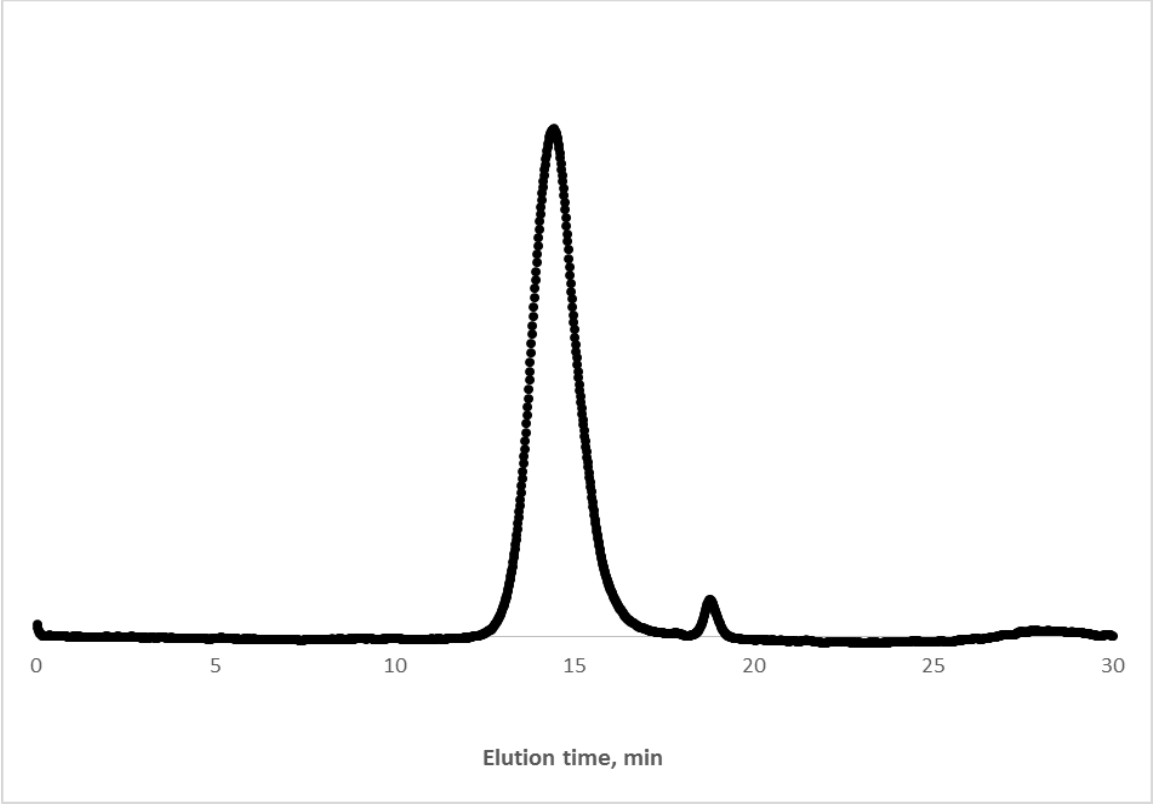

2-49-2A Polymer **6**, Light scattering

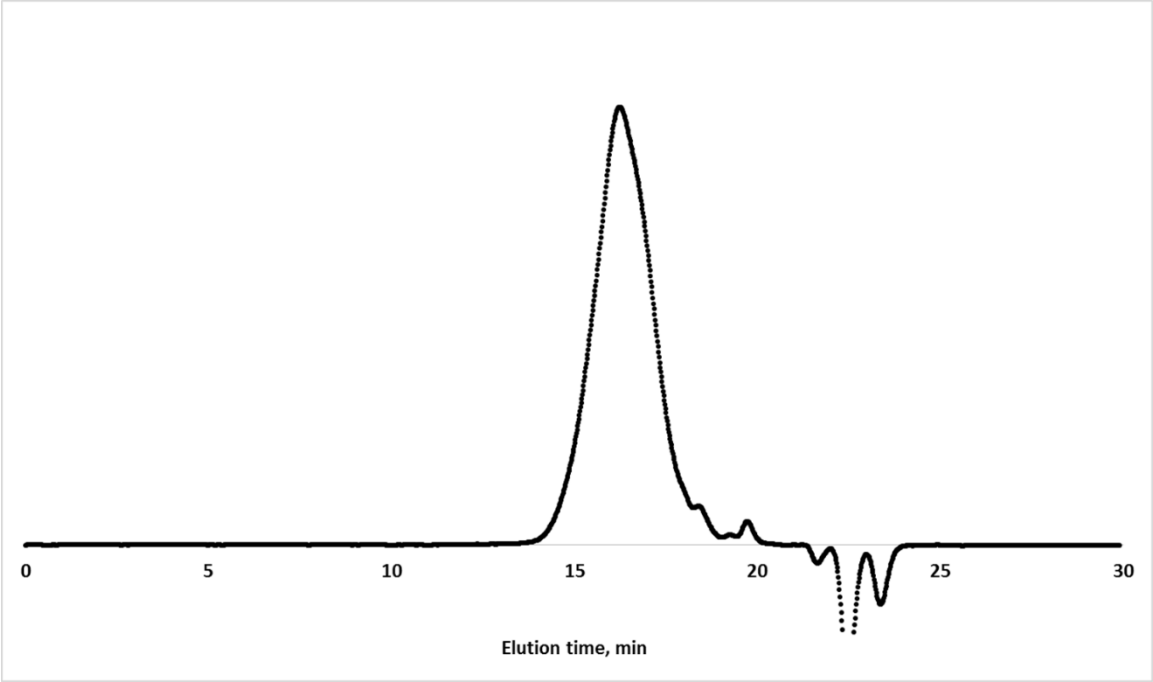

2-142A2 Polymer **7**, Refractive index

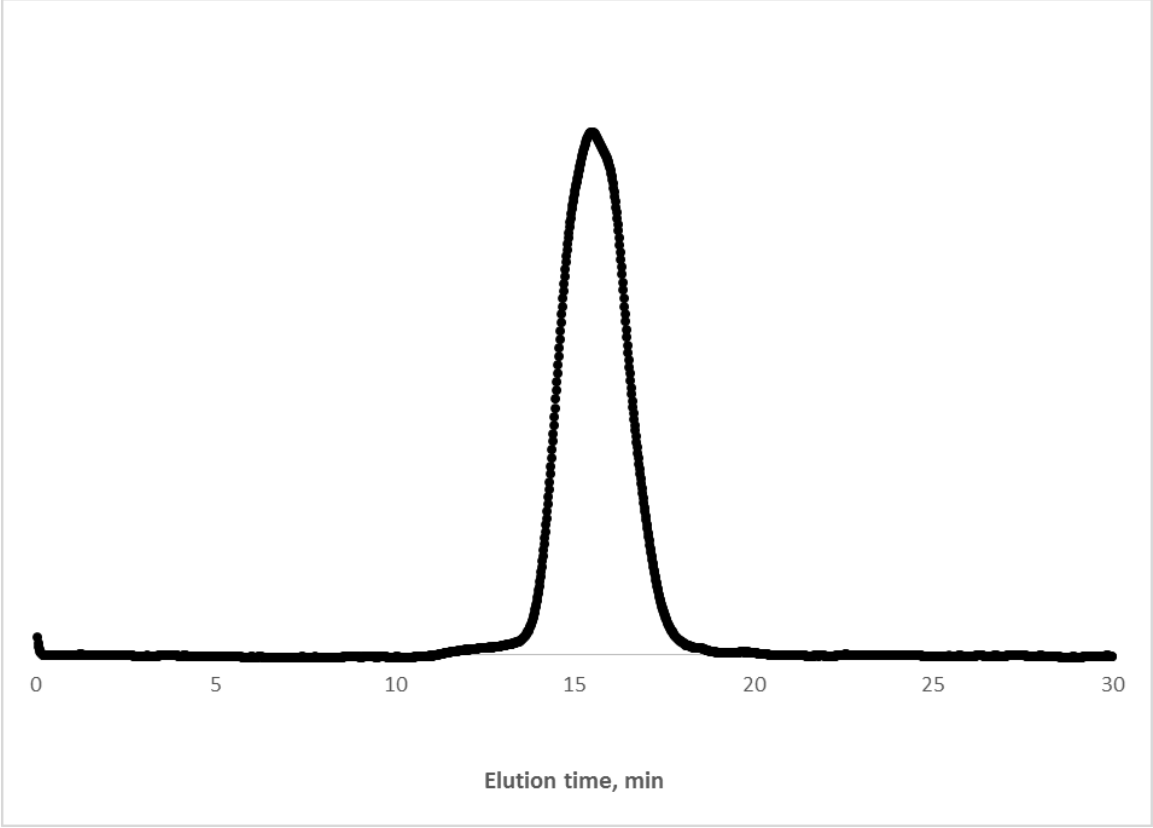

2-142A2 Polymer **7**, Light scattering

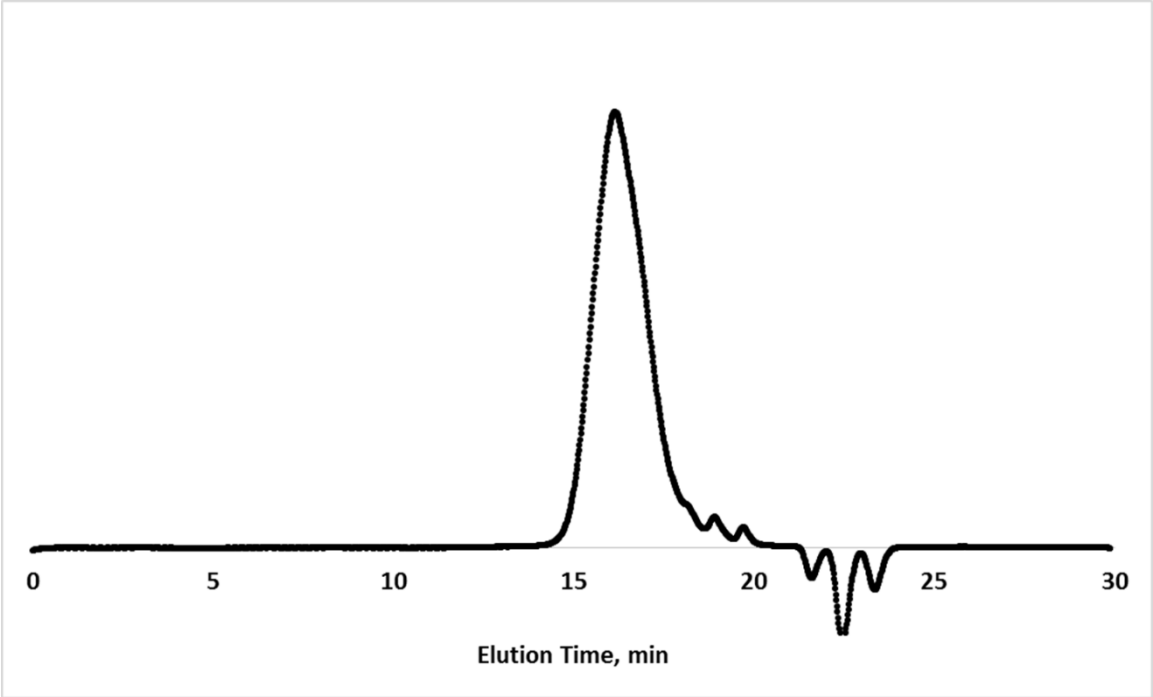

2-146-2 Polymer **8**, Refractive index

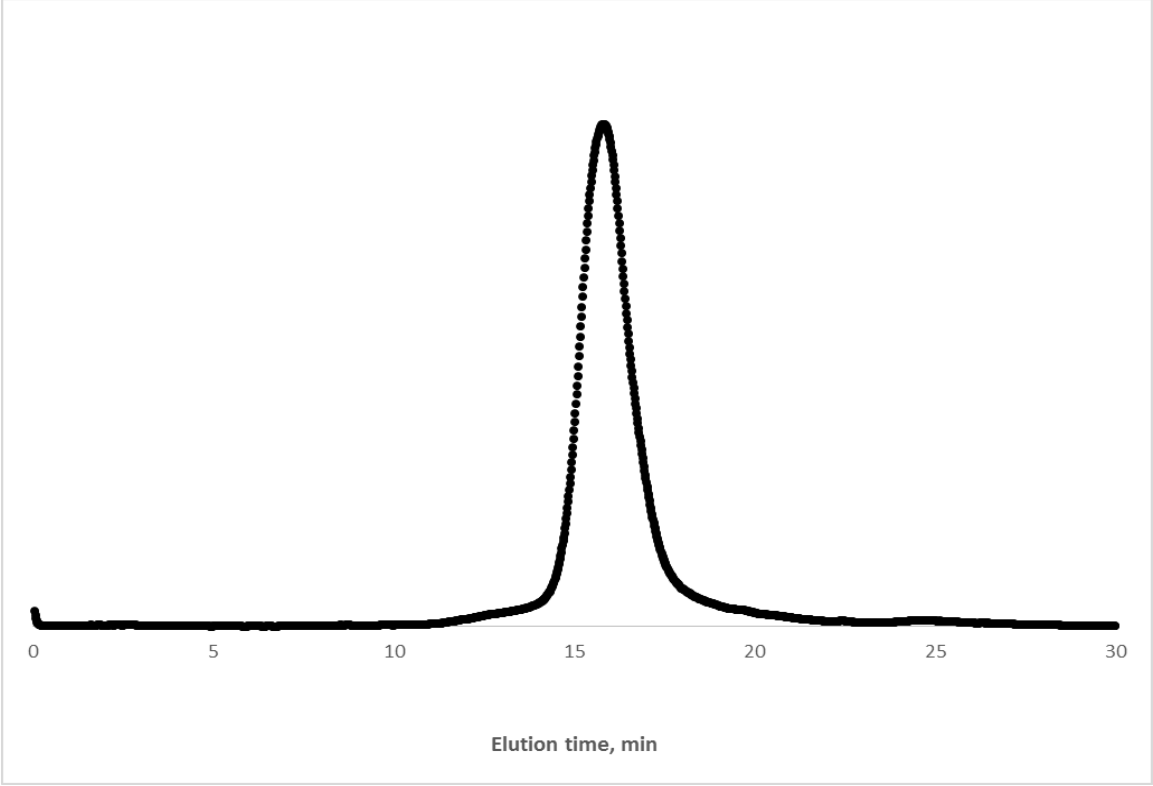

2-146-2 Polymer **8**, Light scattering

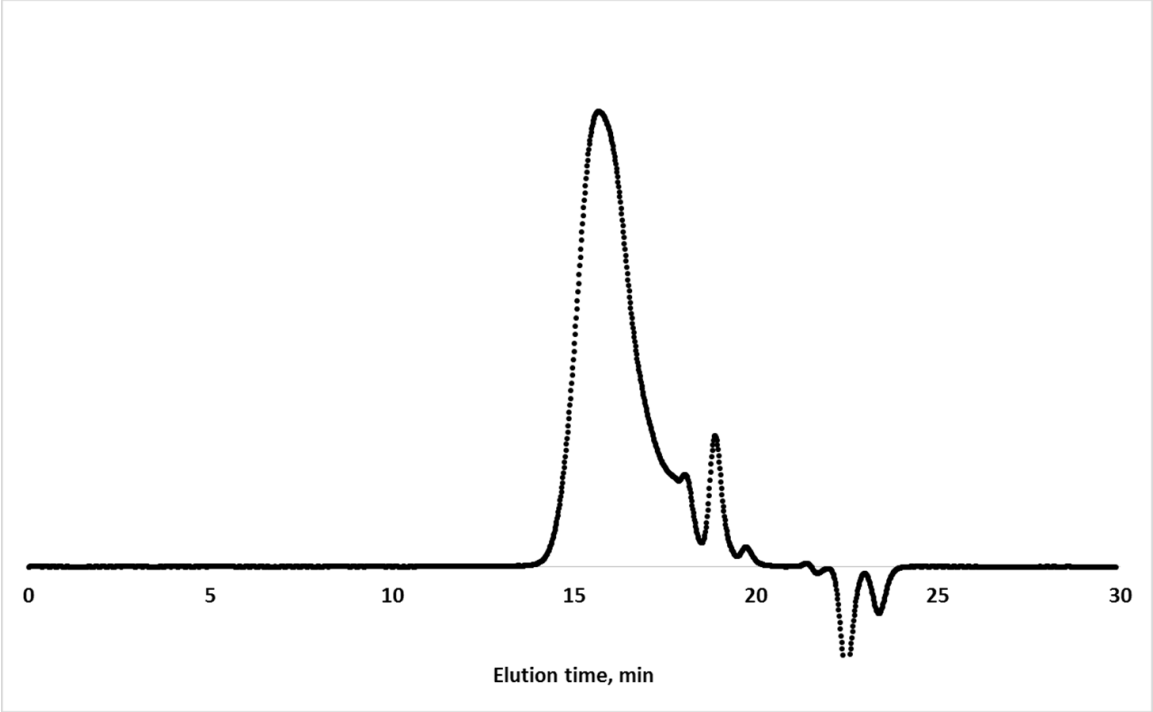

2-142B1 Polymer **9**, Refractive index

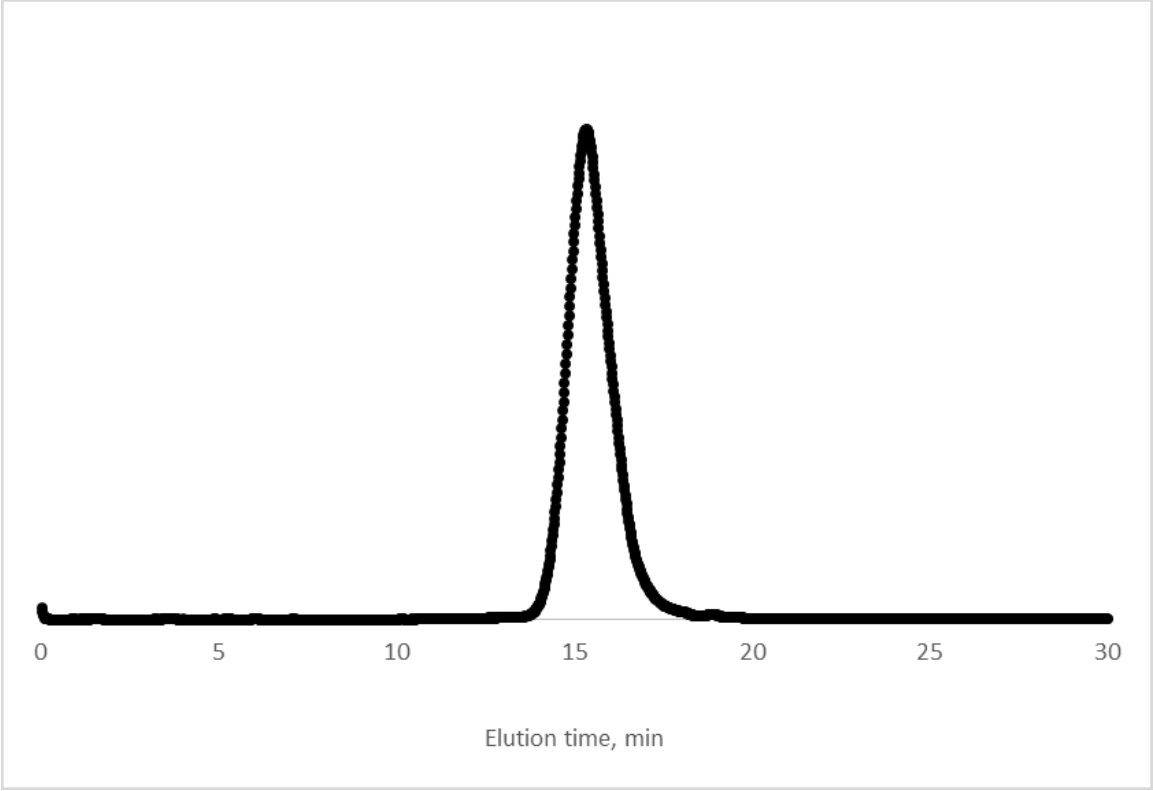

2-142B1 Polymer **9**, Light scattering

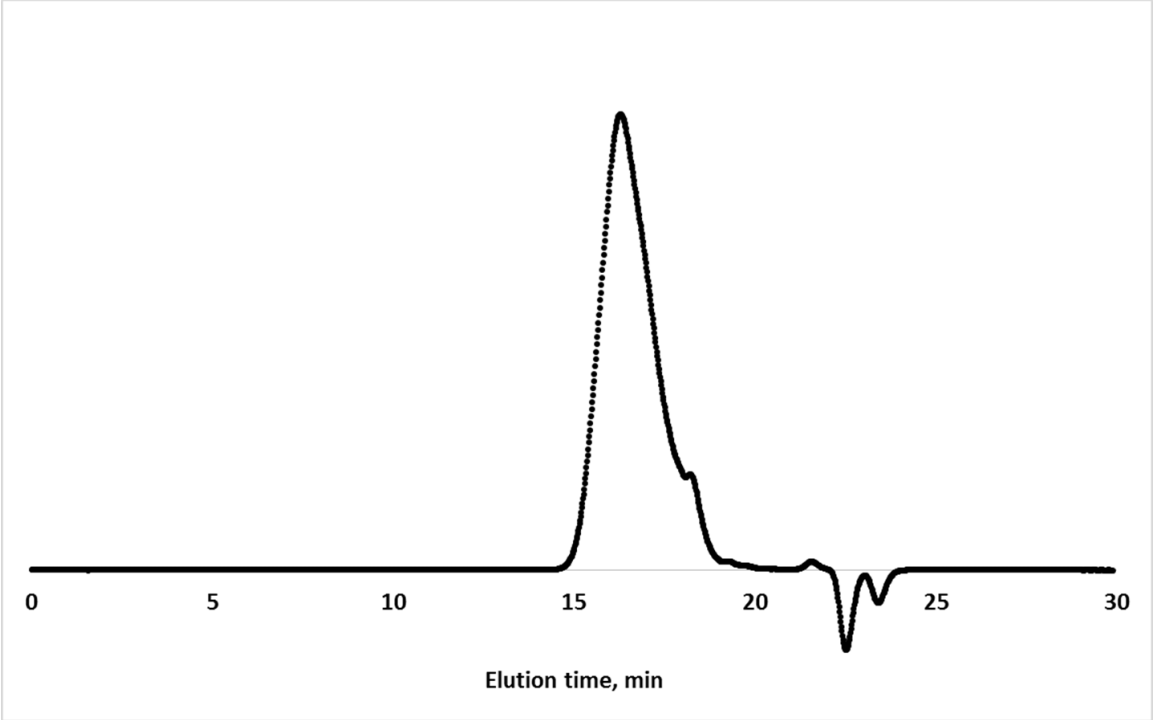

2-183-2 Polymer **10**, Refractive index

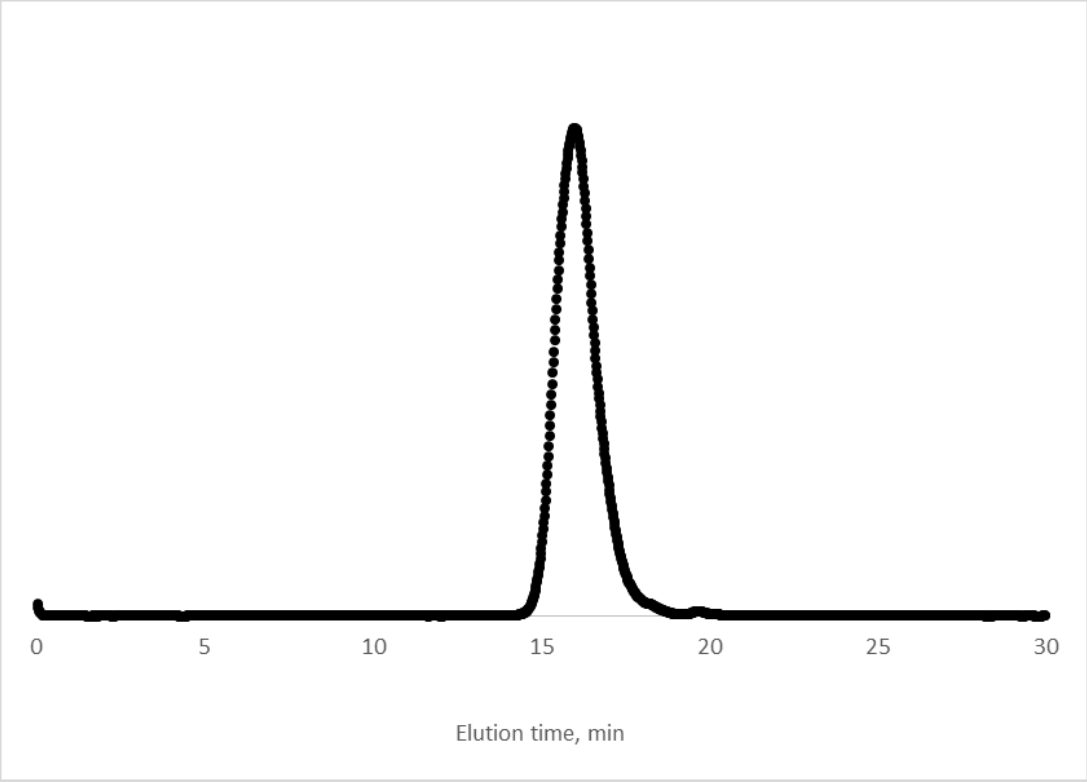

2-183-2 Polymer **10**, Light scattering

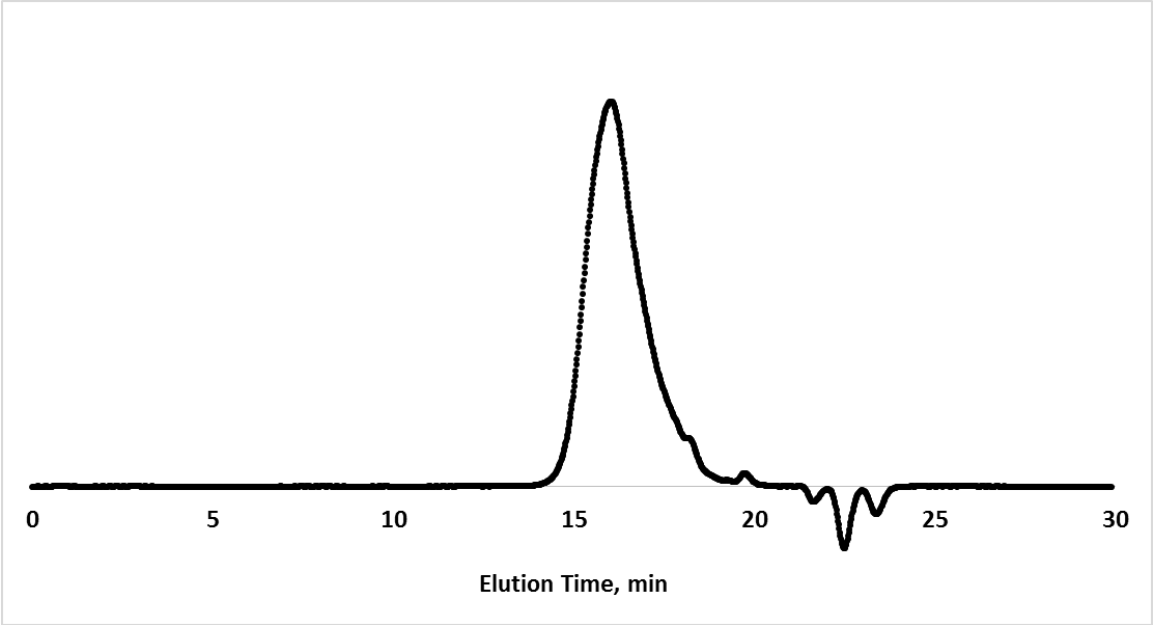

2-142B2 Polymer **11**, Refractive index

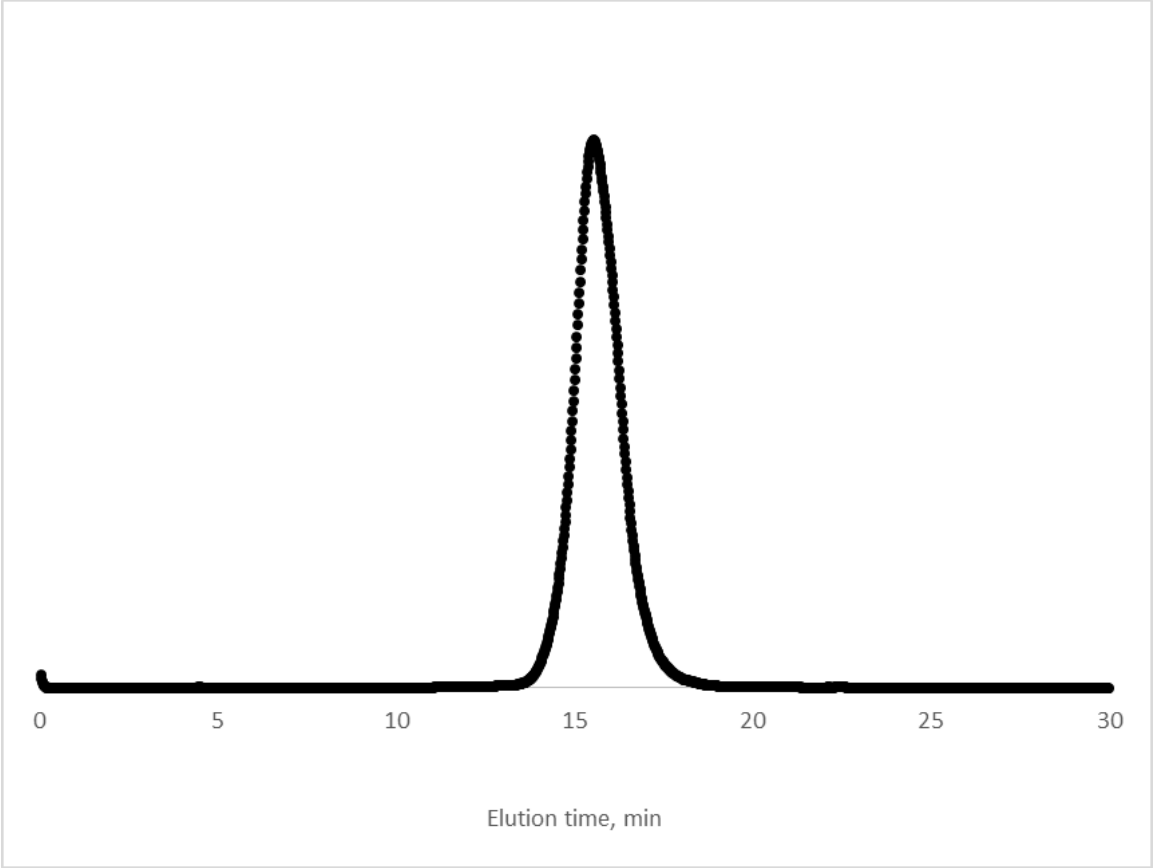

2-142B2 Polymer **11**, Light scattering

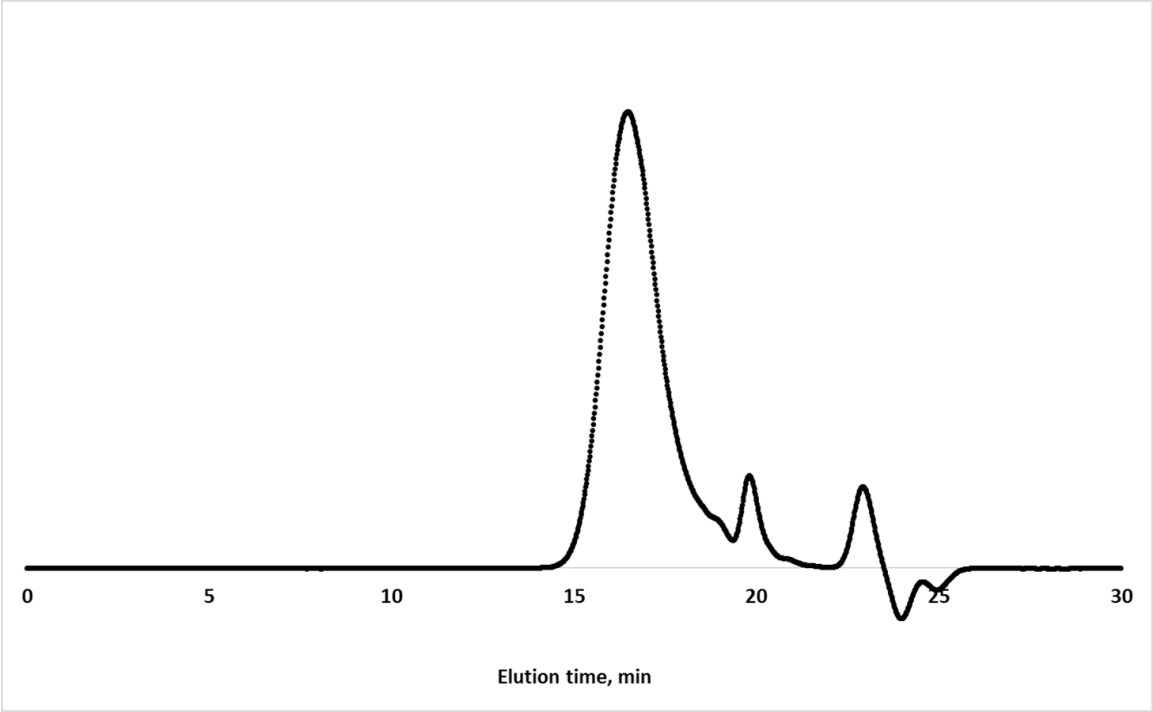

Polymer **12**, Refractive index

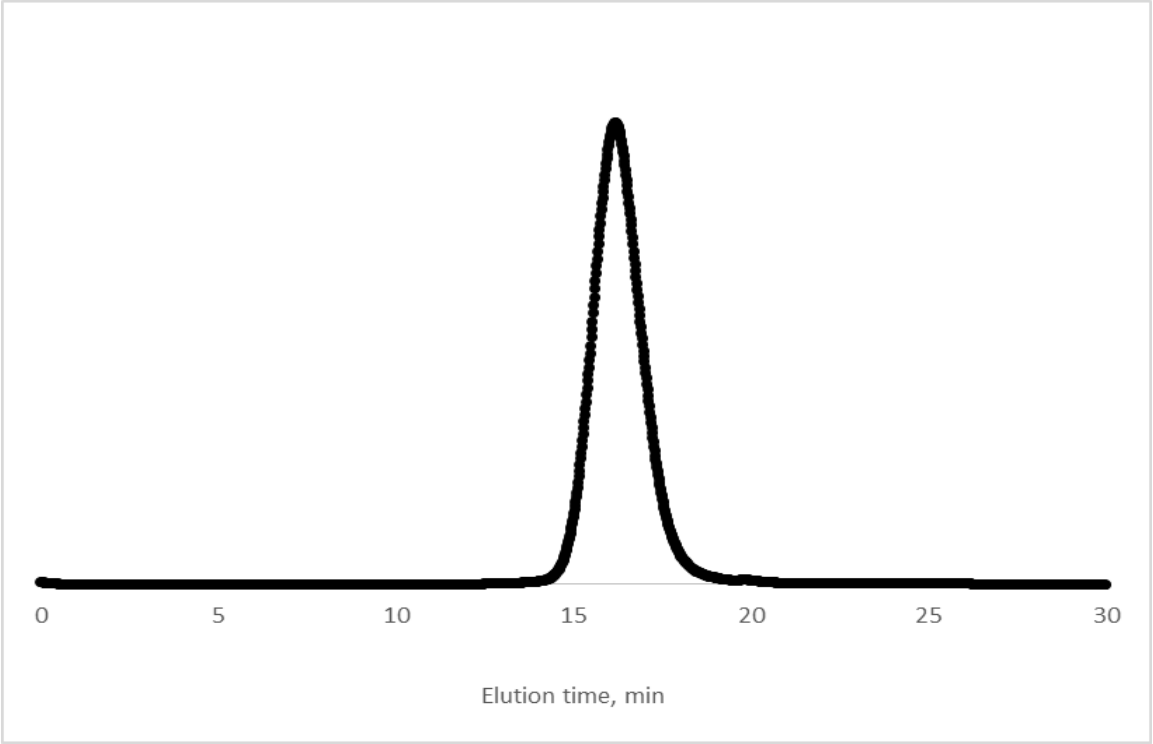

2-47-2 Polymer **12**, Light scattering

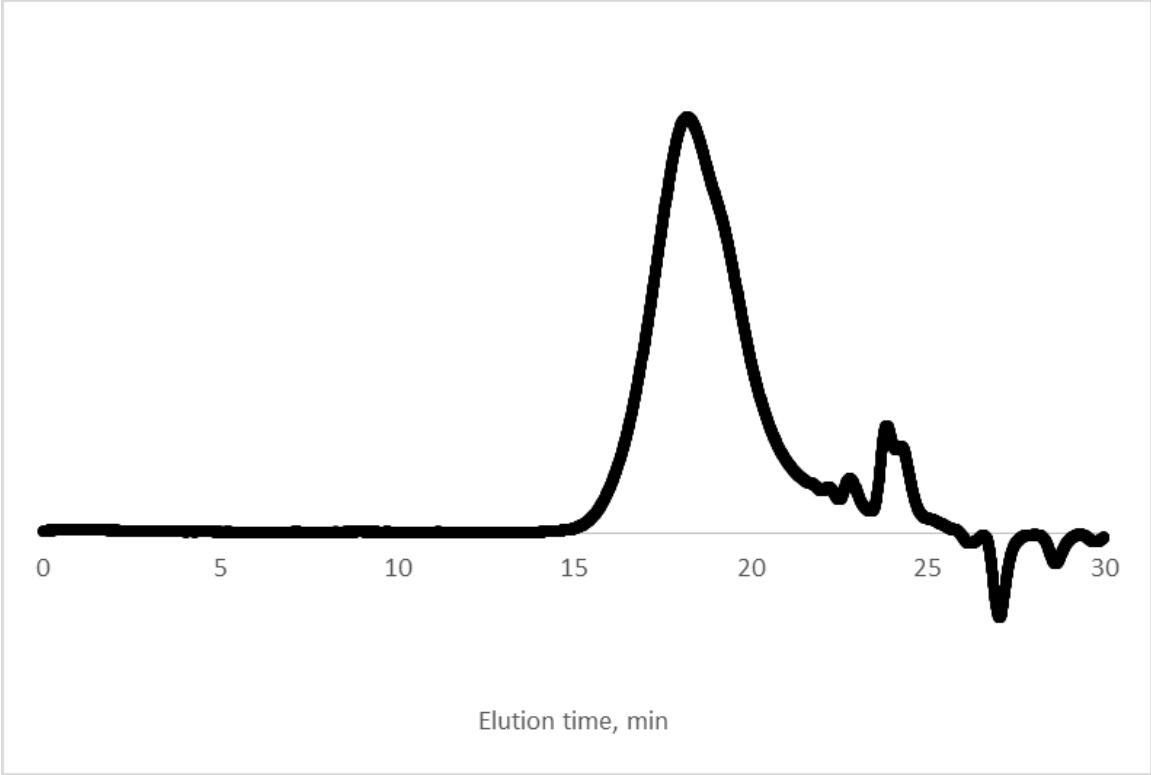

2-22-1 Polymer **13**, Refractive index

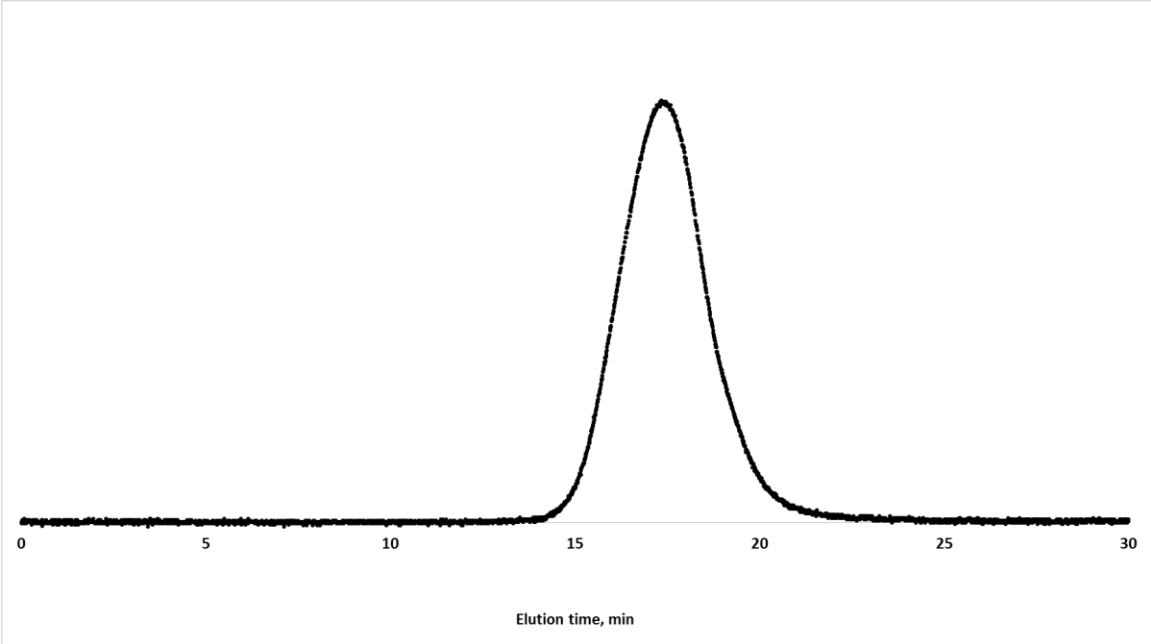

2-22-1 Polymer **13**, Light scattering

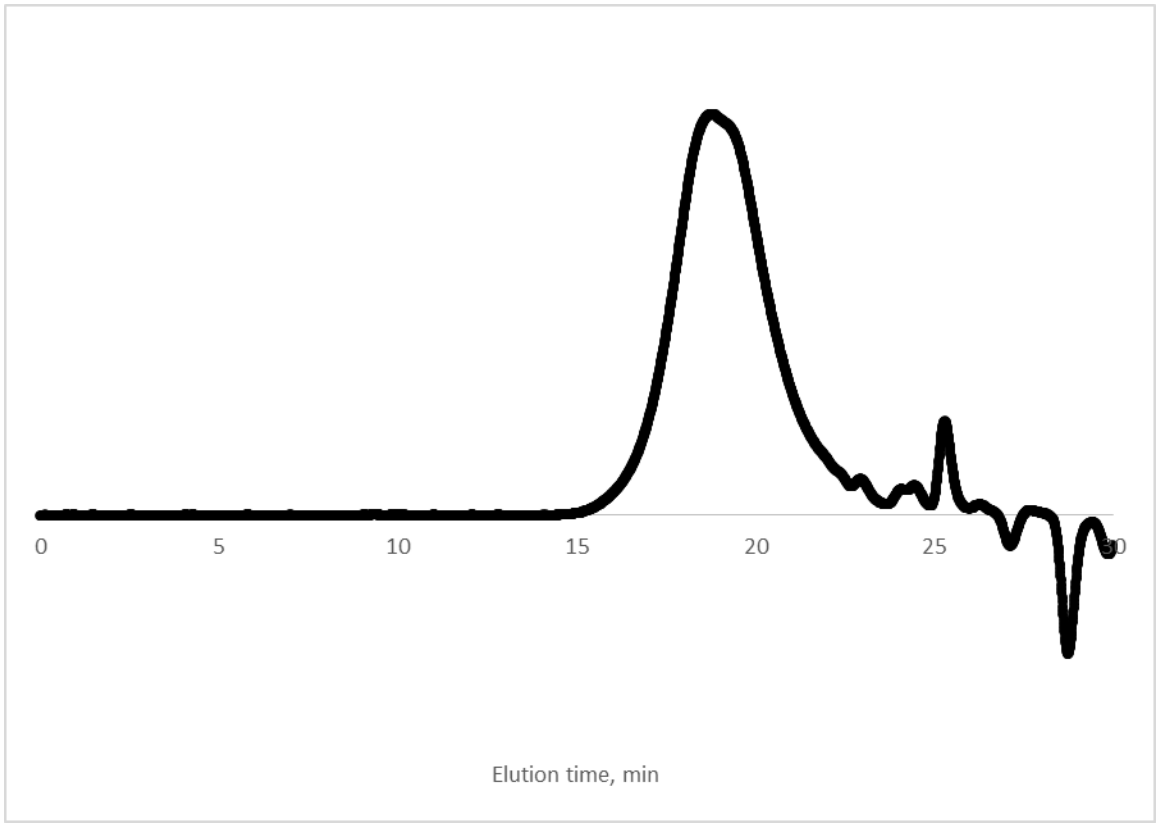

2-36-2 Polymer **14**, Refractive index

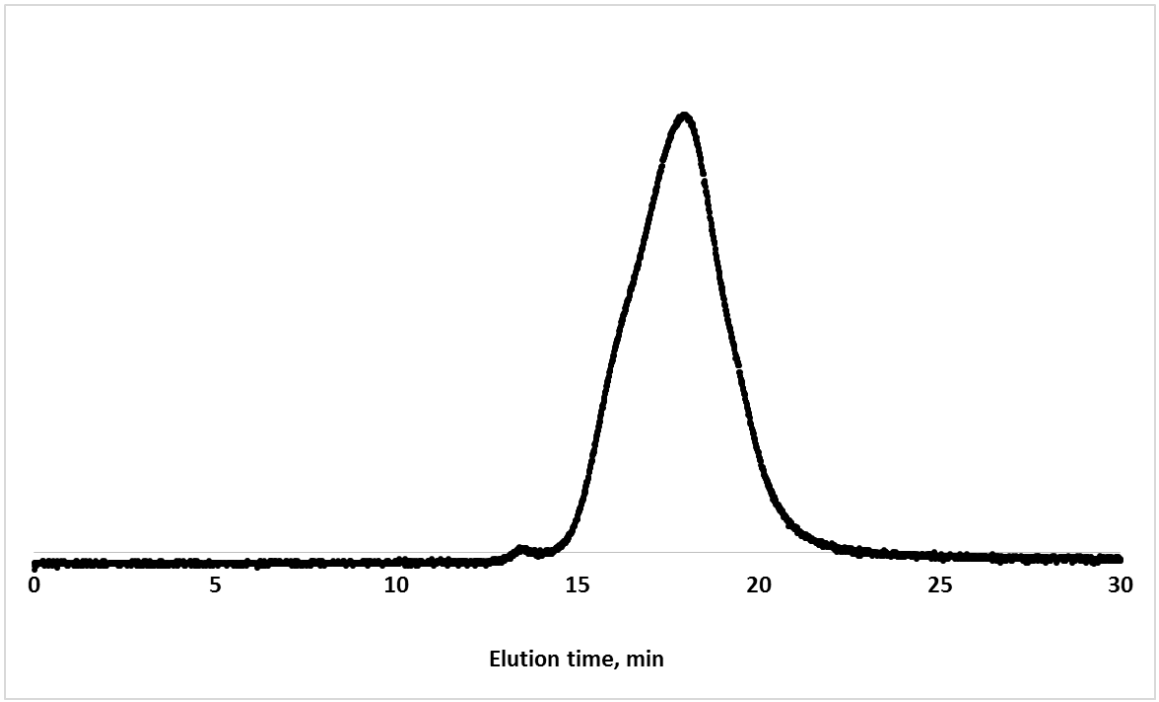

2-36-2 Polymer **14**, Light scattering

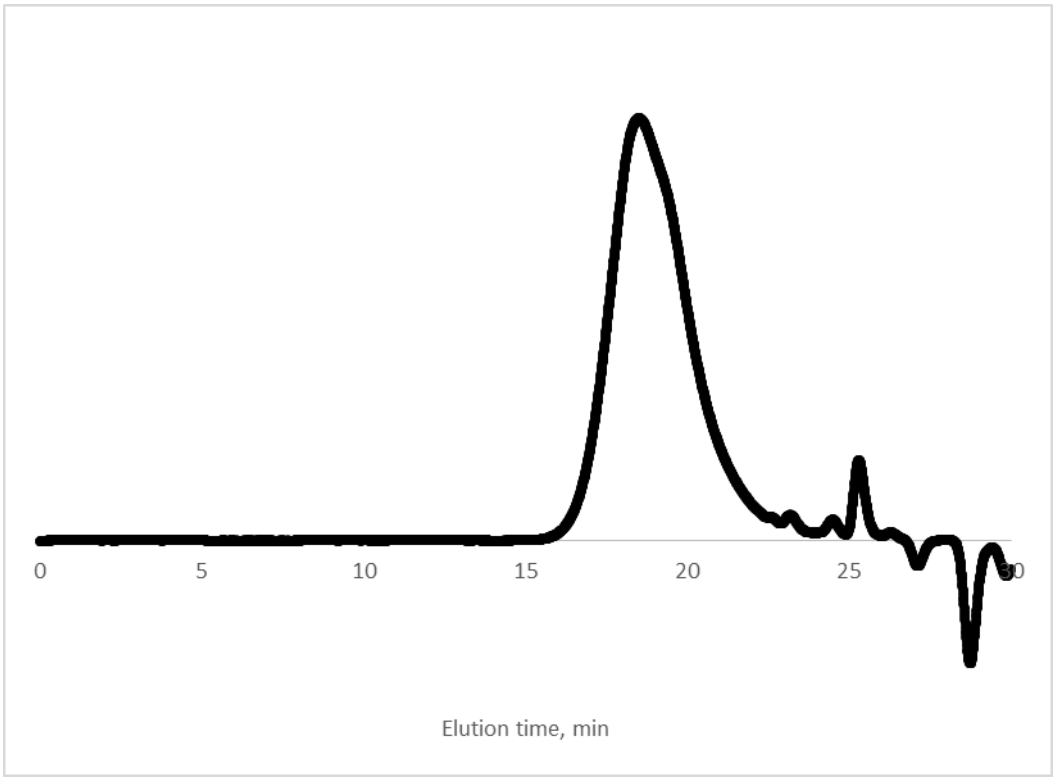

2-37-2 Polymer **15**, Light scattering

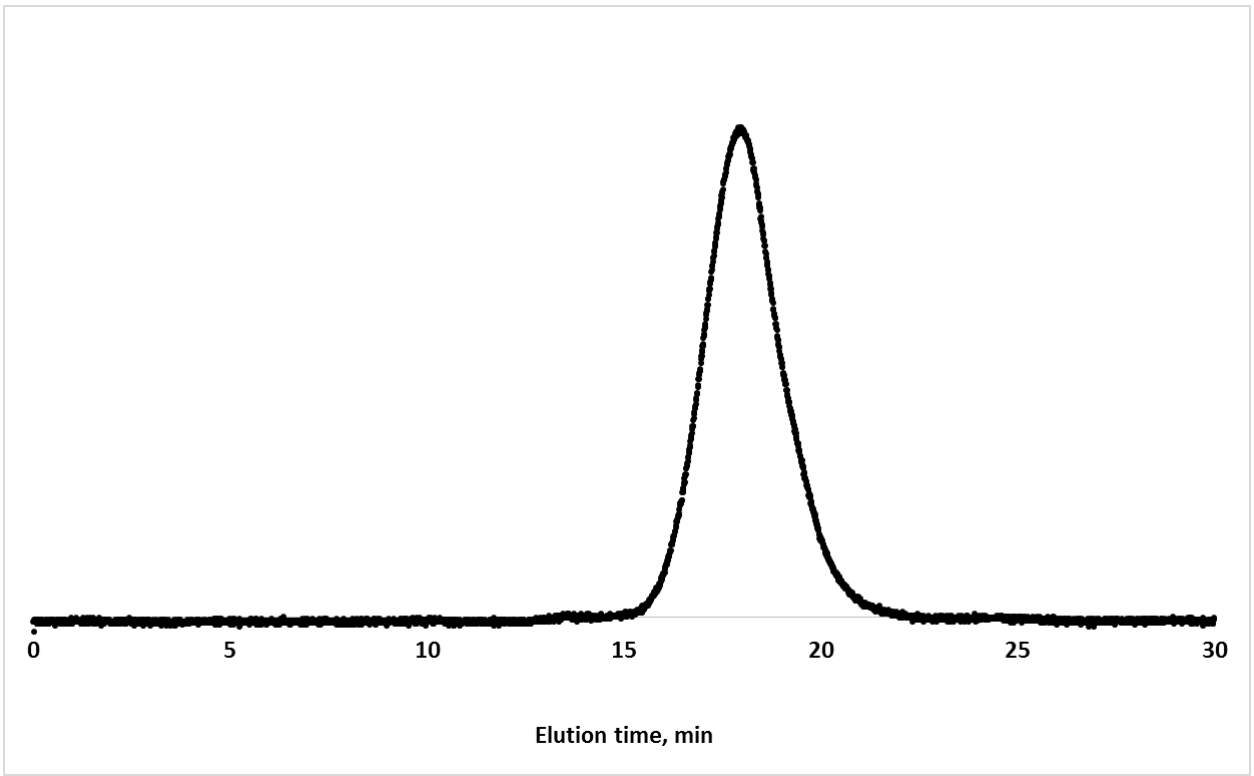

2-37-2 Polymer **15**, Light scattering

DSC Traces

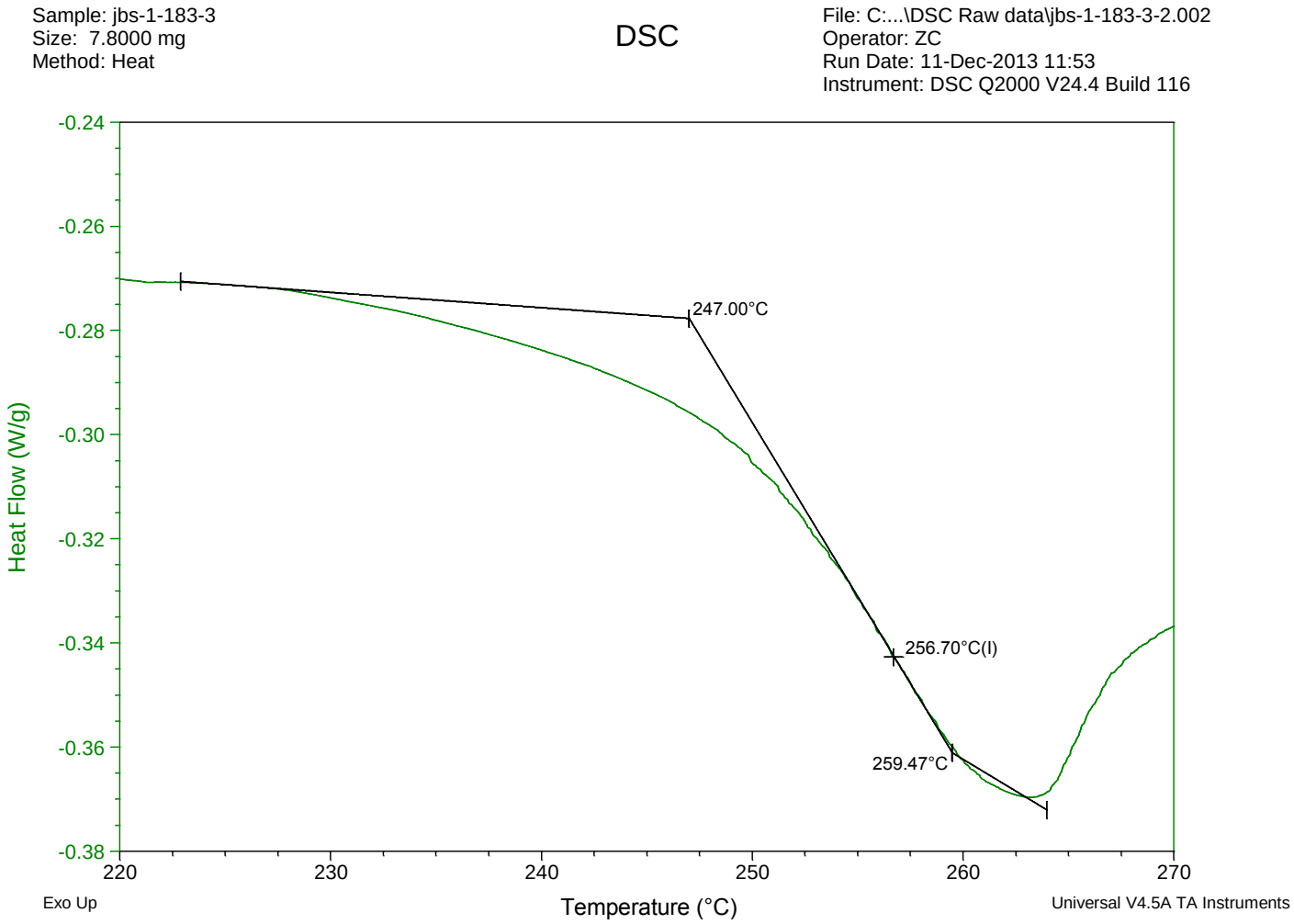

Polymer **1**

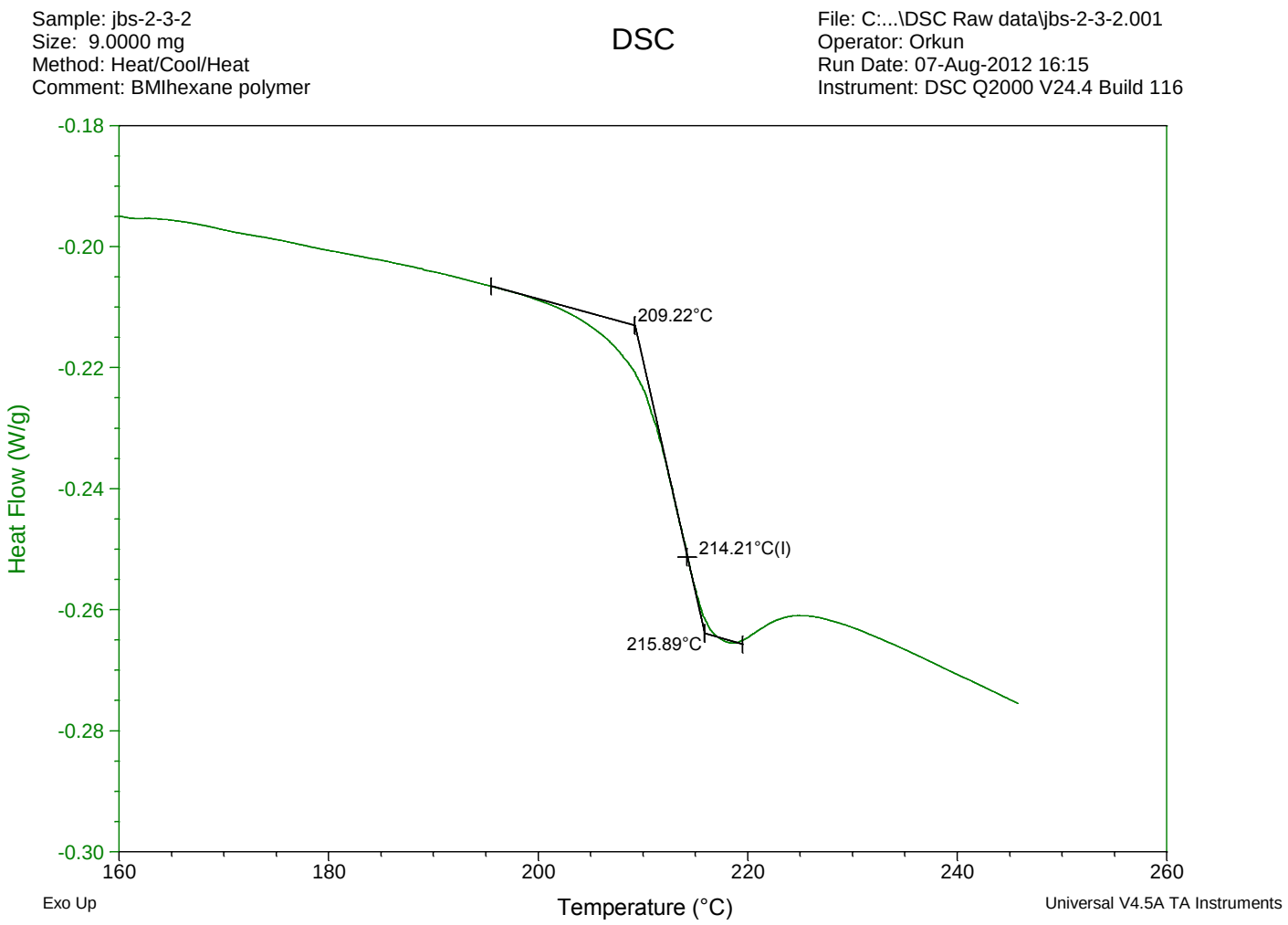
Sample: jbs-2-3-2
Size: 9.0000 mg
Method: Heat/Cool/Heat
Comment: BMIhexane polymer
DSC
File: C:...\DSC Raw data\jbs-2-3-2.001
Operator: Orkun
Run Date: 07-Aug-2012 16:15
Instrument: DSC Q2000 V24.4 Build 116
-0.18
-0.20
-0.22
-0.24
-0.26
-0.28
-0.30
Heat Flow (W/g)
209.22°C
214.21°C(I)
215.89°C
160
180
200
220
240
260
Exo Up
Temperature (°C)
Universal V4.5A TA Instruments

Polymer **2**

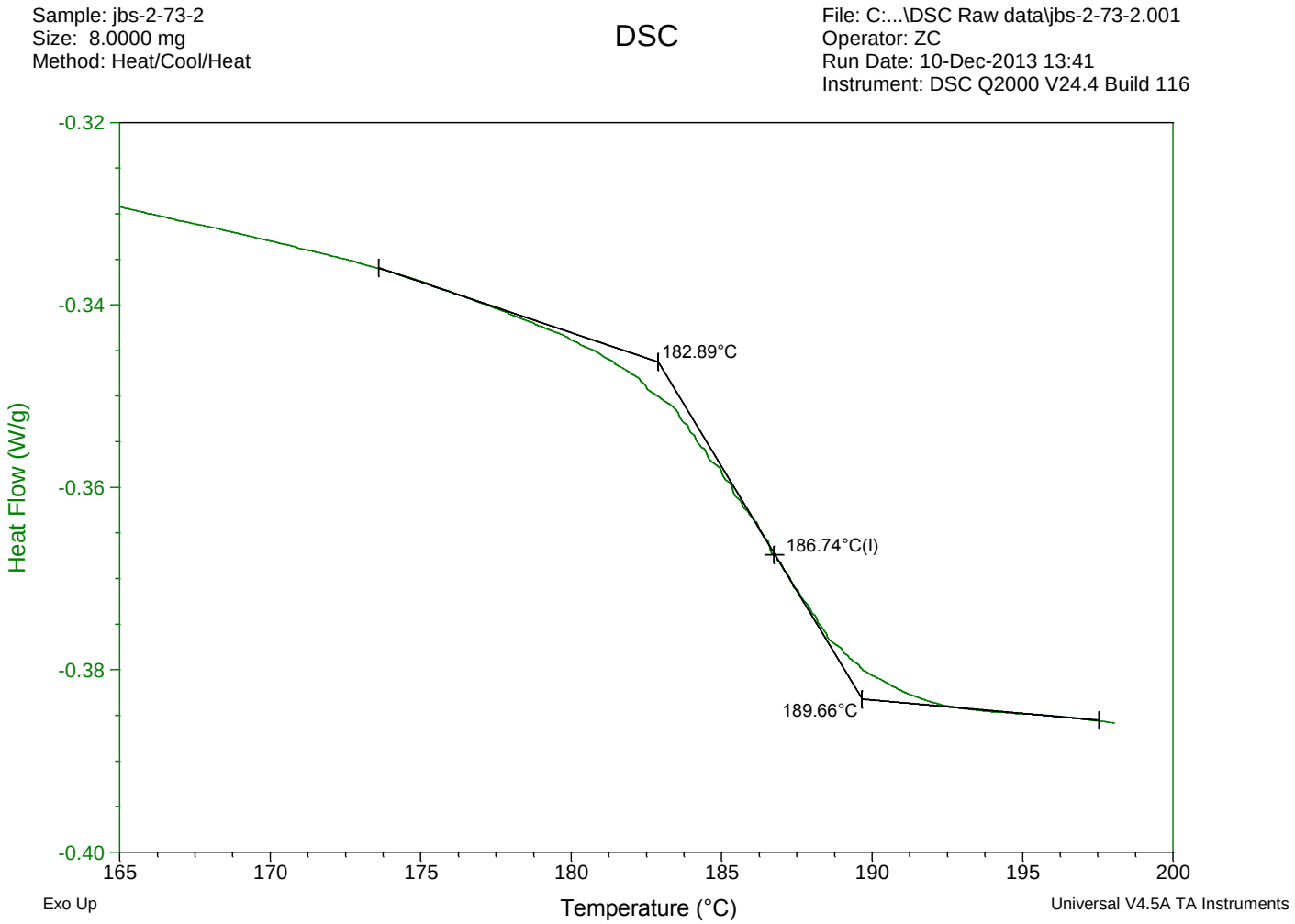
Sample: jbs-2-73-2
Size: 8.0000 mg
Method: Heat/Cool/Heat
DSC
File: C:...\DSC Raw data\jbs-2-73-2.001
Operator: ZC
Run Date: 10-Dec-2013 13:41
Instrument: DSC Q2000 V24.4 Build 116
-0.32
-0.34
-0.36
-0.38
-0.40
Heat Flow (W/g)
182.89°C
186.74°C(I)
189.66°C
165
170
175
180
185
190
195
200
Exo Up
Temperature (°C)
Universal V4.5A TA Instruments

Polymer **3**

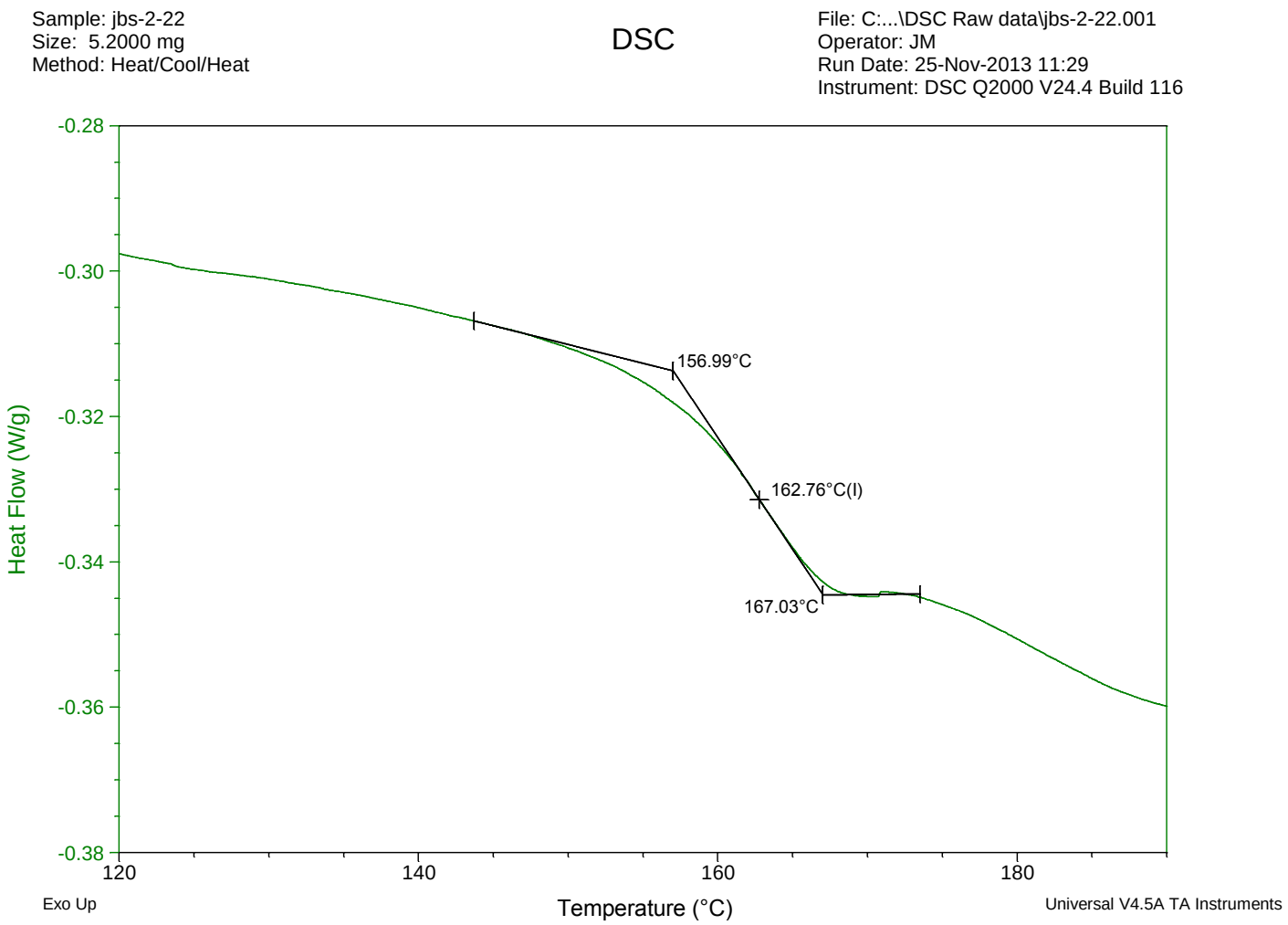
Sample: jbs-2-22
Size: 5.2000 mg
Method: Heat/Cool/Heat
DSC
File: C:...\DSC Raw data\jbs-2-22.001
Operator: JM
Run Date: 25-Nov-2013 11:29
Instrument: DSC Q2000 V24.4 Build 116
-0.28
-0.30
-0.32
-0.34
-0.36
-0.38
Heat Flow (W/g)
156.99°C
162.76°C(I)
167.03°C
120
140
160
180
Exo Up
Temperature (°C)
Universal V4.5A TA Instruments

Polymer **4**

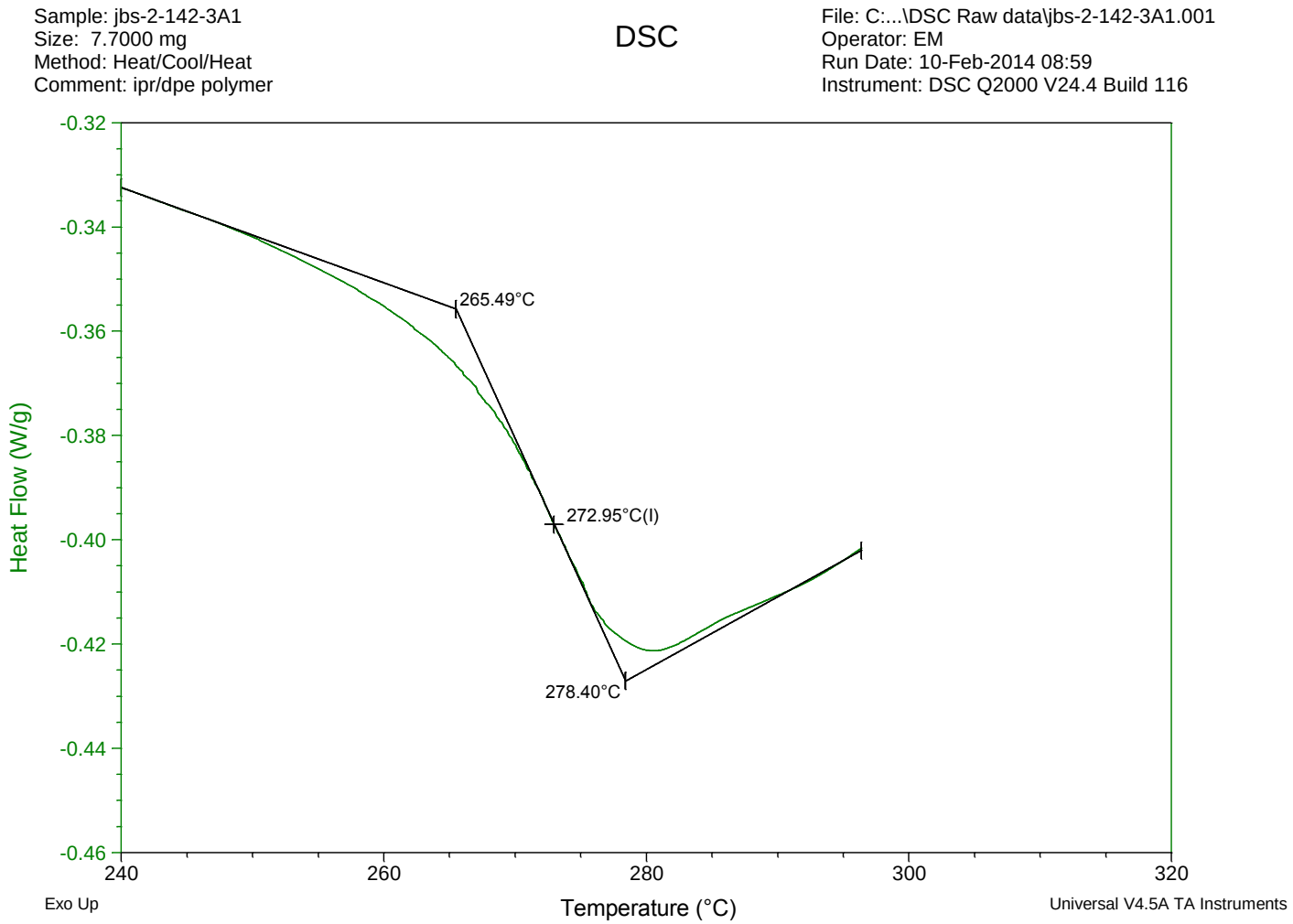
Sample: jbs-2-142-3A1
Size: 7.7000 mg
Method: Heat/Cool/Heat
Comment: ipr/dpe polymer
DSC
File: C:...\DSC Raw data\jbs-2-142-3A1.001
Operator: EM
Run Date: 10-Feb-2014 08:59
Instrument: DSC Q2000 V24.4 Build 116
-0.32
-0.34
-0.36
-0.38
-0.40
-0.42
-0.44
-0.46
Heat Flow (W/g)
265.49°C
272.95°C(I)
278.40°C
240
260
280
300
320
Exo Up
Temperature (°C)
Universal V4.5A TA Instruments

Polymer **5**

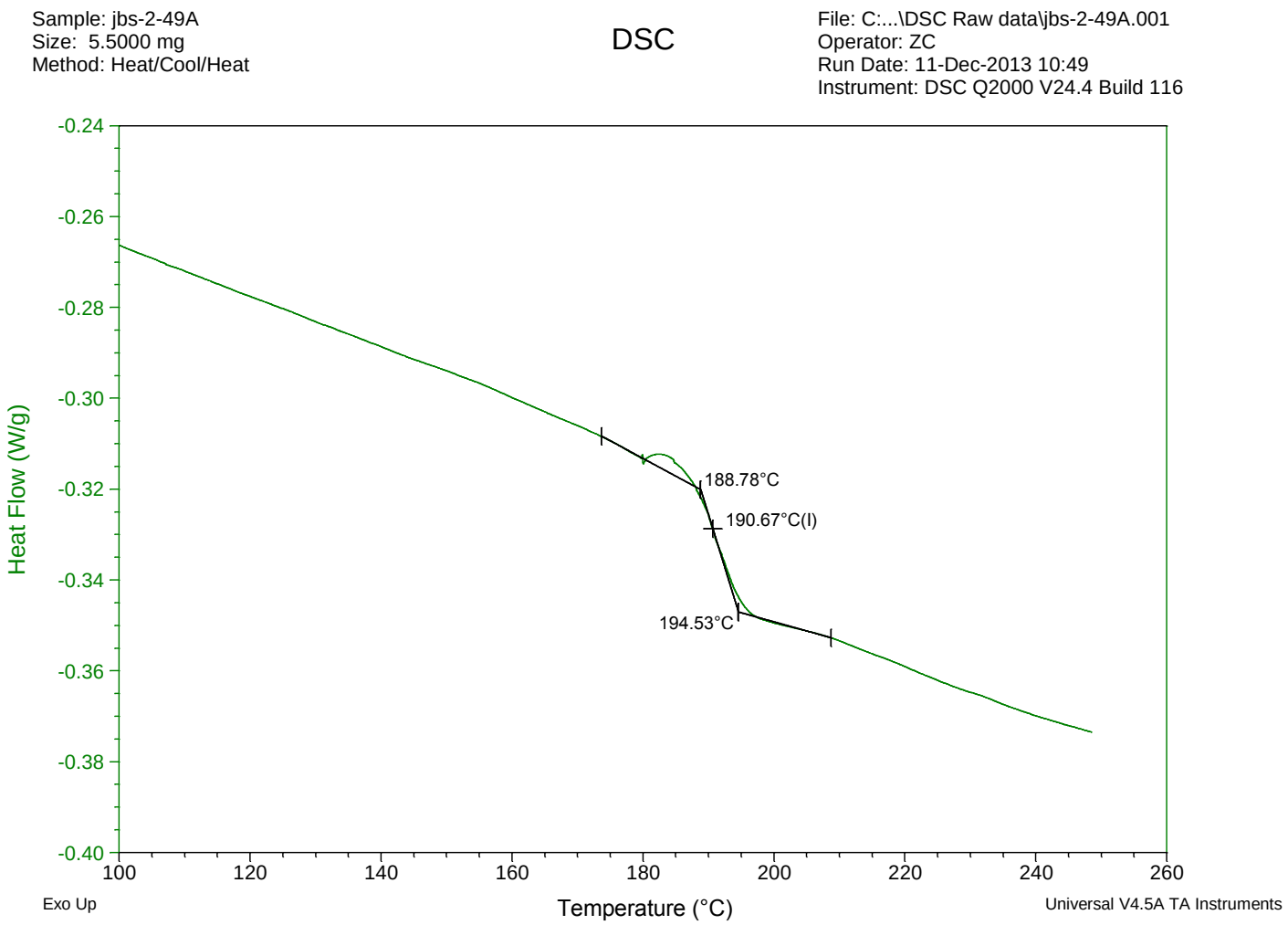
Sample: jbs-2-49A
Size: 5.5000 mg
Method: Heat/Cool/Heat
DSC
File: C:...\DSC Raw data\jbs-2-49A.001
Operator: ZC
Run Date: 11-Dec-2013 10:49
Instrument: DSC Q2000 V24.4 Build 116
Heat Flow (W/g)
-0.24
-0.26
-0.28
-0.30
-0.32
-0.34
-0.36
-0.38
-0.40
188.78°C
190.67°C(I)
194.53°C
100
120
140
160
180
200
220
240
260
Exo Up
Temperature (°C)
Universal V4.5A TA Instruments

Polymer **6**

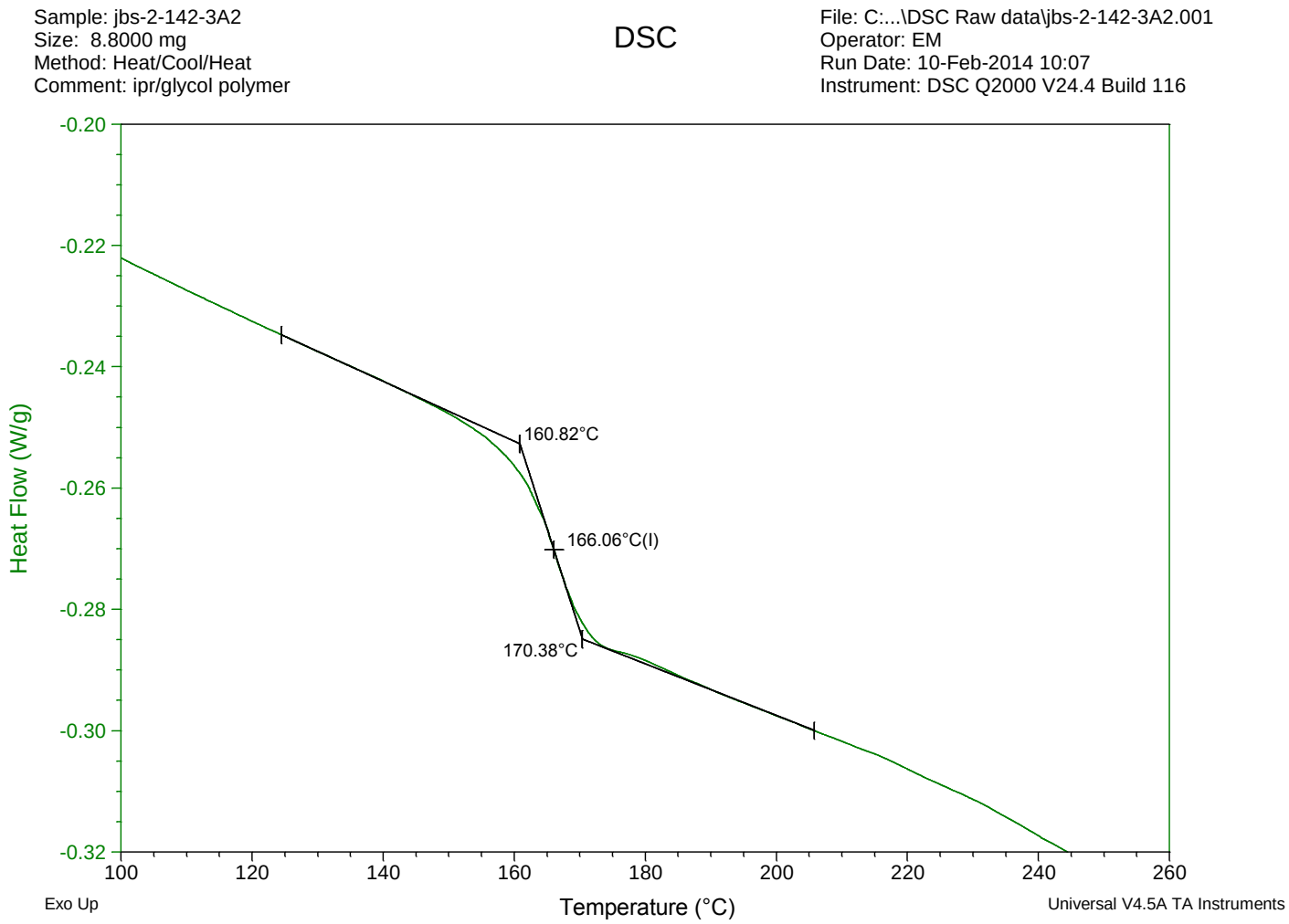
Sample: jbs-2-142-3A2
Size: 8.8000 mg
Method: Heat/Cool/Heat
Comment: ipr/glycol polymer
DSC
File: C:...\DSC Raw data\jbs-2-142-3A2.001
Operator: EM
Run Date: 10-Feb-2014 10:07
Instrument: DSC Q2000 V24.4 Build 116
Heat Flow (W/g)
-0.20
-0.22
-0.24
-0.26
-0.28
-0.30
-0.32
160.82°C
166.06°C(I)
170.38°C
100
120
140
160
180
200
220
240
260
Temperature (°C)
Exo Up
Universal V4.5A TA Instruments

Polymer **7**

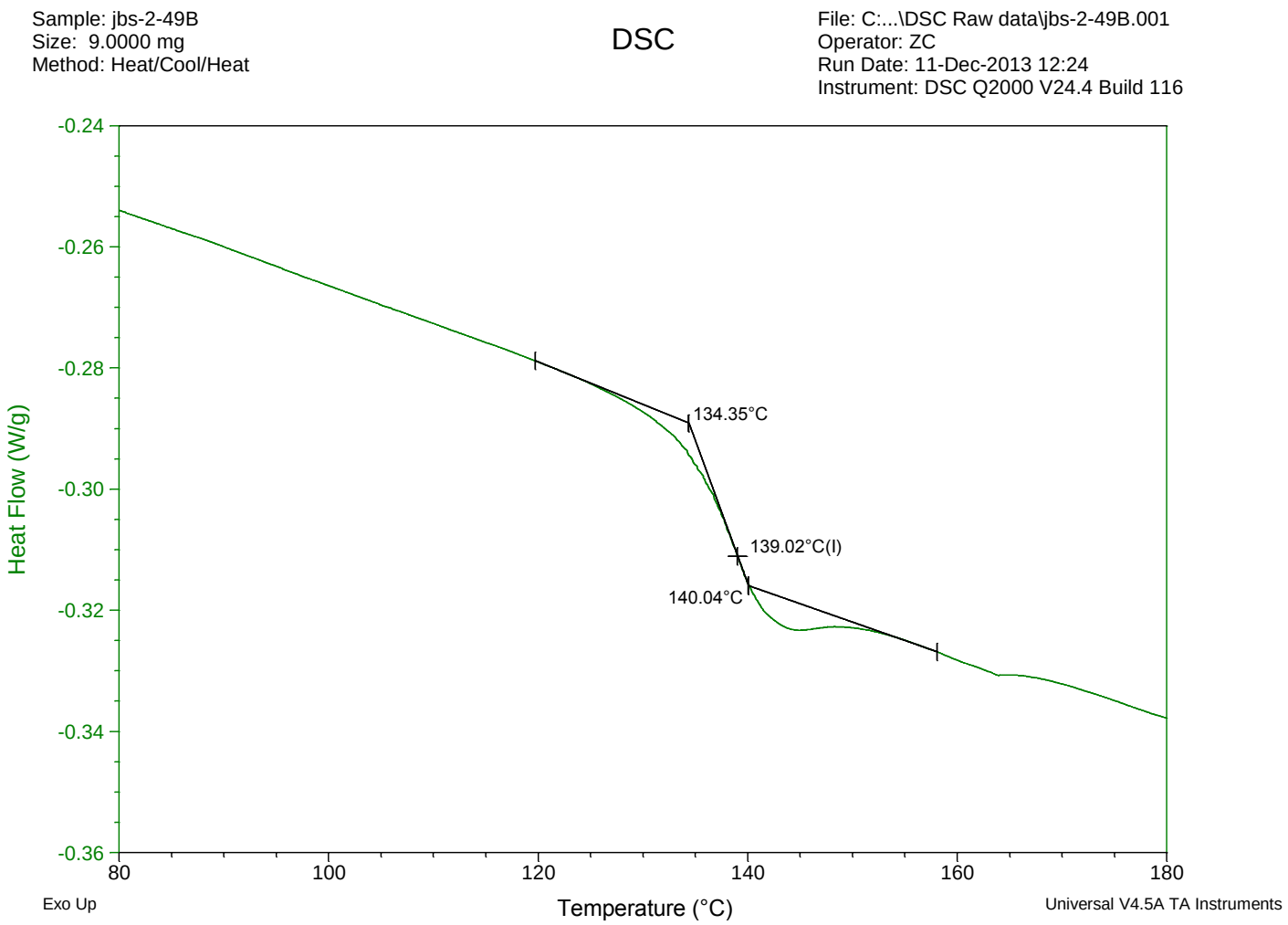
Sample: jbs-2-49B
Size: 9.0000 mg
Method: Heat/Cool/Heat
DSC
File: C:...\DSC Raw data\jbs-2-49B.001
Operator: ZC
Run Date: 11-Dec-2013 12:24
Instrument: DSC Q2000 V24.4 Build 116
-0.24
-0.26
-0.28
-0.30
-0.32
-0.34
-0.36
Heat Flow (W/g)
134.35°C
139.02°C(I)
140.04°C
80
100
120
140
160
180
Exo Up
Temperature (°C)
Universal V4.5A TA Instruments

Polymer **8**

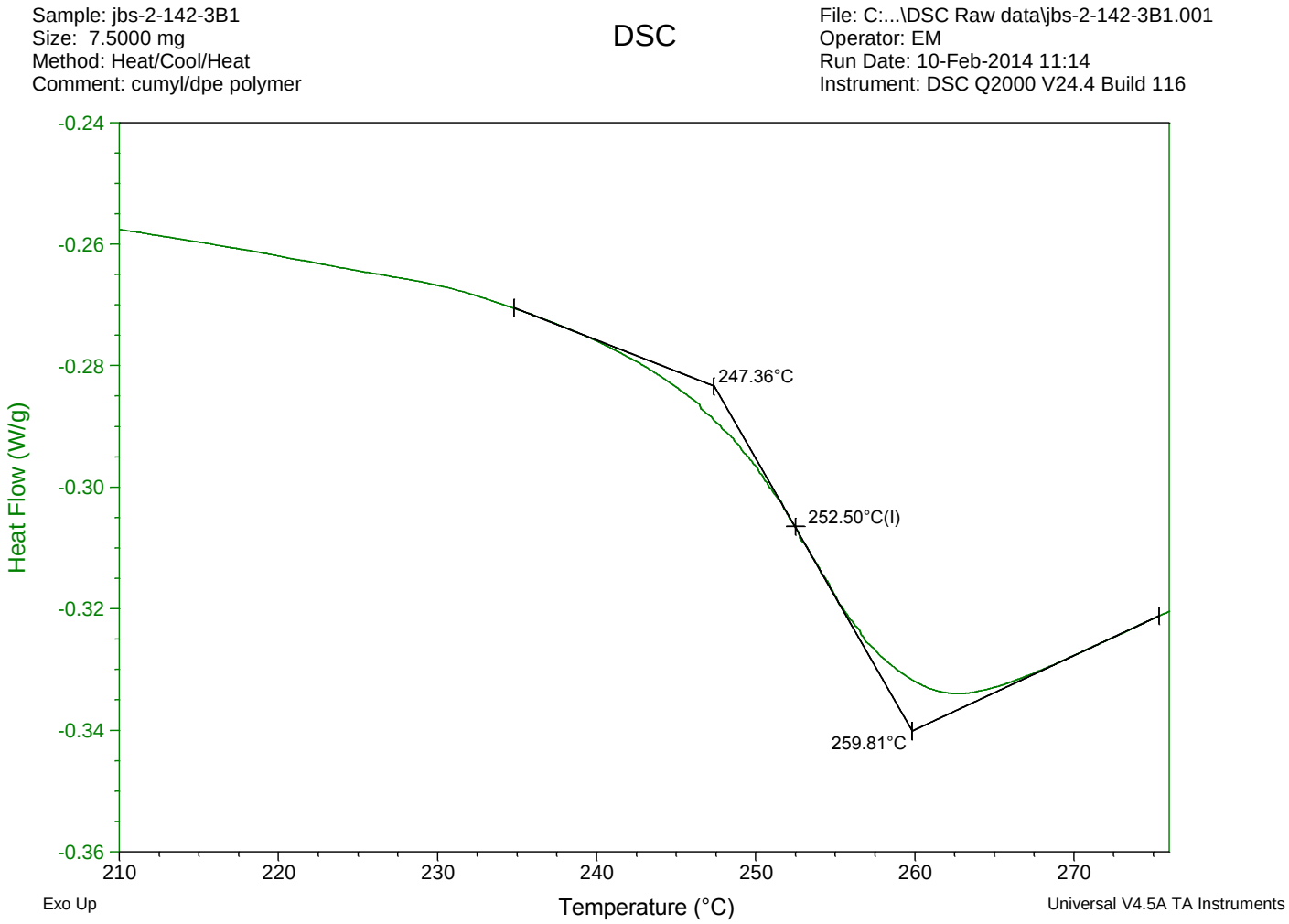
Sample: jbs-2-142-3B1
Size: 7.5000 mg
Method: Heat/Cool/Heat
Comment: cumyl/dpe polymer
DSC
File: C:...\DSC Raw data\jbs-2-142-3B1.001
Operator: EM
Run Date: 10-Feb-2014 11:14
Instrument: DSC Q2000 V24.4 Build 116
-0.24
-0.26
-0.28
-0.30
-0.32
-0.34
-0.36
Heat Flow (W/g)
247.36°C
252.50°C(I)
259.81°C
210
220
230
240
250
260
270
Exo Up
Temperature (°C)
Universal V4.5A TA Instruments

Polymer **9**

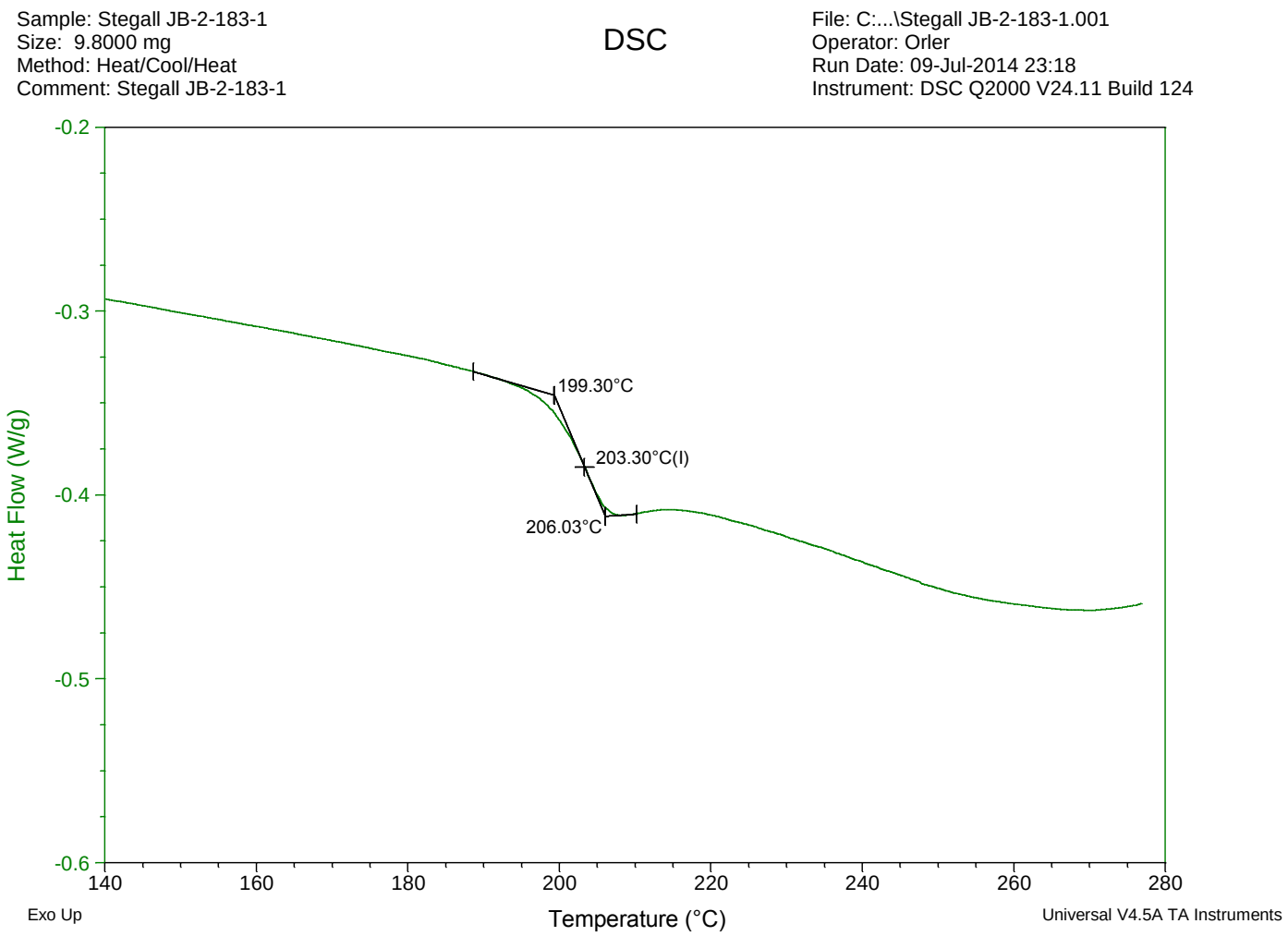
Sample: Stegall JB-2-183-1
Size: 9.8000 mg
Method: Heat/Cool/Heat
Comment: Stegall JB-2-183-1
DSC
File: C:...\Stegall JB-2-183-1.001
Operator: Orler
Run Date: 09-Jul-2014 23:18
Instrument: DSC Q2000 V24.11 Build 124
-0.2
-0.3
-0.4
-0.5
-0.6
Heat Flow (W/g)
199.30°C
203.30°C(I)
206.03°C
140
160
180
200
220
240
260
280
Exo Up
Temperature (°C)
Universal V4.5A TA Instruments

Polymer **10**

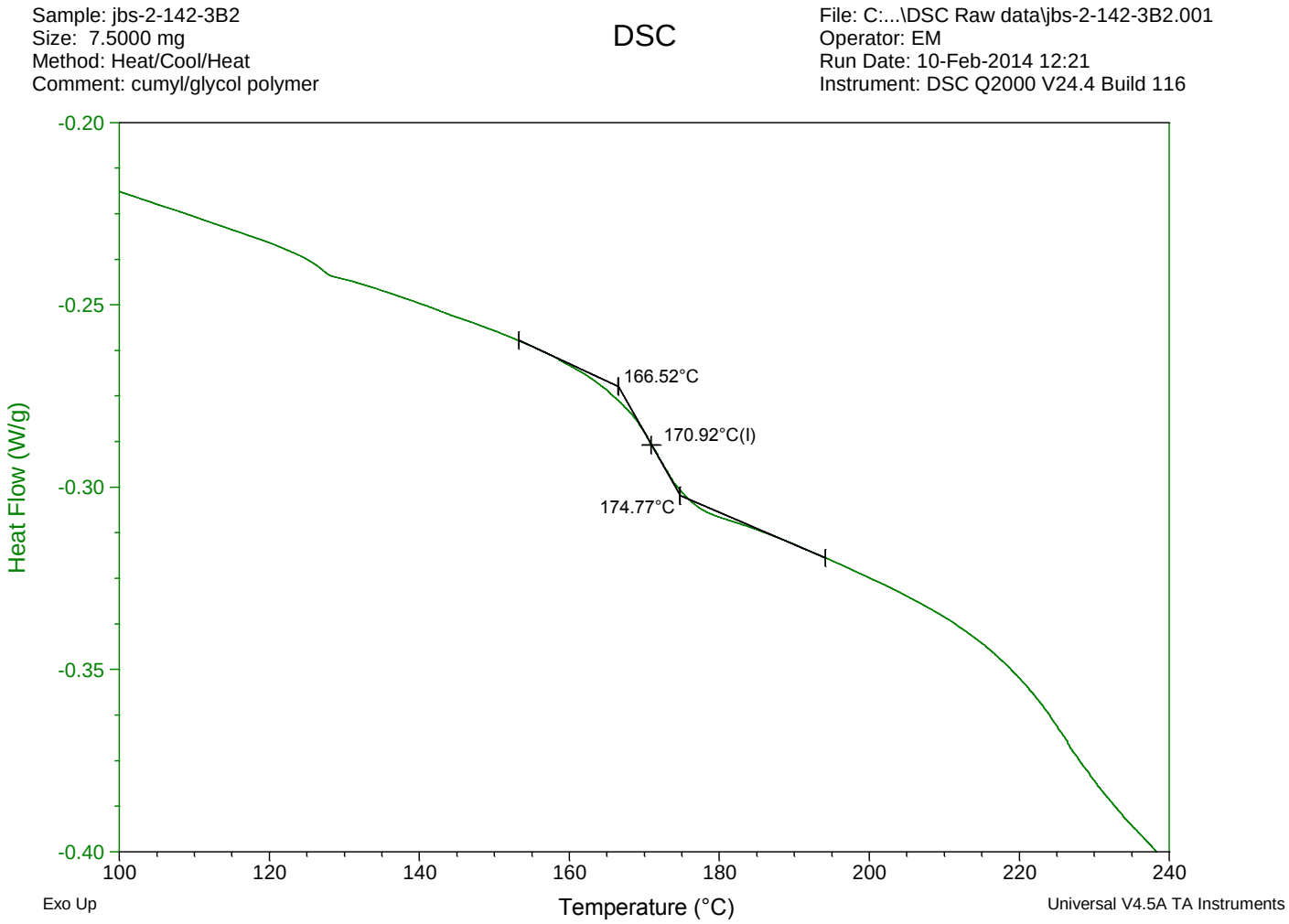
Sample: jbs-2-142-3B2
Size: 7.5000 mg
Method: Heat/Cool/Heat
Comment: cumyl/glycol polymer
DSC
File: C:...\DSC Raw data\jbs-2-142-3B2.001
Operator: EM
Run Date: 10-Feb-2014 12:21
Instrument: DSC Q2000 V24.4 Build 116
-0.20
-0.25
-0.30
-0.35
-0.40
Heat Flow (W/g)
166.52°C
170.92°C(I)
174.77°C
100
120
140
160
180
200
220
240
Exo Up
Temperature (°C)
Universal V4.5A TA Instruments

Polymer **11**

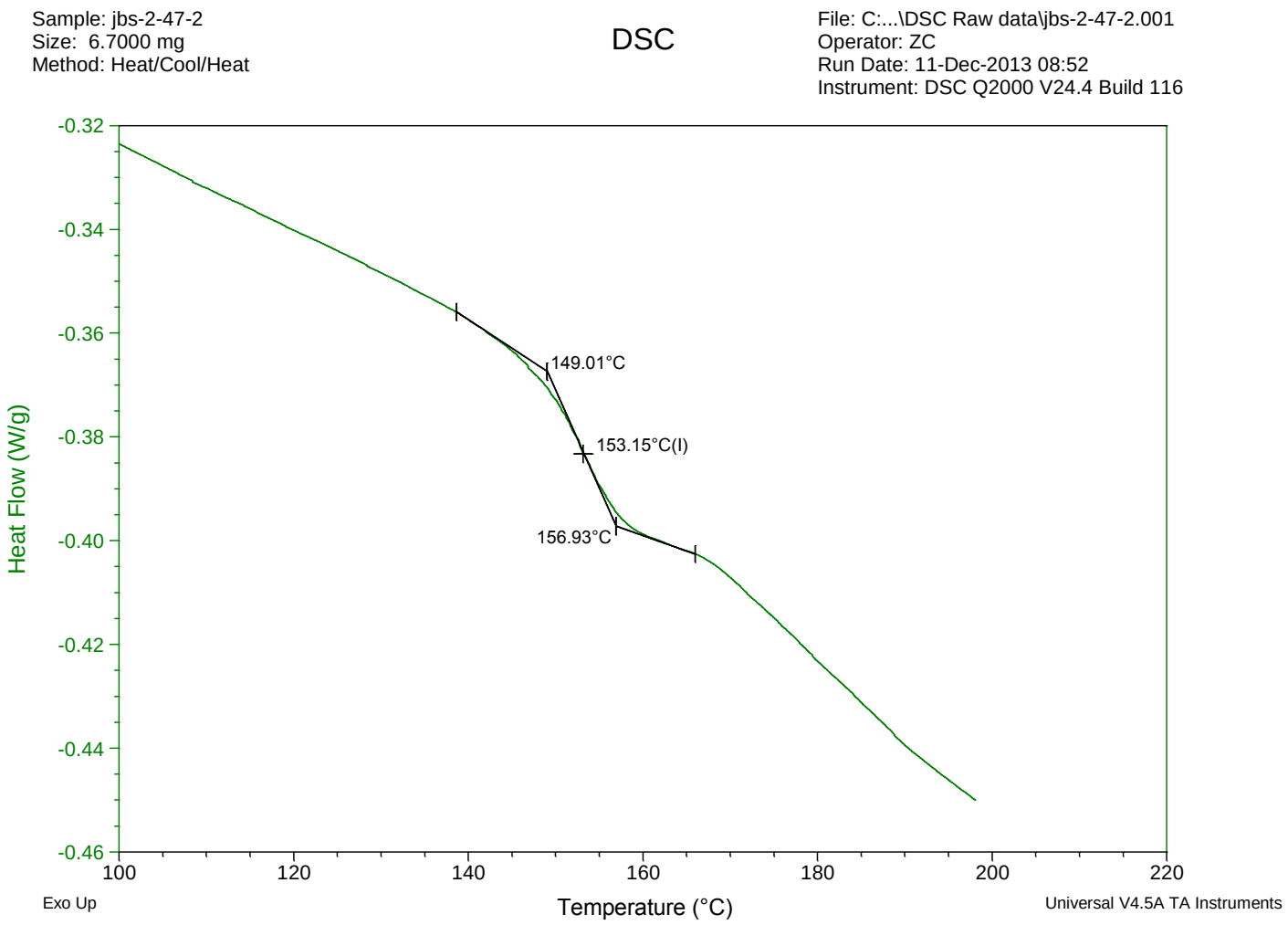
Sample: jbs-2-47-2
Size: 6.7000 mg
Method: Heat/Cool/Heat
DSC
File: C:...\DSC Raw data\jbs-2-47-2.001
Operator: ZC
Run Date: 11-Dec-2013 08:52
Instrument: DSC Q2000 V24.4 Build 116
-0.32
-0.34
-0.36
-0.38
-0.40
-0.42
-0.44
-0.46
Heat Flow (W/g)
149.01°C
153.15°C(I)
156.93°C
100
120
140
160
180
200
220
Exo Up
Temperature (°C)
Universal V4.5A TA Instruments

Polymer **12**

References

1. Fringuelli, F.; Taticchi, A., *The Diels Alder Reaction : Selected Practical Methods*. Wiley: Chichester, 2002.
2. Dag, A.; Aydin, M.; Durmaz, H.; Hizal, G.; Tunca, U., Various polycarbonate graft copolymers via diels-alder click reaction. *J. Polym. Sci., Part A: Polym. Chem.* **2012,** *50* (21), 4476-4483.
3. Gandini, A.; Belgacem, M. N., Furans in Polymer Chemistry. *Prog. Polym. Sci.* **1997,** *22*, 1203-1379.
4. Gandini, A., The furan/maleimide Diels–Alder reaction: A versatile click–unclick tool in macromolecular synthesis. *Prog. Polym. Sci.* **2013,** *38* (1), 1-29.
5. Boutelle, R. C.; Northrop, B. H., Substituent effects on the reversibility of furan-maleimide cycloadditions. *J. Org. Chem.* **2011,** *76* (19), 7994-8002.
6. Pieniazek, S. N.; Houk, K. N., The origin of the halogen effect on reactivity and reversibility of Diels-Alder cycloadditions involving furan. *Angew Chem Int Ed Engl* **2006,** *45* (9), 1442-5.
7. Cativiela, C.; Garcia, J.; Mayoral, J. A.; Salvatella, L., Modelling of Solvent Effects on the Diels-Alder Reaction. *Chem. Soc. Rev.* **1996,** *25*, 209 - 218.
8. Kuramoto, N.; Hayashi, K.; Nagai, K., Thermoreversible Reaction of Diels-Alder Polymer Composed of Difurufuryladipate with Bismaleimidodiphenylmethane. *J. Polym. Sci., Part A: Polym. Chem.* **1994,** *32*, 2501-2504.
9. Gandini, A.; Gousse´, C. c., Diels–Alder polymerization of difurans with bismaleimides. *Polym. Int.* **1999,** *48*, 723-731.
10. Meijer, E. W.; Brunsveld, L.; Folmer, B. J. B.; Sijbesma, R. P., Supramolecular Polymers. *Chem. Rev.* **2001,** *101*, 4071-4098.
11. Jones, M. W.; Strickland, R. A.; Schumacher, F. F.; Caddick, S.; Baker, J. R.; Gibson, M. I.; Haddleton, D. M., Polymeric dibromomaleimides as extremely efficient disulfide bridging bioconjugation and pegylation agents. *J Am Chem Soc* **2012,** *134* (3), 1847-52.
12. Watanabe, M.; Yoshie, N., Synthesis and properties of readily recyclable polymers from bisfuranic terminated poly(ethylene adipate) and multi-maleimide linkers. *Polymer* **2006,** *47* (14), 4946-4952.
13. Teramoto, N.; Arai, Y.; Shibata, M., Thermo-reversible Diels–Alder polymerization of difurfurylidene trehalose and bismaleimides. *Carbohydrate Polymers* **2006,** *64* (1), 78-84.
14. Patel, H. S.; Patel, V. C., New monomers for polyimides. *Des. Monomers Polym.* **2000,** *3*, 191-197.
15. Chujo, Y.; Sada, K.; Saegusa, T., Reversible gelation of polyoxazoline by means of Diels-Alder reaction. *Macromolecules* **1990,** *23* (10), 2636-2641.
16. Stevens, M. P.; Jenkins, A. D., Crosslinking of Polystyrene via Pendant Maleimide Groups. *J. Polym. Sci., Part A: Polym. Chem.* **1979,** *17*, 3675-3685.
17. Canary, S. A.; Stevens, M. P., Thermally Reversible Crosslinking of Polystyrene via the Furan-Maleimide Diels-Alder Reaction. *J. Polym. Sci., Part A: Polym. Chem.* **1992,** *30*, 1755-1760.
18. Chen, X., A Thermally Re-mendable Cross-Linked Polymeric Material. *Science* **2002,** *295* (5560), 1698-1702.
19. Jong Se, P.; Takahashi, K.; Guo, Z.; Wang, Y.; Bolanos, E.; Hamann-Schaffner, C.; Murphy, E.; Wudl, F.; Hahn, H. T., Towards Development of a Self-Healing Composite using a Mendable Polymer and Resistive Heating. *J. Compos. Mater.* **2008,** *42* (26), 2869-2881.
20. Franc, G.; Kakkar, A. K., Diels-Alder "Click" Chemistry in Designing Dendritic Macromolecules. *Chem. Eur. J.* **2009,** *15* (23), 5630-5639.
21. Polaske, N. W.; McGrath, D. V.; McElhanon, J. R., Thermally Reversible Dendronized Step-Polymers Based on Sequential Huisgen 1,3-Dipolar Cycloaddition and Diels−Alder "Click" Reactions. *Macromolecules* **2010,** *43* (3), 1270-1276.

22. McElhanon, J. R.; Wheeler, D. R., Thermally Responsive Dendrons and Dendrimers Based on Reversible Furan-Maleimide Diels-Alder Adducts. *Organic Letters* **2001,** *3* (17), 2681-2683.
23. McElhanon, J. R.; Russick, E. M.; Wheeler, D. R.; Loy, D. A.; Aubert, J. H., Removable foams based on an epoxy resin incorporating reversible Diels-Alder adducts. *Journal of Applied Polymer Science* **2002,** *85* (1496-1502).
24. McElhanon, J. R.; Zifer, T.; Kline, S. R.; Wheeler, D. R.; Loy, D. A.; Jamison, G. M.; Long, T. M.; Rahimian, K.; Simmors, B. A., Thermally Cleavable Surfactants Based on Furan−Maleimide Diels−Alder Adducts. *Langmuir* **2005,** *21*, 3259-3266.
25. Thomas, I. P.; Ramsden, j. A.; Kovacs, T. Z.; Brown, J. M., Covalent Adhesion: Organic Reactivity at a Solid-Solid Interface Through an Inter-Bead Diels-Alder reaction. *Chem. Commun.* **1999**, 2.
26. Stille, J. K.; Plummer, L., Polymerization by the Diels-Alder Reaction. *Journal of Organic Chemistry* **1961,** *26*, 4026-4029.
27. Kennedy, J. P.; Carlson, G. M., Synthesis, Characterization, and Diels-Alder Extension of Cyclopentadiene Telechelic Polyisobutylene. *Journal of Polymer Science Part A: Polymer Chemistry* **1983,** *21*, 3551-3561.
28. Kennedy, J. P.; Castner, K. F., Thermally Reversible Polymer Systems by Cyclopentadienylation. I. A Model for Termination by Cyclopentadienylation of Olefin Polymerization. *Journal of Polymer Science Part A: Polymer Chemistry* **1979,** *17*, 2039-2054.
29. Kennedy, J. P.; Castner, K. F., Thermally Reversible Polymer Systems by Cyclopentadienylation. II. The Synthesis of Cyclopentadiene-Containing Polymers. *Journal of Polymer Science Part A: Polymer Chemistry* **1979,** *17* (7), 2055-2070.
30. Kennedy, J. P.; Carlson, G. M., Synthesis, Characterization, and Diels-Alder Extension of Cyclopentadiene Telechelic Polyisobutylene. III. Silylcyclopentadiene-Telechelic Polyisobutylene. *Journal of Polymer Science Part A: Polymer Chemistry* **1983,** *21* (10), 2973-2986.
31. Murphy, E. B.; Bolanos, E.; Schaffner-Hamann, C.; Wudl, F.; Nutt, S. R.; Auad, M. L., Synthesis and Characterization of a Single-Component Thermally Remendable Polymer Network: Stuadinger and Stille Revisited. *Macromolecules* **2008,** *41* (14), 5203-5209.
32. Murphy, E. B.; Wudl, F., The world of smart healable materials. *Progress in Polymer Science* **2010,** *35* (1-2), 223-251.
33. Zhang, M. Q.; Rong, M. Z., *Self-Healing Polymers and Polymer Composites*. John Wiley and Sons: Hoboken, New Jersey, 2011.
34. Christoffers, J.; Werner, T.; Baro, A.; Fischer, P., Synthesis of a tin-functionalized cyclopentadiene derivative. *Journal of Organometallic Chemistry* **2004,** *689*, 3550-3555.
35. Skattebol, L., Chemistry of Gem-Dihalocyclopropanes-VI. *Tetrahedron* **1967,** *23*, 1107-1117.
36. Deck, P. A.; Jackson, W. F.; Fronczek, F. R., Synthesis of Pentafluorophenyl-Substituted Cyclopentadienes and Their Use as Transition-Metal Ligands. *organometallics* **1996,** *15*, 5287-5291.
37. Deck, P. A.; Kroll, C. E.; Hollis, W. G. J.; Fronczek, F. R., Conformational control of intramolecular arene stacking in ferrocene complexes bearing tert-butyl and pentafluorophenyl substituents. *Journal of Organometallic Chemistry* **2001,** *637*, 107-115.
38. Hughes, R. P.; Kowalski, A. S.; Lomprey, j. R., A New Synthesis of 1,5-Di-tert-butyl-1,3-cyclopentadiene by Dehydration of an Epoxide and Characterization of its Diels-Alder Dimer. *The Journal of organic chemistry* **1996,** *61*, 401-404.
39. Krupka, J., Kinetics of Thermal Dimerizations of Cyclopentadiene and Methylcyclopentadiene and their Co-dimerization. *Petroleum and Coal* **2010,** *52* (4), 290-306.
40. Craig, D., The Rearrangement of endo-3,6-Methylene-l,2,3,6-tetrahydro-cis-phthalic anhydride. *J. Am. Chem. Soc.* **1951,** *73* (10), 4889-4892.

41. Evans, J. P.; Hickory, B. S.; Slebodnick, C.; Deck, P. A., Development of Modular Monomer System for Highly Fluorinated Diels-Alder Polyphenylenes. *Journal of Organic Chemistry* **2011**, Manuscript in preparation.
42. Vladimirskaya, N. B.; Koshutin, V. I.; Smirnov, V. A., Addition of methyl- and phenyllithium to 6,6-dimethylfulvene. *Zh. Org. Khim.* **1975,** *11* (1), 212.
43. Deck, P. A.; Jantunen, K. C.; Taw, F. L.; Kiplinger, J. L., (Pentafluorophenyl)Cyclopentadiene and its Sodium Salt. In *Inorganic Syntheses: Volume 36*, John Wiley & Sons, Inc.: 2014; pp 38-41.
44. Csicsery, S. M., Methylcyclopentadiene Isomers. *J. Org. Chem.* **1960,** *25*, 518-521.
45. Craven, W. J. The Methylcyclopentadienes. Cornell, Cornell University, 1955.
46. Avramenko, G. I.; Sergeyev, N. M.; Ustynyuk, Y. A., NMR spectroscopy of metal cyclopentadienyls VIII. Prototropism and dimerisations of silicon cyclopentadienyls. *Journal of Organometallic Chemistry* **1972,** *37* (1), 89-100.
47. Harvey, S. C., Maleimide as a Dienophile. *J. Am. Chem. Soc* **1949,** *71* (3), 1121-1122.
48. Deck, P. A., Perfluoroaryl-substituted cyclopentadienyl complexes of transition metals. *Coordination Chemistry Reviews* **2006,** *250* (9-10), 1032-1055.
49. Sen, S.; Slebodnick, C.; Deck, P. A., Highly Fluorinated Diels-Alder Polyphenylenes. *Macromolecules* **2011**, Manuscript in preparation.
50. Schwarzer, A.; Weber, E., Influence of Fluorine Substitution on the Crystal Packing of N-phenylmaleimides and Corresponding Phthalimides. *Crystal Growth and Design* **2008,** *8* (8), 2862-2874.
51. Ltd, A. T. A. T. U., CrysAlisPro Software system. Oxford, UK, 2011; Vol. v1.171.35.11.
52. Sheldrick, G. M., "A short history of SHELX". *Acta Cryst.* **2008,** *A64*, 112-122.
53. Dolomanov, O. V.; Bourhis, L. J.; Gildea, R. J.; Howard, J. A. K.; Puschmann, H., *J. Appl. Cryst.* **2009,** *42*, 339-341.
54. Gandini, A.; Silvestre, A. J. D.; Coelho, D., Reversible click chemistry at the service of macromolecular materials. *Polymer Chemistry* **2011,** *2* (1713-1720).
55. Weizman, H.; Nielsen, C.; Weizman, O. S.; Nemat-Nasser, S., Synthesis of a Self-Healing Polymer Based on Reversible Diels–Alder Reaction: An Advanced Undergraduate Laboratory at the Interface of Organic Chemistry and Materials Science. *Journal of Chemical Education* **2011,** *88* (8), 1137-1140.
56. Binder, W. H., Self-Healing Polymers : From Principles to Applications. 1 ed.; Wiley: Hoboken, 2013. http://viva.eblib.com/patron/FullRecord.aspx?p=1163227.
57. Bergman, S. D.; Wudl, F., Mendable polymers. *Journal of Materials Chemistry* **2008,** *18* (1), 41-62.
58. Adzima, B. J.; Aguirre, H. A.; Kloxin, C. J.; Scott, T. F.; Bowman, C. N., Rheological and Chemical Analysis of Reverse Gelation in a Covalently Cross-Linked DA Polymer Network. *Macromolecules* **2008,** *41* (23), 9112-9117.
59. Zhang, R.; Yu, S.; Chen, S.; Wu, Q.; Chen, T.; Sun, P.; Li, B.; Ding, D., Reversible cross-linking, microdomain structure, and heterogeneous dynamics in thermally reversible cross-linked polyurethane as revealed by solid-state NMR. *The journal of physical chemistry. B* **2014,** *118* (4), 1126-37.
60. Salamone, J. C.; Chung, Y.; Clough, S. B., Thermally Reversible, Covalently Crosslinked Polyphosphazenes. *Journal of polymer science. Part A, Polymer chemistry* **1988,** *26*, 2923-2939.
61. Lv, W.; El-Hebshi, Y.; Li, B.; Xia, Y.; Xu, R.; Chen, X., Investigation of thermo-reversibility of polymer crosslinked by reversible covalent bonds through torque measurement. *Polymer Testing* **2013,** *32* (2), 353-358.
62. Wagener, K. B.; Engle, L. P., Thermally Reversible Polymer Linkages. II. Linear Addition Polymers. *Journal of polymer science. Part A, Polymer chemistry* **1993,** *31*, 865-875.

63. Gousse´, C. c.; Gandini, A.; Hodge, P., Application of the Diels-Alder Reaction to Polymers Bearing Furan Moieties. 2. Diels-Alder and Retro-Diels-Alder reactions Involving Furan Rings in Some Styrene Copolymers. *Macromolecules* **1998,** *31* (2), 314-321.
64. Sheridan, R. J.; Bowman, C. N., Understanding the process of healing of thermoreversible covalent adaptable networks. *Polymer Chemistry* **2013,** *4* (18), 4974.
65. Dewar, M. J. S.; Pierini, A. B., Mechanism of the Diels-Alder Reaction. Studies of the Addition of Maleic Anhydride to Furan and Methylfurans. *Journal of the American Chemical Society* **1984,** *106*, 203-208.
66. Rulisek, L.; Sebek, P.; Havlas, Z.; Hrabal, R.; Capek, P.; Svatos, A., An Experimental and Theoretical Study of Stereoselectivity of Furan-Maleic Anhydride and Furan-Maleimide Diels-Alder Reactions. *Journal of Organic Chemistry* **2005,** *70*, 6295-6302.
67. Inglis, A. J.; Nebhani, L.; Altintas, O.; Schmidt, F. G.; Barner-Kowollik, C., Rapid Bonding/Debonding on Demand: Reversibly Cross-Linked Functional Polymers via Diels−Alder Chemistry. *Macromolecules* **2010,** *43* (13), 5515-5520.
68. Kiriazis, A.; Leikoski, T.; Mutilkainen, I.; Yli-Kauhaluoma, J., The Diels-Alder Reaction between Deactivated Dienes and Electron-deficient Dienophiles on solid support Stereoselective synthesis of hexahydro 1,3 diocoisoindoles. *Journal of Combinatorial Chemistry* **2004,** *6* (2), 283-285.
69. Magana, S.; Zerroukhi, A.; Jegat, C.; Mignard, N., Thermally reversible crosslinked polyethylene using Diels–Alder reaction in molten state. *Reactive and Functional Polymers* **2010,** *70* (7), 442-448.
70. Roland, C. D. The Development of Transparent, Processable, Thermally-Responsive Coatings. California Polytechnic State University, 2012.
71. Schmidt, J. R.; Polik, W. F. *WebMO Enterprise* 14.0.007e; 2013.
72. Frisch, M. J.; Trucks, G. W.; Schlegel, H. B.; Scuseria, G. E.; Robb, M. A.; Cheeseman, J. R.; Scalmani, G.; Barone, V.; Mennucci, B.; Petersson, G. A.; Nakatsuji, H.; Caricato, M.; Li, X.; Hratchian, H. P.; Izmaylov, A. F.; Bloino, J.; Zheng, G.; Sonnenberg, J. L.; Hada, M.; Ehara, M.; Toyota, K.; Fukuda, R.; Hasegawa, J.; Ishida, M.; Nakajima, T.; Honda, Y.; Kitao, O.; Nakai, H.; Vreven, T.; Montgomery, J. A., Jr.; Peralta, J. E.; Ogliaro, F.; Bearpark, M.; Heyd, J. J.; Brothers, E.; Kudin, K. N.; Staroverov, V. N.; Kobayashi, R.; Normand, J.; Raghavachari, K.; Rendell, A.; Burant, J. C.; Iyengar, S. S.; Tomasi, J.; Cossi, M.; Rega, N.; Millam, M. J.; Klene, M.; Knox, J. E.; Cross, J. B.; Bakken, V.; Adamo, C.; Jaramillo, J.; Gomperts, R.; Stratmann, R. E.; Yazyev, O.; Austin, A. J.; Cammi, R.; Pomelli, C.; Ochterski, J. W.; Martin, R. L.; Morokuma, K.; Zakrzewski, V. G.; Voth, G. A.; Salvador, P.; Dannenberg, J. J.; Dapprich, S.; Daniels, A. D.; Farkas, Ö.; Foresman, J. B.; Ortiz, J. V.; Cioslowski, J.; Fox, D. J. *Gaussian, Inc.*, Wallingford CT, 2009.
73. Stephens, P. J.; Devlin, F. J.; Chabalowski, C. F.; Frisch, M. J., Ab Initio Calculation of Vibrational Absorption and Circular Dichroism Spectra Using Density Functional Force Fields. *J.Phys.Chem.* **1994,** *98*, 11623-11627.
74. Vosko, S. H.; Wilk, L.; Nusair, M., Accurate spin-dependent electron liquid correlation energies for local spin density calculations: a critical analysis. *Can. J. Phys.* **1980,** *58* 1200-1211.
75. Lee, C.; Yang, W.; Parr, R. G., Development of the Colle-Salvetti correlation-energy formula into a functional of the electron density. *Phys. Rev. B* **1988,** *37*, 785-789.
76. Becke, A. D., Density-functional thermochemistry. III. The role of exact exchange. *J. Chem. Phys.* **1993,** *98*, 5648-5652.
77. Petersson, G. A.; Al-Laham, M. A., A complete basis set model chemistry. II. Open-shell systems and the total energies of the first-row atoms. *J. Chem. Phys.* **1991,** *94*, 6081-6090.
78. Petersson, G. A.; Bennett, A.; Tensfeldt, T. G.; Al-Laham, M. A.; Shirley, W. A.; Mantzaris, J., A complete basis set model chemistry. I. The total energies of closed-shell atoms and hydrides of the first-row atoms. *J. Chem. Phys.* **1988,** *89*, 2193-2218.
79. Stewart, J. J. P., Optimization of parameters for semiempirical methods II. Applications. *J. Comput. Chem.* **1989,** *10* (2), 221.

80. Stewart, J. J. P., Optimization of parameters for semiempirical methods I. Method. *J. Comput. Chem.* **1989,** *10* (2), 209.
81. Spek, A. L., "PLATON, A Multipurpose Crystallographic Tool, Utrecht University, Utrecht, The Netherlands.". *J. Appl. Cryst.* **2003,** *36*, 7-13.
82. Hawrelak, E. J.; Deck, P. A., Analysis of Metallocene-Methyalumoxane Methide Transfer Processes in SOlution Using 19F NMR Spectroscopic Probe. *Organometallics* **2003,** *22*, 3558-3565.
83. Thornberry, M. P.; Slebodnick, C.; Deck, P. A.; Fronczek, F. R., Synthesis and Structure of Piano Stool Complexes Derived from the Tetrakis(pentafluorophenyl)cyclopentadienyl Ligand. *Organometallics* **2001,** *20*, 920-926.
84. Tamagna, C.; Mison, P.; Pascal, T.; Petiaud, R.; Sillion, B., Fluorine-19 NMR monitored thermal imidization of
bicyclo[2.2.2]oct-7-ene systems. *Polymer* **1999,** *40*, 8.
85. Newhouse, T.; Baran, P. S.; Hoffman, R. W., The Economies of Synthesis. *Chemical Society Reviews* **2009,** *38*, 3010 - 3021.
86. He, X.; Sastri, V. R.; Tesoro, G. C., 1,4-Bis(5-methylfurfuryl)benzene Polymerization with siloxane containing dimaleimides. *Makromol. Chem., Rapid Commun.* **1988,** *9*, 191-194.
87. Tesoro, G. C.; Sastri, V. R., Synthesis of Siloxane-containing bis(furans) and polymerization with bis(maleimides). *Ind. Eng. Chem. Prod. Res. Dev.* **1986,** *25*, 444-448.
88. Mikroyannidis, J. A., Synthesis and Diels-Alder polymerization of furfurylidene and furfuryl-substituted maleamic acids. *Journal of Polymer Science Part A, Polymer Chemistry* **1992,** *30*, 125-132.
89. Bauer, R. E.; Grimsdale, A. C.; Muellen, K., Functionalised polyphenylene dendrimers and their applications. *Top. Curr. Chem.* **2005,** *245* (Functional Molecular Nanostructures), 253-286.
90. Yoshie, N.; Saito, S.; Oya, N., A thermally-stable self-mending polymer networked by Diels–Alder cycloaddition. *Polymer* **2011,** *52* (26), 6074-6079.
91. Chen, X.; Dam, M. A.; Ono, K.; Mal, A.; Shen, H.; Nutt, S. R.; Sheran, K.; Wudl, F., A thermally re-mendable cross-linked polymeric material. *Science* **2002,** *295* (5560), 1698-702.
92. Goiti, E.; Huglin, M. B.; Rego, J. M., Thermal Breakdown by the Retro Diels–Alder Reaction of Crosslinking in Poly[styrene-co-(furfuryl methacrylate)]. *Macromolecular Rapid Communications* **2003,** *24* (11), 692-696.
93. Kossmehl, G.; Nagel, H.-I.; Pahn, A., Cross-linking reactions on polyamides by bis- and tris(maleimides). *Angew. Makromol Chem* **1995,** *227*, 139 - 157.
94. Aumsuwan, N.; Urban, M., Reversible releasing of arms from star morphology polymers. *Polymer* **2009,** *50* (1), 33-36.
95. Anslyn, E. V.; Dougherty, D. A., Thermal Pericyclic Reactions. In *Modern Physical Organic Chemistry*, University Science Books: 2006.
96. Charton, M., Application of the Hammett Equation to Nonaromatic Unsaturated Systems. VI. The Diels-Alder Reaction. *Journal of Organic Chemistry* **1966,** *31* (11), 3745 - 3751.
97. Inukai, T.; Kojima, T., Hammett Correlation for the Rates of Diels-Alder Reaction of 2-substituted Butadienes. *Chem. Soc. D: Chem. Commun.* **1969,** (22), 1334 - 1335.
98. Dang, Q.; Liu, Y., An efficient entry to furo[2,3-d]pyrimidines via inverse electron demand Diels–Alder reactions of 2-aminofurans with 1,3,5-triazines. *Tetrahedron Letters* **2009,** *50* (49), 6758-6760.
99. Adams, H.; Elsunaki, T. M.; Ojea-Jimenez, I.; Jones, S.; Meijer, A. J., Diastereoselective cycloadditions and transformations of N-alkyl and N-aryl maleimides with chiral 9-anthrylethanol derivatives. *J. Org. Chem.* **2010,** *75* (18), 6252-62.
100. Sauer, J., Diels-Alder reaction. I. Reactivity of dienophiles towards cyclopentadiene and 9,10-dimethylanthracene. *Chem. Ber.* **1964,** *97* (11), 3183-3207.

101. Gugelchuk, M. M.; Chan, P. C.-M.; Sprules, T. J., Can Remote Substituent Effects Influence Reactivity and Stereoselectivity in the Diels-Alder Cycloadditions of p-Substituted 6-Phenyl-6-methylfulvenes? *J. Org. Chem.* **1994,** *59*, 7723-7731.
102. Hapke, M.; Gutnov, A.; Weding, N.; Spannenberg, A.; Fischer, C.; Benkhäuser-Schunk, C.; Heller, B., Use of the Diels-Alder Cycloaddition of Tetracyclone and Internal Aryl Acetylenes for the Synthesis of Functionalized Atropisomeric Biaryls. *Eur. J. Org. Chem.* **2010,** *2010* (3), 509-514.
103. Singh, P.; Rausch, M. D.; Bitterwolf, T. E., Formation of Synthetic Utility of Benzyl- and Phenylcyclopentadienylthallium. *J. Organomet. Chem.* **1988,** *352* (3), 273 - 382.
104. Farnum, D. G.; Mostashari, A.; Hagedorn, A. A., III, Nuclear magnetic resonance spectra of cyclic 1,3-diphenylallyl cations. 1,3-Orbital interaction. *J. Org. Chem.* **1971,** *36*, 698 - 702.
105. Kang, Y. K.; Lee, H.-K.; Lee, S. S.; Chung, Y. K.; Carpenter, G., Synthesis and structure of new diarene-bridged bi- and polymetallic compounds *Inorg. Chim. Acta* **1997,** *261*, 37 - 44.
106. Panda, T. K.; Gamer, M. T.; Roesky, P. W., An Improved Synthesis of Sodium and Potassium Cyclopentadienide. *Organometallics* **2008,** *22*, 877-878.
107. Deck, P. A.; McCauley, B. D.; Slebodnick, C., Transition metal cyclopentadienyl complexes bearing perfluoro-4-tolyl substituents. *J. Organomet. Chem.* **2006,** *691* (9), 1973-1983.
108. Flack, H. D., On enantiomorph-polarity estimation. *Acta Cryst.* **1983,** *A39*, 876-881.
109. Warren, A. D. Virginia Tech.
110. Pangborn, A. B.; Giardello, M. A.; Grubbs, R. H.; Rosen, R. K.; Timmers, F. J., Safe and Convenient Procedure for Solvent Purification. *Organometallics* **1996,** *15*, 1518-1520.
111. Searle, N. E. Synthesis of N-Aryl-Maleimides. 1948.
112. Barrales-Rienda, J. M.; Ramos, J. G.; Chaves, M. S., Synthesis of N-(fluorophenyl) Maleamic Acids and N-(fluorophenyl) Maleimides. *Journal of Fluorine Chemistry* **1977,** *9*, 293-308.
113. Takeda, S.; Akijama, H.; Kakiuchi, H., Synthesis and Properties of Bismaleimide Resins Containing Ether Bonds. *J. Appl. Polym. Sci.* **1988,** *35*, 1341.
114. White, J. E.; Snider, D. A.; Scaia, M. D., Synthesis and Properties of Some New Polyimidosulfides with Highly Mobile Backbones. *Journal of Polymer Science: Polymer Chemistry Edition* **1984,** *22*, 589-596.
115. Dickert, J. J. J. Phosphorus Derivatives of 4,4'-Disuccinimidobiphenyloxide and Lubricant Compositions Containing Same. U.S. Patent 3,756,951, September 4, 1973, 1973.
116. Mayo, J. D.; Adronov, A., Effect of spacer chemistry on the formation and properties of linear reversible polymers. *Journal of Polymer Science Part A: Polymer Chemistry* **2013,** *51* (23), 5056-5066.
117. Hollandsworth, C. B.; Hollis, W. G.; Deck, P. A.; Slebodnick, C., Metallocene Complexes of Iron and Cobalt Derived from the 4,4’-Bis(η5-cyclopentadienyl)octafluorobiphenyl Ligand. *Organometallics* **1999,** *18* (18), 3610-3614.
118. Gibson, H. W.; Yamaguchi, N.; Jones, J. W., Supramolecular Pseudorotaxane Polymers from Complementary Pairs of Homoditopic Molecules. *Journal of the American Chemical Society* **2003,** *125*, 3522-3533.